Clinical pharmacological and translational research on novel formulations of anticancer drugs

ISBN/EAN: 978-90-6464-216-6

Cover design: Ed Veltkamp, Bosch en Duin, The Netherlands
Sander Veltkamp, Amsterdam, The Netherlands

Printed by: Ponsen & Looijen BV, Wageningen, The Netherlands

Clinical pharmacological and translational research on novel formulations of anticancer drugs

Klinisch farmacologisch en translationeel onderzoek naar nieuwe formuleringen van antikanker middelen
(met een samenvatting in het Nederlands)

PROEFSCHRIFT

ter verkrijging van de graad van doctor
aan de Universiteit Utrecht
op gezag van rector magnificus, prof. dr. J.C. Stoof,
ingevolge het besluit van het college voor promoties
in het openbaar te verdedigen
op woensdag 5 maart 2008 des morgens te 10.30 uur

door

Stephan Alexander Veltkamp

geboren op 23 januari 1977 te Laren

Promotoren:

Prof. Dr. J.H.M. Schellens
Prof. Dr. J.H. Beijnen

The research described in this thesis was performed at the Division of Experimental Therapy and the Department of Medical Oncology, The Netherlands Cancer Institute / Antoni van Leeuwenhoek Hospital and the Department of Pharmacy & Pharmacology, The Netherlands Cancer Institute / Slotervaart Hospital, Amsterdam, The Netherlands.

Publication of this thesis was financially supported by:

Eli Lilly Nederland BV, Houten, The Netherlands
Abbott BV, Hoofddorp, The Netherlands
Merk Sharp & Dohme BV, Haarlem, The Netherlands
The Netherlands Cancer Institute / Antoni van Leeuwenhoek Hospital, Amsterdam, The Netherlands

A person who spills one hour in life has not discovered the value of life yet (Charles Darwin)

Fantasy is more important than knowledge (Albert Einstein)

Aan mijn ouders

Voor Annefloor

Contents

Chapter 1

General introduction

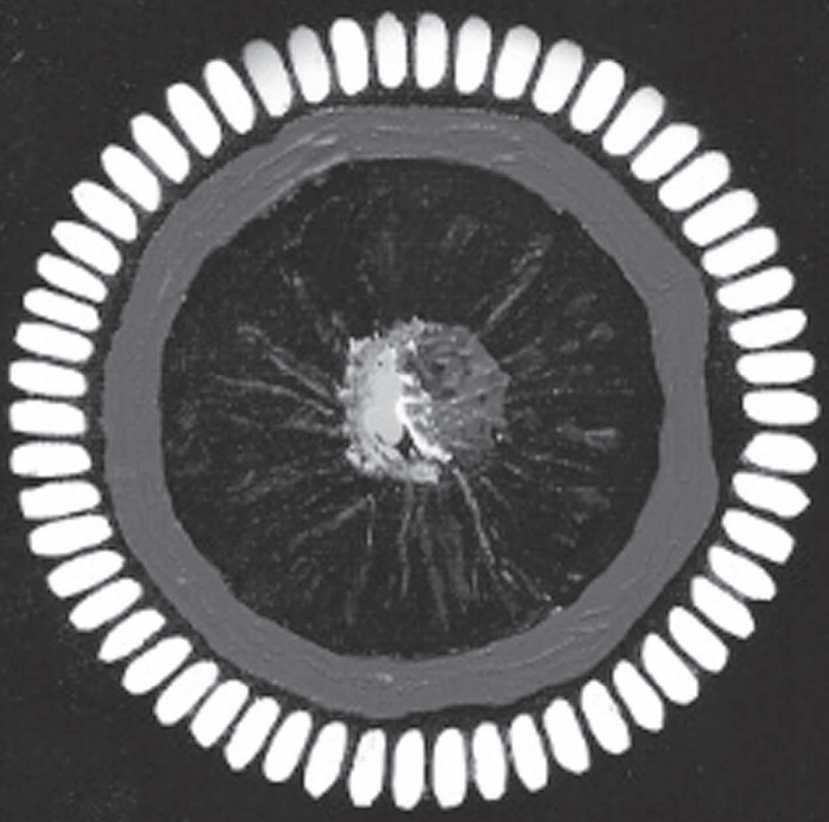

General introduction

Each year, more than 10 million people are diagnosed with cancer worldwide. The most common cancers are lung, breast and colorectal cancer with 1.4, 1.2, and 1.0 million new cases per year (1). Cancer is the second cause of death in The Netherlands (2). In 2003, about 73,000 new cases of cancer were diagnosed and 38,000 people died as a result of the disease (3). In the same year, 21% of the new cancer cases in man were attributed to prostate cancer and 16% to lung cancer, while in women 34% of the incident cancer cases were attributed to breast cancer (3).

Chemotherapy is frequently used in the treatment of patients with solid tumors, including patients with non-small cell lung cancer. At the time of this writing, about 6,440 clinical trials are registered in the USA that perform research to improve the diagnosis and treatment of cancer (4).

Among the chemotherapeutic agents, gemcitabine (5) and paclitaxel (6) are relevant drugs used in single or combination regimens with other anticancer drugs or radiotherapy. However, there is a growing need for new treatment strategies to optimize the clinical use of these anticancer drugs. Antitumor activity can be increased by prolongation of the exposure time of a tumor to adequate concentrations of an anticancer drug. An increase in the exposure of the tumor to the drug can be achieved by continuous drug administration and by targeting the drug to the tumor site. Oral drug administration facilitates the use of continuous dosing regimens and is generally more convenient for patients than intravenous (i.v.) administration. Novel preclinical discoveries are important for the development and application of new drugs and/or drug formulations in patients. Also, the clinical ("bed side") results of the compounds often raise questions that are the basis for new research in preclinical ("bench side") models. This two-way traffic between preclinical and clinical research is called translational research.

Outline of this thesis

The application of prolonged fixed dose rate infusion compared to standard 30-min infusion of gemcitabine and the pharmacology and mechanisms of action of gemcitabine are discussed in **Chapter 2**. Research on the cytotoxicity, metabolism, tissue distribution, and pharmacokinetics of gemcitabine after oral and i.v.

administration in preclinical and clinical studies is described in **Chapter 3**. Clinical studies on novel oral paclitaxel formulations without Cremophor® EL and the application of cyclosporin A to increase the systemic exposure to paclitaxel from these formulations is presented in **Chapter 4**. In **Chapter 5** we describe a clinical pharmacological study with a new polymer prodrug MEN 4901/T-0128 that inhibits topoisomerase I.

References

1. GLOBOCAN 2002 database. Cancer Incidence, Mortality and Prevalence Worldwide. International Agency for Research on Cancer (http://www-dep.iarc.fr).

2. KWF kankerbestrijding (http://www.kwfkankerbestrijding.nl).

3. NKR cijfers 2003. IKC 2007 (http://www.ikcnet.nl/page.php?id=41).

4. National Cancer Institute (http://www.cancer.gov/clinicaltrials).

5. US Food and Drug Administration (FDA). Center for Drug Evaluation and Research (http://www.fda.gov/cder/foi/label/2006/020509s039lbl.pdf).

6. College ter Beoordeling van Geneesmiddelen (http://www.cbg-meb.nl/IB-Teksten/h16265.pdf).

Chapter 2

Fixed dose rate infusion of gemcitabine

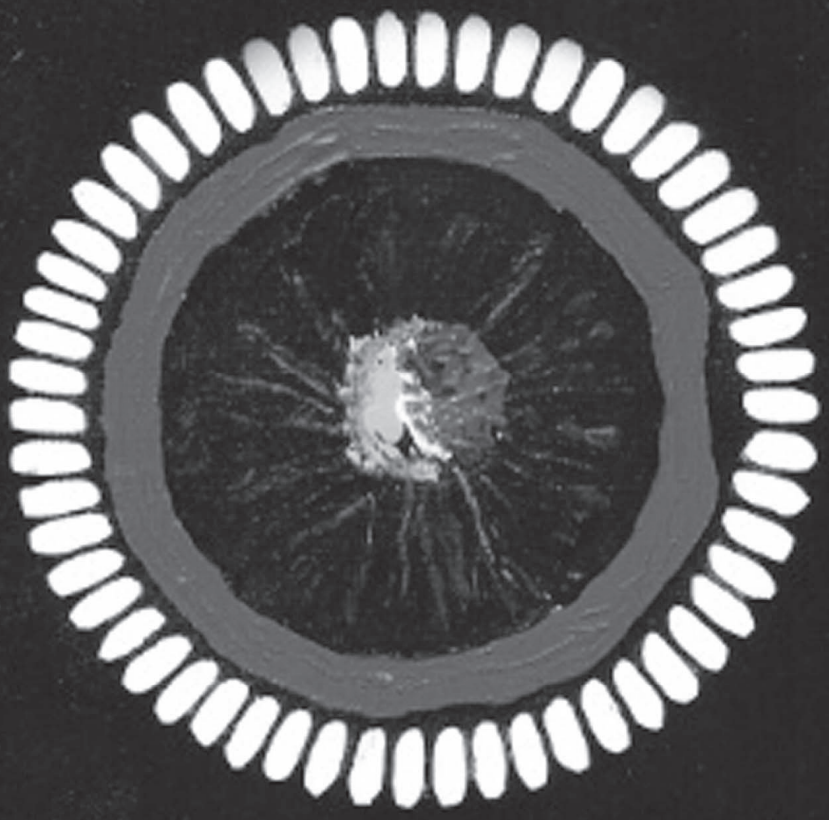

Chapter 2.1

Prolonged versus standard gemcitabine infusion: translation of molecular pharmacology to new treatment strategy

The Oncologist, accepted for publication

Stephan A. Veltkamp
Jos H. Beijnen
Jan H.M. Schellens

Abstract

Gemcitabine is frequently used in the treatment of patients with solid tumors. Gemcitabine is taken up into the cell via human nucleoside transporters (hNTs) and is intracellularly phosphorylated by deoxycytidine kinase (dCK) to its monophosphate and subsequently into its main active triphosphate metabolite (dFdCTP), which is incorporated into DNA and inhibits DNA synthesis. Besides, gemcitabine is extensively deaminated to 2',2'-difluorodeoxyuridine (dFdU), which is largely excreted into the urine. High expression levels of the human equilibrative nucleoside transporter type 1 (hENT1) were associated with a significantly longer overall survival after gemcitabine treatment in patients with pancreatic cancer.

Clinical studies in blood mononuclear and leukemic cells demonstrated that a lower infusion rate of gemcitabine was associated with higher intracellular dFdCTP levels. Prolonged infusion of gemcitabine at a fixed dose rate (FDR) of 10 $mg/m^2/min$ was associated with a higher intracellular accumulation of dFdCTP, higher toxicity and an improved response rate compared to the standard 30-min infusion of gemcitabine in patients with pancreatic cancer.

In the current review, we discuss the molecular pharmacology of nucleoside analogues and the influence of hNTs and dCK on the activity and toxicity of gemcitabine, which is the basis for clinical studies on FDR administration. Furthermore, we discuss the results of FDR dosing in patients. These findings might aid optimal clinical application of gemcitabine in the future.

Introduction

Nucleoside anticancer drugs constitute an important class of antimetabolites that are used in the treatment of hematological malignancies and solid tumors. The pyrimidine nucleoside analogues cytarabine (cytosine arabinoside, ara-C) and gemcitabine (2',2'-difluorodeoxycytidine, dFdC) are frequently used in the treatment of patients with solid tumors and hematological malignancies (1-4). The chemical structures of gemcitabine and cytarabine are depicted in Figure 1.

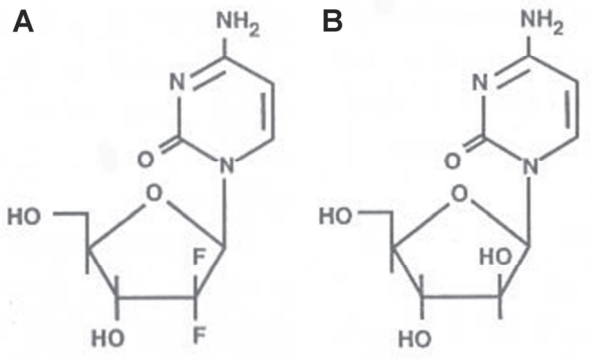

Figure 1. Chemical structure of the pyrimidine nucleosides gemcitabine (A) and cytarabine (B).

Gemcitabine is applied in the clinic either as single agent or in combination with chemotherapeutic agents (5) or radiotherapy (6). It is usually administered intravenously (i.v.) at a dose of 1000-1250 mg/m^2 as 30-min infusion on days 1 and 8 of a 21-day or days 1, 8, and 15 of a 28-day cycle. Preclinical studies in human tumor cell lines and xenografts showed that intracellular accumulation of gemcitabine triphosphate (dFdCTP), the active metabolite of gemcitabine, is dependent on the total exposure time and rate of administration of gemcitabine (7-10). Different gemcitabine dosing schedules have been investigated in the clinic (5). Standard gemcitabine infusion of 1000 mg/m^2 in 30 min (~33 mg/m^2/min) was shown to saturate deoxycytidine kinase (dCK) and intracellular formation of dFdCTP. Prolonged gemcitabine infusion at a fixed dose rate (FDR) of 10 mg/m^2/min was investigated to increase intracellular accumulation of dFdCTP, aiming to enhance antitumor activity of gemcitabine and the response rate in

patients. This FDR approach was derived from earlier studies on cytarabine that showed an increase in the AUC of cytarabine triphosphate (ara-CTP), the active metabolite of cytarabine, in leukemic cells of patients following prolonged infusion times of cytarabine (11, 12). The activity and toxicity of gemcitabine depends on the dose and dosing schedule (13, 14). In various randomized clinical trials, FDR administration was compared with standard 30-min infusion of gemcitabine. Up to date there are not yet sufficiently powered studies that demonstrate that FDR administration leads to a significantly improved treatment outcome in patients as opposed to standard gemcitabine infusion.

In the current review, we discuss the molecular pharmacology of nucleoside analogues and the influence of hNTs and dCK on the activity and toxicity of gemcitabine that is the basis for preclinical and clinical studies on FDR dosing as opposed to standard gemcitabine administration, of which trial results are summarized. These findings can be relevant for the optimal use of gemcitabine in patients in the future.

Molecular pharmacology of nucleoside anticancer drugs

Uptake by human nucleoside transporters

The nucleoside anticancer drugs gemcitabine and cytarabine are hydrophilic compounds. Their uptake into cells is largely dependent on the activity of human equilibrative nucleoside transporters (hENTs) and human concentrative nucleoside transporters (hCNTs) (15-18). The hENTs are capable of transporting pyrimidine and purine nucleosides from outside to inside the cell and vice versa, and are widely distributed in most human cells (19). The hCNTs transport substrates, such as pyrimidine and purine nucleosides, only from outside to inside the cell, and are highly expressed in liver (20), kidney (21, 22), and intestine (23, 24). hCNTs generally have a higher affinity for transport of nucleosides than hENTs (e.g. hCNT1 has a ten-fold higher affinity for gemcitabine than hENT1).

Metabolism: Activation and deactivation

Gemcitabine and cytarabine are phosphorylated by dCK into their corresponding monophosphate form, which is the rate-limiting step in the formation of their active triphosphate metabolite, which is incorporated into DNA, thereby inhibiting DNA

synthesis and DNA repair. Gemcitabine and cytarabine are extensively deaminated by cytidine deaminase (CDA) (7, 25) in liver, kidney, and plasma to their corresponding uracil metabolites 2',2'-difluorodeoxyuridine (dFdU) and arabinosyluracil (ara-U), respectively. These metabolites have much lower cytotoxicity compared to their parent compounds. Because of this rapid deamination, the elimination half-life ($t_{1/2}$) of gemcitabine and cytarabine is short, ranging between 10 and 30 min.

Mechanisms of action of gemcitabine

The chemical structures of dFdC, dFdU, and dFdCTP and the metabolic scheme and proposed pharmacological actions of gemcitabine and metabolites are depicted in Figure 2. dFdCTP, the main active metabolite of gemcitabine competes with deoxycytidine triphosphate (dCTP) for incorporation into DNA. Once dFdCTP is incorporated, two phosphate molecules are split off, leaving dFdCMP in the DNA chain. Once dFdCTP is incorporated into DNA, only one more natural deoxynucleoside triphosphate (dNTP) can be incorporated, after which DNA replication terminates. dFdCMP is resistant to removal from the DNA strand by proof-reading enzymes (i.e. polymerase ε), thus impairing its ability to repair the DNA strand, a mechanism also known as "masked-chain termination". In addition, gemcitabine diphosphate (dFdCDP) inhibits ribonucleotide reductase (RR) (26), thereby depleting dCTP pools and facilitating incorporation of dFdCTP into DNA. As depicted in Figure 2, gemcitabine has various self-potentiating mechanisms of action contributing to the maintenance of dFdCDP and dFdCTP levels for prolonged periods of time.

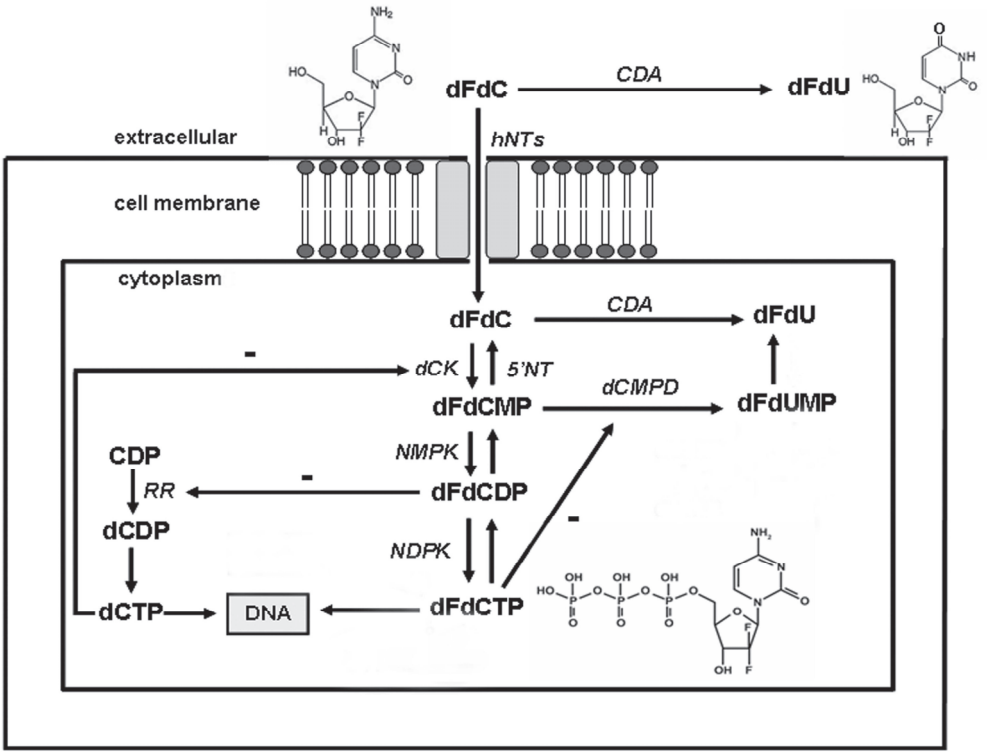

Figure 2. Chemical structures of dFdC, dFdU, and dFdCTP and metabolic scheme and proposed pharmacological mechanisms of action of gemcitabine and metabolites. dFdC is taken up by human nucleoside transporters (hNTs) into the cell. dFdC is intracellularly phosphorylated by deoxycytidine kinase (dCK) to its monophosphate (dFdCMP), and subsequently into its active diphosphate (dFdCDP) and triphosphate (dFdCTP) metabolites. dFdCTP is incorporated into deoxyribonucleic acid (DNA), thereby competing with deoxycytidine triphosphate (dCTP) for incorporation. dFdCDP inhibits ribonucleotide reductase (RR), which inhibits the conversion of cytidine diphosphate (CDP) to deoxycytidine diphosphate (dCDP) and inhibits synthesis of dCTP, leading to an elevation of the intracellular dFdCTP/dCTP ratio and into enhanced incorporation of dFdCTP into DNA. Since dCTP inhibits dCK, decreased dCTP pools can result in higher dCK activity and an increase in phosphorylation of dFdC to its active metabolites. dFdC is deaminated by cytidine deaminase (CDA) to 2',2'-difluorodeoxyuridine (dFdU). dFdCMP can be dephosphorylated to dFdC by 5´-nucleotidase (5´-NT) and deaminated to 2',2'-difluorodeoxyuridine monophosphate (dFdUMP) by deoxycytidylate deaminase (dCMPD). dFdCTP can inhibit dCMPD, which stimulates its own formation.

Preclinical pharmacology of gemcitabine

Nucleoside cytotoxicity

High intracellular accumulation of dFdCTP and incorporation into DNA is associated with increased sensitivity to gemcitabine in preclinical tumor models (9). Clonogenic survival assays demonstrated that the loss of cell viability increased with increasing gemcitabine concentrations and suggested intracellular retention of active gemcitabine metabolites for prolonged periods of time (27, 28). The elimination of dFdCTP was found to be dependent of the intracellular concentration of dFdCTP. Elimination of dFdCTP was linear with a $t_{1/2}$ of about 3.6 h at lower concentrations (< 50 μM) and became biphasic at higher dFdCTP concentrations (> 100 μM) with an initial $t_{1/2}$ of about 1 h, and an apparent terminal half-life of about 19 h in leukemic cells (10).

Intracellular accumulation of active metabolites and cytotoxicity of gemcitabine are influenced by multiple factors, such as by 1) the dosing schedule, 2) phosphorylation/activation (dCK), 3) cellular transport (hNTs), 4) degradation/inactivation (CDA), and by 5) genetic factors (e.g. single nucleotide polymorphisms in genes encoding for dCK and CDA) (29-32). In this review, we discuss the effect of the dosing schedule and the role of dCK and hNTs on the activity and toxicity of gemcitabine.

The importance of dCK

Phosphorylation of gemcitabine to dFdCMP by dCK was shown to be the rate-limiting step in the formation of dFdCTP (33, 34). The affinity of dCK is higher for gemcitabine than for cytarabine and other nucleoside anticancer drugs (e.g. cladribine and fludarabine) (35). The activity of dCK is an important factor in the overall cytotoxicity of gemcitabine. A2780 human ovarian carcinoma cell lines deficient in dCK were resistant to gemcitabine (36). Increased expression of dCK cDNA in HT-29 human colon carcinoma xenografts in nude mice positively correlated with enhanced dFdCTP accumulation and with the antitumor activity of gemcitabine (37).

The importance of hNTs

Transport of gemcitabine occurs particularly by hCNT1, hENT1, and hENT2 (18, 38, 39) and is saturable (40). Sensitivity to gemcitabine positively correlated with the expression of hENT1 (41) and hENT1-deficient cells were highly resistant to cytotoxicity by gemcitabine and cytarabine (42-44). Inhibitors of nucleoside transporters, such as nitrobenzylmercaptopurine riboside (NBMPR), a specific hENT1-inhibitor at low nanomolar concentrations, and dipyridamole, a hENT1/2 inhibitor, reduced sensitivity to gemcitabine by 39- and 1800-fold (18). hENT1 transports gemcitabine with high affinity and low capacity, whereas, hENT2 transports gemcitabine with low affinity and high capacity (40). Restoration of hCNT1 activity in human pancreatic cancer cells positively correlated with the cytotoxicity of gemcitabine (45).

Clinical pharmacology of gemcitabine

Gemcitabine is generally administered as a standard 30-min infusion at a dose of 1000 mg/m^2 once weekly for 3 weeks at a 4-weekly cycle. Following i.v. administration, gemcitabine has a short $t_{1/2}$ (~ 8-20 min) due to rapid deamination to dFdU (46), which has a long $t_{1/2}$ (~ 50 h) and is largely excreted in the urine (47). dFdCTP peak concentrations were obtained within 30 min of the end of infusion, and dFdCTP elimination was linear at low concentrations, and became biphasic at high concentrations in leukemic and blood mononuclear cells (46, 48, 49). The long retention time of dFdCTP likely contributes to the fact that gemcitabine has activity against both rapidly proliferating, as well as slowly dividing tumors.

dCK and intracellular levels of nucleoside triphosphates

Gemcitabine was shown to be a good substrate for phosphorylation by dCK having a K_m value of 5-10 μM (50, 51). Inhibition of the reaction was shown at higher substrate concentrations (50). Therefore, it was expected that the rate of phosphorylation became saturated at gemcitabine concentrations above 20 μM, with a negative effect on phosphorylation at higher levels. Clinical pharmacokinetic studies strongly suggested that the rate of intracellular accumulation of dFdCTP was saturated at gemcitabine concentrations of 15-20 μM

in plasma (46, 52), which were achieved with gemcitabine infusions at a dose rate of 8 to 10 mg/m^2/min (52). Standard 30-min infusion of gemcitabine at doses of 800-2600 mg/m^2 generates gemcitabine plasma concentrations of 20-60 μM, which exceeds levels at which the formation of dFdCTP becomes saturated (46, 49), and which may also inhibit the process of phosphorylation of gemcitabine (50). Consequently, cells are not able to phosphorylate a substantial portion of the infused drug and the main portion of gemcitabine is deaminated to dFdU. These findings suggested that dose schedules resulting in gemcitabine plasma concentrations of 15-20 μM were optimal to achieve maximal intracellular dFdCTP levels. Additionally, maximal accumulation of dFdCTP was likely achieved by more prolonged infusions at a dose rate that resulted in maintenance of a gemcitabine plasma concentration that saturated the formation of gemcitabine nucleotides.

The formation of ara-CTP was also saturable during high dose cytarabine therapy at cytarabine plasma concentrations above 10 μM (53-55). Exposure to ara-CTP in acute leukemic blasts positively correlated with response following administration of cytarabine either at an intermittent schedule (56) or by continuous infusion. Non-linear elimination of ara-CTP was observed at high dose regimens of cytarabine, corresponding to plasma concentrations above 100 μM (57-59).

The role of hNTs in the cytotoxicity of nucleosides

In 21 patients with pancreatic cancer treated with gemcitabine, hENT1 expression levels correlated with median overall survival (OS). Patients with high expression levels of hENT1 had a significantly longer OS of 25.7 months (95% CI: 17.6-33.7 months) compared to the OS of 8.5 months (95% CI: 7.0-9.9 months) in patients with low levels of hENT1 (60). Additionally, characterization of gene expression patterns in tumor specimens of 102 patients with pancreatic cancer revealed that patients with high expression of hENT1 had a significantly longer OS of 25.7 months compared with 12.4 months in patients with low transcription levels ($p < 0.001$) (61).

Prolonged infusion of gemcitabine (1200-2800 mg/m^2) at a FDR of 10 mg/m^2/min was safe and resulted in cumulative myelotoxicity with a lower maximum tolerated dose (MTD) compared to standard 30-min gemcitabine infusion (62). Prolonged gemcitabine infusion at low dose-levels (300 mg/m^2 in 6 h) was associated with

more pronounced non-hematological toxicity (e.g. ALT/AST elevations) (63, 64). This might be due to more pronounced accumulation of gemcitabine into the liver (high hCNT1 expression) compared to other tissues. Because of the higher affinity of hCNT1 than hENT1 for gemcitabine, prolonged infusion of gemcitabine at a low dose-level might allow selective uptake of gemcitabine into tumor cells with high expression of hCNT1, while sparing bone marrow cells that predominantly contain hENTs.

Intracellular accumulation of ara-CTP in leukemic cells of patients was limited and directly correlated with the number of membrane nucleoside transporters at low (< 1 μM) cytarabine concentrations (65-67) after low dose cytarabine therapy (100-200 mg/m^2/day) (68, 69). Concordant with these findings, patients with AML who did not respond to cytarabine therapy (100-200 mg/m^2/day) demonstrated low cytarabine uptake and low numbers of NBMPR binding sites in leukemic blasts (70). Thus, at low cytarabine plasma concentrations, transport of cytarabine by hNTs is the rate-limiting step, whereas at high cytarabine concentrations, intracellular phosphorylation of cytarabine by dCK becomes the rate-limiting step in the formation of ara-CTP.

Co-administration of an inhibitor of hENT1 to cytarabine enhanced its cytotoxicity towards cells that co-expressed hENTs and hCNTs, which was explained by inhibition of efflux of cytarabine by hENT1, and enhanced intracellular uptake by hCNT1.

Concept of FDR dosing of gemcitabine

Gemcitabine plasma concentrations of 20-60 μM are achieved following a standard 30-min infusion of gemcitabine 1000-1200 mg/m^2, which exceeds the levels of 15-20 μM at which dCK becomes saturated (46, 48, 49, 51). Prolongation of the duration of infusion of gemcitabine at lower dose-levels might increase the intracellular concentration of dFdC. In addition, it leads to the maintenance of plasma gemcitabine concentrations at levels at which dCK is saturated for prolonged periods of time, which increases intracellular accumulation of dFdCTP (48, 71). This strategy was hypothesized to result in a higher antitumor activity of gemcitabine in patients. Clinical studies on prolonged administration of gemcitabine at a FDR (e.g. 10 mg/m^2/min) compared to standard 30-min infusion (e.g. 30 mg/m^2/min) will be discussed in the next chapters.

Phase I/II dose finding studies investigating prolonged (FDR) and standard infusion of gemcitabine

Grunewald and co-workers demonstrated in a small subset of patients that prolongation of the infusion duration of gemcitabine at a dose of 800 mg/m^2 increased the AUC of dFdCTP in leukemic cells (Table 1) (48). In a dose-escalating study (10-1000 mg/m^2 gemcitabine) they showed that prolonged 60-min dosing of 800 mg/m^2 (~ 400 mg/m^2 in 30 min), resulting in plasma gemcitabine concentrations of 20 μM, led to a 4-fold increase in AUC of dFdCTP compared to 30-min infusion of 790 mg/m^2, after which gemcitabine concentrations of 60 μM were obtained (49). No significant increase in the AUC for dFdCTP was observed at gemcitabine plasma concentration above 20 μM (49). In a different dose-escalating study with gemcitabine (10-1000 mg/m^2), Abbruzzese and colleagues demonstrated that after the end of a 30-min infusion, plasma levels of gemcitabine decreased rapidly ($t_{1/2}$ ~ 8 min) due to deamination to dFdU (46). Both the rate of accumulation (μM/h) and the maximum concentration (μM) of dFdCTP in mononuclear cells increased with the gemcitabine dose up to 350 mg/m^2, corresponding with gemcitabine plasma concentrations of 15-20 μM, without further increase at higher dose-levels, suggesting saturation of the intracellular formation of dFdCTP (46). Administration of gemcitabine (1200-6400 mg/m^2) at a FDR of 10 mg/m^2/min resulted in a linear increase in the AUC of dFdCTP with the infusion time and with the dose (52). Additionally, inhibition of DNA synthesis in circulating blasts increased proportionally with the AUC of dFdCTP. A study by Touroutoglou and colleagues showed that FDR gemcitabine (1200-2800 mg/m^2) was safe and well tolerated (62). Once-weekly administration of gemcitabine for 7 weeks of a 8-weekly cycle and FDR dosing of 1000 mg/m^2 in 150 min demonstrated that intracellular levels of dFdCTP in PBMCs increased linearly with the infusion duration (72). The C_{max} of dFdCTP was 1.4-fold higher after FDR compared to standard gemcitabine administration. Similarly, Gandhi and colleagues demonstrated that levels of dFdCTP in AML blasts increased linearly with the infusion time following FDR gemcitabine dosing (73). An abrupt decrease in DNA synthesis to values of 5-20% of the pre-treatment value at 1 h after infusion was observed and DNA synthesis remained inhibited until 24 h after start

of infusion. Moreover, dATP pools decreased during gemcitabine infusion up to 24 h after start of infusion. Bengala and co-workers found that FDR gemcitabine infusion in patients with advanced pancreatic adenocarcinoma resulted in a median time to progression (TTP) of 4.8 months, a median OS of 7 months, and a 1-year survival rate (SR) of 21.9% (74). The AUC of dFdU, the main deaminated metabolite of gemcitabine, and OS significantly correlated with the expression and activity of cytidine deaminase ($p < 0.05$). Studies on prolonged infusion of gemcitabine during 3, 4, 6, and 24 h at low dose-levels in patients with advanced solid tumors found low MTD values between 180 and 450 mg/m^2 (75-78). Besides treatment with single agent gemcitabine, FDR infusion of gemcitabine has been investigated in combination with other chemotherapeutic agents, such as carboplatin and cisplatin. Soo and colleagues found that combination therapy of carboplatin (AUC = 5 mg/ml*min) with gemcitabine administered as 75-min infusion at a dose of 750 mg/m^2 was active and tolerable in patients with NSCLC and resulted in plasma gemcitabine concentrations above 10 μM (79). Others found that combination of carboplatin (AUC = 5 mg/ml*min) with gemcitabine administered as 120-min infusion at a dose of 1200 mg/m^2 resulted in a median TTP of 7.0 months and an OS of 12.0 months (80). The gemcitabine concentration at the end of infusion correlated positively with the percentage reduction in leukocytes and platelets. Prolonged infusion of gemcitabine (120-250 mg/m^2) over 6 h with cisplatin 75 mg/m^2 had an acceptable toxicity profile (81). Median TTP was 6 months and the 1-year SR was 40%. Prolonged gemcitabine infusion over 96 h at doses between 1 and 25 mg/m^2/day resulted mainly in non-hematological toxicities (e.g. mucositis, fever, rash) in contrast to studies with shorter infusion durations (< 2 h), predominantly resulting in myelotoxicity (82).

Table 1. Summary of phase I/II dose finding studies on prolonged FDR and standard infusion of gemcitabine.

Tumor Type	n	P	Dose schedule	Intracellular dFdCTP	Toxicity	MTD	Response	Reference
Leukemia	4	I	800 mg/m^2 in 1 h (13 mg/m^2/min) 800 mg/m^2 in 2 h (7 mg/m^2/min) 800 mg/m^2 in 3 h (4 mg/m^2/min) d 1, 8, 15 q 4w	Median AUC (range): 140 (66-252) h*µM (n = 4) Median AUC (range): 217 (129-1012) h*µM (n = 4) Median AUC (range): 432 (430-435) h*µM (n = 2)	Thrombocytopenia was observed in 2 patients with chronic lymphocytic leukemia after the first two infusion schedules of 1 h and 2 h (G, not further specified)	NR	NR	Grunewald et al. [48]
Solid; various types	29	I	790 mg/m^2 in 0.5 h (26 mg/m^2/min) 800 mg/m^2 in 1 h (13 mg/m^2/min) d 1, 8, 15 q 4w	Median AUC (range): 19 (19-23) h*µM (n = 3) Median AUC (range): 98 (55-174) h*µM (n = 5)	NR	NR	NR	Grunewald et al. [49]
Solid; various types	50	I	22.5, 35, 53 , 80 ,120, 180, 225, 350, 525, 790 , 1000 mg/m^2 in 0.5 h (0.8-33 mg/m^2/min) d 1, 8, 15 q 4w	C_{max}: 18-284 µM, C_{max} increased with dose (no statistical significance and no dFdCTP AUC values were reported)	DLT was myelosuppression: G 3/4 thrombocytopenia, G 3 anemia, G 3 granulocytopenia at 525, 790, and 1000 mg/m^2 with somewhat higher incidence at higher doses Rash (n = 5) at 525 mg/m^2 and higher dose-levels N/V and anorexia were mild and appeared not to be dose-dependent	790 mg/m^2	PR 2/47 (4%)	Abbruzesse et al. [46]
Leukemia	22	I	1200, 1500, 2400, 3600, 4800, 6400 mg/m^2 (10 mg/m^2/min) d 1, 8, 15 q 4w	AUC: 11-7217 h*µM, AUC increased with dose (no statistical significance reported)	G 3 thrombocytopenia with pulmonary hemorrhage (n = 1) at 2400 mg/m^2 G 4 skin ulceration (n = 1) and G 4 mucositis (n = 1) at 6400 mg/m^2 G 1/2 N/V (n = 6), mucositis and stomatitis seemed to be dose-dependent (n, G, and dose-levels not further specified)	4800 mg/m^2	No CR observed	Grunewald et al. [52]

Table 1. Continued.

Tumor Type	n	P	Dose schedule	Intracellular dFdCTP	Toxicity	MTD	Response	Reference
Solid; various types	31	I	1200, 1500, 1800, 2250, and 2800 mg/m^2 (10 mg/m^2/min) d 1, 8, 15 q 4w	NR	G 3/4 granulocytopenia, G 3 thrombocytopenia at dose-levels of 1500-2800 mg/m^2, without major differences in incidence and severity All dose-levels could safely be administered during the first course, however, there appeared to be cumulative myelosuppression	2250 mg/m^2	CR 1/30 (3%) PR 2/30 (7%)	Touroutoglou et al. [62]
Soft tissue sarcoma	56	II	1000 mg/m^2 in 0.5 h (33 mg/m^2/min) 1000 mg/m^2 in 2.5 h (~6.7 mg/m^2/min) d 1, 8, 15, 22, 29, 36, 42 q 8w	Median C_{max} (range): 120 (50-310) µM (n = 9) Median C_{max} (range): 170 (65-445) µM (n = 7) Median C_{max} = 1.4-fold higher after FDR dosing (p = 0.016)	Mainly G 3/4 neutropenia (n = 6), G 3/4 thrombocytopenia (n = 5), G 3 anemia (n = 2), G 3 ALT (n = 2), and G 1/2 fatigue (n = 11)	NR	PR 7/39 (18%) Survival = 13.9 months	Patel et al. [72]
Acute myeloid leukemia	19	I	4800, 6000, 7200 9240, 10,800 mg/m^2 (10 mg/m^2/min) d 1 q 3-4w	C_{max}: 133-970 µM (high interpatient variability likely due to inability of the cells to accumulate dFdCTP because of variation in phosphorylation of gemcitabine to dFdCTP)	G2/3 mucositis at all dose-levels G2 diarrhea at 7200 mg/m^2 G2 N/V at 7200, 9240, and 10,800 mg/m^2 G3 rash at 9240, 10,800 mg/m^2	~ 7200-9240 mg/m^2	PR 1/19 (5%)	Gandhi et al. [73]
Advanced pancreatic cancer	23	I	3000-7000 mg/m^2 in 5-11.7 h (10 mg/m^2/min) d 1, q 2w	NR	G 4 mucositis at 7000 mg/m^2 Other toxicities were: G 3/4 neutropenia, G 3 anemia, G 3 thrombocytopenia, G 2 diarrhea, G 2 fever (n, and dose-levels not specified)	6500 mg/m^2	CR 1/18 (6%) PR 3/18 (17%) SD 7/18 (39%) TTP = 4.8 months OS = 7 months 1-year SR = 1.9%	Bengala et al. [74]

Table 1. Continued.

Tumor Type	n	P	Dose schedule	Intracellular dFdCTP	Toxicity	MTD	Response	Reference
NSCLC	24	I	10, 20, 40, 80, 120, 180, 210 mg/m^2 in 24 h (0.007-0.15 mg/m^2/min) d 1, 8, 15 q 4w	NR	G 2/3 leucopenia, G 2 neutropenia, G2 anemia, G 3 N/V, G 2 ALT, G 2/3 lethargy, and G 2/3 mucositis, which seemed to increase in severity and incidence with dose	180 mg/m^2	PR 5/24 (21%)	Anderson et al. [75]
Solid; various types	47	I	300 mg/m^2 in 0.5 h, 1 h, 2 h, 3 h, 4.5 h, and 6 h 875 mg/m^2 in 0.5 h, and 1 h (0.8-29 mg/m^2/min) d 1, 8, 15 q 4w	NR	DLT: leucopenia at 6 h infusion schedule of which the severity increased with duration of infusion No DLTs, however incidence of leucopenia was higher at the 1 h compared to the 0.5 h schedule G 2/3 AST/ALT elevations increased with the infusion duration	300 mg/m^2 in 6 h	PR 8/47 (17%)	Pollera et al. [63]
Breast cancer	16	I	200, 250, and 300 mg/m^2 in 6 h (0.56-0.83 mg/m^2/min) d 1, 8, 15 q 4w	NR	Myelosuppression was generally mild at all dose-levels and consisted mainly of neutropenia. Elevations in liver transaminases was the predominant non-hematological toxicity and tended to occur earlier and with increased intensity at higher dose-levels and at higher cumulative dosis	250 mg/m^2	CR 1/16 (6%) PR 1/16 (6%) SD 7/16 (44%)	Akrivakis et al. [78]
Solid; Various types	27	I	300, 400, 450, and 500 mg/m^2 in 3 h (1.7-2.8 mg/m^2/min) d 1, 8, 15 q 4w	NR	Myelosuppression appeared to be the most common toxicity with an increase in incidence with dose	450 mg/m^2	NR	Maurel et al. [76]
Solid tumors; various types	21	I	350 mg/m^2 400 mg/m^2 450 mg/m^2 in 4 h (1.5-1.9 mg/m^2/min)	NR	0 DLTs 2 DLTs; G 4 thrombocytopenia and G 3 mucositis (n = 1), G 3 AST/ALT (n = 1) 4 DLTs; G 4 neutropenia (n = 1), G 3 ALT (n = 1), G 4 thrombocytopenia (n = 2)	400 mg/m^2	PR 2/16 (13%) SD 5/16 (31%)	Schmid et al. [77]

Table 1. Continued.

Tumor Type	n	P	Dose schedule	Intracellular dFdCTP	Toxicity	MTD	Response	Reference
NSCLC	15	I	600 mg/m^2 in 1 h (n = 3) 750 mg/m^2 in 1.25 h (n = 6) 900 mg/m^2 in 1.5 h (n = 6) (10 mg/m^2/min) d 1, 8 q 3w	NR	0 DLTs DLTs; G 3 neutropenia (n = 1) DLTs; G 3 liver failure (n = 1), G 3 thrombocytopenia (n = 1)	900 mg/m^2	PR 2/10 (20%) SD 5/10 (50%)	Soo et al. [79]
NSCLC	23	II	1200 mg/m^2 in 2 h (10 mg/m^2/min) *plus carboplatin (AUC 5)* d 1, 8 q 3w	NR	Main toxicities were G 3/4 thrombocytopenia (n = 9), G 3/4 neutropenia (n = 7), and G 3/4 anemia (n = 6) Main non-hematological toxicities were G 4 elevated AST (n = 1) G 3 rash (n = 1), and G 1/2 alopecia (n = 12)	NR	PR 10/21 (48%) SD 7/21 (33%) TTP = 6 months 1-year SR = 40%	Wang et al. [80]
NSCLC	61	I/ II	130-210 mg/m^2 in 6 h (n = 21) 250 mg/m^2 in 6 h (n = 40) (< 0.4-0.7 mg/m^2/min) *plus cisplatin (75 mg/m^2)* d 1, 8 q 3w	NR	No DLTs Mainly anemia, neutropenia and alopecia of which the incidence and/or severity was higher at the dose level of 250 mg/m^2 compared to the lower dose-levels.	NR	CR 1/61 (2%) PR 27/61 (44%) SD 20/61 (33%)	Zwitter et al. [81]
Advanced solid tumors and lymphoma	34	I	1, 2, 4, 6, 7, 8, 9, 10, 15, 20, and 25 mg/m^2/d as 96 h infusion (< 0.2 mg/m^2/min) d 1, q 2w or 3w	NR	Myelosuppression was uncommon. DLTs were dyspnea, mucositis, fever, and hypotension at dose-levels of 10-25 mg/m^2/d.	~24 mg/m^2 q 2w or 32 mg/m^2 q 3w	SD 6/34 (18%)	Rajdev et al. [82]

n, number of patients; P, phase of the study; DLTs, dose-limiting toxicities; MTD, maximum tolerated dose; dFdCTP, gemcitabine triphosphate; C_{max}, maximum concentration; AUC, area under the concentration-time curve; G, CTC Grade (calculated based on CTC criteria version 3.0, when data were given as number of cells/mm^3); N/V, nausea/vomiting; ALT, alanine transaminase; AST, aspartate transaminase; NSCLC, non-small cell lung cancer; CR, complete response; PR, partial response; SD, stable disease; TTP, time to progression; OS, overall survival; SR, survival rate; NR, not reported. Toxicities ≥ CTC Grade 2 are reported.

Phase II/III randomized trials comparing FDR with standard dosing of gemcitabine

A study in 48 Asian patients with unresectable hepatocellular carcinoma treated with first-line single agent gemcitabine 1250 mg/m^2 either as 30-min or FDR infusion in 2 h resulted in a TTP and median OS of 46 and 97 days, respectively, without statistically significant differences in response and toxicity between the two treatment schedules (83) (Table 2). A randomized phase II study by Tempero et al. in 92 patients with pancreatic cancer compared standard infusion (2200 mg/m^2 in 30 min) with FDR infusion (1500 mg/m^2 in 150 min) of gemcitabine (84). The dose-levels for each dosing regimen were based on the established MTD for gemcitabine in previous studies (62, 85, 86), which permitted comparison of clinical responses at equitoxic gemcitabine doses between both dosing schedules. They found that the concentration of dFdCTP in PBMCs increased linearly with the infusion time up to 188 μM at the end of the 150-min infusion, while infusion of the higher dose in 30-min resulted in a plateau in dFdCTP concentration of 103 μM at 1 hour after the end of infusion. However, no AUC values of dFdCTP were reported. The 1- and 2-year SR was significantly higher following FDR compared to standard gemcitabine infusion ($p = 0.007$; Table 2). Furthermore, OS was improved for patients in the FDR arm compared to the standard arm (5.0 vs. 8.0 months, $p = 0.013$), but time to treatment failure (TTF), their primary endpoint, was similar between standard and FDR infusion of gemcitabine (1.8 vs. 2.0 months, $p = 0.09$). The fact that the difference in OS was not statistically significant may be due to insufficient power of the study. It was surprising that the advantage in survival in the FDR group was not accompanied by an improvement in TTF. According to the authors, TTF may not be a good predictor for survival benefit, because this endpoint may be influenced by other factors, such as poor tolerance to therapy and clinical deterioration. Furthermore, twice as much patients in the FDR arm compared to the standard arm received second-line chemotherapy, which might have influenced survival. On the other hand, possibly more patients receiving FDR gemcitabine were able to proceed to second-line treatment based on a better performance status. Patients receiving FDR infusion experienced more hematological toxicities than patients treated with standard gemcitabine; grade 3/4

thrombocytopenia (37.2% vs. 10.2%), neutropenia (48.8% vs. 26.5%), and grade 4 anemia (9.3% vs. 2%). In summary, although the results have to be interpreted carefully, the pharmacological and clinical findings of the study supported a FDR infusion strategy for gemcitabine.

A randomized phase II study by Soo and colleagues, investigating combination therapy of carboplatin (AUC = 5 mg/ml*min) with either standard 30-min infusion or FDR gemcitabine (750 mg/m^2 over 75 min), demonstrated that the mean C_{max} of gemcitabine in plasma was significantly lower following FDR infusion (21 μM) compared to standard infusion (41 μM) (87). The mean AUC of dFdCTP in blood mononuclear cells, however, was comparable between both dosing schedules (Table 2). Furthermore, TTP, OS, 1-year SR, and hematological toxicity were comparable between both treatment arms (Table 2). A randomized phase II study by Cappuzzo and colleagues demonstrated no significant differences in response rate (RR), and OS between FDR and standard gemcitabine dosing (88). However, FDR dosing resulted in a higher incidence of grade 3/4 neutropenia compared to standard infusion of gemcitabine (49.2% vs. 17.9%, $p < 0.001$). A randomized phase II study in patients with advanced NSCLC treated with cisplatin 80 mg/m^2 plus gemcitabine, resulted in a median TTP of 6 months (range: 1-26 months) and 8 months (range: 2-21 months) following standard and FDR infusion of gemcitabine, respectively (89). Median OS was 13 months for both treatment schedules, which were tolerated with cumulative incidence of grade 3/4 neutropenia and thrombocytopenia of 27% and 15%, respectively. Recently, a phase III randomized trial assessed whether prolonged infusion of gemcitabine (1200 mg/m^2 in 120 min) could improve OS in patients with advanced NSCLC compared to first-line treatment with cisplatin 80 mg/m^2 plus gemcitabine 1200 mg/m^2 as 30-min infusion. Prolonged administration of gemcitabine did not improve OS, but resulted in more pronounced vomiting and fatigue (90).

Table 2. Summary of Phase II/III randomized studies comparing prolonged FDR with standard infusion of gemcitabine.

Tumor Type	n	P	Dose schedule	Intracellular dFdCTP	Toxicity	Response	Reference
Hepatic cancer	25	II Randomized	1250 mg/m^2 in 0.5 h (42 mg/m^2/min)	NR	44% G 3/4 hematological and 76% non-hematological toxicity	PR 1/25 (4%)	Guan et al. [83]
In total 50 patients were enrolled; 2 patients did not receive study treatment	23		1250 mg/m^2 in 2 h (10 mg/m^2/min) d 1, 8 q 3w		35% G3/4 hematological and 52% non-hematological toxicity No statistical differences between the treatment arms	No PR observed No significant difference in OS between both schedules	
Pancreatic cancer	49	II Randomized	2200 mg/m^2 in 0.5 h (73 mg/m^2/min)	Median C_{max} (range): 188 (44-533) µM	G 3/4 neutropenia (26.5%), G 3/4 thrombocytopenia (10.2%), G 4 anemia (2%)	PR 2/49 (4%) OS = 5 months 1-year SR = 9% 2-year SR = 2% TTF = 1.8 months	Tempero et al. [84]
No reason for the difference in number of patients between the two arms was given	43		1500 mg/m^2 in 2.5 h (10 mg/m^2/min) d 1, 8, 15 q 4w	Median C_{max} (range): 398 (111-682) µM	G 3/4 neutropenia (48.8%), G 3/4 thrombocytopenia (37.2%), G 4 anemia (9.3%)	PR 1/43 (2%) OS = 8 months 1-year SR = 29% 2-year SR = 18% TTF = 2.1 months TTF: p = 0.09 OS: p = 0.013 2-year SR: p = 0.007	
NSCLC	38	II Randomized	1000 mg/m^2 in 0.5 h (33 mg/m^2/min)	Mean AUC (± SD): 585 ± 304 h*µM	G 3/4 anemia (31%), G 3/4 neutropenia (68%), G 3/4 thrombocytopenia (59%)	PR 16/38 (42%) OS = 9.6 months 1-year SR = 36% TTP = 5.2 months	Soo et al. [87]
	38		750 mg/m^2 in 1.25 h (10 mg/m^2/min) *Plus carboplatin* d 1, 8 q 3w	Mean AUC (± SD): 537 ± 188 h*µM	G 3/4 anemia (33%), G 3/4 neutropenia (75%), G 3/4 thrombocytopenia (52%) No significant differences observed	PR 13/38 (34%) OS = 7.0 months 1-year SR = 32% TTP = 5.3 months No significant differences observed	

Table 2. Continued.

Tumor Type	n	P	Dose schedule	Intracellular dFdCTP	Toxicity	Response	Reference
NSCLC In total 121 patients were enrolled; 4 patients did not receive study treatment	56	II Randomized	1500 mg/m^2 in 0.5 h (50 mg/m^2/min)	NR	G 3/4 neutropenia (17.9%), G 3 leucopenia (10.7%), G 3 anemia (5.4%), pulmonary toxicity (12.5%)	CR 1/56 (2%) PR 8/56 (14%) SD 24/56 (43%) Overall RR = 16% TTP = 4 months 1-year SR = 42.6% OS = 9 months	Cappuzzo et al. [88]
	61		1500 mg/m^2 in 2.5 h (10 mg/m^2/min) d 1, 8 q 3w		G 3/4 neutropenia (49.2%), G 3/4 leucopenia (31.2%), G 3 anemia (3.3%), G 3/4 paresthesias (4.9%), pulmonary toxicity (3.3%) ANC: p = 0.0002	PR 6/61 (10%) SD 31/61 (51%) Overall RR = 10% TTP = 4.5 months 1-year SR = 39% OS = 9 months No significant differences observed	
NSCLC	57	II Randomized	1000 mg/m^2 in 0.5 h	NR	G 3/4 neutropenia (24%), G 3/4 thrombocytopenia (11%), G 3/4 anemia (2%)	PR 15/57 (26%) SD 19/57 (33%) TTP = 6 months OS = 13 months 1-year SR = 52%	Ceribelli et al. [89]
	56		1000 mg/m^2 in 1.7 h (10 mg/m^2/min) *Plus cisplatin* d 1, 8, 15 q 4w		G 3/4 neutropenia (30%), G 3/4 thrombocytopenia (18%), G 3/4 anemia (11%) No significant differences observed	PR 19/55 (34%) SD 15/55 (27%) TTP = 8 months OS = 13 months 1-year SR = 51% No significant differences observed	
NSCLC	200	III Randomized	1200 mg/m^2 in 0.5 h	NR	No significant differences were noted in the occurrence and severity of the majority of all toxicities	CR 3/200 (2%) PR 64/200 (32%) SD 51/200 (26%) TTP = 5.5 months OS = 11 months Overall RR = 34%	Gridelli et al. [90]
	200		1200 mg/m^2 in 2 h *Plus cisplatin* d 1, 8 q 3w		G 2/3/4 vomiting occured more frequently in the prolonged infusion schedule (28%) as opposed to the standard schedule (18%)	CR 2/200 (1%) PR 55/200 (28%) SD 62/200 (31%) TTP = 5.8 months OS = 12 months Overall RR = 29% No significant differences observed	

n, number of patients; P, phase of the study; dFdCTP, gemcitabine triphosphate; C_{max}, maximum concentration; AUC, area under the concentration-time curve; G, CTC Grade (calculated based on CTC criteria version 3.0, when data were given as number of cells/mm^3); NSCLC, non-small cell lung cancer; RR, response rate; CR, complete response; PR, partial response; SD, stable disease; TTP, time to progression; TTF, time to treatment failure; OS, overall survival; SR, survival rate; NR, not reported. Toxicities ≥ CTC Grade 2 are reported.

Discussion and future perspectives

In summary, various clinical studies have shown that prolonged i.v. gemcitabine administration over 1-24 h at lower rates of infusion (< 30 mg/m^2/min) can be safely administered and has remarkable antitumor activity in patients with advanced solid tumors. Overall, there was a trend that prolonged infusion of gemcitabine resulted in a somewhat higher degree of non-hematological toxicity (e.g. elevations in transaminases) compared to standard 30-min infusion, after which myelosuppression was the most common toxicity. The FDR strategy (e.g. 10 mg/m^2/min) resulted in gemcitabine plasma concentrations at levels at which dCK becomes saturated for prolonged periods of time and led to higher AUC values of dFdCTP in mononuclear and leukemic cells compared to standard gemcitabine infusion (e.g. 33 mg/m^2/min). Concordant with these findings, one would expect FDR gemcitabine to result into higher concentrations of dFdCTP in solid tumors of patients. However, *in vivo* metabolism and/or transport of gemcitabine might be somewhat different between blood mononuclear, leukemic, and solid tumor cells, for example due to differences in expression of metabolic enzymes and hNTs. Thus far, not many studies have determined dFdCTP concentrations in tumor tissue following gemcitabine therapy. A study in 30 patients with head and neck cancer treated with i.v. gemcitabine (50-300 mg/m^2) over 30 min, resulted in dFdCTP concentrations of 733-3817 pmol/g tumor biopsy, which was suggested to produce potent radiosensitization based on *in vitro* studies (91). In a phase I trial in 52 patients with refractory solid cancers, 30-min infusion of gemcitabine 1500 mg/m^2 resulted in 70 pmol dFdCTP/g wet weight tumor biopsy of patients with head and neck cancer (n = 2) (92).

Overall, clinical studies provide pharmacological evidence for an advantage of prolonged FDR dosing above standard 30-min infusion of gemcitabine, based on the increase in dFdCTP exposure in blood mononuclear cells, which could be used to further optimise gemcitabine treatment. Thus far, only the study by Tempero and co-workers demonstrated an advantage of FDR infusion as opposed to standard gemcitabine in terms of survival of patients. Recently, a phase III study compared OS of standard gemcitabine 1000 mg/m^2/30 min once weekly x 7 weeks over 56 days followed by once weekly x 3 weeks every 28 days (A) versus FDR gemcitabine 1500 mg/m^2/150 min once weekly x 3 weeks every 28 days (B) or

FDR gemcitabine 1000 mg/m^2/100 min on day 1 + oxaliplatin 100 mg/m^2 on day 2 every 14 days (C) in 750 patients with advanced metastatic cancer (93). An interim analysis showed a median OS of 4.96, 6.01, and 6.47 months for arm A, B, and C, respectively without significant differences between the three treatment arms. In general, pancreatic cancer is an unresponsive disease and other anticancer drugs than gemcitabine are needed for the treatment of this type of cancer. New well powered randomized clinical studies are warranted to establish the optimal dose and infusion duration of gemcitabine providing the greatest antitumor activity with acceptable toxicity in other types of cancer than pancreatic cancer. Furthermore, future studies should assess relationships between the exposure to dFdCTP in PBMCs and solid tumors following prolonged FDR and standard gemcitabine therapy. These studies should prove whether prolonged FDR gemcitabine dosing is a better treatment option compared to standard gemcitabine.

References

1 Rustum YM, Raymakers RA. 1-Beta-arabinofuranosylcytosine in therapy of leukemia: preclinical and clinical overview. Pharmacol Ther 1992;56:307-321.

2 Abratt RP, Bezwoda WR, Falkson G, et al. Efficacy and safety profile of gemcitabine in non-small-cell lung cancer: a phase II study. J Clin Oncol 1994;12:1535-1540.

3 Rizzieri DA, Bass AJ, Rosner GL, et al. Phase I evaluation of prolonged-infusion gemcitabine with mitoxantrone for relapsed or refractory acute leukemia. J Clin Oncol 2002;20:674-679.

4 Perez-Manga G, Lluch A, Alba E, et al. Gemcitabine in combination with doxorubicin in advanced breast cancer: final results of a phase II pharmacokinetic trial. J Clin Oncol 2000;18:2545-2552.

5 Van Moorsel CJ, Peters GJ, Pinedo HM. Gemcitabine: Future Prospects of Single-Agent and Combination Studies. The Oncologist 1997;2:127-134.

6 Pauwels B, Korst AE, Lardon F, et al. Combined modality therapy of gemcitabine and radiation. The Oncologist 2005;10:34-51.

7 Plunkett W, Huang P, Xu YZ, et al. Gemcitabine: metabolism, mechanisms of action, and self-potentiation. Semin Oncol 1995;22:3-10.

8 Plunkett W, Huang P, Gandhi V. Preclinical characteristics of gemcitabine. Anticancer Drugs 1995;6:7-13.

9 Ruiz van Haperen VW, Veerman G, Boven E, et al. Schedule dependence of sensitivity to 2',2'-difluorodeoxycytidine (Gemcitabine) in relation to accumulation and retention of its triphosphate in solid tumour cell lines and solid tumours. Biochem Pharmacol 1994;48:1327-1339.

10 Heinemann V, Xu YZ, Chubb S, et al. Cellular elimination of 2',2'-difluorodeoxycytidine 5'-triphosphate: a mechanism of self-potentiation. Cancer Res 1992;52:533-539.

11 Heinemann V, Estey E, Keating MJ, et al. Patient-specific dose rate for continuous infusion high-dose cytarabine in relapsed acute myelogenous leukemia. J Clin Oncol 1989;7:622-628.

12 Plunkett W, Liliemark JO, Estey E, et al. Saturation of ara-CTP accumulation during high-dose ara-C therapy: pharmacologic rationale for intermediate-dose ara-C. Semin Oncol 1987;14:159-166.

13 Kaye SB. Gemcitabine: current status of phase I and II trials. J Clin Oncol 1994;12:1527-1531.

14 Boven E, Schipper H, Erkelens CA, et al. The influence of the schedule and the dose of gemcitabine on the anti-tumour efficacy in experimental human cancer. Br J Cancer 1993;68:52-56.

15 Pastor-Anglada M, Molina-Arcas M, Casado FJ, et al. Nucleoside transporters in chronic lymphocytic leukaemia. Leukemia 2004;18:385-393.

16 Wiley JS, Jones SP, Sawyer WH, et al. Cytosine arabinoside influx and nucleoside transport sites in acute leukemia. J Clin Invest 1982;69:479-489.

17 White JC, Rathmell JP, Capizzi RL. Membrane transport influences the rate of accumulation of cytosine arabinoside in human leukemia cells. J Clin Invest 1987;79:380-387.

18 Mackey JR, Mani RS, Selner M, et al. Functional nucleoside transporters are required for gemcitabine influx and manifestation of toxicity in cancer cell lines. Cancer Res 58:4349-4357.

19 Baldwin SA, Mackey JR, Cass CE, et al. Nucleoside transporters: molecular biology and implications for therapeutic development. Mol Med Today 1999;5:216-224.

20 Ritzel MW, Yao SY, Ng AM, et al. Molecular cloning, functional expression and chromosomal localization of a cDNA encoding a human Na+/nucleoside cotransporter (hCNT2) selective for purine nucleosides and uridine. Mol Membr Biol 1998;15:203-211.

21 Wang J, Su SF, Dresser MJ, et al. Na(+)-dependent purine nucleoside transporter from human kidney: cloning and functional characterization. Am J Physiol 1997;273:F1058-F1065.

22 Gutierrez MM, Brett CM, Ott RJ, et al. Nucleoside transport in brush border membrane vesicles from human kidney. Biochim Biophys Acta 1992;1105:1-9.

23 Patil SD, Unadkat JD. Sodium-dependent nucleoside transport in the human intestinal brush-border membrane. Am J Physiol 1997;272:G1314-G1320.

24 Chandrasena G, Giltay R, Patil SD, et al. Functional expression of human intestinal Na+-dependent and Na+-independent nucleoside transporters in Xenopus laevis oocytes. Biochem Pharmacol 1997;53:1909-1918.

25 Camiener GW, Smith CG. Studies of the enzymatic deamination of cytosine arabinoside. I. Enzyme distribution and species specificity. Biochem Pharmacol 1965;14:1405-1416.

26 Heinemann V, Xu YZ, Chubb S, et al. Inhibition of ribonucleotide reduction in CCRF-CEM cells by 2',2'-difluorodeoxycytidine. Mol Pharmacol 1990;38:567-572.

27 Hertel LW, Boder GB, Kroin JS, et al. Evaluation of the antitumor activity of gemcitabine (2',2'-difluoro-2'-deoxycytidine). Cancer Res 1990;50:4417-4422.

28 Huang P, Chubb S, Hertel LW, et al. Action of 2',2'-difluorodeoxycytidine on DNA synthesis. Cancer Res 1991;51:6110-6117.

29 Galmarini CM, Mackey JR, Dumontet C. Nucleoside analogues: mechanisms of drug resistance and reversal strategies. Leukemia 2001;15:875-890.

30 Fukunaga AK, Marsh S, Murry DJ, et al. Identification and analysis of single-nucleotide polymorphisms in the gemcitabine pharmacologic pathway. Pharmacogenomics J 2004;4:307-314.

31 Maring JG, Groen HJ, Wachters FM, et al. Genetic factors influencing pyrimidine-antagonist chemotherapy. Pharmacogenomics J 2005;5:226-243.

32 Joerger M, Bosch TM, Doodeman VD, et al. Novel deoxycytidine kinase gene polymorphisms: a population screening study in Caucasian healthy volunteers. Eur J Clin Pharmacol 2006;62:681-684.

33 Gandhi V, Plunkett W. Modulatory activity of 2',2'-difluorodeoxycytidine on the phosphorylation and cytotoxicity of arabinosyl nucleosides. Cancer Res 1990;50:3675-3680.

34 Shewach DS, Reynolds KK, Hertel L. Nucleotide specificity of human deoxycytidine kinase. Mol Pharmacol 1992;42:518-524.

35 Plunkett W, Gandhi V. Nucleoside analogs: Celllular pharmacology, mechanisms of action, and strategies for combination therapy. In: B. D. Cheson, M. J. Keating and W. Plunkett, Nucleoside analogs in cancer therapy, pp. 1-36. Marcel Dekker, Inc.: New York, 1997.

36 Ruiz van Haperen VW, Veerman G, Eriksson S, et al. Development and molecular characterization of a 2',2'-difluorodeoxycytidine-resistant variant of the human ovarian carcinoma cell line A2780. Cancer Res 1994;54:4138-4143.

37 Blackstock AW, Lightfoot H, Case LD, et al. Tumor uptake and elimination of 2',2'-difluoro-2'-deoxycytidine (gemcitabine) after deoxycytidine kinase gene transfer: correlation with in vivo tumor response. Clin Cancer Res 2001;7:3263-3268.

38 Ritzel MW, Ng AM, Yao SY, et al. Recent molecular advances in studies of the concentrative Na+-dependent nucleoside transporter (CNT) family: identification and characterization of novel human and mouse proteins (hCNT3 and mCNT3) broadly selective for purine and pyrimidine nucleosides (system cib). Mol Membr Biol 2001;18:65-72.

39 Lostao MP, Mata JF, Larrayoz IM, et al. Electrogenic uptake of nucleosides and nucleoside-derived drugs by the human nucleoside transporter 1 (hCNT1) expressed in Xenopus laevis oocytes. FEBS Lett 2000; 481:137-140.

40 Mackey JR, Yao SY, Smith KM, et al. Gemcitabine transport in xenopus oocytes expressing recombinant plasma membrane mammalian nucleoside transporters. J Natl Cancer Inst 1999;91:1876-1881.

41 Jansen WJ, Pinedo HM, van der Wilt CL, et al. The influence of BIBW22BS, a dipyridamole derivative, on the antiproliferative effects of 5-fluorouracil, methotrexate and gemcitabine in vitro and in human tumour xenografts. Eur J Cancer 1995;31A:2313-2319.

42 Gati WP, Paterson AR, Larratt LM, et al. Sensitivity of acute leukemia cells to cytarabine is a correlate of cellular es nucleoside transporter site content measured by flow cytometry with SAENTA-fluorescein. Blood 1997;90:346-353.

43 Galmarini CM, Thomas X, Calvo F, et al. Potential mechanisms of resistance to cytarabine in AML patients. Leuk Res 2002;26:621-629.

44 Achiwa H, Oguri T, Sato S, et al. Determinants of sensitivity and resistance to gemcitabine: the roles of human equilibrative nucleoside transporter 1 and deoxycytidine kinase in non-small cell lung cancer. Cancer Sci 2004;95:753-757.

45 Garcia-Manteiga J, Molina-Arcas M, Casado FJ, et al. Nucleoside transporter profiles in human pancreatic cancer cells: role of hCNT1 in 2',2'-difluorodeoxycytidine- induced cytotoxicity. Clin Cancer Res 2003;9:5000-5008.

46 Abbruzzese JL, Grunewald R, Weeks EA, et al. A phase I clinical, plasma, and cellular pharmacology study of gemcitabine. J Clin Oncol 1991;9:491-498.

47 Zhang L, Sinha V, Forgue ST, et al. Model-based drug development: the road to quantitative pharmacology. J Pharmacokinet Pharmacodyn 2006;33:369-393.

48 Grunewald R, Kantarjian H, Keating MJ, et al. Pharmacologically directed design of the dose rate and schedule of 2',2'-difluorodeoxycytidine (Gemcitabine) administration in leukemia. Cancer Res 1990;50:6823-6826.

49 Grunewald R, Abbruzzese JL, Tarassoff P, et al. Saturation of 2',2'-difluorodeoxycytidine 5'-triphosphate accumulation by mononuclear cells during a phase I trial of gemcitabine. Cancer Chemother Pharmacol 1991;27:258-262.

50 Shewach DS, Reynolds KK, Hertel L. Nucleotide specificity of human deoxycytidine kinase. Mol Pharmacol 1992;42:518-524.

51 Bouffard DY, Laliberte J, Momparler RL. Kinetic studies on 2',2'-difluorodeoxycytidine (Gemcitabine) with purified human deoxycytidine kinase and cytidine deaminase. Biochem Pharmacol 1993;45:1857-1861.

52 Grunewald R, Kantarjian H, Du M, et al. Gemcitabine in leukemia: a phase I clinical, plasma, and cellular pharmacology study. J Clin Oncol 1992;10:406-413.

53 Plunkett W, Iacoboni S, Estey E, et al. Pharmacologically directed ara-C therapy for refractory leukemia. Semin Oncol 1985;12:20-30.

54 Estey E, Plunkett W, Dixon D, et al. Variables predicting response to high dose cytosine arabinoside therapy in patients with refractory acute leukemia. Leukemia 1987;1:580-583.

55 Estey EH, Keating MJ, McCredie KB, et al. Cellular ara-CTP pharmacokinetics, response, and karyotype in newly diagnosed acute myelogenous leukemia. Leukemia 1990;4:95-99.

56 Kantarjian HM, Estey EH, Plunkett W, et al. Phase I-II clinical and pharmacologic studies of high-dose cytosine arabinoside in refractory leukemia. Am J Med 1986;81:387-394.

57 Early AP, Preisler HD, Slocum H, et al. A pilot study of high-dose 1-beta-D-arabinofuranosylcytosine for acute leukemia and refractory lymphoma: clinical response and pharmacology. Cancer Res 1982;42:1587-1594.

58 Capizzi RL, Yang JL, Cheng E, et al. Alteration of the pharmacokinetics of high-dose ara-C by its metabolite, high ara-U in patients with acute leukemia. J Clin Oncol 1983;1:763-771.

59 Liliemark JO, Plunkett W, Dixon DO. Relationship of 1-beta-D-arabinofuranosylcytosine in plasma to 1-beta-D-arabinofuranosylcytosine 5'-triphosphate levels in leukemic cells during treatment with high-dose 1-beta-D-arabinofuranosylcytosine. Cancer Res 1985;45:5952-5957.

60 Spratlin J, Sangha R, Glubrecht D, et al. The absence of human equilibrative nucleoside transporter 1 is associated with reduced survival in patients with gemcitabine-treated pancreas adenocarcinoma. Clin Cancer Res 2004;10:6956-6961.

61 Giovannetti E, Del Tacca M, Mey V, et al. Transcription analysis of human equilibrative nucleoside transporter-1 predicts survival in pancreas cancer patients treated with gemcitabine. Cancer Res 2006;66:3928-3935.

62 Touroutoglou N, Gravel D, Raber MN, et al. Clinical results of a pharmacodynamically-based strategy for higher dosing of gemcitabine in patients with solid tumors. Ann Oncol 1998;9:1003-1008.

63 Pollera CF, Ceribelli A, Crecco M, et al. Prolonged infusion gemcitabine: a clinical phase I study at low- (300 mg/m2) and high-dose (875 mg/m2) levels. Invest New Drugs 1997;15:115-121.

64 Storniolo AM, Allerheiligen SR, Pearce HL. Preclinical, pharmacologic, and phase I studies of gemcitabine. Semin Oncol 1997;24: S7.

65 White JC, Rathmell JP, Capizzi RL. Membrane transport influences the rate of accumulation of cytosine arabinoside in human leukemia cells. J Clin Invest 1987;79:380-387.

66 Wiley JS, Jones SP, Sawyer WH. Cytosine arabinoside transport by human leukaemic cells. Eur J Cancer Clin Oncol 1983;19:1067-1074.

67 Jamieson GP, Snook MB, Wiley JS. Saturation of intracellular cytosine arabinoside triphosphate accumulation in human leukemic blast cells. Leuk Res 1990;14:475-479.

68 Weinstein HJ, Griffin TW, Feeney J, et al. Pharmacokinetics of continuous intravenous and subcutaneous infusions of cytosine arabinoside. Blood 1982;59:1351-1353.

69 Ho DH, Brown NS, Benvenuto J, et al. Pharmacologic studies of continuous infusion of arabinosylcytosine by liquid infusion system. Clin Pharmacol Ther 1977;22:371-374.

70 Wiley JS, Jones SP, Sawyer WH, et al. Cytosine arabinoside influx and nucleoside transport sites in acute leukemia. J Clin Invest 1982;69:479-489.

71 Veerman G, Ruiz van Haperen VW, Vermorken JB, et al. Antitumor activity of prolonged as compared with bolus administration of 2',2'-difluorodeoxycytidine in vivo against murine colon tumors. Cancer Chemother Pharmacol 1996;38:335-342.

72 Patel SR, Gandhi V, Jenkins J, Papadopolous N, et al. Phase II clinical investigation of gemcitabine in advanced soft tissue sarcomas and window evaluation of dose rate on gemcitabine triphosphate accumulation. J Clin Oncol 2001;19:3483-3489.

73 Gandhi V, Plunkett W, Du M, et al. Prolonged infusion of gemcitabine: clinical and pharmacodynamic studies during a phase I trial in relapsed acute myelogenous leukemia. J Clin Oncol 2002;20:665-673.

74 Bengala C, Guarneri V, Giovannetti E, et al. Prolonged fixed dose rate infusion of gemcitabine with autologous haemopoietic support in advanced pancreatic adenocarcinoma. Br J Cancer 2005;93:35-40.

75 Anderson H, Thatcher N, Walling J, et al. A phase I study of a 24 hour infusion of gemcitabine in previously untreated patients with inoperable non-small-cell lung cancer. Br J Cancer 1996;74:460-462.

76 Maurel J, Zorrilla M, Puertolas T, et al. Phase I trial of weekly gemcitabine at 3-h infusion in refractory, heavily pretreated advanced solid tumors. Anticancer Drugs 2001;12:713-717.

77 Schmid P, Schweigert M, Beinert T, et al. Prolonged infusion of gemcitabine in advanced solid tumors: a phase-I-study. Invest New Drugs 2005;23:139-146.

78 Akrivakis K, Schmid P, Flath B, et al. Prolonged infusion of gemcitabine in stage IV breast cancer: a phase I study. Anticancer Drugs 1999;10:525-531.

79 Soo RA, Lim HL, Wang LZ, et al. Phase I trial of fixed dose-rate gemcitabine in combination with carboplatin in chemonaive advanced non-small-cell lung cancer: a Cancer Therapeutics Research Group study. Cancer Chemother Pharmacol 2003;52:153-158.

80 Wang L, Wu X, Huang M, et al. The efficacy and relationship between peak concentration and toxicity profile of fixed-dose-rate gemcitabine plus carboplatin in patients with advanced non-small-cell lung cancer. Cancer Chemother Pharmacol 2007;60:211-218.

81 Zwitter M, Kovac V, Smrdel U, et al. Phase I-II trial of low-dose gemcitabine in prolonged infusion and cisplatin for advanced non-small cell lung cancer. Anticancer Drugs 2005;16:1129-1134.

82 Rajdev L, Goldberg G, Hopkins U, et al. A Phase I Trial of Gemcitabine Administered as a 96-h Continuous Intravenous Infusion in Patients with Advanced Carcinoma and Lymphoma. Med Oncol 2006;23:369-376.

83 Guan Z, Wang Y, Maoleekoonpairoj S, et al. Prospective randomised phase II study of gemcitabine at standard or fixed dose rate schedule in unresectable hepatocellular carcinoma. Br J Cancer 2003;89:1865-1869.

84 Tempero M, Plunkett W, Ruiz Van Haperen VW., et al. Randomized phase II comparison of dose-intense gemcitabine: thirty-minute infusion and fixed dose rate infusion in patients with pancreatic adenocarcinoma. J Clin Oncol 2003;21:3402-3408.

85 Fossella FV, Lippman SM, Shin DM, et al. Maximum-tolerated dose defined for single-agent gemcitabine: a phase I dose-escalation study in chemotherapy-naive patients with advanced non-small-cell lung cancer. J Clin Oncol 1997;15:310-316.

86 Brand R, Capadano M, Tempero M. A phase I trial of weekly gemcitabine administered as a prolonged infusion in patients with pancreatic cancer and other solid tumors. Invest New Drugs 1997;15:331-341.

87 Soo RA, Wang LZ, Tham LS, et al. A multicentre randomised phase II study of carboplatin in combination with gemcitabine at standard rate or fixed dose rate infusion in patients with advanced stage non-small-cell lung cancer. Ann Oncol 2006;17:1128-1133.

88 Cappuzzo F, Novello S, De Marinis MF, et al. A randomized phase II trial evaluating standard (50 mg/min) versus low (10 mg/min) infusion duration of gemcitabine as first-line treatment in advanced non-small-cell lung cancer patients who are not eligible for platinum-based chemotherapy. Lung Cancer 2006;52:319-325.

89 Ceribelli A, Gridelli C, De Marinis MF, et al. Prolonged gemcitabine infusion in advanced non-small cell lung carcinoma: a randomized phase II study of two different schedules in combination with cisplatin. Cancer 2003;98:337-343.

90 Gridelli C, Gallo C, Ceribelli A, et al. Factorial phase III randomised trial of rofecoxib and prolonged constant infusion of gemcitabine in advanced non-small-cell lung cancer: the GEmcitabine-COxib in NSCLC (GECO) study. Lancet Oncol 2007;8:500-512.

91 Eisbruch A, Shewach DS, Bradford CR, et al. Radiation concurrent with gemcitabine for locally advanced head and neck cancer: a phase I trial and intracellular drug incorporation study. J Clin Oncol 2001;19:792-799.

92 Peters GJ, Clavel M, Noordhuis P, et al. Clinical phase I and pharmacology study of gemcitabine (2', 2'-difluorodeoxycytidine) administered in a two-weekly schedule. J Chemother 2007;19:212-221.

93 Poplin E, Levy DE, Berlin J, et al. Phase III trial of gemcitabine (30-minute infusion) versus gemcitabine (fixed-dose-rate infusion [FDR]) versus gemcitabine + oxaliplatin (GEMOX) in patients with advanced pancreatic cancer (E6201) (abstract). ASCO 2006;24.

Chapter 3

Preclinical and clinical pharmacological studies on oral and i.v. gemcitabine

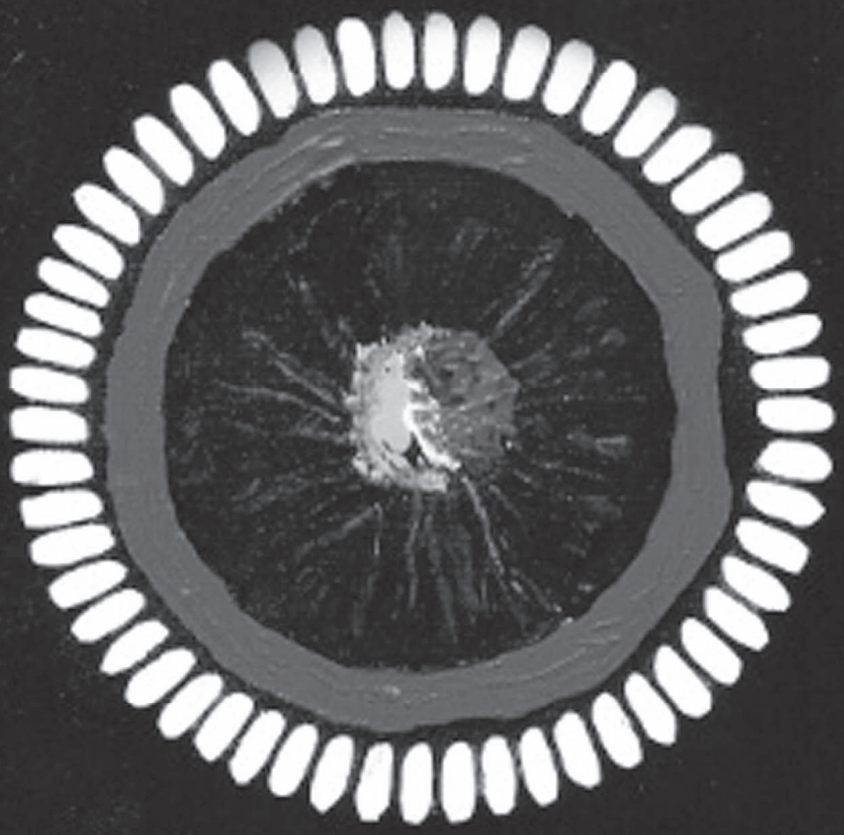

Chapter 3.1

New insights into the *in vitro* pharmacology and cytotoxicity of gemcitabine and its metabolite 2',2'-difluorodeoxyuridine

Submitted for publication

Stephan A. Veltkamp
Dick Pluim
Monique A.J. van Eijndhoven
Marije J. Bolijn
Felix H.G. Ong
Rajgopal Govindarajan
Jash Unadkat
Jos H. Beijnen
Jan H.M. Schellens

Abstract

In a clinical study with oral gemcitabine (2',2'-difluorodeoxycytidine, dFdC), 2',2'-difluorodeoxyuridine (dFdU) was extensively formed and accumulated after multiple oral dosing. Here, we have investigated the *in vitro* cytotoxicity, cellular uptake, efflux, biotransformation and nucleic acid incorporation of dFdC and dFdU.

Short- and long-term cytotoxicity assays were used to assess the cytotoxicity of dFdC and dFdU in human hepatocellular carcinoma HepG2, human lung carcinoma A549, and Madin-Darby canine kidney (MDCK) cell lines transfected with the human concentrative or equilibrative nucleoside transporter 1 (hCNT1 or hENT1), or empty vector. Radiolabeled dFdC and dFdU were used to determine cellular uptake, efflux, biotransformation, and incorporation into DNA and RNA. The compounds dFdC, dFdU, and their phosphorylated metabolites were quantified by HPLC with UV and radioisotope detection.

dFdU monophosphate (dFdU-MP), diphosphate (dFdU-DP), and triphosphate (dFdU-TP) were formed from dFdC and dFdU. dFdU-TP was incorporated into DNA and RNA. The AUC of dFdC-TP and dFdU-TP and their extent of incorporation into DNA and RNA inversely correlated with the IC_{50} of dFdC and dFdU, respectively. The cellular uptake and cytotoxicity of dFdU were significantly enhanced by hCNT1. dFdU inhibited cell cycle progression and its cytotoxicity significantly increased on longer duration of exposure.

dFdU is taken up into cells with high affinity by hCNT1 and phosphorylated to its dFdU-TP metabolite. dFdU-TP is incorporated into DNA and RNA, which correlated with dFdU cytotoxicity. These data provide strong evidence that dFdU can significantly contribute to the cytotoxicity of dFdC, which warrants further investigation.

Introduction

Gemcitabine (2',2'-difluorodeoxycytidine, dFdC), a pyrimidine nucleoside anticancer drug, has proven antitumor activity both *in vitro* and *in vivo* (1-6). dFdC is transported into cells by human nucleoside transporters (hNTs) (7). dFdC is intracellularly phosphorylated by deoxycytidine kinase (dCK) to its monophosphate (dFdC-MP) and subsequent phosphorylation by nucleoside kinases results in the formation of the active diphosphate (dFdC-DP) and triphosphate (dFdC-TP) metabolites (4). dFdC-TP competes with the natural substrate deoxycytidine triphosphate (dCTP) for incorporation into DNA (8), thereby inhibiting DNA synthesis and blocking cells in the early S phase (5). dFdC-DP inhibits ribonucleotide reductase (RR) (9), ultimately leading to a depletion of dCTP pools and facilitating incorporation of dFdC-TP into DNA. Moreover, dFdC can potentiate its own cytotoxic effect via other pathways (10, 11). Alternatively, dFdC is deaminated by cytidine deaminase (CDA; EC 3.5.4.5) (10), which is highly expressed in human liver (12), to 2',2'-difluorodeoxyuridine (dFdU), of which the activity is uncertain. The chemical structures of dFdC and dFdU as well as the proposed biotransformation and pharmacological mechanisms of action of dFdC are depicted in Figure 1.

dFdC is a high affinity substrate for the human concentrative nucleoside transporter type 1 (hCNT1) (apparent K_m values of 12-36 μM) and is transported at lower affinity by the human equilibrative nucleoside transporter type 1 (hENT1) (apparent K_m values of 120-200 μM) (7, 13). It has been shown that the uptake of dFdC and its cytotoxicity significantly increased following co-administration with nitrobenzylmercaptopurine riboside (NBMPR), an inhibitor of hENT mediated transport (14). Expression of hCNT1 was shown to correlate with toxicity of dFdC *in vitro* in human pancreatic adenocarcinoma cell lines (15) and expression of hENT1 with overall survival in patients with pancreatic cancer (16). hENT1 is an ubiquitous transporter with significant variability in tissue abundance (17), while hCNT1 is considered to have more restricted distribution, with high expression in liver and kidney (18).

In a clinical study on continuous low dose oral dFdC in patients with advanced solid tumors, dFdU was extensively formed via first-pass metabolism and

accumulated, most likely in the liver (submitted). One patient treated at 8 mg oral dFdC once daily for 14 days of a 21-day cycle experienced lethal hepatotoxicity. Pathological examination revealed severe drug induced liver necrosis.

We hypothesized that dFdU might contribute to the toxicity and/or antitumor activity of dFdC and might become hepatotoxic after liver accumulation following chronic oral dFdC administration. We speculated that dFdU is phosphorylated to its triphosphate (dFdU-TP) and subsequently incorporated into DNA and/or RNA. In addition, we hypothesized that dFdU is taken up by cells with high affinity by hCNT1.

The aims of this study were to investigate the cytotoxicity, effects on cell cycle distribution, cellular uptake, efflux, biotransformation, and nucleic acid incorporation of dFdU and its parent compound dFdC *in vitro* using human hepatocellular carcinoma HepG2, human lung carcinoma A549, and Madin-Darby canine kidney (MDCK) cells transfected with either hCNT1, hENT1 or empty vector.

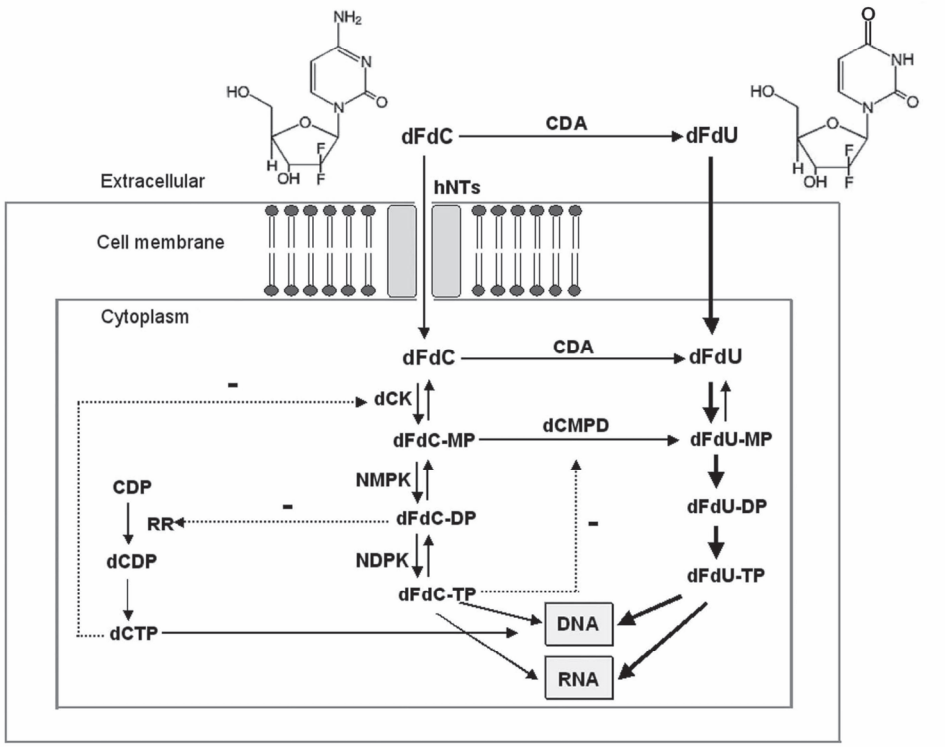

Figure 1. Proposed biotransformation and pharmacological actions of dFdC and its metabolites with chemical structures of dFdC and dFdU. The Figure presents uptake of dFdC by hNTs and phosphorylation by deoxycytidine kinase (dCK) to its monophosphate (dFdC-MP), and by human nucleoside monophosphate and diphosphate kinases (NMPK and NDPK) into its diphosphate (dFdC-DP) and triphosphate (dFdC-TP) metabolites. dFdC-TP is incorporated into RNA and particularly into DNA, thereby competing with deoxycytidine triphosphate (dCTP) for incorporation. dFdC-DP inhibits ribonucleotide reductase (RR), which inhibits the conversion of cytidine diphosphate (CDP) to deoxycytidine diphosphate (dCDP) and depletes dCTP pools, resulting in less inhibition of dCK and elevation of the intracellular dFdC-TP/dCTP ratio, ultimately resulting into enhanced incorporation of dFdC-TP into DNA. dFdC is deaminated by cytidine deaminase (CDA) to 2',2'-difluorodeoxyuridine (dFdU). dFdC-MP is converted to difluorodeoxyuridine monophosphate (dFdU-MP) by deoxycytidylate deaminase (dCMPD). dFdC-TP can inhibit dCMPD, thereby stimulating its own formation. Novel pathways found in this study are presented with arrows in bold. dFdU is taken up into cells by the action of hNTs and phosphorylated to its monophosphate (dFdU-MP), diphosphate (dFdU-DP) and its triphosphate (dFdU-TP), which is incorporated into DNA and RNA.

Material and methods

Antibodies

FITC-labelled goat anti-rabbit IgG antibody was purchased from Molecular Probes, Inc. (Eugene, OR). Mouse anti-bromodeoxyuridine was purchased from Dakocytomation (Glostrup, Denmark). Anti-mouse IgG-FITC was derived from Sigma-Aldrich Chemie GmbH (Steinheim, Germany).

Reagents

dFdC, dFdU, dFdC-MP, dFdC-DP, dFdC-TP, dFdU-MP, dFdU-DP, dFdU-TP and CDA (activity: 2 μmol/min/mg for cytidine) were kindly provided by Eli Lilly and Company (Indianapolis, CA, USA). Tetrahydrouridine (THU) was obtained from Calbiochem (San Diego, CA, USA) and nitrobenzylthioinosine (nitrobenzylmercaptopurine riboside, NBMPR) from Biomol Research Laboratories Inc. (PA, USA). [^{3}H]-dFdC (21.3 Ci/mmol), [^{3}H]-thymidine (20 Ci/mmol) and [^{3}H]-uridine (16.2 Ci/mmol) were purchased from Moravek Biochemicals Inc. (Brea, CA, USA). [^{3}H]-dFdU was synthesized out of [^{3}H]-dFdC via enzymatic conversion by CDA. Nuclease P_1 (NP_1) (endonuclease activity: 1000 μmol/min/mg protein) was purchased from Roche Diagnostics GmbH (Penzberg, Germany) and thymidine kinase 1 (TK1) (activity: 2-12 μmol/min/mg protein for thymidine) was purchased from Biaffin GmbH & Co KG (Kassel, Germany). Crystal violet and glutardialdehyde were obtained from Merck KgaA (Darmstadt, Germany). All other chemicals were purchased from Sigma (St. Louis, MO, USA).

Cell culture

HepG2, A549, and MDCK cells transfected with either hCNT1, hENT1, or empty vector (mock) (19), were cultured in Roswell Park Memorial Institute (RPMI) 1640 medium, Dulbecco's modified Eagles medium (DMEM), and modified Eagle's minimum essential medium (MEM), respectively. Medium was supplemented with 100 units/mL penicillin, 100 μg/mL streptomycin and 10% fetal bovine serum (FBS). All cell lines were routinely tested for absence of *Mycoplasma*. All experiments were performed with exponentially growing cells. Cells were treated with drugs after a period of 12 h for the cells to attach.

Sulphorhodamine B cytotoxicity assay

Cells in 200 µL/well were plated in 96-wells plates and dFdC and dFdU were added in serial dilutions for 48, 72, and 96 h. Cells were washed and stained with Sulforhodamine B (20, 21). Extinction was measured at 540 nm with a microplate reader (BioTek Instruments, Winooski, VT, USA). The data were fitted to a sigmoidal concentration-response curve, and cytotoxicity was determined by calculation of the inhibitory concentration at 50% cell death (IC_{50}) using GraphPad prism version 4.0 for Windows (GraphPad Software, San Diego, CA, USA). Control wells (untreated) were set at 100% survival.

Clonogenic survival assay

Cells in 2 mL medium were plated in 6-wells plates and dFdC and dFdU were added at varying concentrations. Cells were allowed to form colonies over a period of maximal 14 days after addition of drugs, which were subsequently fixed and stained with 0.2% crystal violet/2.5% glutardialdehyde. The number of colonies was counted with a Colcount (Oxford Optronix, Oxford, UK) and visually confirmed under a light microscope to contain at least 50 cells. Cell survival was corrected for plating efficiency.

Cell cycle analysis

HepG2 and A549 cells in 2 mL medium were plated in 6-wells plates. dFdC and dFdU were added for 8, 24, 48, and 72 h and labelled with iododeoxuridine (IUdR) (22). In brief, nuclei were isolated and incubated with a mouse anti-bromodeoxyuridine antibody, which binds to IUdR (1:50), followed by 30 min incubation with FITC-conjugated anti-mouse antibody (1:50). Finally, propidium iodide (PI) was added to stain total DNA. Flow cytometry was carried out using a FACScan flow cytometer.

Nucleoside and nucleotide extraction and analysis

Separation, identification, and quantification of dFdC, dFdU, dFdC-MP, dFdC-DP, dFdC-TP, dFdU-MP, dFdU-DP, and dFdU-TP were performed using ion-pairing reversed phase high performance liquid chromatography (HPLC) (Beckman Coulter, Inc., CA, USA) with ultraviolet (UV) and off-line radioisotope detection (Packard, Instrument Co., Inc., CT, USA). A C18 HDO column, 5 µm, 150 x 4.6

mm (Uptisphere, Interchrom, France) was used with a column temperature of 40 °C, a 1:1 mixture of Ultima-flow and mobile phase, and a flow rate of 1.0 mL/min. The mobile phase consisted of a mixture of eluent A (80 mM potassium phosphate pH 7.0, 11 mM tetrabutylamine, and 1.0% MeOH) mixed with eluent B (80 mM potassium phosphate pH 7.0, and 10% MeOH) in the following gradient: t = 0-10 min:17% B; t = 10-65 min:22% B; t = 65-85 min:100% B, and t = 85-90 min:17% B. System suitability was assessed using a mixture of reference standards of dFdC, dFdU, dFdC-MP, dFdC-DP, dFdC-TP, dFdU-MP, dFdU-DP, and dFdU-TP prior to each sequence. Radioactivity was determined with a Tri-Carb® 2800 TR liquid scintillation analyzer (Perkin Elmer, USA). Metabolites were quantified based on the radioactivity of the metabolite peak relative to the radioactivity of [^{3}H]-dFdC or [^{3}H]-dFdU with correction for the total amount of drug. The concentration of cellular protein was determined by the Bio-Rad Protein Assay (23) and was used to correct for differences in amount of isolated cells between samples. In HepG2 and A549 cells, cell number and cell volume were determined by a Casy 1 cell counter (Schärfe System GmbH, Reutlingen, Germany) to be able to calculate micromolar concentrations of dFdC-TP.

Synthesis of [^{3}H]-dFdU and determination of phosphorylation by TK1

[^{3}H]-dFdU was synthesized from [^{3}H]-dFdC via conversion by CDA. A mixture of 1.0 mL [^{3}H]-dFdC (1.0 mCi/mL), 80 µL CDA (134 µg/mL), and 8.9 mL 10mM Tris-HCl pH 7.5 was incubated for 60 min at 37 °C. The solution was snap-frozen on a dry ice/ethanol bath, freeze-dried, and the pellet was dissolved in 500 µL eluent (10 mM NaH_2PO_4, 2.0% MeOH pH 6.0) and injected onto the HPLC. [^{3}H]-dFdU was identified with UV and radioisotope detection as described above. The reference compounds dFdC and dFdU were used prior to each sequence to assess system suitability. The elution times for dFdC and dFdU were 15 and 26 min, respectively. The [^{3}H]-dFdU fraction was collected, freeze-dried and the pellet was dissolved in 1.0 mL Milli-Q. The recovery was calculated based on the radioactivity of [^{3}H]-dFdU relative to the radioactivity of the initial [^{3}H]-dFdC solution, and purity was checked by HPLC. Recovery and purity were > 97% and > 99%, respectively.

Phosphorylation of [^{3}H]-dFdC, [^{3}H]-dFdU and [^{3}H]-thymidine (positive control) was investigated by incubation with TK1 (in 50 mM TrisHCl pH 7.6, 0.5 mM

$MgCl_2$, 0.1% Tween 20, and 2.5 mM ATP in 0.9% NaCl) at 37 °C for 30 min, after which the mixture was placed at 100 °C for 2 min, following centrifugation at 21,000 x *g* for 5 min and injection of the supernatant onto the HPLC.

Cellular uptake and biotransformation of dFdC and dFdU

Cells in 10 mL medium/well were plated in 8 cm dishes, and incubated for 4, 12, and 24 h with [^{3}H]-dFdC or [^{3}H]-dFdU (40 x 10^6 dpm/well) complemented with cold dFdC and dFdU, respectively to total concentrations of 0.5 and 5.0 µM (and 5 nM dFdC and 500 µM dFdU in HepG2 cells). dFdC was co-incubated with 100 µM THU, a competitive inhibitor of CDA (24-26), to reduce deamination of dFdC to dFdU to compare relative toxicity of dFdC with dFdU. Experiments were stopped, medium was collected, and cells were washed thrice with 10 mL ice cold Phosphate Buffered Saline (PBS). Subsequently, cells were scraped in 10 mL ice cold PBS, transferred into a 15 mL tube, and centrifuged at 1100 x *g* at 0 °C for 5 min. After removal of the supernatant, cells were resuspended into 200 µL ice cold PBS. Twenty µL was used to determine the protein concentration. The remaining solution was mixed with MeOH to a final concentration of 60% and placed at -20 °C for 2 h to precipitate proteins and to extract dFdC, dFdU, and their phosphorylated metabolites. After centrifugation at 21,000 x *g* for 5 min, the supernatant was freeze-dried, resuspended in 240 µL eluent A, sonificated for 5 min, and centrifuged at 21,000 x *g* for 5 min. The supernatant was collected for analysis of dFdC, dFdU, and phosphorylated metabolites by HPLC. A comparable procedure was performed for medium.

Incorporation of dFdC-TP and dFdU-TP into DNA and RNA

Cells in 10 mL medium were plated in 8 cm dishes and incubated for 24 h with [^{3}H]-dFdC or [^{3}H]-dFdU (100 x 10^6 dpm/dish) both complemented with cold drugs to total concentrations of 0.5 µM (and 5 nM dFdC and 500 µM dFdU in HepG2 cells). After termination of the experiments, medium was discarded, and cells were washed thrice with 10 mL ice cold PBS. Subsequently, cells were scraped in 10 mL ice cold PBS, transferred into a 15 mL tube, centrifuged at 1100 x *g* at 0 °C for 5 min and the supernatant was discarded. From the remaining cell pellet, DNA and RNA were purified using a QIAamp® DNA Mini Kit and RNeasy Mini Kit,

respectively (Qiagen Inc., CA, USA). Purity was determined by a Nanodrop ND-1000 spectrophotometer (NanoDrop Technologies, Inc., DE, USA). After purification, 80 µL of DNA/RNA solution (maximal 100 µg DNA/RNA) was diluted with 420 µL 50 mM ammonium acetate pH 5.0 and digested by addition of 6 µL NP-1 (0.5 units/µL) at 60 °C for 3 h. Final solutions were freeze-dried, resuspended in eluent A, centrifuged at 21,000 x *g* for 5 min, and the supernatant was collected for quantification of dFdC-MP and dFdU-MP and determination of the amount of incorporated dFdC-TP and dFdU-TP. The amount of DNA and RNA that was synthesized during treatment with dFdC or dFdU was assessed by co-incubation of the cells with [^{3}H]-thymidine and [^{3}H]-uridine (10 x 10^6 dpm each). Two wells were treated with non-radioactive drugs only following incubation with [^{3}H]-thymidine or [^{3}H]-uridine for 10 min to exclude any non-specific binding of drugs to DNA/RNA. Total amounts of incorporated dFdC-TP and dFdU-TP were expressed as pmol/mg DNA or RNA to compare within cell lines and in pmol drug/µmol synthesized DNA or RNA to be able to compare between cell lines, which had different DNA and RNA content.

Transport of dFdC and dFdU by hCNT1

MDCK-hCNT1, and -mock cells in 1.0 mL medium/well were plated in 24-wells plates. Transport experiments were carried out in sodium-containing transport buffer (20 mM Tris-HCl, 3 mM K_2HPO_4, 1 mM $MgCl_2.6H_2O$, 2 mM $CaCl_2$, 5 mM glucose, 130 mM NaCl, pH 7.4) or sodium-free transport buffer in which NaCl was replaced by 130 mM N-methyl-D-glucamine pH 7.4. Cells were pre-incubated for 15 min at 37 °C with 250 µL transport buffer in sodium-containing or sodium-free transport buffer containing 10 µM NBMPR (27). Subsequently, 250 µL of the corresponding transport buffer containing [^{3}H]-dFdC or [^{3}H]-dFdU (150,000 dpm/well) both complemented with cold dFdC and dFdU, respectively at varying concentrations were added for 15 min at 37 °C. Experiments were stopped, medium was discarded, and cells were washed thrice with 1.0 mL ice cold PBS. Cells were lysed in 500 µL 1N NaOH for 30 min at 37 °C, resuspended, radioactivity was counted and protein concentration was determined.

Efflux of dFdC and dFdU

HepG2 and A549 cells in 1.0 mL medium/well were plated in 24-wells plates. Cells were loaded with [^{3}H]-dFdC (40 x 10^6 dpm) for 15 min at a total concentration of 15 µM or with [^{3}H]-dFdU for 4 h complemented with cold drug to 5 µM. The short period of time and relatively high dFdC concentration were chosen to prevent metabolism of dFdC, and to obtain measurable amounts of dFdC. After loading the cells, medium was replaced by fresh medium and samples were taken at t = 0, 5, 10, 30, and 60 min. Cells were washed thrice, scraped and resuspended in ice cold PBS, centrifuged at 21,000 x *g* for 5 min, the supernatant was discarded, and cells were resuspended in 200 µL ice cold PBS. The protein concentration was determined and nucleosides and nucleotides were quantified.

In vitro pharmacokinetic and statistical analysis

The cellular pharmacokinetic parameters of dFdC, dFdU, dFdC-MP, dFdC-DP, dFdC-TP, dFdU-MP, dFdU-DP, and dFdU-TP were determined by non-compartmental analysis, using WinNonLin™ (version 5.0.1, Pharsight Corporation, Mountain View, CA, USA). The area under the intracellular concentration-time curve (AUC) up to the last measured concentration-time point (AUC_{0-24}) was determined using the trapezoidal method. Furthermore, the maximal observed drug concentration (C_{max}) and the terminal half-life ($t_{1/2}$) were determined. Pharmacokinetic parameters were reported as mean ± standard deviation (SD) ($n \geq 3$). Two-sided unpaired Student t-tests were applied on the log-transformed values of the IC_{50}. Relationships between 1) the dFdC or dFdU concentration that was added to HepG2 cells and the intracellular levels of metabolites, 2) the AUC of dFdC-TP/dFdU-TP and the IC_{50} of dFdC/dFdU, 3) the extent of incorporation into DNA/RNA of dFdC-TP/dFdU-TP and the IC_{50} of dFdC/dFdU, and 4) the AUC of dFdC-TP/dFdU-TP and the extent of incorporation into DNA/RNA were assessed by scatter plots and Spearman correlation coefficients. Statistical analysis was performed using SPSS 15.0 (SPSS Inc., Chicago, IL, USA). Differences were considered to be statistically significant when $p < 0.05$.

Results

Cytotoxicity of dFdU is highly dependent on time-period of drug exposure and influenced by expression of hCNT1

The IC_{50} of dFdC and dFdU decreased 13-fold and 196-fold, respectively in HepG2 cells and 3.5-fold and 48-fold, respectively in A549 cells when the exposure time was increased from 72 h to 14 days (Table 1A). The IC_{50} for dFdC at 72 h was about 94,000-fold, 113,000-fold, and 2500-fold lower than for dFdU in HepG2, A549, and MDCK-hCNT1 cells, respectively. THU lowered the IC_{50} of dFdC about 2-fold in HepG2 and A549 cells ($p = 0.005$ for both). The cytotoxicity at 72 h for dFdC and dFdU was about 3 to 4-fold higher in HepG2 compared to A549 cells ($p = 0.005$ for dFdC and $p < 0.001$ for dFdU). hENT1-MDCK cells had a 3-fold higher sensitivity to dFdC compared to mock cells ($p = 0.032$) without significant differences for dFdU (Table 1B). hCNT1-overexpression resulted in a 3 to 4-fold increase in cytotoxicity of dFdC ($p = 0.015$) and dFdU ($p < 0.001$). These data demonstrate that dFdC cytotoxicity is significantly affected by CDA activity and expression of hENT1 and dFdU cytotoxicity is significantly influenced by expression of hCNT1.

Table 1A. IC_{50} of dFdC and dFdU in HepG2 and A549 cells at different time-periods of exposure.

Drug	IC_{50} (nM)	
	HepG2	A549
dFdC		
t = 48 h	16 ± 0.9	47 ± 11
t = 72 h	5.2 ± 0.9	16 ± 1.7
+ 100 µM THU	2.5 ± 0.6	9.2 ± 1.1
t = 96 h	3.2 ± 0.5	9.6 ± 0.1
t = 14 d	0.4 ± 0.07	4.5 ± 0.4
dFdU (x10^3)		
t = 48 h	3126 ± 501	3924 ± 390
t = 72 h	491 ± 32	1812 ± 140
t = 96 h	210 ± 21	1161 ± 180
t = 14 d	2.5 ± 0.3	38 ± 0.6

IC_{50}, inhibitory concentration at 50% cell death; THU, tetrahydrouridine.

Table 1B. IC_{50} of dFdC and dFdU in MDCK-cells at different time-periods of exposure.

Drug	IC_{50} (nM)		
	MDCK-mock	**MDCK-hENT1**	**MDCK-hCNT1**
dFdC			
t = 48 h	412 ± 13	141 ± 16	114 ± 4.0
t = 72 h	262 ± 7.7	93 ± 9.7	33 ± 3.0
t = 96 h	154 ± 58	54 ± 26	46 ± 8.0
dFdU (x10^3)			
t = 48 h	12645 ± 2118	5724 ± 1530	923 ± 54
t = 72 h	2136 ± 33	2067 ± 144	82 ± 7.8
t = 96 h	1041 ± 33	922 ± 44	344 ± 7.4

IC_{50}, inhibitory concentration at 50% cell death.

dFdU induces cell cycle arrest

Figure 2 depicts representative dot plots of HepG2 cells after 48 h treatment with dFdU 0-6000 μM (E-H) and dFdC 0-100 nM (I-L). Similar to dFdC, dFdU caused a concentration dependent arrest in the early S phase. These effects were also time dependent and similar results were found in A549 cells (data not shown).

Nucleosides and nucleotides were simultaneously identified and quantified using a sensitive HPLC assay with UV and radioisotope detection

The nucleosides and nucleotides eluted at the following retention times: dFdC: t = 6.7 min, dFdU: t = 10.3 min, dFdC-MP: t = 14.5 min, dFdU-MP: t = 23 min, dFdC-DP: t = 34 min, dFdU-DP: t = 70 min, dFdC-TP: t = 75 min, and dFdU-TP: t = 81 min. In HepG2 cells, 1 mg of cellular protein corresponded to 12 x 10^6 cells with a volume of 17 fL per cell (n = 36) and to 13 x 10^6 cells with a volume of 14 fL per cell in A549 cells (n = 36). The limit of detection (LOD) for each of the detected metabolites in whole cell lysate was 1.5 fmol, corresponding to 2.5 fmol/mg protein in HepG2 cells, 3.8 fmol/mg protein in A549 cells, and 15 fmol/mg protein in MDCK-hCNT1 cells. The LOD for each metabolite in DNA and RNA was 0.6 fmol, corresponding to 8.0 fmol/mg DNA and 2.0 fmol/mg RNA (HepG2 cells), 8.0 fmol/mg DNA and 2.7 fmol/mg RNA (A549 cells), and 24 fmol/mg DNA and 4.0 fmol/mg RNA (MDCK-hCNT1 cells). No dFdC-MP or dFdU-MP were detected after incubation of [^{3}H]dFdC or [^{3}H]-dFdU with TK1, while [^{3}H]-thymidine was completely phosphorylated to its monophosphate form.

dFdU-TP is intracellularly formed and its accumulation positively correlated with the cytototoxicity of dFdU

The concentration versus time profiles for dFdC, dFdU and phosphorylated metabolites in HepG2 cells and the AUC values after incubation with 0.5 µM dFdU and 0.5 µM dFdC + 100 µM THU are depicted in Figure 2A-D. The PK parameters of all metabolites in all cell lines are summarized in Table 2. In HepG2 cells, the $t_{1/2}$ values for dFdU, dFdC-TP, and dFdU-TP were 13 h, 12 h, and 7 h respectively, demonstrating relatively long retention of these metabolites in the cell (Figure 2, Table 2). The total AUC of dFdC-TP was 1687, 1140, and 547 h*pmol/mg protein contributing to 56%, 67%, and 27% of the total intracellular drug content in HepG2, A549, and MDCK-hCNT1 cells, respectively (Table 2). Co-administration of dFdC with THU in HepG2 cells resulted in a 1.5 to 2-fold increase in intracellular dFdC, dFdC-MP, dFdC-DP, and dFdC-TP, consistent with the higher cytotoxicity of dFdC when co-administered with THU. dFdU-MP, dFdU-DP, and dFdU-TP were the only detected metabolites following incubation with dFdU (Figure 2, Table 2). This demonstrates that dFdU itself enters the cell and is further phosphorylated to its metabolites (Figure 1). The nucleotides of dFdU contributed for 47%, 15%, and 8% to the total intracellular drug content following dFdU treatment in HepG2, A549, and MDCK cells, respectively, demonstrating relatively high phosphorylation of dFdU in HepG2 cells. The total AUC of the dFdU nucleotides following treatment with dFdC + THU was 26-fold and 14-fold higher than after treatment with dFdU in HepG2 and A549 cells, respectively, while intracellular levels of dFdU were not very different. This suggests that the dFdU nucleotides were primarily formed via deamination of dFdC-MP by dCMP deaminase following incubation with dFdC plus THU in these cell lines.

In HepG2 cells, the AUC of dFdC-TP after dFdC treatment increased with the concentration of dFdC in the range from 5 nM-0.5 µM-5 µM ($r = 0.949$, $p = 0.001$). Intracellular drug accumulation increased up to 20 µM dFdC reaching a plateau at higher concentrations (data not shown). The AUC of dFdU-TP after incubation with dFdU increased linearly in the range from 0.5 µM-5 µM-500 µM ($r = 0.949$, $p = 0.001$).

In HepG2 cells treated at the IC_{50} of 5 nM dFdC or 500 µM dFdU, the AUC of dFdC-TP (45 ± 5.4 h*pmol/mg protein) was approximately 7-fold lower than the

AUC of dFdU-TP (309 ± 63 h*pmol/mg protein) after dFdU treatment (Table 2, Figure 3A and B).

The pattern of accumulation of dFdC and its metabolites was dependent on the incubation concentration of dFdC. In HepG2 cells, treated with dFdC at a concentration of 5 nM, dFdC, dFdU, dFdC nucleotides, and dFdU nucleotides contributed for 5%, 1%, 82%, and 12%, respectively to the total recovered intracellular drug content, while these values were 1%, 0.06%, 98% and 0.94%, respectively following incubation at 0.5 µM dFdC. Additionally, C_{max} of dFdC-TP was 2.1 pmol/mg protein (~ 10 µM) at 5 nM dFdC, which increased to 121 pmol/mg protein (~ 556 µM) at 0.5 µM dFdC. This difference in the pattern of dFdC metabolism was also found in MDCK-hCNT1 cells between 0.5 µM and 5 µM dFdC. This suggests that at high dFdC concentrations, resulting in high dFdC-TP concentrations, less deamination of dFdC-MP to dFdU-MP takes place.

Significant inverse correlations were found for the IC_{50} of dFdC with the AUC of dFdC-TP ($r = -0.917$, $p = 0.001$) and for the IC_{50} of dFdU after dFdU treatment with the AUC of dFdU-TP ($r = -0.950$, $p = 0.001$) (Figure 3D and E).

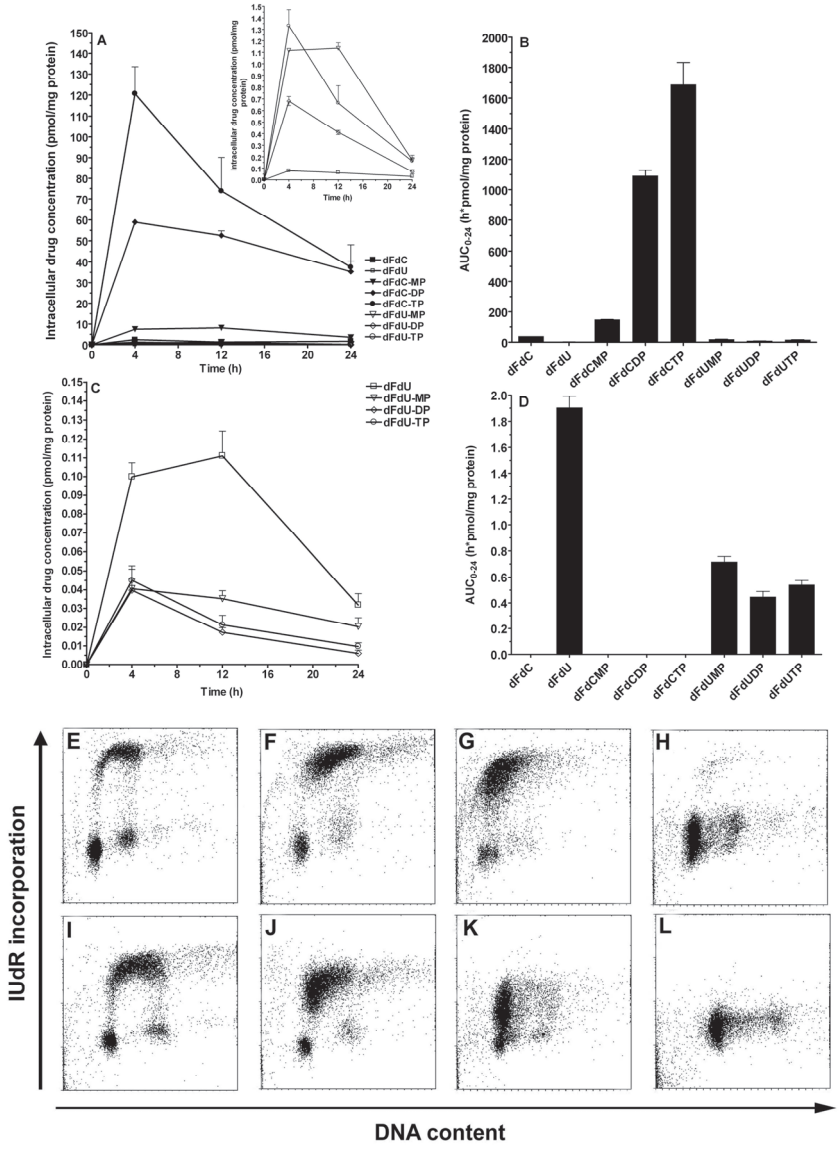

Figure 2. Intracellular concentration versus time profiles of dFdC, dFdU, and phosphorylated metabolites and corresponding $AUC_{0\text{-}24}$ values in HepG2 cells after incubation with 0.5 µM dFdC + 100 µM THU (A and B) and 0.5 µM dFdU (C and D). The insert in Figure A depicts the profiles for dFdU and its phosphorylated metabolites only. Effects on cell cycle distribution after 48 h are depicted for control (untreated) cells (E and I) and after treatment with dFdU 500 µM (F), 1000 µM (G), and 6000 µM (H), and dFdC 10 nM (J), 20 nM (K), and 100 nM (L). Cells were labeled with IUdR for determination of the S-phase fraction (top region, positive for IUdR) and stained with PI for distinguishing G_1 (bottom left region) from G_2-M cells (bottom right region).

Table 2. PK of dFdC, dFdU and their nucleotides and DNA and RNA incorporation in cell lines. Data are presented as mean ± SD.

HepG2								
5 nM dFdC + THU	**dFdC**	**dFdU**	**dFdC-MP**	**dFdC-DP**	**dFdC-TP**	**dFdU-MP**	**dFdU-DP**	**dFdU-TP**
C_{max} (pmol/mg protein)	0.2 ± 0.01	0.03 ± 0.01	0.5 ± 0.05	1.4 ± 0.2	2.1 ± 0.1	0.3 ± 0.1	0.2 ± 0.04	0.3 ± 0.03
$AUC_{0\text{-}24}$ (h*pmol/mg protein)	6.3 ± 0.5	1.0 ± 0.1	14 ± 0.7	44 ± 5.4	45 ± 5.4	6.7 ± 1.4	4.0 ± 0.7	5.0 ± 0.4
0.5 µM dFdC + THU	**dFdC**	**dFdU**	**dFdC-MP**	**dFdC-DP**	**dFdC-TP**	**dFdU-MP**	**dFdU-DP**	**dFdU-TP**
C_{max} (pmol/mg protein)	2.5 ± 0.4	0.1 ± 0.01	8.2 ± 0.3	59 ± 1.0	121 ± 13	1.1 ± 0.04	0.7 ± 0.04	1.3 ± 0.1
$AUC_{0\text{-}24}$ (h*pmol/mg protein)	38 ± 0.2	1.2 ± 0.2	148 ± 2.3	1090 ± 64	1687 ± 253	19 ± 0.7	8.6 ± 0.4	16 ± 2.2
$t_{1/2}$ (h)	n.d.	13 ± 1.9	10 ± 2.1	33 ± 18	12 ± 0.7	6.0 ± 0.5	6.0 ± 0.6	7.0 ± 0.9
DNA (pmol/µmol)	n.a.	n.a.	n.a.	n.a.	1600 ± 300	n.a.	n.a.	20 ± 1.0
RNA (pmol/µmol)	n.a.	n.a.	n.a.	n.a.	400 ± 30	n.a.	n.a.	10 ± 2.0
0.5 µM dFdU	**dFdC**	**dFdU**	**dFdC-MP**	**dFdC-DP**	**dFdC-TP**	**dFdU-MP**	**dFdU-DP**	**dFdU-TP**
C_{max} (pmol/mg protein)	n.d.	0.1 ± 0.01	n.d.	n.d.	n.d.	0.04 ± 0.01	0.04 ± 0.01	0.05 ± 0.01
$AUC_{0\text{-}24}$ (h*pmol/mg protein)	n.d.	1.9 ± 0.2	n.d.	n.d.	n.d.	0.7 ± 0.1	0.5 ± 0.1	0.5 ± 0.1
$t_{1/2}$ (h)	n.d.	10 ± 0.9	n.d.	n.d.	n.d.	21 ± 7.0	8.0 ± 0.8	9.0 ± 2.0
DNA (pmol/µmol)	n.a.	n.a.	n.a.	n.a.	n.a.	n.a.	n.a.	10 ± 2.0
RNA (pmol/µmol)	n.a.	n.a.	n.a.	n.a.	n.a.	n.a.	n.a.	6.0 ± 1.0
500 µM dFdU	**dFdC**	**dFdU**	**dFdC-MP**	**dFdC-DP**	**dFdC-TP**	**dFdU-MP**	**dFdU-DP**	**dFdU-TP**
C_{max} (pmol/mg protein)	n.d.	74 ± 9.0	n.d.	n.d.	n.d.	45 ± 3	21 ± 2.6	15 ± 3.4
$AUC_{0\text{-}24}$ (h*pmol/mg protein)	n.d.	2090 ± 167	n.d.	n.d.	n.d.	1098 ± 58	557 ± 45	309 ± 63

Table 2. Continued.

A549								
0.5 µM dFdC + THU	**dFdC**	**dFdU**	**dFdC-MP**	**dFdC-DP**	**dFdC-TP**	**dFdU-MP**	**dFdU-DP**	**dFdU-TP**
C_{max} (pmol/mg protein)	0.8 ± 0.1	0.3 ± 0.1	4.6 ± 1.0	26 ± 4.6	64 ± 13	0.1 ± 0.03	0.2 ± 0.06	0.3 ± 0.03
$AUC_{0\text{-}24}$ (h*pmol/mg protein)	14 ± 1.3	5.7 ± 1.4	80 ± 8	446 ± 47	1140 ± 184	1.6 ± 0.2	4.0 ± 0.8	4.9 ± 0.1
DNA (pmol/µmol)	n.a.	n.a.	n.a.	n.a.	910 ± 11	n.a.	n.a.	n.a.
RNA (pmol/µmol)	n.a.	n.a.	n.a.	n.a.	130 ± 30	n.a.	n.a.	n.a.
0.5 µM dFdU	**dFdC**	**dFdU**	**dFdC-MP**	**dFdC-DP**	**dFdC-TP**	**dFdU-MP**	**dFdU-DP**	**dFdU-TP**
C_{max} (pmol/mg protein)	n.d.	0.2 ± 0.1	n.d.	n.d.	n.d.	0.03 ± 0.01	0.02 ± 0.001	0.002 ± 0.001
$AUC_{0\text{-}24}$ (h*pmol/mg protein)	n.d.	3.3 ± 0.4	n.d.	n.d.	n.d.	0.3 ± 0.03	0.1 ± 0.02	0.03 ± 0.02
DNA (pmol/µmol)	n.a.	n.a.	n.a.	n.a.	n.a.	n.a.	n.a.	5.0 ± 0.6
RNA (pmol/µmol)	n.a.	n.a.	n.a.	n.a.	n.a.	n.a.	n.a.	0.7 ± 0.4
MDCK-hCNT1								
0.5 µM dFdC + THU	**dFdC**	**dFdU**	**dFdC-MP**	**dFdC-DP**	**dFdC-TP**	**dFdU-MP**	**dFdU-DP**	**dFdU-TP**
C_{max} (pmol/mg protein)	7.3 ± 1.4	24 ± 5	15 ± 0.8	61 ± 7.7	66 ± 6.1	6.6 ± 0.6	4.7 ± 0.4	7.5 ± 0.3
$AUC_{0\text{-}24}$ (h*pmol/mg protein)	62 ± 11	387 ± 80	184 ± 19	576 ± 46	547 ± 42	110 ± 16	56 ± 7.2	70 ± 2.4
DNA (pmol/µmol)	n.a.	n.a.	n.a.	n.a.	400 ± 60	n.a.	n.a.	5.0 ± 0.8
RNA (pmol/µmol)	n.a.	n.a.	n.a.	n.a.	80 ± 10	n.a.	n.a.	2.0 ± 0.5
0.5 µM dFdU	**dFdC**	**dFdU**	**dFdC-MP**	**dFdC-DP**	**dFdC-TP**	**dFdU-MP**	**dFdU-DP**	**dFdU-TP**
C_{max} (pmol/mg protein)	n.d.	35 ± 3.7	n.d.	n.d.	n.d.	0.6 ± 0.1	0.5 ± 0.1	0.6 ± 0.1
$AUC_{0\text{-}24}$ (h*pmol/mg protein)	n.d.	630 ± 26	n.d.	n.d.	n.d.	11 ± 0.5	8.0 ± 0.9	6.6 ± 0.7
DNA (pmol/µmol)	n.a.	n.a.	n.a.	n.a.	n.a.	n.a.	n.a.	20 ± 2.0
RNA (pmol/µmol)	n.a.	n.a.	n.a.	n.a.	n.a.	n.a.	n.a.	10 ± 2.0

n.a., not applicable; n.d., not detectable.

dFdU-TP is incorporated into DNA and RNA and its incorporation positively correlates with the cytotoxicity of dFdU

Both dFdC-TP and dFdU-TP were incorporated into nucleic acids favoring DNA over RNA (Table 2). Strong inverse correlations were found for the IC_{50} for dFdC with the amount of incorporated dFdC-TP into DNA ($r = -0.856$, $p = 0.003$) and RNA ($r = -0.933$, $p = 0.001$) and for the IC_{50} for dFdU following dFdU treatment with the amount of incorporated dFdU-TP into DNA ($r = -0.850$, $p = 0.004$) and RNA ($r = -0.910$, $p = 0.001$) (Figure 3F and G). As expected, significant positive correlations were found for the AUC of dFdC-TP and the extent of incorporation of dFdC-TP into DNA ($r = 0.867$, $p = 0.002$) and RNA ($r = 0.933$, $p = 0.001$) and for the AUC of dFdU-TP after treatment with dFdU with the extent of incorporation of dFdU-TP into DNA ($r = 0.942$, $p = 0.001$) and RNA ($r = 0.900$, $p = 0.001$).

In HepG2 cells treated at IC_{50} concentrations of dFdC or dFdU, the amount of dFdC-TP incorporated into DNA was only 1.3-fold lower ($p = 0.05$) compared to the amount of dFdU-TP incorporated into DNA following dFdU treatment (Figure 3C and Table 2), suggesting equal intrinsic toxicity of dFdC-TP and dFdU-TP. The ratio's of the amount of dFdC-TP in DNA over the AUC of dFdC-TP and the amount of dFdU-TP in DNA over the AUC of dFdU-TP were 0.22 and 0.04, respectively, suggesting 5.5-fold higher efficiency of dFdC-TP than dFdU-TP for incorporation into DNA. In addition, the ratio of dFdU-TP in DNA over the AUC of dFdU-TP was 0.008 after 5 nM dFdC, which was 5-fold lower than after treatment with 500 μM dFdU, probably because of the lack of competition between dFdU-TP and dFdC-TP for incorporation following dFdU treatment.

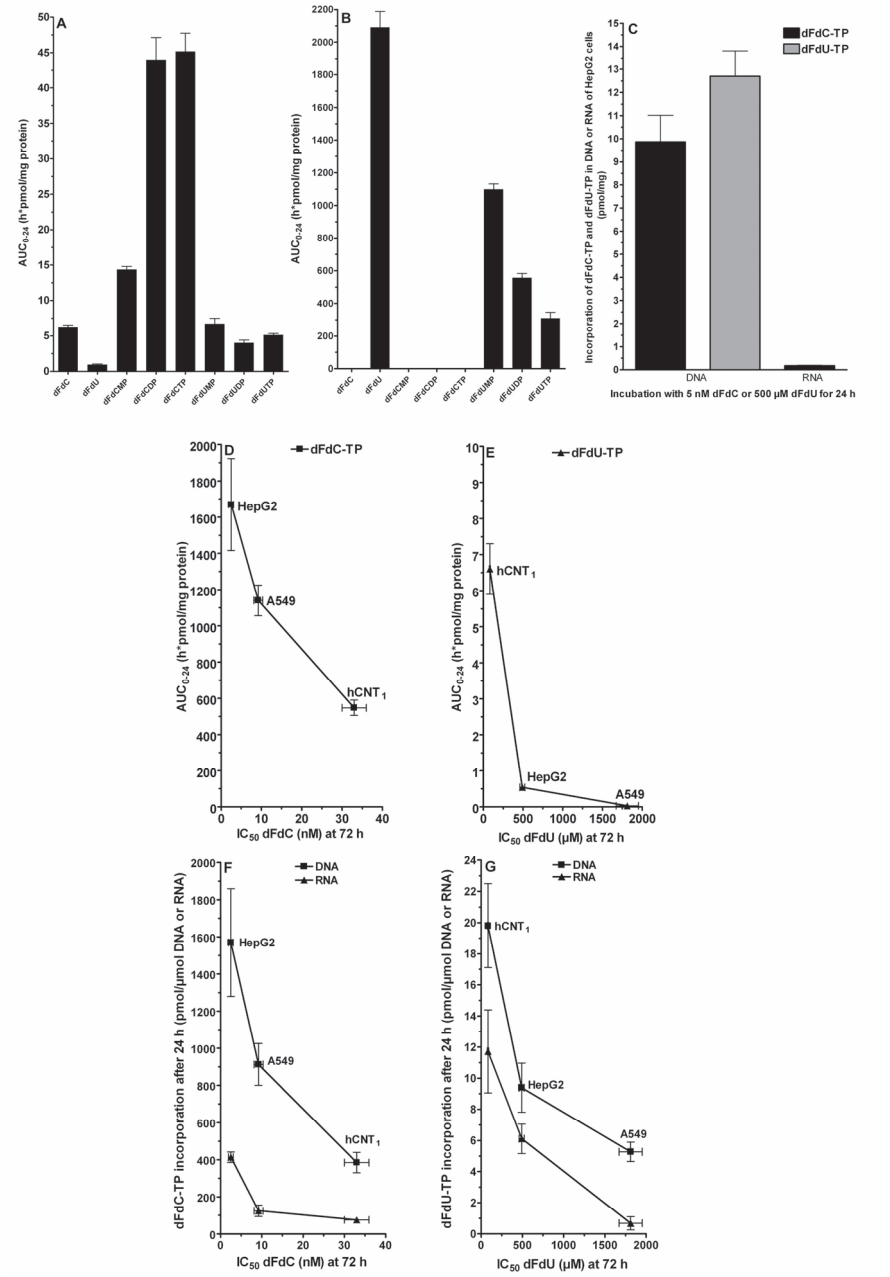

Figure 3. AUC values of dFdC, dFdU, and nucleotides in HepG2 cells after 5 nM dFdC (A), 500 µM dFdU (B) and nucleic acid incorporation of dFdC-TP and dFdU-TP (C). Relationships between the $AUC_{0\text{-}24}$ of dFdC-TP (D) and dFdU-TP (E) and extent of DNA and RNA incorporation of dFdC-TP (F) and dFdU-TP (G) with the IC_{50} values of dFdC and dFdU in HepG2, A549, and MDCK-hCNT1 cells. Incorporation of dFdU-TP into RNA was below the LOQ.

Transport of dFdU and dFdC is mediated by hCNT1

The uptake of dFdC and dFdU significantly increased with the concentration of the drugs (Figure 4). Transport of both dFdC and dFdU was significantly enhanced in the presence of sodium, required as co-transporter for hCNT1-mediated transport (Figure 4A). As expected, uptake of dFdC and dFdU in MDCK-hCNT1 cells in the absence of sodium decreased to levels comparable with those in the MDCK-mock cells (Figure 4A and 4B).

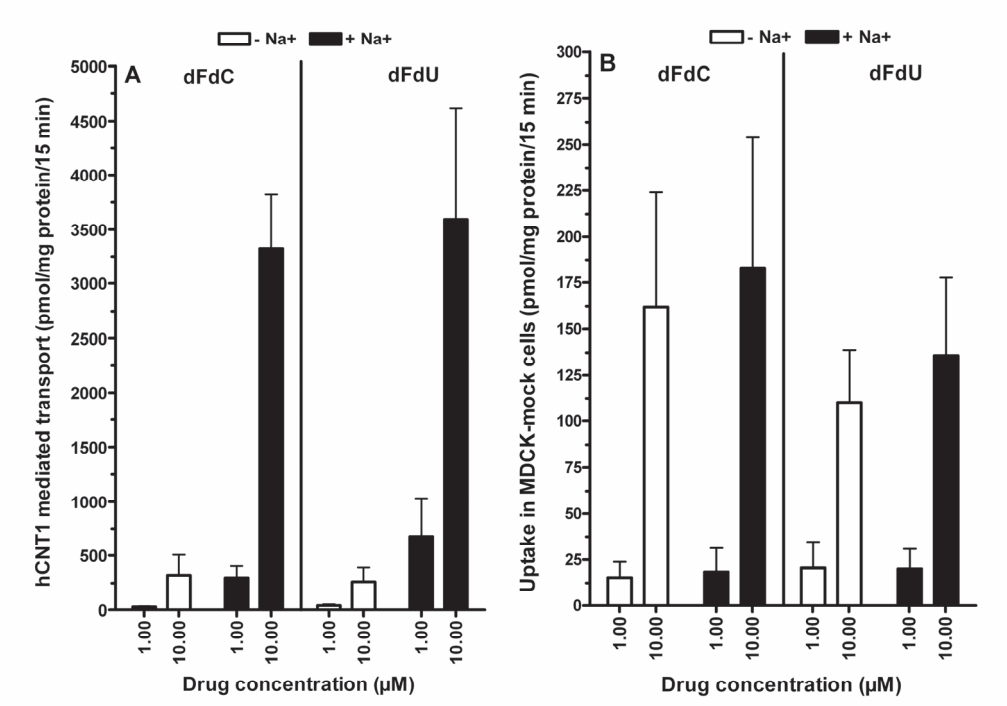

Figure 4. Uptake of dFdC and dFdU in MDCK-hCNT1 (A) and MDCK-mock (B) cells in the presence and absence of sodium.

dFdU and dFdC are effluxed

After loading the HepG2 and A549 cells and release in drug-free medium, intracellular concentrations of dFdC rapidly decreased to 10% of the initial concentration within 10 min without significant formation of dFdU and phosphorylated metabolites. In HepG2 cells, the elimination pattern of dFdC and dFdU was biphasic with a rapid elimination during the first 10 min ($t_{1/2,\alpha}$ = 2.6 min)

followed by a slower elimination from 10 to 60 min ($t_{1/2,\beta}$ = 28 min). Elimination of dFdU was also biphasic with an initial rapid elimination ($t_{1/2,\alpha}$ = 9.2 min) followed by a slower elimination ($t_{1/2,\beta}$ = 90 min). These results demonstrate that dFdC and dFdU were rapidly effluxed with a slower elimination rate of dFdU compared to dFdC.

Discussion

This is the first study that demonstrates the formation of dFdU-MP, dFdU-DP and dFdU-TP from dFdC and dFdU. It shows that dFdU is a good substrate for hCNT1 and is intracellularly phosphorylated and incorporated into DNA and RNA. The AUC and extent of incorporation of dFdU-TP and dFdC-TP into DNA and RNA inversely correlate with the IC_{50} of dFdU and dFdC, respectively.

The IC_{50} values for dFdC and dFdU in our study were somewhat higher compared to the IC_{50} values at 48h for dFdC of 0.6-11 nM in A2780, C26-10, and WiDr cell lines (28) and the IC_{50} value at 24 h for dFdU of 252 µM in H292 cells (29). This could be due to differences in expression/activity of uptake and efflux transporters and in metabolic enzymes. The IC_{50} for dFdU of 2.5 µM (~660 ng/mL) following 14 days incubation was of the same order of magnitude as the plasma concentrations of dFdU (~700 ng/mL) in patients treated with multiple low doses of oral dFdC in our phase I study. Treatment with dFdU clearly caused an arrest of cells in the early S phase, consistent with findings in ECV304 and H292 cells (29).

The relatively high amount of dFdU nucleotides in HepG2 cells treated at 5 nM dFdC (corresponding with 10 µM dFdC-TP) compared to the higher 0.5 µM dFdC concentration (corresponding with 556 µM dFdC-TP) was possibly due to less inhibition of dCMP deaminase by dFdC-TP, leading to increased deamination of dFdC-MP. dFdC-TP concentrations of 460 µM were shown to cause 50% inhibition of dCMP deaminase activity (11). The intracellular concentrations of dFdC-DP of 271 µM in HepG2 cells and 132 µM in A549 cells likely caused maximal inhibition of RR, since the IC_{50} for inhibition of RR was shown to be 0.3 µM following dFdC treatment (9). The dFdC-TP concentrations of 10 pmol/10^6 cells in HepG2 cells and 5 pmol/10^6 cells in A549 cells at 4 h treatment with 0.5 µM dFdC were somewhat lower compared to the dFdC-TP values of 40 pmol/10^6

A2780 cells, 20 pmol/10^6 WiDr cells, and 20 pmol/10^6 C26-10 cells following 4 h incubation with 1.0 µM dFdC (28), consistent with the higher IC_{50} values found in our investigated solid tumor cell lines. The higher uptake of dFdC and dFdU in HepG2 compared to A549 cells might have been associated with the higher gene expression of hCNT1 in HepG2 than in A549 cells measured by QT-PCR (data not shown).

In patients who were treated with 8 mg oral dFdC in our phase I study, plasma concentrations of dFdC were close to 1 ng/mL (~ 4 nM) and the AUC_{0-24} of dFdC-TP was 78 h*pmol/mg protein in PBMCs, which was comparable to the AUC_{0-24} in HepG2 cells of 45 h*pmol/mg protein after 5 nM dFdC. The AUC_{0-24} of dFdU-TP in PBMCs was 129 h*pmol/mg protein and increased to 927 h*pmol/mg protein following daily oral dosing for 14 days, which was 182-fold higher compared to the dFdU-TP AUC_{0-24} of 5.1 h*pmol/mg protein after 5 nM dFdC and 3-fold higher than the dFdU-TP AUC_{0-24} of 309 h*pmol/mg protein after 500 µM dFdU in HepG2 cells. Thus, *in vivo* in patients there is a relatively high exposure to dFdU-TP in PBMCs, possibly due to differences in uptake, efflux, and biotransformation of dFdC and/or dFdU between PBMCs and human solid tumor cell lines.

Both dFdC and dFdU were effluxed from HepG2 and A549 cells, possibly by hENT1, which was found to be expressed in both cell lines in the QT-PCR experiments (data not shown). The presence of dFdC-MP, dFdU-MP and dFdU-TP in the medium suggest that cells are able to efflux nucleoside phosphates. To our knowledge only multidrug resistance protein (MRP) 4 and 5 were shown to transport nucleoside monophosphates but with low affinity and without having significant effects on resistance to dFdC (30-32). Further studies should elucidate possible efflux transporters for these compounds. Theoretically, THU might have inhibited in part the uptake of dFdC and dFdU by inhibition of hNTs after simultaneous administration. However, this is unlikely based on the increase in uptake and cytotoxicity of dFdC after co-incubation with THU in this study, consistent with previous findings for cytarabine plus THU in hepatocytes (33).

This study demonstrated high transport of dFdU by hCNT1, which is highly expressed in liver (18, 34), kidney (35, 36), and intestine (37, 38). This might cause high (re)uptake of dFdU into the liver in patients, leading to high exposures to dFdU in the liver for prolonged periods of time. Cytotoxicity of dFdU in MDCK-

hCNT1 cells highly exceeded the cytotoxicity in hENT1 cells, consistent with the high transport of dFdU by hCNT1 (7, 15).

This study clearly demonstrated phosphorylation of dFdU to its nucleotides in all tested cell lines in contrast to previous statements (10). No phosphorylation of dFdU to dFdU-MP by cytosolic TK1 was observed, consistent with the low affinity of dFdU for TK1 (39). Possibly, dFdU is phosphorylated in part by other cytosolic enzymes and/or by TK2 in mitochondria, which warrants further investigation.

In conclusion, the unique new findings of this study are: 1) the high uptake of dFdU by hCNT1, 2) the formation of dFdU-DP and dFdU-TP from dFdC and dFdU, 3) the incorporation of dFdU-TP into DNA and RNA, and 4) the significant correlations between the AUC and DNA/RNA incorporation of dFdC-TP/dFdU-TP and the cytotoxicity of dFdC and dFdU. High exposure levels to dFdU combined with significant phosphorylation to dFdU-TP and high levels of incorporation of dFdU-TP into DNA/RNA could contribute to the toxicity and or antitumor activity of dFdC *in vivo*, which warrant further investigation.

Acknowledgements

We thank Stefan Vink for support with the flow cytometry analysis and Eli Lilly for providing dFdC, dFdU and phosphorylated metabolites.

References

1. Hertel LW, Boder GB, Kroin JS, et al. Evaluation of the antitumor activity of gemcitabine (2',2'-difluoro-2'-deoxycytidine). Cancer Res 1990;50:4417-22.

2. Noble S, Goa KL. Gemcitabine. A review of its pharmacology and clinical potential in non-small cell lung cancer and pancreatic cancer. Drugs 1997;54:447-72.

3. Braakhuis BJ, van Dongen GA, Vermorken JB, Snow GB. Preclinical in vivo activity of 2',2'-difluorodeoxycytidine (Gemcitabine) against human head and neck cancer. Cancer Res 1991;51:211-4.

4. Heinemann V, Hertel LW, Grindey GB, Plunkett W. Comparison of the cellular pharmacokinetics and toxicity of 2',2'-difluorodeoxycytidine and 1-beta-D-arabinofuranosylcytosine. Cancer Res 1988;48:4024-31.

5. Grunewald R, Kantarjian H, Du M, Faucher K, Tarassoff P, Plunkett W. Gemcitabine in leukemia: a phase I clinical, plasma, and cellular pharmacology study. J Clin Oncol 1992;10:406-13.

6. Boven E, Schipper H, Erkelens CA, Hatty SA, Pinedo HM. The influence of the schedule and the dose of gemcitabine on the anti-tumour efficacy in experimental human cancer. Br J Cancer 1993;68:52-6.

7. Mackey JR, Yao SY, Smith KM, et al. Gemcitabine transport in xenopus oocytes expressing recombinant plasma membrane mammalian nucleoside transporters. J Natl Cancer Inst 1999;91:1876-81.

8. Huang P, Chubb S, Hertel LW, Grindey GB, Plunkett W. Action of 2',2'-difluorodeoxycytidine on DNA synthesis. Cancer Res 1991;51:6110-7.

9. Heinemann V, Xu YZ, Chubb S, et al. Inhibition of ribonucleotide reduction in CCRF-CEM cells by 2',2'-difluorodeoxycytidine. Mol Pharmacol 1990;38:567-72.

10. Plunkett W, Huang P, Xu YZ, Heinemann V, Grunewald R, Gandhi V. Gemcitabine: metabolism, mechanisms of action, and self-potentiation. Semin Oncol 1995;22:3-10.

11. Heinemann V, Xu YZ, Chubb S, et al. Cellular elimination of 2',2'-difluorodeoxycytidine 5'-triphosphate: a mechanism of self-potentiation. Cancer Res 1992;52:533-9.

12. Camiener GW, Smith CG. Studies of the enzymatic deamination of cytosine arabinoside. I. Enzyme distribution and species specificity. Biochem Pharmacol 1965;14:1405-16.

13. Pastor-Anglada M, Molina-Arcas M, Casado FJ, Bellosillo B, Colomer D, Gil J. Nucleoside transporters in chronic lymphocytic leukaemia. Leukemia 2004;18:385-93.

14. Mackey JR, Mani RS, Selner M, et al. Functional nucleoside transporters are required for gemcitabine influx and manifestation of toxicity in cancer cell lines. Cancer Res 1998;58:4349-57.

15. Garcia-Manteiga J, Molina-Arcas M, Casado FJ, Mazo A, Pastor-Anglada M. Nucleoside transporter profiles in human pancreatic cancer cells: role of hCNT1 in 2',2'-difluorodeoxycytidine- induced cytotoxicity. Clin Cancer Res 2003;9:5000-8.

16. Spratlin J, Sangha R, Glubrecht D, et al. The absence of human equilibrative nucleoside transporter 1 is associated with reduced survival in patients with gemcitabine-treated pancreas adenocarcinoma. Clin Cancer Res 2004;10:6956-61.

17. Huang QQ, Yao SY, Ritzel MW, Paterson AR, Cass CE, Young JD. Cloning and functional expression of a complementary DNA encoding a mammalian nucleoside transport protein. J Biol Chem 1994;269:17757-60.

18. Govindarajan R, Bakken AH, Hudkins KL, et al. In situ hybridization and immunolocalization of concentrative and equilibrative nucleoside transporters in the human intestine, liver, kidneys, and placenta. Am J Physiol Regul Integr Comp Physiol 2007;293:R1809-22.

19. Lai Y, Bakken AH, Unadkat JD. Simultaneous expression of hCNT1-CFP and hENT1-YFP in Madin-Darby canine kidney cells. Localization and vectorial transport studies. J Biol Chem 2002;277:37711-7.

20. Voigt W. Sulforhodamine B assay and chemosensitivity. Methods Mol Med 2005;110:39-48.

21. Skehan P, Storeng R, Scudiero D, et al. New colorimetric cytotoxicity assay for anticancer-drug screening. J Natl Cancer Inst 1990;82:1107-12.

22. Begg AC, Moonen L, Hofland I, Dessing M, Bartelink H. Human tumour cell kinetics using a monoclonal antibody against iododeoxyuridine: intratumour sampling variations. Radiother Oncol 1988;11:337-47.

23. Bradford MM. A rapid and sensitive method for the quantitation of microgram quantities of protein utilizing the principle of protein-dye binding. Anal Biochem 1976;72:248-54.

24. Cohen RM, Wolfenden R. Cytidine deaminase from Escherichia coli. Purification, properties and inhibition by the potential transition state analog 3,4,5,6-tetrahydrouridine. J Biol Chem 1971;246:7561-5.

25. Stoller RG, Myers CE, Chabner BA. Analysis of cytidine deaminase and tetrahydrouridine interaction by use of ligand techniques. Biochem Pharmacol 1978;27:53-9.

26. Laliberte J, Marquez VE, Momparler RL. Potent inhibitors for the deamination of cytosine arabinoside and 5-aza-2'-deoxycytidine by human cytidine deaminase. Cancer Chemother Pharmacol 1992;30:7-11.

27. Lai Y, Tse CM, Unadkat JD. Mitochondrial expression of the human equilibrative nucleoside transporter 1 (hENT1) results in enhanced mitochondrial toxicity of antiviral drugs. J Biol Chem 2004;279:4490-7.

28. Ruiz van Haperen VW, Veerman G, Boven E, Noordhuis P, Vermorken JB, Peters GJ. Schedule dependence of sensitivity to 2',2'-difluorodeoxycytidine (Gemcitabine) in relation to accumulation and retention of its triphosphate in solid tumour cell lines and solid tumours. Biochem Pharmacol 1994;48:1327-39.

29. Pauwels B, Korst AE, Pattyn GG, et al. Cell cycle effect of gemcitabine and its role in the radiosensitizing mechanism in vitro. Int J Radiat Oncol Biol Phys 2003;57:1075-83.

30. Reid G, Wielinga P, Zelcer N, et al. Characterization of the transport of nucleoside analog drugs by the human multidrug resistance proteins MRP4 and MRP5. Mol Pharmacol 2003;63:1094-1103.

31. Chen ZS, Lee K, Walther S, et al. Analysis of methotrexate and folate transport by multidrug resistance protein 4 (ABCC4): MRP4 is a component of the methotrexate efflux system. Cancer Res 2002;62:3144-50.

32. Pratt S, Shepard RL, Kandasamy RA, Johnston PA, Perry W III, Dantzig AH. The multidrug resistance protein 5 (ABCC5) confers resistance to 5-fluorouracil and transports its monophosphorylated metabolites. Mol Cancer Ther 2005;4:855-63.

33. Riva C, Barra Y, Carcassonne Y, Cano JP, Rustum Y. Effect of tetrahydrouridine on metabolism and transport of 1-beta-D-arabinofuranosylcytosine in human cells. Chemotherapy 1992;38:358-66.

34. Ritzel MW, Yao SY, Ng AM, Mackey JR, Cass CE, Young JD. Molecular cloning, functional expression and chromosomal localization of a cDNA encoding a human Na+/nucleoside cotransporter (hCNT2) selective for purine nucleosides and uridine. Mol Membr Biol 1998;15:203-11.

35. Wang J, Su SF, Dresser MJ, Schaner ME, Washington CB, Giacomini KM. Na(+)-dependent purine nucleoside transporter from human kidney: cloning and functional characterization. Am J Physiol 1997;273:F1058-65.

36. Gutierrez MM, Brett CM, Ott RJ, Hui AC, Giacomini KM. Nucleoside transport in brush border membrane vesicles from human kidney. Biochim Biophys Acta 1992;1105:1-9.

37. Patil SD, Unadkat JD. Sodium-dependent nucleoside transport in the human intestinal brush-border membrane. Am J Physiol 1997;272:G1314-20.

38. Chandrasena G, Giltay R, Patil SD, Bakken A, Unadkat JD. Functional expression of human intestinal Na+-dependent and Na+-independent nucleoside transporters in Xenopus laevis oocytes. Biochem Pharmacol 1997;53:1909-18.

39. Wang J, Su C, Neuhard J, Eriksson S. Expression of human mitochondrial thymidine kinase in Escherichia coli: correlation between the enzymatic activity of pyrimidine nucleoside analogues and their inhibitory effect on bacterial growth. Biochem Pharmacol 2000;59:1583-8.

Chapter 3.2

Extensive metabolism and liver accumulation of gemcitabine following multiple oral and intravenous administration in mice

Submitted for publication

Stephan A. Veltkamp

Dick Pluim

Olaf van Tellingen

Jos H. Beijnen

Jan H.M. Schellens

Abstract

In a clinical study with oral gemcitabine (2',2'-difluorodeoxycytidine, dFdC), we found that gemcitabine was hepatotoxic and extensively metabolized to 2',2'-difluorodeoxyuridine (dFdU) after continuous oral dosing. The main metabolite dFdU had a long terminal half-life in particular after oral administration. Our hypothesis was that dFdU and/or phosphorylated metabolites of gemcitabine accumulated in the liver after multiple oral dosing.

In this study, mice were treated with oral or i.v. dFdC administered at a single dose (1qdx1d) or at multiple doses once daily for 7 days (1qdx7d) or seven times daily (7qdx1d). Plasma, liver, kidneys, and lungs were collected at several time-points. Urine samples were collected after i.v. administration of dFdC and peripheral blood mononuclear cells after 7qdx1d dosing of dFdC. The nucleosides dFdC and dFdU as well as the nucleotides dFdC-MP, dFdC-DP, dFdC-TP, dFdU-MP, dFdU-DP, and dFdU-TP were simultaneously quantified by high performance liquid chromatography with ultraviolet and radioisotope detection.

We demonstrate that phosphorylated metabolites of both dFdC and dFdU are formed in mice, primarily consisting of dFdC-MP, dFdC-TP and dFdU-TP. Interestingly, multiple dosing of dFdC leads to substantial hepatic and renal accumulation of dFdC-TP and dFdU-TP, which has a more pronounced liver accumulation after oral than after i.v. dosing. The presence of dFdC-MP, dFdC-TP and dFdU-TP in plasma and urine suggests efflux of these potentially toxic metabolites. Our results show that dFdU, dFdC-TP, and dFdU-TP accumulate in the liver after multiple dosing of dFdC and might contribute to the hepatotoxicity of oral dFdC, which warrants further investigation.

Introduction

Gemcitabine (2',2'-difluorodeoxycytidine, dFdC), a pyrimidine nucleoside anticancer drug, is used in the treatment of patients with a variety of solid tumors (1, 2). Transport by human nucleoside transporters (hNTs) enables dFdC to enter cells (3). Gemcitabine is intracellularly phosphorylated by deoxycytidine kinase (dCK) to its monophosphate (dFdC-MP) and subsequently into its active diphosphate and triphosphate metabolites (4). Gemcitabine triphosphate (dFdC-TP) is incorporated into DNA (5), thereby competing with the natural substrate deoxycytidine triphosphate (dCTP), resulting in inhibition of DNA synthesis (6). In addition, gemcitabine diphosphate (dFdC-DP) inhibits ribonucleotide reductase (RR), which depletes dCTP pools en facilitates incorporation of dFdC-TP into DNA. Also, dFdC can potentiate its own cytotoxic effect via multiple mechanisms of action (7, 8). Alternatively, dFdC is deaminated to 2',2'-difluorodeoxyuridine (dFdU) by cytidine deaminase (CDA), which is highly expressed in human liver an mice kidney (9).

In a clinical study, dFdC was orally administered at continuous dosing regimens at low dose-levels in patients with advanced solid tumors (submitted). The exposure to dFdC was low due to extensive first-pass metabolism to dFdU. Additionally, we found dFdU triphosphate (dFdU-TP) at high exposure levels in peripheral blood mononuclear cells (PBMCs). One patient treated with 8 mg oral dFdC once-daily for 14 days of a 21-day cycle experienced severe hepatic and renal toxicity and died on day 13 of the second cycle. Pathological examination revealed severe drug induced liver necrosis. Pharmacokinetic analysis demonstrated a long terminal half-life of dFdU of 89 h possibly as a result of liver accumulation and slow release into the plasma. Based on these findings, we hypothesized that continuous daily oral dosing of dFdC results in liver accumulation of dFdU and/or phosphorylated metabolites in patients, possibly associated with the hepatotoxicity of dFdC. We recently found that dFdU is efficiently transported by the human concentrative nucleoside transporter type 1 (hCNT1), which is highly expressed in kidney and liver (10). Furthermore, dFdU was found to be phosphorylated to its monophosphate (dFdU-MP), diphosphate (dFdU-DP) and triphosphate (dFdU-TP). Interestingly, dFdU-TP was incorporated into DNA and RNA, which correlated with the cytotoxicity of dFdU (submitted). The chemical structures of dFdC and

dFdU as well as the proposed biotransformation and pharmacological mechanisms of action of dFdC and metabolites are depicted in Figure 1.

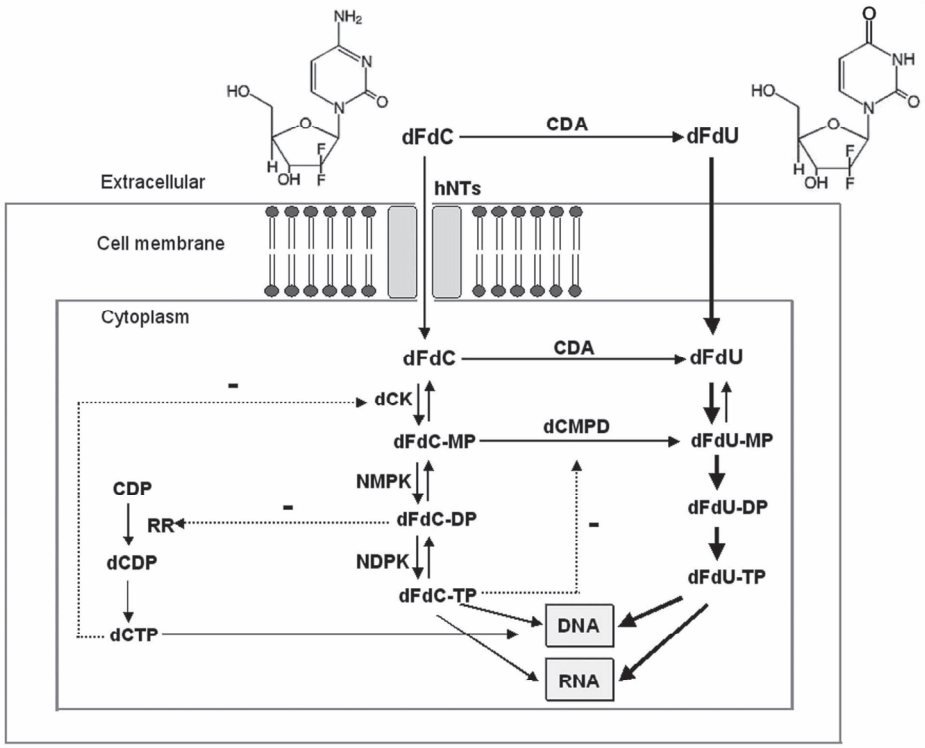

Figure 1. Chemical structures of dFdC and dFdU and proposed biotransformation and pharmacological actions of dFdC and its metabolites. dFdC is taken up by hNTs and phosphorylated by deoxycytidine kinase (dCK) to its monophosphate (dFdC-MP), and by human nucleoside monophosphate and diphosphate kinases (NMPK and NDPK) into its diphosphate (dFdC-DP) and triphosphate (dFdC-TP) metabolites. dFdC-TP is incorporated into RNA and particularly into DNA, thereby competing with deoxycytidine triphosphate (dCTP) for incorporation. dFdC-DP inhibits ribonucleotide reductase (RR), which inhibits the conversion of cytidine diphosphate (CDP) to deoxycytidine diphosphate (dCDP) and depletes dCTP pools resulting in less inhibition of dCK and stimulation of phosphorylation of dFdC. dFdC is deaminated by cytidine deaminase (CDA) to 2',2'-difluorodeoxyuridine (dFdU). dFdC-MP is converted to difluorodeoxyuridine monophosphate (dFdU-MP) by deoxycytidylate deaminase (dCMPD). dFdC-TP can inhibit dCMPD thereby decreasing deamination of dFdC-MP. Both dFdC, dFdC-MP, dFdC-DP, dFdC-TP, and dFdU monophosphate (dFdU-MP), diphosphate (dFdU-DP), and triphosphate (dFdU-TP) were formed *in vivo* (present study). In vitro studies revealed that dFdU is a high affinity substrate for transport by hCNT1 and is phosphorylated to dFdU-TP and incorporated into DNA and RNA (submitted).

Shipley and colleagues investigated the pharmacokinetics (PK) of dFdC in plasma after single i.v. administration at a dose of 20 mg/kg (11). However, no phosphorylated metabolites were quantified and no drug exposures in tissues were determined. Dose-responsive intestinal lesions and hepatotoxicity were found in mice after single oral dFdC administration at high doses of 333-500 mg/kg (12).
The aims of this study were to assess the PK and metabolism of dFdC in mice and to investigate whether the drug accumulates in the liver following multiple oral and i.v. dosing of dFdC, which we couldn't measure in patients. Gemcitabine was administered to mice at a low dose-level of 0.1 mg/kg to compare the PK to that in patients treated with low doses of 1-8 mg oral dFdC. The following dosing schedules were investigated: 1) a single dose on day 1 (1qdx1d) or 2) once daily dosing for 7 days (1qdx7d), and 3) 7 times dosing on day 1 (7qdx1d). A treatment period of maximal 7 days was chosen to reduce the discomfort for the mice. The 7qdx1d (every 1.5 h) dosing regimen of oral dFdC was compared with 1qdx7d (every 24 h) dosing, because of the approximately 15-fold higher clearance of dFdU in mice than in patients, to mimic the PK as observed in man at multiple oral dosing. Furthermore, we assessed the excretion of dFdC and its metabolites in urine and the exposure levels in PBMCs, which are often used as surrogate for tumor tissue in assessment of the PK-PD relationships for dFdC.

Material and methods

Materials

The nucleosides dFdC and dFdU, and the nucleotides dFdC-MP, dFdC-DP, dFdC-TP, dFdU-MP, dFdU-DP, dFdU-TP were kindly provided by Eli Lilly and Company (Indianapolis, CA, USA). Tetrahydrouridine (THU) was obtained from Calbiochem (La Jolla, CA, USA). Calf intestine alkaline phosphatase (AP) (activity: 1 μmol 4-nitrophenyl phosphate/min/unit protein) was purchased from Roche Diagnostics GmbH (Penzberg, Germany). Adenosine triphosphate ($Na_2ATP.3H_2O$) was obtained from Boehringer Mannheim (Almere, The Netherlands). [^{3}H]-dFdC (21.3 Ci/mmol) was purchased from Moravek Biochemicals Inc. (Brea, CA, USA) and [γ^{32}P]-ATP was obtained from Amersham Life Science (Amersham, UK).

Animals

Mice were housed and handled according to institutional guidelines complying with Dutch legislation. Animals used in this study were female wild-type mice (FVB) between 9 and 14 weeks of age. Animals were kept in a temperature controlled environment with a 12-h light/12-h dark cycle, and received a standard diet (AM-II; Hope Farms, Woerden, The Netherlands) and acidified water *ad libitum*.

Drug preparation, administration, and collection of samples

The dFdC stock solution was diluted with NaCl 0.9% to a final concentration of 10 µg/mL. A tracer quantity of 5 µCi (~ 12 x 10^6 dpm) [^{3}H]-dFdC was added to the dFdC solution. Mice received dFdC at a low dose of 0.1 mg/kg either orally by gavage into the stomach or by i.v. injection into the tail vein. Each test group consisted of 3 mice per time-point. Blood samples (1 mL) were taken at t = 0.08, 0.25, 4, 8, and 24 h after administration. Mice were anesthetized with methoxyflurane, their blood was collected by cardiac puncture, and they were sacrified by cervical dislocation followed by collection of urine (for i.v. dFdC only), and liver, kidney and lungs were removed. Whole blood was immediately transferred to a 3 mL ethylenediaminetetraacetic acid (EDTA) vacutainer on ice containing 100 µg THU (10 µL of a 10 mg/mL THU solution) to prevent any *ex vivo* deamination of dFdC. The plasma fraction of the blood samples was collected after centrifugation at 2000 x *g* at 4 °C for 5 min. The buffycoat was carefully collected for isolation of PBMCs. The buffycoat was diluted with 10 mL red blood cell (RBC) lysis buffer, and placed on ice for 20 min. The sample was centrifuged at 2000 x *g* at 4 °C for 5 min, and washed twice with ice cold PBS. The PBMC pellet was resuspended in 100 µL ice cold PBS. The cellular protein content was determined by the Bio-Rad Protein Assay (13) and was used to correct for differences in number of isolated cells between samples. Cell number was determined using a coulter counter (Beckman, Mijdrecht, The Netherlands). Plasma, PBMCs, urine, and organ samples were immediately weighed and snap-frozen in liquid nitrogen followed by storage at -80 °C until analysis.

Nucleoside and nucleotide extraction, recovery, and analysis

Samples were thawed on ice and tissues were homogenized in 4% (m/v) bovine serum albumin (5 mL for liver, and 3 mL for kidneys and lungs). Then, 600 µL MeOH 100% was added to 400 µL of plasma, urine, and tissue homogenate, vortex-mixed and placed at -20 °C for 2 h to precipitate proteins. Then, each mixture was centrifuged at 21,000 x *g* for 5 min, and the supernatant was dried overnight in a speedvac at room temperature. The pellet was dissolved by sonication for 15 min in 500 µL elution buffer (10 mM potassium phosphate pH 7.0, 10 mM tetrabutylamine (TBA)). The mixture was transferred onto an OASIS column after equilibration of the column with 2 x 1 mL Milli-Q, 2 x 1 mL MeOH 100%, 2 x 1 mL Milli-Q, and 2 x 1 mL elution buffer. The column was rinsed twice with 500 µL elution buffer and the eluate was discarded. Subsequently, nucleosides and nucleotides were eluted from the column using 500 µL MeOH 60% and the eluate was dried in a speedvac for approximately 3 h at room temperature. The dry pellet was resuspended in 100 µL eluent A (80 mM potassium phosphate pH 7.0, 11 mM TBA, and 1.0% MeOH), sonicated for 5 min, centrifuged at 21,000 x g for 5 min and the supernatant was collected for analysis.

The recovery of nucleosides and nucleotides from plasma, liver, and kidney was checked by spiking tissue homogenates with [^{3}H]-dFdC, [^{3}H]-dFdU, and [^{32}P]-ATP (as a surrogate nucleotide) complemented with cold drug to total concentrations of 39, 193, and 963 ng/mL. Extraction was performed as described above.

Separation, identification, and quantification of dFdC, dFdU, dFdC-MP, dFdC-DP, dFdC-TP, dFdU-MP, dFdU-DP, and dFdU-TP were performed using ion-pairing reversed phase high performance liquid chromatography (HPLC) (Beckman Coulter, Inc., CA, USA) with ultraviolet (UV) and off-line radioisotope detection (Packard, Instrument Co., Inc., CT, USA). A C18 HDO column, 5 µm, 150 x 4.6 mm (Uptisphere, Interchrom, France) was used with a column temperature of 40 °C, a 1:1 mixture of Ultima-flow and eluent, and a flow rate of 1.0 mL/min. The injection volume was 95 µL. The mobile phase consisted of a mixture of eluent A (80 mM potassium phosphate pH 7.0, 11 mM TBA, and 1.0% MeOH) mixed with eluent B (80 mM potassium phosphate pH 7.0, and 10% MeOH) in the following gradient: t = 0-10 min: 17% B; t = 10-65 min: 22% B; t = 65-85 min: 100% B, and t = 85-90 min; 17% B. A mixture of the reference compounds dFdC, dFdU, dFdC-MP, dFdC-DP, dFdC-TP, dFdU-MP, dFdU-DP, and dFdU-TP was used prior to

each sequence to assess system suitability. The radioactivity was determined with a Tri-Carb® 2800 TR Liquid Scintillation analyzer (Perkin Elmer, USA). Gemcitabine and its metabolites were identified based on their retention time and quantified by their radioactivity relative to the total administered radioactivity of [^{3}H]-dFdC multiplied by the total amount of drug.

Dephosphorylation of metabolites in liver homogenates

Liver homogenates obtained and prepared from 3 mice at 4 h after the last dose of 7qdx1d oral dFdC were pooled. Previous analysis revealed the presence of dFdC, dFdU, dFdC-MP, dFdC-DP, dFdC-TP, dFdU-MP, dFdU-DP, and dFdU-TP in these liver homogenates. Four fractions of 400 µL liver homogenate each were mixed with 600 µL MeOH 100%, stored for 2 h at -20 °C to precipitate proteins, and centrifuged at 21,000 x *g* for 5 min. The supernatants of the four fractions were transferred into a new vial and dried in a speedvac. The dried pellets were dissolved in eluting buffer followed by OASIS extraction and purification as described above. The pellets were again pooled after dissolving in 500 µL of a mixture containing 10 mM TrisHCl pH 8.0, 100 mM NaCl, 10 mM $MgCl_2$ and 1 mM $ZnCl_2$ with 2 units AP or without AP (negative control) and incubated at 37 °C for 4 h. Samples were lyophilized overnight and solubilized in 100 µL eluent A. The nucleosides and nucleotides were analyzed by HPLC with UV and radioisotope detection to confirm the identification of the phosphorylated metabolites.

Stability of nucleosides and nucleotides

Stability was assessed by spiking freshly obtained plasma, liver and kidney homogenates of 3 blank mice with [^{3}H]-dFdC, [^{3}H]-dFdU, and [^{32}P]-ATP supplemented with cold drugs to a total concentration of 963 ng/mL. Extraction and analysis of dFdC, dFdU, and ATP was performed as described above. Stability was determined at t = 0, t = 1 week, and t = 1 month after storage at -80 °C followed directly by OASIS solid phase extraction and HPLC analysis as described previously.

Pharmacokinetic and statistical analysis

The pharmacokinetic parameters of dFdC, dFdU, dFdC-MP, dFdC-DP, dFdC-TP, dFdU-MP, dFdU-DP, and dFdU-TP were determined by non-compartmental analysis, using WinNonLin™ (version 5.0.1, Pharsight Corporation, Mountain View, CA, USA). The area under the concentration-time curve (AUC) up to the last measured concentration-time point (AUC_{0-8}; AUC_{0-24}) was calculated using the trapezoidal method. Furthermore, the overall terminal half-life ($t_{1/2}$) was determined. The apparent clearance (Cl) and volume of distribution (V_d) were calculated for dFdC. The apparent oral bioavailability (F) of dFdC was calculated by the formula: F = AUC_{0-24} p.o./AUC_{0-24} i.v. * 100%. The plasma clearance of dFdU, dFdC-MP, dFdC-TP, and dFdU-TP was estimated by the formula: Cl = V * (Cu/Cp) (14), in which V presents the urine volume produced over 24 h, and Cu and Cp present the mean concentration between 4 and 24 h in urine and plasma, respectively. Pharmacokinetic parameters were reported as mean ± standard deviation (SD) ($n \geq 3$). Two-sided unpaired Student t tests were applied on the log-transformed values of the PK parameters to compare the groups. Statistical analysis was performed using SPSS 15.0 (SPSS Inc., Chicago, IL, USA). Differences were considered to be statistically significant when $p < 0.05$.

Results

Nucleosides and nucleotides were simultaneously quantified using a sensitive HPLC assay with radioisotope detection

The detected compounds eluted at the following retention times: dFdC: t = 6.7 min, dFdU: t = 10.3 min, dFdC-MP: t = 14.5 min, dFdU-MP: t = 23 min, dFdC-DP: t = 34 min, dFdU-DP: t = 70 min, dFdC-TP: t = 75 min, and dFdU-TP: t = 81 min. The mean weight of the PBMC dry pellet was 12.3 ± 4.9 mg, corresponding to 186 ± 84 µg PBMC protein and 1.1 ± 0.7 x 10^6 PBMCs (~ 5.9 x 10^6 PBMCs/mg protein) (n = 7). The limit of detection (LOD) for each of the metabolites was 14 fmol, corresponding to 147 fmol/mL plasma and urine or g tissue and PBMCs (~ 9.7 fmol/mg PBMC protein or 1.6 fmol/10^6 PBMCs). dFdC, dFdU and ATP (193 ng/mL) demonstrated reproducible recovery from liver (83 ± 5.7%, 82 ± 4.9%, and 65 ± 3.4%, respectively). The recovery of dFdC, dFdU, and ATP from the liver was similar at lower spiked concentrations and comparable for kidneys and plasma.

Treatment of liver homogenates with AP resulted in a decrease in the concentrations of all nucleotides (e.g. 33-fold for dFdC-MP, 23-fold for dFdC-TP, and 38-fold for dFdU-TP) and led to an expected increase in concentrations of dFdC and dFdU. After one month of storage at -80 °C, dFdC, dFdU, and ATP showed good stability in liver (97 ± 3.0%, 97 ± 2.9% and 96 ± 3.2%, respectively), kidneys (99 ± 4.6%, 94 ± 7.2% and 91 ± 3.7%, respectively), plasma (104 ± 4.8%, 98 ± 5.0%, and 97 ± 7.2%, respectively), and urine (100 ± 3.6%, 102 ± 7.0%, and 95 ± 5.9%, respectively).

Accumulation of dFdU, dFdC-MP, dFdC-TP and dFdU-TP in liver and kidney after multiple dosing of dFdC

The concentration versus time profiles for dFdC, dFdU, and their phosphorylated metabolites in plasma, liver, kidney, and lung following 1qdx1d oral dFdC 0.1 mg/kg are presented in Figure 2. The AUC_{0-24} values following oral administration of dFdC at the 1qdx1d and 1qdx7d dosing schedules are presented in Figure 3. The PK parameters of dFdC and its main metabolites following 1qdx1d, 1qdx7d, and 7qdx1d are summarized in Table 1 (oral dosing) and 2 (i.v. dosing). The nucleosides dFdC and dFdU as well as the nucleotides dFdC-MP, dFdC-TP, and dFdU-TP were detected in liver, kidney, lung, and in plasma and urine, suggesting efflux of the hydrophilic phosphorylated metabolites. The nucleotides dFdC-DP, dFdU-MP and dFdU-DP were detectable at very low concentrations at a few time points only in plasma, liver, kidney, and lung after oral and i.v. administration of dFdC, suggesting relatively high instability of these metabolites *in vivo* in mice.

Maximum concentrations of dFdC and dFdU in plasma and organs were achieved at about 15 min after oral administration (Figure 2), demonstrating rapid uptake and distribution of dFdC and fast metabolism to dFdU. The time to the maximum concentration (T_{max}) could not be determined accurately based on the sparse data points. Following i.v. administration, dFdC was very rapidly cleared from plasma and tissue with a rapid decline in concentration between 5 and 15 min ($t_{1/2,\alpha}$ ~ 0.17 h) followed by a slower decline up to 4 h ($t_{1/2,\beta}$ ~ 2 h). The concentration of dFdU in plasma and organs decreased from 0.25 to 8 h ($t_{1/2,\alpha}$ ~ 4 h) followed by a slower decrease up to 24 h ($t_{1/2,\beta}$ ~ 6 h) (Table 1, Figure 2).

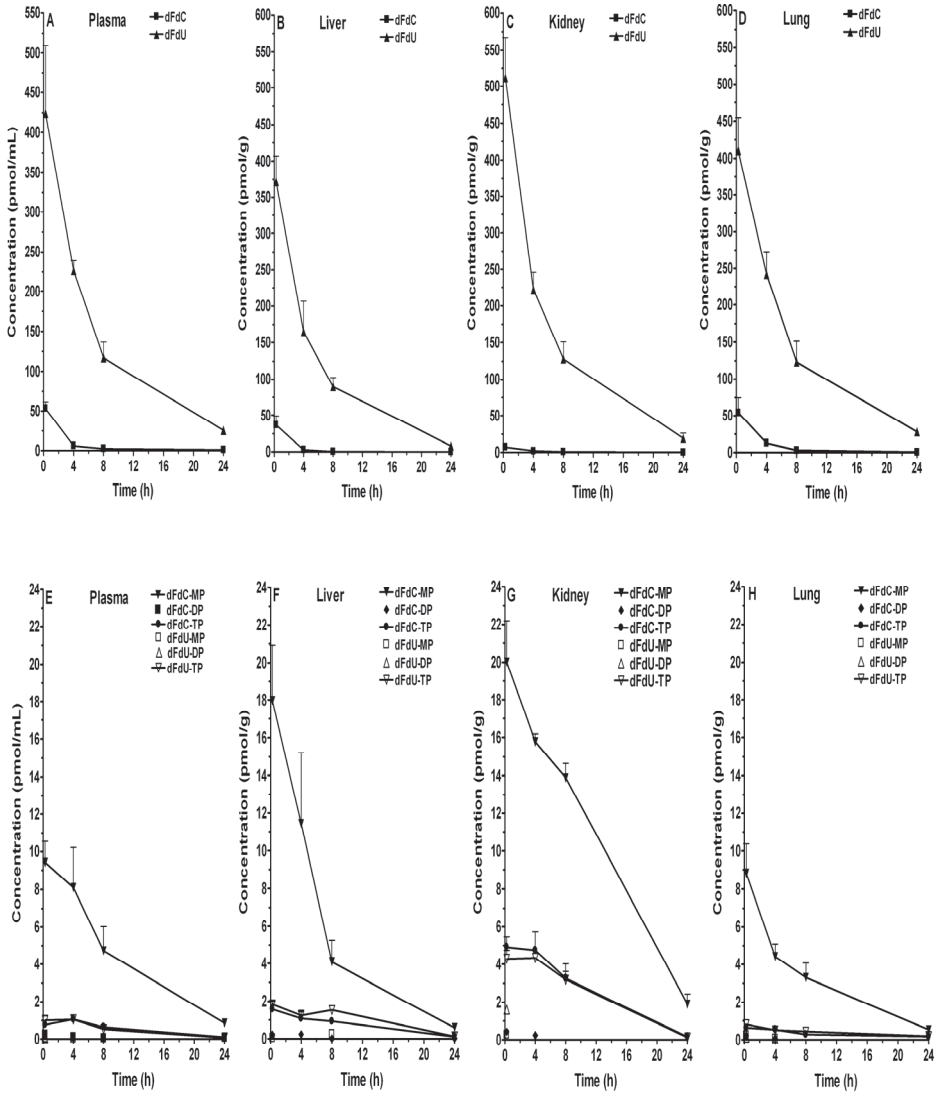

Figure 2. Concentration versus time profiles of dFdC, dFdU, dFdC-MP, dFdC-TP, and dFdU-TP in plasma (A and E), liver (B and F), kidney (C and G), and lung (D and H) after single oral dosing on day 1 (1qdx1d) of dFdC 0.1 mg/kg. Concentrations of dFdC-DP, dFdU-MP, and dFdU-DP were measurable at a few time-points only.

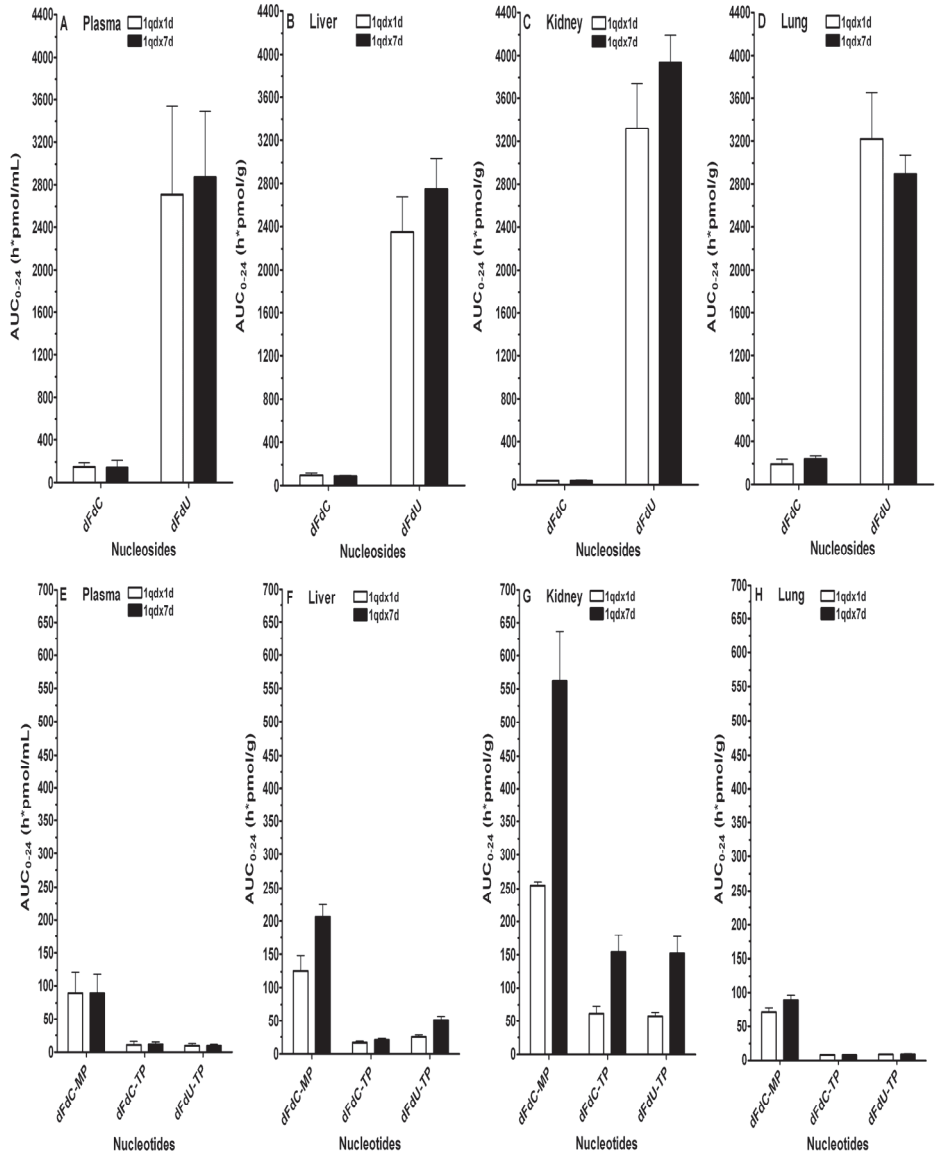

Figure 3. Systemic exposure (AUC_{0-24}) to dFdC, dFdU, and the main phosphorylated metabolites in plasma (A and E), liver (B and F), kidney (C and G), and lung (D and H) after a single dose on day 1 (1qdx1d) and multiple once daily dosing for 7 days (1qdx7d) of oral dFdC 0.1 mg/kg.

Table 1. PK of dFdC, dFdU and their nucleotides in plasma, liver, kidney, lung, and PBMCs following 1qdx1d, 1qdx7d, and 7qdx1d dosing of oral dFdC 0.1 mg/kg. Data are presented as mean ± SD.

Oral - 1qdx1d					
Plasma	**dFdC**	**dFdU**	**dFdC-MP**	**dFdC-TP**	**dFdU-TP**
AUC_{0-8} (h*pmol/ml)	136 ± 20	1957 ± 255	60 ± 7	7 ± 1	7 ± 1
AUC_{0-24} (h*pmol/ml)	157 ± 36	2708 ± 827	89 ± 33	11 ± 5	10 ± 3
$t_{1/2}$ (h)	n.a.	5.7 ± 1.1	6.7 ± 1.2	5.7 ± 0.2	6.9 ± 1.2
Liver					
AUC_{0-8} (h*pmol/g)	63 ± 47	1562 ± 254	88 ± 12	9 ± 2	12 ± 1
AUC_{0-24} (h*pmol/g)	68 ± 46	2347 ± 333	126 ± 22	17 ± 2	25 ± 3
Kidney					
AUC_{0-8} (h*pmol/g)	25 ± 0.1	2142 ± 185	129 ± 3	35 ± 6	32 ± 2
AUC_{0-24} (h*pmol/g)	36 ± 0.1	3319 ± 426	255 ± 5	62 ± 11	58 ± 6
Lung					
AUC_{0-8} (h*pmol/g)	165 ± 51	2005 ± 247	41 ± 2	4 ± 0.1	4 ± 0.1
AUC_{0-24} (h*pmol/g)	195 ± 49	3217 ± 434	72 ± 6	8 ± 1	9 ± 0.1
Oral - 1qdx7d					
Plasma	**dFdC**	**dFdU**	**dFdC-MP**	**dFdC-TP**	**dFdU-TP**
AUC_{0-8} (h*pmol/ml)	113 ± 72	1794 ± 559	89 ± 22	6 ± 2	6 ± 2
AUC_{0-24} (h*pmol/ml)	149 ± 68	2870 ± 622	89 ± 30	12 ± 3	10 ± 2
$t_{1/2}$ (h)	n.a.	6.1 ± 0.7	5.9 ± 0.5	9.5 ± 2.3	7.7 ± 3.0
Liver					
AUC_{0-8} (h*pmol/g)	16 ± 3.1	1947 ± 226	145 ± 20	11 ± 2	29 ± 3
AUC_{0-24} (h*pmol/g)	22 ± 3.9	2748 ± 289	207 ± 18	21 ± 2	51 ± 6
Kidney					
AUC_{0-8} (h*pmol/g)	27 ± 3.8	2642 ± 162	282 ± 42	88 ± 14	89 ± 11
AUC_{0-24} (h*pmol/g)	38 ± 4.0	3935 ± 260	563 ± 74	154 ± 25	152 ± 25
Lung					
AUC_{0-8} (h*pmol/g)	210 ± 27	1908 ± 138	51 ± 5	4 ± 0.1	5 ± 1
AUC_{0-24} (h*pmol/g)	245 ± 27	2893 ± 180	89 ± 7	8 ± 0.1	9 ± 1
Oral - 7qdx1d					
Plasma	**dFdC**	**dFdU**	**dFdC-MP**	**dFdC-TP**	**dFdU-TP**
AUC_{0-8} (h*pmol/ml)	79 ± 22	9706 ± 410	271 ± 44	36 ± 4	36 ± 7
Liver					
AUC_{0-8} (h*pmol/g)	30 ± 4	7033 ± 366	200 ± 4	45 ± 6	217 ± 10
PBMCs					
AUC_{0-8} (h*pmol/g)	58 ± 11	1202 ± 63	6.8	16 ± 8	14 ± 7

n.a.; not applicable.

Table 2. PK of dFdC, dFdU and their nucleotides in plasma, liver, kidney, and PBMCs following 1qdx1d, 1qdx7d, and 7qdx1d i.v. dosing of dFdC 0.1 mg/kg. Data are presented as mean ± SD.

IV - 1qdx1d					
Plasma	**dFdC**	**dFdU**	**dFdC-MP**	**dFdC-TP**	**dFdU-TP**
AUC_{0-8} (h*pmol/ml)	327 ± 36	2129 ± 48	64 ± 4	9 ± 1	7 ± 1
AUC_{0-24} (h*pmol/ml)	350 ± 39	3185 ± 85	102 ± 9	13 ± 1	11 ± 1
$t_{1/2}$ (h)	1.8 ± 0.3	4.4 ± 0.6	3.9 ± 0.6	4.5 ± 1.3	4.0 ± 0.7
Cl (l/kg/h)	1.0 ± 0.1	n.a.	n.a.	n.a.	n.a.
V_d (l/kg)	12 ± 1.6	n.a.	n.a.	n.a.	n.a.
Liver					
AUC_{0-8} (h*pmol/g)	106 ± 35	1878 ± 227	168 ± 36	15 ± 1	24 ± 2
AUC_{0-24} (h*pmol/g)	110 ± 35	2716 ± 155	210 ± 41	22 ± 1	37 ± 1
Kidney					
AUC_{0-8} (h*pmol/g)	15 ± 1.0	3520 ± 219	297 ± 28	122 ± 4	78 ± 9
AUC_{0-24} (h*pmol/g)	21 ± 1.5	4976 ± 668	530 ± 53	225 ± 18	147 ± 19
IV - 1qdx7d					
Plasma	**dFdC**	**dFdU**	**dFdC-MP**	**dFdC-TP**	**dFdU-TP**
AUC_{0-8} (h*pmol/ml)	348 ± 14	2495 ± 75	58 ± 4	9 ± 1	9 ± 1
AUC_{0-24} (h*pmol/ml)	377 ± 40	4673 ± 131	114 ± 9	16 ± 1	16 ± 1
$t_{1/2}$ (h)	2.0 ± 0.3	5.9 ± 0.5	6.1 ± 1.0	8.1 ± 1.0	6.9 ± 0.8
Liver					
AUC_{0-8} (h*pmol/g)	124 ± 32	2185 ± 32	199 ± 16	16 ± 2	29 ± 3
AUC_{0-24} (h*pmol/g)	131 ± 32	3578 ± 158	284 ± 20	30 ± 5	55 ± 2
Kidney					
AUC_{0-8} (h*pmol/g)	15 ± 2.0	3555 ± 289	336 ± 33	150 ± 16	115 ± 13
AUC_{0-24} (h*pmol/g)	27 ± 4.0	5570 ± 377	657 ± 80	284 ± 37	208 ± 21
IV - 7qdx1d					
Plasma	**dFdC**	**dFdU**	**dFdC-MP**	**dFdC-TP**	**dFdU-TP**
AUC_{0-8} (h*pmol/ml)	182 ± 148	9284 ± 1018	271 ± 34	37 ± 7	34 ± 6
Liver					
AUC_{0-8} (h*pmol/g)	89 ± 53	6985 ± 143	353 ± 279	61 ± 11	101 ± 15
PBMCs					
AUC_{0-8} (h*pmol/g)	125 ± 42	2242 ± 380	5.6 ± 2.9	15 ± 2	16 ± 2

n.a.; not applicable.

The mean plasma AUC_{0-24} of dFdC was 157 h*pmol/mL after a single oral dose of dFdC and 350 h*pmol/mL following single i.v. administration of dFdC (Table 1), demonstrating an apparent oral dFdC bioavailability of about 45%. In all organs, dFdU was the most prominent metabolite after oral and i.v. dFdC administration (Tables 1 and 2). The ratio of dFdU AUC_{0-24}/dFdC AUC_{0-24} was about two-fold higher after a single oral dose of dFdC (ratio = 17) compared to a single i.v. dose of dFdC (ratio = 9), indicating first-pass metabolism of dFdC to dFdU.

The AUC_{0-24} of dFdC was 2.3-fold significantly lower ($p < 0.01$) and the exposure to dFdC-MP, dFdC-TP, and dFdU-TP was 1.4-fold, 1.5-fold, and 2.5-fold higher ($p < 0.01$) in liver compared to plasma following single oral dFdC administration. In kidneys, the exposure to dFdC was 4.4-fold lower and the AUC_{0-24} values of dFdC-MP, dFdC-TP, and dFdU-TP were 2.9-fold, 5.6-fold, 5.8-fold significantly higher compared to plasma. Thus, exposure to dFdC-MP, dFdC-TP, and dFdU-TP was significantly higher in liver and kidneys compared to plasma. In lung tissue, the AUC_{0-24} of dFdC was relatively high without major differences in exposure to dFdU, dFdC-MP, dFdC-TP, and dFdU-TP compared to plasma.

Multiple oral dosing of dFdC once daily for seven days (1qdx7d) resulted in a significant increase in the exposure to dFdC-MP (1.6-fold) and dFdU-TP (2.0-fold) in the liver and increase in the exposure to dFdC-MP (2.2-fold), dFdC-TP (2.5-fold) and dFdU-TP (2.6-fold) in the kidneys (all $p < 0.01$) (Table 1, Figure 3). In contrast, no accumulation was seen in lung tissue. Multiple i.v. dosing (1qdx7d) of dFdC resulted in a lower 1.2 to 1.5-fold increase in dFdC-MP, dFdC-TP, and dFdU-TP in liver and kidneys (Table 2).

Interestingly, when dFdC was administered orally at the 7qdx1d dosing schedule, a significant decrease in liver exposure (AUC_{0-8}) to dFdC (1.9-fold) and increase in exposure to dFdU (3.6-fold), dFdC-TP (4.1-fold), and dFdU-TP (7.5-fold) ($p < 0.001$) compared to 1qdx7d oral dFdC were observed (Table 1, Figure 4). A similar pattern was observed following i.v. administration of 7qdx1d dFdC compared to 1qdx7d dosing of dFdC, however, the exposure to dFdU-TP increased 3.5-fold (Table 2).

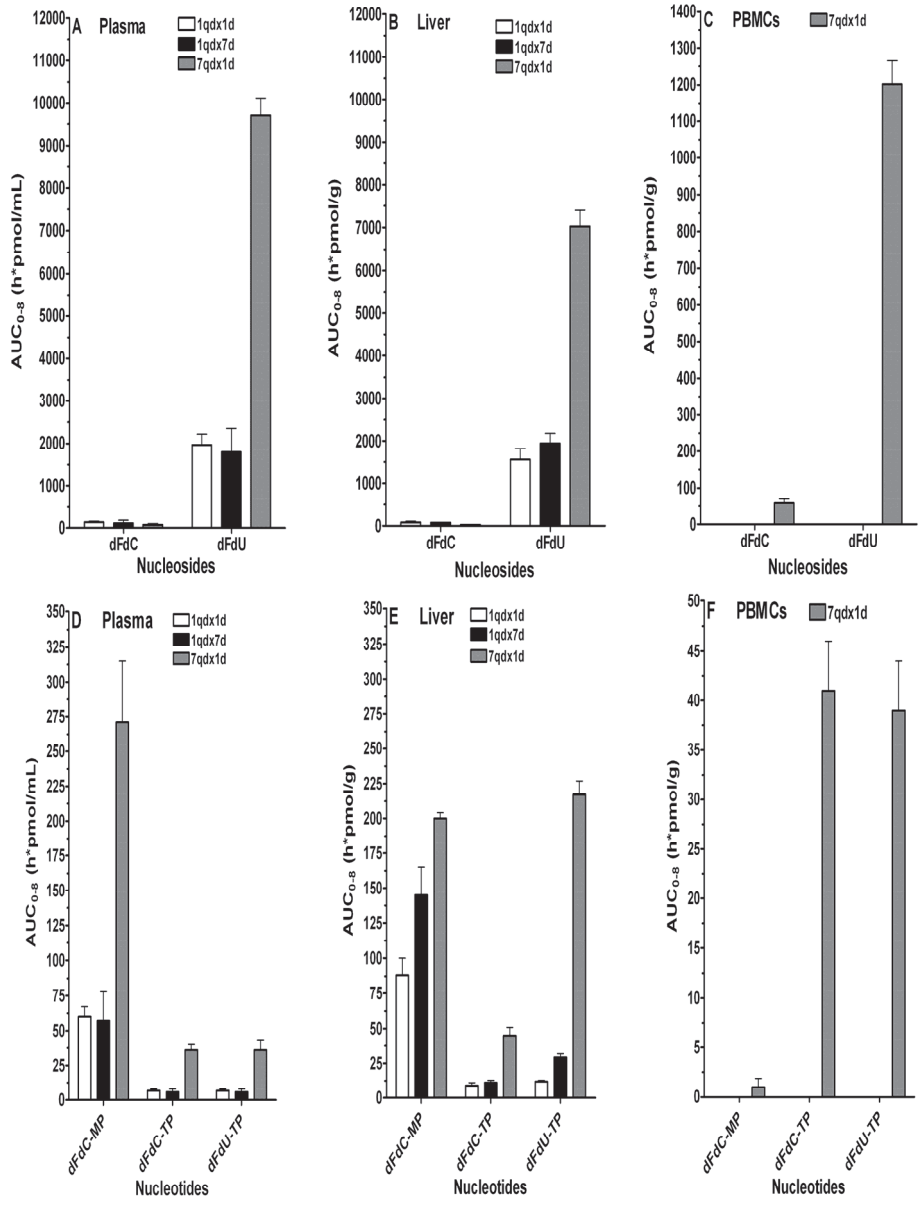

Figure 4. Comparison of the systemic exposures (AUC_{0-8}) to dFdC, dFdU, and the main phosphorylated metabolites in plasma (A and D), liver (B and E) and PBMCs (C and F) following oral administration of dFdC 0.1 mg/kg at three different dosing schedules: 1qdx1d, 1qdx7d, and 7qdx1d.

These results demonstrate that dFdU, dFdC-MP, dFdC-TP and dFdU-TP significantly accumulate following multiple oral and i.v. administrations of dFdC and that liver accumulation of dFdU-TP is more pronounced following multiple oral compared to i.v. administration of dFdC.

The $AUC_{0\text{-}8}$ values of dFdC-TP and dFdU-TP following oral administration of dFdC 7qdx1d were only about 2-fold lower in PBMCs compared to plasma. However, the exposure to dFdC-MP was 40-fold lower ($p < 0.001$) in PBMCs compared to plasma, which suggests high efflux of dFdC-MP from these cells. Furthermore, the exposure to dFdU-TP in the liver was 16-fold ($p < 0.001$) higher compared to PBMCs and 6-fold higher ($p < 0.001$) compared to plasma.

Besides dFdC and dFdU, also dFdC-TP, dFdU-TP, and particularly dFdC-MP were excreted in the urine following dFdC administration (Figure 5).

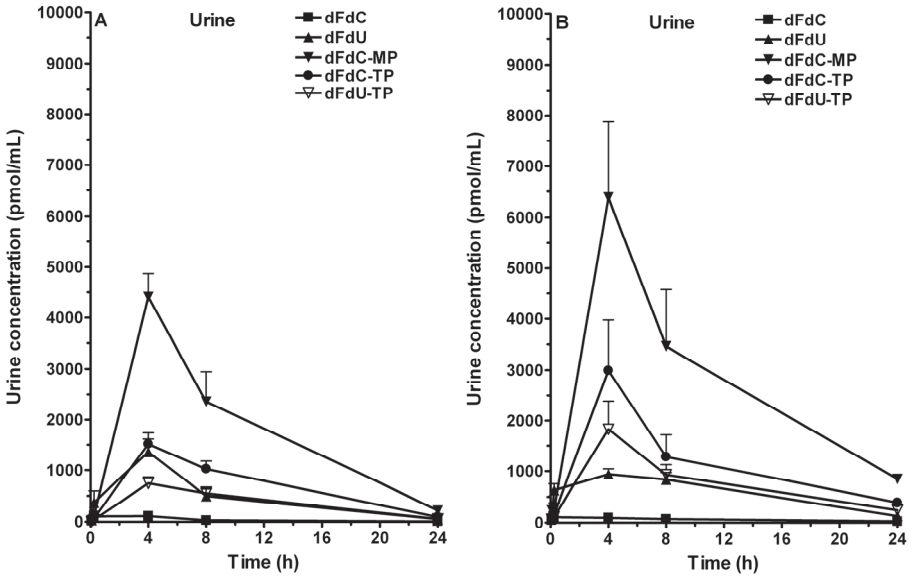

Figure 5. Excretion of dFdC, dFdU, dFdC-MP, dFdC-TP, and dFdU-TP in urine after 1qdx1d (A) and 1qdx7d (B) administration of i.v. dFdC 0.1 mg/kg.

Although we did not collect total urine within the first 24 h, we estimated the clearance of the main excreted metabolites after i.v. dFdC 0.1 mg/kg (see methods). From previous metabolic cage experiments performed at our institute, it is known that FVB wild-type mice between 9 and 14 weeks of age (n = 16) produce approximately 1.3 ± 0.5 mL of urine in 24 h (~ 0.903 µL/min). Estimated

values of Cl of dFdC-MP, dFdC-TP, dFdU-TP, and dFdU after a single i.v. dose of dFdC were 368 µL/min, 833 µL/min, 521 µL/min, and 4 µL/min, respectively.

Discussion

This study provides new insights into the *in vivo* PK and metabolism of dFdC in mice and was initiated to better understand the biotransformation, disposition and safety of oral dFdC in patients. It identifies and quantifies for the first time dFdC, dFdU, dFdC-MP, dFdC-DP, dFdC-TP, dFdU-MP, dFdU-DP and dFdU-TP in liver, kidney, lung, plasma, and urine. Previous studies in animal models only investigated the PK of dFdC after i.v. administration at relatively high dose-levels (11, 15, 16).

The elimination half-life of dFdU in patients ($t_{1/2}$ ~ 89 h) was substantially higher compared to mice ($t_{1/2}$ ~ 6 h) following oral administration of dFdC. From a clinical study with i.v. dFdC 120-1000 mg/m^2, it was suggested that the long terminal elimination phase of dFdU in patients was possibly a result from renal reabsorption of dFdU (17). It is known that the proximal tubule of the kidney is capable of nucleoside reabsorption (18, 19). Reabsorption of dFdU might occur by the action of human equilibrative and/or concentrative nucleoside transporters (hENTs and/or hCNTs), which are expressed in human kidney and liver (10, 20, 21). Our recent findings, demonstrating that dFdU is a high affinity substrate for hCNT1 and to a lesser extent for hENT1, strongly support the possibility of active uptake of dFdU in kidney and liver. Since dFdC is extensively deaminated to dFdU following first-pass metabolism in the liver, which highly expresses CDA, this might result into a more pronounced hepatic accumulation of the drug in patients following oral dFdC administration.

In C57BL/6J mice, the creatinine clearance, which reflects glomerular filtration rate (GFR) was reported to be 255 ± 68 µL/min (22). Thus, the estimated clearance of dFdU of 4 µL/min in this study suggests that dFdU is actively reabsorbed from the kidneys. The estimated values for the clearance of dFdC-MP, dFdC-TP, and dFdU-TP suggest that these hydrophilic phosphorylated compounds are excreted at a rate which approximates the GFR.

The fact that dFdC-MP, dFdC-TP, and dFdU-TP were found in plasma and urine suggests that cells can eliminate these hydrophilic nucleotides, consistent with our

in vitro experiments which demonstrated the presence of these compounds in culture medium of human solid tumor cell lines incubated with dFdC (submitted). It is likely that hepatocytes and other cell types have active efflux mechanisms to eliminate these potentially toxic compounds. So far it is unknown which transporters exactly contribute to this phenomenon. Multidrug resistance protein (MRP) 4 and 5 were shown to transport nucleoside monophosphates, however, with low affinity and without having a significant effect on resistance to dFdC (23, 24). Future studies are warranted to elucidate possible efflux transporters for these compounds.

A significantly higher exposure to dFdC-TP and dFdU-TP was found in liver and kidneys compared to lung tissue following a single oral and i.v. dose of dFdC. This might be explained by a higher uptake of dFdC and dFdU and/or higher expression of phosphorylating kinases in liver and kidney compared to lung tissue. Interestingly, multiple dosing of dFdC in mice resulted in significant accumulation of dFdU, dFdC-TP and dFdU-TP and a more pronounced hepatic accumulation of dFdU-TP after oral compared to i.v. administration. From our *in vitro* experiments in human hepatocellular HepG2 cells, we know that dFdU-TP was formed directly from dFdU (submitted). In addition, we found that dFdU-TP was formed via deamination of dFdC-MP by deoxycytidylate deaminase (dCMPD) to dFdU-MP when dFdC was co-administered with the CDA inhibitor THU. More importantly, the AUC of dFdU-TP and its extent of incorporation into DNA significantly correlated with the cytotoxicity of dFdU. Additionally, dFdU-TP and dFdC-TP had a comparable extent of DNA incorporation in HepG2 cells at equitoxic concentrations of dFdC and dFdU.

The maximum concentration of dFdC in plasma and organs was achieved shortly after oral administration, indicating rapid absorption of dFdC from the gastrointestinal tract into the systemic circulation and rapid distribution of dFdC into tissues. In addition, maximum concentrations of dFdU were also achieved shortly after oral administration, likely as a result of rapid deamination of dFdC. Although dFdU was likely formed via deamination of dFdC in the liver, it might have been formed in part pre-systemically via deamination of dFdC in the gut wall after which dFdU could be taken up into the liver and systemic circulation. The ratio of the plasma $AUC_{0\text{-}24}$ of dFdU over dFdC was 0.7 after a single i.v. dose of 20 mg/kg dFdC (11). This value was 13-fold and 24-fold higher after i.v. and oral

administration of a low dose of 0.1 mg/kg dFdC in this study, suggesting that deamination of dFdC becomes a more prominent route of metabolism at lower doses of dFdC, which is consistent with our *in vitro* findings in human solid tumor cell lines (submitted). The ratio's of the AUC of dFdU over dFdC were 92, 35, and 16 in kidney, liver and lung, respectively following single oral administration of dFdC. The higher ratio's in kidney and liver compared to lung could be due to the lower exposure to dFdC as a result of a relatively high extent of phosphorylation of dFdC in kidney and liver.

The dFdU/dFdC AUC ratio of 1000 in the patients who were administered a single oral dose of dFdC 1-8 mg was more than 50-fold higher compared to the mice who received a single dose of 0.1 mg/kg oral dFdC. This demonstrates a much higher extent of first-pass metabolism of dFdC to dFdU in humans compared to mice, consistent with the high expression of CDA in human liver (9). Furthermore, we observed a difference in exposure to dFdC-TP and dFdU-TP between mouse and man. The $AUC_{0\text{-}8}$ of both dFdC-TP and dFdU-TP in PBMCs of mice was about 2.7 h*pmol/mg protein (~ 40 h*pmol/g) after 7qdx1d administration of 0.1 mg/kg dFdC. In contrast, the $AUC_{0\text{-}8}$ values of dFdC-TP and dFdU-TP in PBMCs from patients were about 39 h*pmol/mg protein and 60 h*pmol/mg protein, respectively following a single oral dose of 8 mg dFdC and about 40 h*pmol/mg protein and 470 h*pmol/mg protein following once daily oral dosing for 14 days (1qdx14d). This might indicate a higher extent of nucleoside phosphorylation in PBMCs of humans compared to mice, possibly due to a higher expression of phosphorylating kinases in human cells compared to mouse cells, which was also suggested for fludarabine (25). In mice, dFdU accumulated 3.6-fold in plasma and dFdU-TP 9-fold in liver following 7qdx1d dosing compared to a single dose of oral dFdC. Similarly, dFdU accumulated 5.5-fold in plasma and dFdU-TP accumulated 7-fold in PBMCs of patients following 1qdx14d dosing compared to a single oral dose of dFdC.

In conclusion, this study demonstrates that dFdU-TP and dFdC-TP are extensively formed *in vivo* in mice following oral and i.v. administration of dFdC. Multiple administrations of dFdC resulted in a significant increase in dFdU, dFdC-TP and dFdU-TP in liver and kidney. Preferential accumulation of dFdC-TP and dFdU-TP in the liver, in particular after oral administration of dFdC associated with their cytotoxic potential may explain hepatotoxicity as observed in patients. Future

studies should address the potential toxicity and antitumor activity of dFdU-TP relative to dFdC-TP *in vivo*. This study also emphasizes the differences in PK of oral dFdC between humans and mice. The findings are evident for the application of continuous dosing regimens of dFdC and for the development of oral formulations of dFdC and might contribute to an improved efficacy/toxicity balance of dFdC in patients in the future.

Acknowledgements

We are grateful to Tessa Buckle for her logistical assistance in providing the mice and Eli Lilly for providing dFdC, dFdU and phosphorylated metabolites.

References

1 Hertel LW, Boder GB, Kroin JS, Rinzel SM, Poore GA, Todd GC, et al. Evaluation of the antitumor activity of gemcitabine (2',2'-difluoro-2'-deoxycytidine). Cancer Res 1990;50:4417-4422.

2 Noble S, Goa KL. Gemcitabine. A review of its pharmacology and clinical potential in non-small cell lung cancer and pancreatic cancer. Drugs 1997;54:447-472.

3 Mackey JR, Yao SY, Smith KM, Karpinski E, Baldwin SA, Cass CE, et al. Gemcitabine transport in xenopus oocytes expressing recombinant plasma membrane mammalian nucleoside transporters. J Natl Cancer Inst 1999;91:1876-1881.

4 Heinemann V, Hertel LW, Grindey GB, Plunkett W. Comparison of the cellular pharmacokinetics and toxicity of 2',2'-difluorodeoxycytidine and 1-beta-D-arabinofuranosylcytosine. Cancer Res 1988;48:4024-4031.

5 Huang P, Chubb S, Hertel LW, Grindey GB, Plunkett W. Action of 2',2'-difluorodeoxycytidine on DNA synthesis. Cancer Res 1991;51:6110-6117.

6 Grunewald R, Kantarjian H, Du M, Faucher K, Tarassoff P, Plunkett W. Gemcitabine in leukemia: a phase I clinical, plasma, and cellular pharmacology study. J Clin Oncol 1992;10:406-413.

7 Plunkett W, Huang P, Xu YZ, Heinemann V, Grunewald R, Gandhi V. Gemcitabine: metabolism, mechanisms of action, and self-potentiation, Semin Oncol 1995;22:3-10.

8 Heinemann V, Xu YZ, Chubb S, Sen A, Hertel LW, Grindey GB, et al. Cellular elimination of 2',2'-difluorodeoxycytidine 5'-triphosphate: a mechanism of self-potentiation. Cancer Res 1992;52:533-539.

9 Camiener GW, Smith CG. Studies of the enzymatic deamination of cytosine arabinoside. I. Enzyme distribution and species specificity, Biochem Pharmacol 1965;14:1405-1416.

10 Govindarajan R, Bakken AH, Hudkins KL, Lai Y, Casado FJ, Pastor-Anglada M, et al. In situ hybridization and immunolocalization of concentrative and equilibrative nucleoside transporters in the human intestine, liver, kidneys, and placenta. Am J Physiol Regul Integr Comp Physiol 2007;293:R1809-R1822.

11 Shipley LA, Brown TJ, Cornpropst JD, Hamilton M, Daniels WD, Culp HW. Metabolism and disposition of gemcitabine, and oncolytic deoxycytidine analog, in mice, rats, and dogs. Drug Metab Dispos 1992;20:849-855.

12 Horton ND, Young JK, Perkins EJ, Truex LL. Toxicity of single-dose oral gemcitabine in mice (abstract). Proc Amer Assoc Cancer Res 2004;45:486.

13 Bradford MM. A rapid and sensitive method for the quantitation of microgram quantities of protein utilizing the principle of protein-dye binding. Anal Biochem 1976;72:248-254.

14 Roland M, Tozer TN. Clinical pharmacokinetics: Concepts and applications, Williams & Wilkins: Philadelphia, 1995.

15 Kawai M, Esumi Y, Ishizaki M, Gunji S, Seki H. Metabolism of gemcitabine in rat and dog. Xenobiotica 1995;25:405-416.

16 Esumi Y, Mitsugi K, Takao A, Seki H, Kawai M. Disposition of gemcitabine in rat and dog after single and multiple dosings. Xenobiotica 1994;24:805-817.

17 Abbruzzese JL, Grunewald R, Weeks EA, Gravel D, Adams T, Nowak B, et al. A phase I clinical, plasma, and cellular pharmacology study of gemcitabine. J Clin Oncol 1991;9:491-498.

18 Kuttesch JF, Nelson JA. Renal handling of 2'-deoxyadenosine and adenosine in humans and mice. Cancer Chemother Pharmacol 1982;8:221-229.

19 Lee CW, Cheeseman CI, Jarvis SM. Na+- and K+-dependent uridine transport in rat renal brush-border membrane vesicles. Biochim Biophys Acta 1988;942:139-149.

20 Damaraju VL, Elwi AN, Hunter C, Carpenter P, Santos C, Barron GM, et al. Localization of broadly selective equilibrative and concentrative nucleoside transporters, hENT1 and hCNT3, in human kidney. Am J Physiol Renal Physiol 2007;293:F200-F211.

21 Gutierrez MM, Brett CM, Ott RJ, Hui AC, Giacomini KM. Nucleoside transport in brush border membrane vesicles from human kidney. Biochim Biophys Acta 1992;1105:1-9.

22 Dunn SR, Qi Z, Bottinger EP, Breyer MD, Sharma K. Utility of endogenous creatinine clearance as a measure of renal function in mice. Kidney Int 2004;65:1959-1967.

23 Reid G, Wielinga P, Zelcer N, De Haas M, Van Deemter L, Wijnholds J, et al. Characterization of the transport of nucleoside analog drugs by the human multidrug resistance proteins MRP4 and MRP5. Mol Pharmacol 2003;63:1094-1103.

24 Pratt S, Shepard RL, Kandasamy RA, Johnston PA, Perry W, et al. The multidrug resistance protein 5 (ABCC5) confers resistance to 5-fluorouracil and transports its monophosphorylated metabolites. Mol Cancer Ther 2005;4:855-863.

25 Plunkett W, Gandhi V. Nucleoside analogs: Celllular pharmacology, mechanisms of action, and strategies for combination therapy. In: Nucleoside analogs in cancer therapy; Cheson BD, Keating MJ, Plunkett W (eds.) 1997;1-36. Marcel Dekker, Inc.: New York.

Chapter 3.3

Oral administration of gemcitabine in patients with refractory tumors: a clinical and pharmacological study

Clinical Cancer Research, accepted for publication

Stephan A. Veltkamp
Robert S. Jansen
Sophie Callies
Dick Pluim
Carla M. Visseren-Grul
Hilde Rosing
Susanne Kloeker-Rhoades
Valerie A.M. Andre
Jos H. Beijnen
Christopher A. Slapak
Jan H.M. Schellens

Abstract

To determine the toxicity, tolerability, pharmacokinetics (PK) and pharmacodynamics (PD), and preliminary antitumor activity of oral gemcitabine (2',2'-difluorodeoxycytidine, dFdC) in patients with cancer.

Patients with advanced or metastatic cancer refractory to standard therapy were eligible. Gemcitabine was administered orally starting at 1 mg once-daily (QD) using dose escalation with 3 patients per dose-level. Patients received one of two dosing schemes: A) QD dosing for 14 days of a 21-day cycle, B) every-other-day (QOD) dosing for 21 days of a 28-day cycle. PK were assessed by measuring concentrations of dFdC and 2',2'-difluorodeoxyuridine (dFdU) in plasma and gemcitabine triphosphate (dFdCTP) in peripheral blood mononuclear cells (PBMCs), and PD by measuring the effect on T-cell proliferation.

Thirty patients entered the study. Oral gemcitabine was generally well tolerated. The MTD was not reached. Mainly moderate gastrointestinal toxicities occurred except for one patient who died after experiencing grade 4 hepatic failure during cycle two. One patient with a leiomyosarcoma had stable disease during 2 years and 7 months. Systemic exposure to dFdC was low with an estimated bioavailability of 10%. dFdC was highly converted to dFdU, probably via first pass metabolism and dFdU had a long terminal half-life (~89 h). Concentrations of dFdCTP in PBMCs were low, but high levels of dFdUTP, the phosphorylated metabolite of dFdU, were detected.

Systemic exposure to oral gemcitabine was low due to extensive first-pass metabolism to dFdU. Moderate toxicity combined with hints of activity warrant further investigation of the concept of prolonged exposure to gemcitabine.

Introduction

Gemcitabine (2',2'-difluorodeoxycytidine, dFdC), a pyrimidine antimetabolite, is used in the treatment of patients with various solid tumors (1, 2). It is currently formulated in an intravenous (i.v.) solution (Gemzar®) and usually administered as 30-min infusion at a dose of 1000-1250 mg/m^2 on days 1 and 8 of a 21-day or days 1, 8, and 15 of a 28-day cycle. Gemcitabine is taken up into cells by nucleoside transporters (3) and is intracellularly phosphorylated to gemcitabine monophosphate (dFdCMP) by deoxycytidine kinase (dCK, EC 2.7.1.74) and subsequently converted by other kinases into its active diphosphate (dFdCDP) and triphosphate (dFdCTP) forms (1, 4). dFdCTP competes with the natural substrate deoxycytidine triphosphate (dCTP) for incorporation into DNA, thereby inhibiting DNA synthesis (5, 6) and blocking cells in the early S phase of the cell cycle (7). In addition, dFdCDP inhibits ribonucleotide reductase (RR) (8) ultimately resulting into depletion of dCTP pools and enhanced incorporation of dFdCTP into DNA. Moreover, gemcitabine can potentiate its own cytotoxic effect via other pathways (6, 9). Besides, dFdC is extensively deaminated by cytidine deaminase (CDA, EC 3.5.4.5) (9) into 2',2'-difluorodeoxyuridine (dFdU), which has been reported to be present mainly in liver of humans and kidney of mice (10). Clinical studies showed that dFdU has a long terminal half-life ($t_{1/2}$; ~50 h) and is largely excreted in the urine (> 90% of the dose) (11).

Preclinical studies demonstrated that the efficacy and tolerability of gemcitabine was highly dose schedule dependent (1, 12). Clinical studies suggested that protracted or continuous administration of i.v. gemcitabine results in higher antitumor activity in cancer patients (13, 14). dFdCTP levels have been measured in peripheral blood mononuclear cells (PBMCs) and leukemic cells of patients treated with i.v. gemcitabine to investigate the PK-PD relationships of gemcitabine (15-17). Intracellular exposure to dFdCTP and its incorporation into DNA increased with the concentration of gemcitabine (5) and dFdCTP accumulation correlated with gemcitabine cytotoxicity (18-20). One possibility to investigate pharmacodynamic effects of gemcitabine is by assessing the effect on T-cell proliferation, which was shown to be inhibited by gemcitabine at low concentrations of about 3 nM (21, 22).

It was postulated that continuous treatment with oral gemcitabine might be efficacious in human malignancies. Additionally, oral dosing would be more convenient for patients than i.v. gemcitabine administration. Oral gemcitabine demonstrated antitumor activity against human colon, lung, and prostate tumor xenografts in mice following once daily dosing for 14 days (0.5-3 mg/kg), and every-other-day dosing for seven doses (1.25-10 mg/kg) (unpublished). Marginal hematological toxicity and dose-responsive intestinal lesions and enteropathy were found in mice after single oral gemcitabine administration at high doses (23).
Based on the promising antitumor activity in several human tumor xenografts, and the marginal hematological toxicity in preclinical models, a phase I study was started to investigate the feasibility of oral gemcitabine at a continuous dosing schedule in patients with advanced refractory solid tumors. The following dosing schedules were investigated: once-daily (QD) dosing for 14 days of a 21-day cycle (Part A) or every-other-day (QOD) dosing for 21 days of a 28-day cycle (Part B). Because of the observation of dose-limiting intestinal lesions in mice (23), a starting dose of 0.6 mg/m^2/day corresponding to 1 mg/day was chosen for Part A.
The objectives of this study were to: i) determine the toxicity, tolerability, and maximum tolerated dose (MTD), ii) preliminary antitumor activity, and iii) the pharmacokinetics (PK) and pharmacodynamics (PD) of oral gemcitabine in both dosing schedules.

Patients and methods

Eligibility

Patients with histologically or cytologically confirmed advanced and/or metastatic cancer for which no treatment of higher priority existed were eligible. Other eligibility criteria were: age ≥ 18 years, performance status (PS) ≤ 2 on the Eastern Cooperative Oncology Group (ECOG) scale, and an estimated life expectancy of ≥ 3 months. Previous therapy, including chemotherapy, hormonal therapy, radiotherapy, had to be discontinued for at least 4 weeks before study entry and 6 weeks in the case of mitomycin-C or nitrosourea. Patients had to have adequate bone marrow function, defined as absolute neutrophil count (ANC) ≥ 1.5 x 10^9/L, platelets ≥ 100 x 10^9/L, and hemoglobin ≥ 5.6 mmol/L, and adequate renal and

hepatic function defined as serum creatinine ≤ 1.5 the upper limit of normal (ULN), serum bilirubin ≤ 1.5 times the ULN and alanine transaminase (ALT) and aspartate transaminase (AST) ≤ 2.5 times the ULN (or ≤ 5 times the ULN in the case of tumor involvement in the liver). The study protocol was approved by the local Medical Ethics Committee and all patients had to give written informed consent.

Treatment plan and study design

Patients started with gemcitabine QD for 14 days of a 21-day cycle (Part A). Gemcitabine was orally administered as capsule(s) with one glass of tap water within 1 hour after breakfast. Cohorts of 3 patients per dose-level were used. A low flat starting dose of 1 mg in Part A and the introduction of one week of rest were chosen based on the preclinical toxicology studies and criteria by DeGeorge et al (24). If no dose-limiting toxicity (DLT) was reported during the first cycle in the first 3 patients at any dose-level, the dose was escalated to the next dose-level. Dose-levels were initially set at 2, 4, 8, 12, 15, and 20 mg. If one DLT occurred, 3 additional patients were enrolled at that dose-level. DLTs were defined as any of the following events occurring during the first treatment cycle and related to study treatment: any grade 4 hematological toxicity lasting longer than 5 days, or grade 3 or grade 4 non-hematological toxicity (except for untreated nausea and vomiting). The MTD was defined as one dose-level below the dose-level at which 2 out of 6 patients experienced a DLT. By protocol, the second part of the study (Part B) was planned to start upon identification of the MTD in Part A. In Part B, patients were to receive oral gemcitabine QOD for 21 days of a 28-day cycle. The starting dose in Part B was planned to be at the established MTD for Part A, because toxicity in Part B was expected to be milder. Subsequently, dose escalation proceeded to the next dose-levels. An additional 6 patients were planned to be treated at the dose-level determined to be the MTD for Part B.

Drug formulation

Gemcitabine (LY188011) was provided by Eli Lilly and Company (Indianapolis, USA) as capsules containing gemcitabine as hydrochloride salt equivalent to 1 mg,

5 mg, or 15 mg of gemcitabine. The capsules were stored in the refrigerator at 2-8 °C.

Patient evaluation and follow-up

Pre-treatment evaluation included a complete medical history and physical examination, vital signs, ECG, chest x-ray, hematology (hemoglobin, white blood cells (WBCs), platelets, neutrophils, lymphocytes), serum chemistry (bilirubin, alkaline phosphatase (AP), AST, ALT, blood urea nitrogen (BUN), creatinine, calcium, glucose, total protein, albumin, sodium, and potassium), and pregnancy test (if indicated). Before each cycle, the physical examination and vital signs were repeated, hematology and serum chemistry were checked, and any concomitant medication was noted. During each cycle, hematology was checked on day 7 and 14 in Part A and day 7, 14, and 21 in Part B (± 3 days). Serum chemistry was checked on day 7 in Part A and day 14 in Part B (± 3 days). All toxicities were graded according to the Common Toxicity Criteria (CTC) version 2.0. If hematological toxicity (ANC < 1.0 x 10^9/L for 5 days or platelets < 50 x 10^9/L) or non-hematological toxicity (grade 3/4, excluding nausea and vomiting) was observed within a cycle, the dose was reduced or was held until recovery and re-treatment was allowed according to protocol. No new cycle of gemcitabine was allowed unless the ANC was ≥ 1.0 x 10^9/L and platelets ≥ 100 x 10^9/L. If treatment was held for longer than 3 weeks for toxicity reasons, the patient had to be removed from the study. Dose adjustments had to take into account the capsule strengths available (1, 5, and 15 mg) and therefore dose reductions had to be rounded down to the nearest increment. Tumor assessments were performed by radiological imaging and/or tumor measurement of palpable or visible examination at baseline and day 1 of every other cycle and were evaluated according to the RECIST criteria (25).

Analysis of dFdC and dFdU

For analysis of dFdC and dFdU in plasma, blood samples were collected during cycle 1 on day 1 and 2 at 0.5, 1, 2/3, 4, 6, 8, and 24 h after oral administration of gemcitabine. On day 14 (Part A) and 21 (Part B) samples were collected at the following time points: predose, 0.5, 1, 2, 4, 6, 8, 24 h, 48-72 h, and 7 days (day

21/28) (± 1 day) after oral intake of gemcitabine. Blood samples of 3 mL of venous blood were drawn into sodium-heparinized tubes containing 500 µg tetrahydrouridine (THU) (Calbiochem, La Jolla, CA, USA) to prevent *ex vivo* conversion of dFdC to dFdU, immediately placed on ice and centrifuged for 5 min at 1500 x *g*. Plasma was collected and stored at -20 °C until analysis. dFdC and dFdU (analytical standards) and [$^{13}C_2$][$^{15}N_3$]-dFdC and [$^{13}C_4$][$^{15}N_2$]-dFdU (internal standards) were obtained from Lilly Research Laboratories (Indianapolis, USA). Plasma samples were thawed, vortex-mixed, and centrifuged at 2000 x *g* for 5 min, and 100 µL of plasma sample was transferred into a 2.0 mL well of a 96-wells plate (Tomtec Quadra96). The same was performed for the analytical standards, quality controls (QCs) and blank plasma. A volume of 300 µL of Milli-Q was transferred to blank plasma and 300 µL of internal standard (IS) working solution was added to the study samples. The OASIS HLB column for solid-phase extraction (SPE) was conditioned by 500 µL MeOH and 500 µL Milli-Q. The samples with IS were mixed 5 times and transferred to the extraction plate, and washed with 500 µL Milli-Q. Then, dFdC, dFdU, and internal standards were eluted with 200 µL MeOH. The eluate was collected and evaporated until dryness under nitrogen at 65 °C for 45 min. Samples were reconstituted at room temperature in 200 µL Milli-Q water, vortex-mixed for 30 s, centrifuged at 2000 x *g* for 5 min and the supernatant was collected for analysis. Separation of the analytes was performed by high pressure liquid chromatography (Agilent technologies, Palo Alto, CA, USA) using an Ace 5 C18 HL column (2.1 mm x 50 mm, 5.0 µm). The column was maintained at room temperature. The mobile phase consisted of a mixture of water (A) and MeOH with 1% formic acid (B) using the following gradient: t = 0: 100% A, t = 0.25 min: 25% B, t = 2.0 min: 100% B, and t = 3.0 min: 100% A. The injection volume was 20 µL and the total run time was 4 minutes. The analytes were detected and quantified using a PE Sciex API 4000 tandem mass spectrometer with a turbo V ionspray source operating in the positive ion mode. The ionspray voltage was kept at 3.5 kV with a source temperature of 650 °C. The following mass-to-charge (*m/z*) transitions were monitored: *m/z* 264 to 112 for dFdC, *m/z* 265 to 113 for dFdU, *m/z* 269 to 117 for [$^{13}C_2$][$^{15}N_3$]-dFdC and *m/z* 271 to 119 for [$^{13}C_4$][$^{15}N_2$]-dFdU. The assay validation data showed that the inter-assay accuracy for dFdC ranged from 0.1% to 6.5%, and the inter-assay

precision ranged from 2.0% to 3.7%, while for dFdU the inter-assay accuracy ranged from -1.2% to 6.9% and the inter-assay precision ranged from 1.3% to 6.8%. The lower and upper limit of quantification (LLOQ and ULOQ) of both dFdC and dFdU in human plasma were 0.5 ng/mL and 500 ng/mL, respectively. Samples above the ULOQ were diluted and re-analyzed.

Analysis of dFdCTP

For the quantification of dFdCTP in PBMCs, blood samples were collected during cycle 1 on day 1 and 14 (Part A) or 21 (Part B) at 1, 4, 8, and 24 h and on day 21 (Part A) or 28 (Part B) (± 1 day) after oral administration of gemcitabine. Blood samples of 15 mL of venous blood were drawn in sodium-heparinized tubes and immediately placed on ice. The tubes were centrifuged at 4 °C for 5 min at 1500 x *g*, and PBMCs were isolated and dFdCTP concentrations in PBMCs were determined as described previously using our validated LC-MS/MS assay (26). The LLOQ of dFdCTP in PBMCs was 0.277 ng/mg protein corresponding to 0.047 ng/10^6 cells (= 94 fmol/10^6 cells).

To investigate whether dFdUTP, the triphosphate form of dFdU, was formed in PBMCs, the *m/z* transition of 503 to 159 was monitored. Blank human PBMCs were spiked with the reference compound dFdUTP and the response ratio (including ion suppression and MS response) was determined. We compared the response ratio of dFdCTP/IS with dFdUTP/IS and used this factor to quantify the response ratio's in the PBMC samples based on the dFdCTP/IS calibration curve. IS, dFdCTP and dFdUTP had similar elution times.

T-cell proliferation assay

An explorative functional T-cell proliferation assay was used to characterize the effect of the treatment on T-cell proliferation in patients as a pharmacodynamic surrogate marker for bone marrow toxicity and or activity of oral gemcitabine. T-cell proliferation index (PI) of both CD_4^+ and CD_8^+ T-cells was determined during cycle 1. In brief, samples were taken on day 1 (predose), on day 14 (Part A) and 21 (Part B) 1 hour after oral dosing, and on day 21 (Part A) and 28 (Part B) (±1 day). Samples of healthy volunteers were taken as a control. For each sample, 16 mL whole blood was collected in BD Vacutainer® CPT™ tubes with sodium citrate (BD, Franklin Lakes, NJ, USA) and after centrifugation PBMCs were isolated and

resuspended in medium. Cells were counted and 0.5 x 10^6 PBMCs in 1 mL were plated in 9 wells of a 24-well plate; 3 wells were used for flow cytometry settings, 2 for internal positive control, and 4 wells for the samples (2 of these wells were pre-coated with anti-CD3 to stimulate T-cell proliferation). Cells were cultured for 3 days. Then, 10 µL of anti-CD4-FITC and anti-CD8-PE antibody were added to 500 µL of the samples. After washing and centrifugation, cells were taken up in 450 µL washing buffer. A volume of 50 µL of flow-count beads was added to all samples. Both CD_4^+ and CD_8^+ T-cells were counted within 1 h using fluorescent-activated cell sorting (FACS). The PI was calculated by the ratio of cell number after stimulation and cell number without stimulation of proliferation.

PK/PD and statistical analysis

The pharmacokinetic parameters of dFdC and dFdU in plasma, and of dFdCTP and dFdUTP in PBMCs were determined by non-compartmental analysis, using WinNonLin™ (version 5.0.1, Pharsight Corporation, Mountain View, CA, USA). The area under the plasma concentration time curve was determined up to 24 h (AUC_{0-24}) and up to the last measured concentration-time point extrapolated to infinity ($AUC_{0-\infty}$) with the linear logarithmic trapezoidal method using the slope of the terminal part of the logarithmic concentration versus time curve (λ_z). The maximal observed drug concentration (C_{max}) was obtained directly from the experimental data. The terminal half-life ($t_{1/2}$) was determined for dFdU. PI values of CD_4^+ and CD_8^+ T-cells were calculated as described above. The pharmacokinetic parameters were reported as median and range.

The software package Statistical Product and Service Solutions (version 12.1.1 for Windows, SPSS Inc., Chicago, IL, USA) was used for statistical analysis. Paired Student t-tests were applied on the log-transformed values of the pharmacokinetic parameters to investigate the differences between day 14 (Part A) or 21 (Part B) and day 1. ANOVA and Bonferoni post-hoc tests were conducted to investigate any differences in PI between day 1, 14, and 21 (Part A) and 1, 21, and 28 (Part B). Differences were considered to be statistically significant at $p < 0.05$.

Pharmacokinetic modeling

The non-linear mixed effects modeling program NONMEM (version V, level 1.1, double precision) (27) was used to develop a pharmacokinetic model for dFdU following oral gemcitabine. The apparent clearance (Cl/F), apparent volume of distribution (V/F), and the absorption rate constant (k_a) of dFdU were estimated. From the PK of i.v. administered gemcitabine, it is known that almost all of the administered gemcitabine dose (> 90%) is excreted into the urine as dFdU (11), hence the fraction of the total gemcitabine dose that is converted into dFdU (F_m) is almost 1. Additionally, it is known that gemcitabine is extensively metabolized to dFdU by first-pass metabolism in the liver, in which CDA is highly expressed (10). Interindividual variability (IIV) on PK parameters was estimated using an exponential error model. Model selection was based on a number of criteria, such as the exploratory analysis of the goodness of the fit plots, the estimates and the confidence intervals of the fixed and random parameters, and the minimum value of the objective function. Finally, based on mean and variance parameters from the final model, 1000 Monte-Carlo simulations were carried out in order to generate the 95% population prediction interval using NONMEM. A Bayesian analysis using WinBUGS version 1.4 was applied to the dFdC pharmacokinetic data. The Bayesian PK model fitted was a two-compartment disposition PK model with first order absorption rate constant. The distribution of the PK parameters in the population was assumed to be log normal. Previously reported PK parameters following i.v. gemcitabine 500-3600 mg/m^2 in 353 patients were used as informative priors for the total and inter-compartmental clearance, and the central and peripheral volume of distribution (11, 28). These studies with i.v. gemcitabine 1000 mg/m^2 as 30 min infusion showed a median C_{max} of dFdC of 40000 ng/mL (range: 28000 - 52000 ng/mL) and indicated a dose and time independent clearance of dFdC and dFdU. In addition, CDA has a reported K_m for gemcitabine of 290 ± 20 µmol/L corresponding to 76850 ± 5300 ng/mL (29). These data indicate no saturation of CDA following i.v. administration of gemcitabine at clinical doses.

Results

Patient characteristics, dose-levels tested and main drug-related toxicities

Thirty patients were treated in this study (18 in Part A, 12 in Part B) and their characteristics are presented in Table 1.

Table 1. Patient characteristics.

		n
Gender	Male	21
	Female	9
Age	Median	58
	Range	24-73
Race	Caucasian	28
	Hispanic	1
	Other	1
Tumor types	Colon	2
	Adenocarcinoma of unknown primary	3
	Sarcoma	5
	Lung adenocarcinoma	1
	Prostate	4
	Rectum	2
	Cholangiocarcinoma	1
	Ovarian	3
	Cervical	1
	Papillary adenocarcinoma	1
	Pancreas adenocarcinoma	2
	Vater's papil	1
	Parotis gland adenocarcinoma	1
	Squamous cell carcinoma	1
	Mesothelioma	1
	Melanoma	1
Performance status	0	3
	1	21
	2	6
Previous therapy	Hormonal therapy	4
	Radiotherapy	16
	Surgery	22
	Chemotherapy	26

The following dose-levels of gemcitabine were tested: 1 mg, 2 mg, 4 mg, 6 mg, 8 mg (Part A) and 8 mg, 12 mg, 16 mg, and 20 mg (Part B). Oral gemcitabine was generally well tolerated without any DLTs, except for one patient treated with 8 mg daily gemcitabine as described below. All patients were evaluable for safety. The hematological and non-hematological toxicities are presented in Table 2.

Table 2. Drug related toxicities: Maximum grade across all cycles per dosing regimen and dose-level. Data are reported as number of patients.

Adverse events		**Part A**						**Part B**				
	Dose-levels (mg)	1	2	4	6	8	Total	8	12	16	20	Total
	No. of pts. evaluable	3	3	6	3	3	18	3	3	3	3	12
Hematological	CTC Grade											
Anemia	1	1	0	0	0	0	1	0	0	0	0	0
	2	0	0	0	0	1	1	0	0	0	0	0
Leukocytopenia**	1	0	0	1	0	0	1	0	0	1	0	1
Neutropenia**	1	0	0	0	0	0	0	0	0	1	0	1
Thrombocytopenia**	1	0	0	1	0	1	2	1	0	1	0	2
Non-hematological												
Vomiting	1	0	1	0	0	0	1	0	0	0	2	2
	2	0	0	0	0	2	2	1	0	0	0	1
	3	1	0	2	0	0	3	0	0	0	0	0
Nausea	1	0	1	2	0	1	4	1	1	1	1	4
	2	0	0	0	0	0	0	0	0	0	1	1
	3	0	0	1	0	1*	2	0	0	0	0	0
Fatigue	1	0	1	0	1	0	2	0	0	0	0	0
	2	0	0	1	0	1	2	0	0	0	0	0
	3	0	0	0	0	1*	1	0	0	0	0	0
Anorexia	1	0	0	0	0	0	0	0	0	0	1	1
	3	0	0	0	0	1*	1	0	0	0	0	0
DIC	3	0	0	0	0	1*	1	0	0	0	0	0
Diarrhea	1	1	1	0	0	0	2	0	0	0	0	0
	2	0	0	2	0	0	2	0	0	0	0	0
Constipation	1	1	0	1	0	0	2	0	0	0	0	0
	2	0	0	1	0	0	1	0	0	0	0	0
Abdominal pain	1	0	0	0	1	0	1	0	0	0	0	0
	2	0	0	0	0	0	0	0	0	1	0	1
Headache	2	0	0	0	0	0	0	0	0	0	1	1
GI (other)	2	0	0	0	0	0	0	0	0	0	1	1
Renal (other)	2	0	1	0	0	0	1	0	0	0	0	0
Stomatitis/pharyngitis	2	0	0	1	0	0	1	0	0	0	0	0
Alopecia	1	0	0	0	0	0	0	0	1	0	0	1
Fever	1	0	0	1	0	0	1	0	0	0	0	0
Myalgia	1	0	0	0	0	0	0	0	0	0	1	1
Neuropathy	1	0	0	1	0	0	1	0	0	0	0	0
Rigors	1	0	0	0	0	0	0	0	0	0	1	1
Elevated AST	4	0	0	0	0	1*	1	0	0	0	0	0
Elevated ALT	4	0	0	0	0	1*	1	0	0	0	0	0
Elevated creatinine	2	0	1	0	0	0	1	0	0	0	0	0

DIC, disseminated intravascular coagulation; GI, gastrointestinal; AST, aspartate transaminase; ALT, alanine transaminase. * Grade 3/4 toxicities in the single patient with severe hepatic and renal failure.** Not designated as drug related on the case report form.

The most prominent drug related non-hematological toxicities were nausea (37% of patients) and vomiting (30% of patients). Hematological toxicity was mild and did not exceed CTC grade 2. In Part A, a total of 39 drug related adverse events (AEs) were experienced by 11 out of 18 patients; 74% of these were ≤ grade 2. In Part B, 19 AEs were experienced by 6 out of 12 patients; all ≤ grade 2 (Table 2). Of these 58 observed AEs, 55% were grade 1, 28% were grade 2 and 17% were grade 3 and 4 (corresponding to 4 patients in Part A). GI related toxicities (i.e. vomiting,

nausea, abdominal pain, constipation, diarrhea, and anorexia) corresponded to 53% and 50% of the grade 1 and grade 2 AEs, respectively. In Part A, 54% of the toxicities were GI related of which 52% were grade 2/3 and in Part B 53% were GI related of which 30% were grade 2/3.

Fourteen patients experienced one or more serious adverse events (SAEs), of which only 4 patients in Part A (1 at 1 mg, 2 at 4 mg and 1 at 8 mg) experienced SAEs related to the study drug. For three of these patients, the nature of these SAEs were vomiting and nausea and were not considered DLTs. A 68-year old male with an adenocarcinoma of unknown primary (ACUP) treated with 8 mg once daily oral gemcitabine was considered to have a toxic death. The first cycle was almost uneventful. However, nine days after the initiation of the second cycle he developed fever (T = 38.8 °C), followed by the following DLTs: grade 4 liver and kidney failure with rapid steep increases in ALT (2424 U/L) and AST (2781 U/L), γ-GT (237 U/L), LDH (3360 U/L), ureum (24.6 mmol/L), and creatinine (200 μmol/L), grade 3 fatigue, nausea, anorexia, and grade 3 disseminated interstitial coagulation (DIC). All cultures were negative. Ultrasound of liver and kidney demonstrated normal caliber of liver and biliary ducts, with however, an aberrant corticomedullar differentiation and a strongly reduced blood flow in the left kidney. Treatment with oral gemcitabine and co-medication (simvastatin, irbesartan/hydrochloorthiazide, oxazepam and omeprazol) were stopped, and the patient was given i.v prednisone 1 mg/kg. Despite this, his clinical situation deteriorated and 5 days later the patient died. Obduction revealed severe toxic induced liver necrosis, which was likely related to the study drug. Other possible causes for severe liver toxicity, such as viral infections (hepatitis B and C), liver metastasis, and alcohol abuses were excluded and an interaction between gemcitabine and co-medication was unlikely.

Due to this lethal toxicity, the dose of the other patient on 8 mg daily treatment was de-escalated to 4 mg and this dose-level was expanded by inclusion of 3 extra patients. Review of safety and pharmacokinetic data of the first 18 patients enrolled in five dose-levels (1, 2, 4, 6, and 8 mg) in Part A led to the pharmacologically-driven decision to stop enrollment in Part A in the absence of a MTD. The exposure to dFdC and dFdCTP was low and variable at all dose-levels. It was expected that the dosing schedule in Part B would allow higher doses of oral

gemcitabine to be safely administered, possibly leading to increased dFdC exposure. Dose escalation in Part B was carried out from 8 to 12, 16, up to 20 mg and stopped at that level in the absence of a MTD, because of the low systemic exposure to dFdC and dFdCTP without a significant increase with dose.

Response

Twenty-seven of the thirty patients were evaluable for response. The total number of cycles of therapy completed by all patients was 112. Seven patients (23%) had stable disease (SD) and twenty patients (67%) developed progressive disease (PD). Of the seven patients with SD, 5 subjects were treated in Part A at the dose-levels of 2 mg (n = 1), 4 mg (n = 2), 6 mg (n = 1), and 8 mg (n = 1), and 2 subjects were treated in Part B at the dose-levels of 12 mg (n = 1) and 16 mg (n = 1). The patients with SD had the following tumor types: leiomyosarcoma (1x; 39 cycles), cholangiocarcinoma (1x; 2 cycles), ovarian carcinoma (1x; 4 cycles), adenocarcinoma of unknown primary (ACUP) (2x; 2 and 2 cycles each), adenocarcinoma of the pancreas (1x; 8 cycles), and adenocarcinoma of the parathyroid gland (1x; 6 cycles). One female patient with advanced leiomyosarcoma (LMS) who had been treated with doxorubicin and ifosfamide received therapy with oral gemcitabine 2 mg QD for 14 days of a 3-weekly cycle. She tolerated the therapy well with only a few delays in the start of new treatment cycles due to two to three-fold increased liver enzyme values that were also present before start of therapy (at start: AST = 66 U/L [ULN = 40 U/L], ALT = 124 U/L [ULN = 45 U/L]). She had SD for 27 cycles of therapy and then had to switch to 5 mg QOD for 21 days of a 4-weekly cycle, because the supply of 1 mg capsules was exhausted. She received another 12 cycles of therapy. After having SD for 39 cycles the therapy was stopped, because she developed increased liver enzyme values (AST = 180 U/L, ALT = 246 U/L), which was likely caused by oral gemcitabine. Other causes of increasing liver enzyme values, such as viral infections (e.g. hepatitis B), co-medication, and liver metastasis were excluded. Treatment had to be held for more than 3 weeks as a result of the increased liver function tests, and the patient was required by protocol to stop study treatment. She was on study for 2 years and 7 months. Concentrations of dFdC and dFdU in plasma and levels of dFdCTP in PBMCs during cycle 1 were comparable to those of the other patients.

PK/PD of gemcitabine

Blood sampling for PK/PD purposes was performed in all 30 patients. The pharmacokinetic parameters of dFdC, dFdU, dFdCTP, and dFdUTP are shown in Table 3A and 3B. Concentration versus time profiles are depicted in Figure 1, and C_{max} values are demonstrated in Figure 2. Systemic exposure to dFdC was low and variable at all dose-levels due to extensive first-pass metabolism to dFdU and no dose dependent increase in exposure to dFdC was observed (Figure 1 and 2). For dFdC, C_{max} values are presented only, because AUC and $t_{1/2}$ could not be precisely calculated. Median bioavailability of gemcitabine was estimated at 10% (range: 5 - 17%) using prior information about disposition pharmacokinetics of dFdC in a Bayesian analysis. Because the study was terminated, it was decided not to give the patients a low dose of i.v. gemcitabine that was planned at the end of the study for calculation of the bioavailability of oral gemcitabine.

The systemic exposure to dFdU increased with dose following single and multiple administration and showed accumulation following QD and QOD dosing of oral gemcitabine (Figure 1 and 2). This is explained by the long terminal half-life of dFdU of about 89 h. As expected, accumulation of dFdU was approximately twice as high following QD (about 5 to 6- fold) compared to QOD dosing (about 2.5 to 3-fold) (Figure 2).

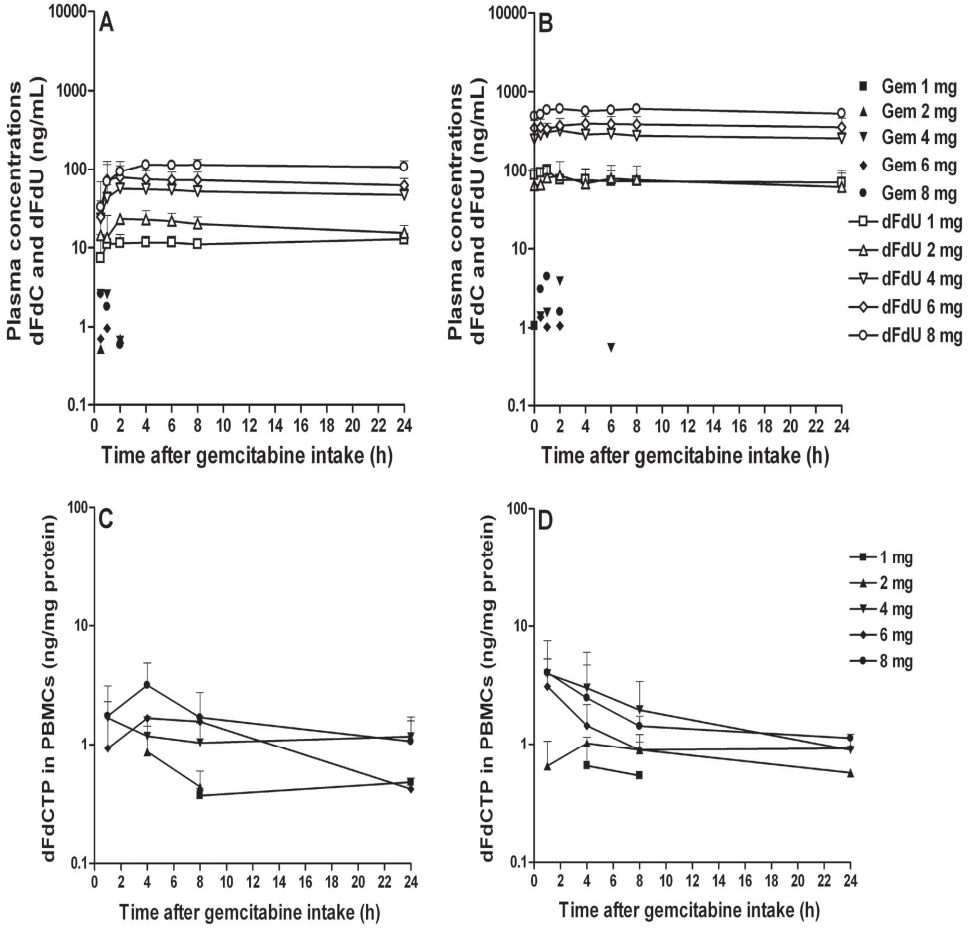

Figure 1. Concentration versus time curves of dFdC (ng/mL) and dFdU (ng/mL) in plasma on day 1 (A) and 14 (B) and of dFdCTP in PBMCs (ng/mg protein) on day 1 (C) and 14 (D) after daily administration of oral gemcitabine. Data are presented as mean ± SD on a semi-logarithmic scale.

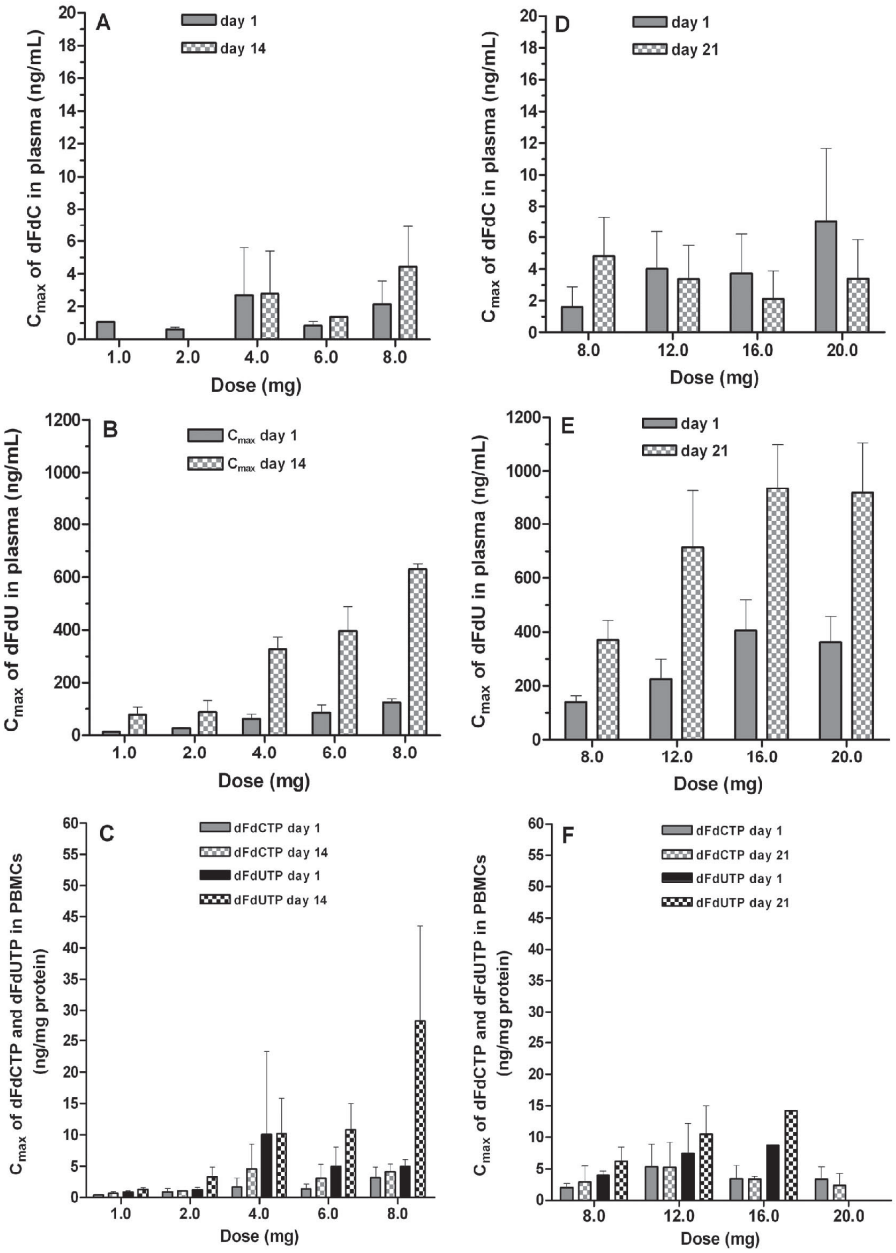

Figure 2. C_{max} of dFdC, dFdU, dFdCTP, and dFdUTP in Part A (A, B, and C) and Part B (D, E, and F) on day 1 and day 14 (Part A) and day 1 and 21 (Part B) after oral administration of gemcitabine. Data are presented as mean ± SD.

The dFdU PK data support the estimation of an empirical one-compartment model with first order absorption rate constant for dFdU. The final pharmacokinetic parameter estimates of dFdU are summarized in Table 4.

Table 4. Pharmacokinetic parameter estimates of dFdU.

Parameter	Mean	RSE (%)
Cl/F (L/h)	0.471	5.52
V/F (L)	0.485	30.5
K_a (h^{-1})	0.008	5.03
F	1 fixed	-
Interindividual variability		
IIV - Cl (%)	25.3	31.5
IIV - V (%)	140	53.8
IIV - K_a (%)	18.8	54.7
Proportional error (%)	33	39.4

RSE = relative standard error, Cl/F = apparent clearance, V/F = apparent volume of distribution, K_a = absorption rate constant from peripheral compartment into central compartment, F = bioavailability, IIV = interindividual variability.

The parameter values for dFdU show that the K_a (~ 0.008 h^{-1}), which represents the input rate into the plasma, is much slower than the K_e (1 h^{-1}), which represents the elimination rate from the plasma. Thus, the rate-limiting step of the PK of dFdU following oral administration of gemcitabine was determined to be the input rate of dFdU into plasma (k_a = 0.008 h^{-1}, $t_{1/2}$ input = 94 h). The apparent clearance of dFdU after oral gemcitabine was 0.471 L/h. As previously reported, following i.v. administration of gemcitabine, the k_a of dFdU (input rate into plasma = elimination rate from plasma) is 4 h^{-1}, the $t_{1/2}$ is about 50 h, and the clearance is about 1-2 L/h. The differences in apparent clearance and elimination half-life of dFdU between oral and i.v. administration of gemcitabine show that first-pass metabolism is the rate-limiting step in the PK of dFdU after oral administration. Hence, dFdC is most likely metabolized in the liver and dFdU is slowly released into the systemic circulation. Thus, the PK of dFdU after oral administration of gemcitabine is indicative of a "flip-flop" phenomenon. The estimate of the apparent volume of distribution for dFdU from the model must be interpreted with caution because of the uncertainty in the calculation of this parameter in case of "flip-flop" PK. The goodness of fit of the model was assessed by simulation of the dFdU

pharmacokinetic profiles and comparison with the observed data following 20 mg of oral gemcitabine (data not shown). The pharmacokinetic model predicted significant accumulation of dFdU into the first-pass metabolising organs, most likely the liver.

Concentrations of dFdCTP in PBMCs were detectable by our sensitive assay up to 24 h after oral administration of low dose gemcitabine. The C_{max} of dFdCTP slightly increased with dose (Figure 2) but showed high interpatient variability. The mean AUC of dFdCTP in PBMCs (Part A+B) was 32 h*ng/mg protein (~12.8 h*pmol/10^6 cells) after single oral administration of 8 mg gemcitabine.

We hypothesized that dFdUTP was formed following administration of gemcitabine. Indeed, a significant peak eluting just after the dFdCTP peak was detected and dFdUTP eluted at the same retention time as the peak in the patient samples. Exposure to dFdUTP was higher compared to dFdCTP at almost all dose-levels. C_{max} and AUC of dFdUTP increased with dose of oral gemcitabine (Table 3 and Figure 2; dFdUTP levels were available for all patients, except for the patients at the 20 mg dose-level). The mean value of the dose normalized AUC of dFdUTP (AUC dFdUTP/gemcitabine dose) for all dose-levels in Part A after single dosing on day 1 (11 h*ng/mg protein) and multiple dosing on day 14 (35 h*ng/mg protein) was significantly higher ($p = 0.001$) than the AUC dFdCTP/gemcitabine dose on day 1 (4.0 h*ng/mg protein) and day 14 (6.2 h*ng/mg protein). These observations about the intracellular PK of dFdUTP and dFdCTP are consistent with the higher plasma levels of dFdU relative to dFdC following oral gemcitabine administration.

The values for the PI of CD_4^+ and CD_8^+ T-cells showed high interpatient variability and no significant inhibiting effects of oral gemcitabine therapy on T-cell PI could be detected in Part A and B, consistent with the low hematological toxicity and low systemic exposure to gemcitabine. We recently determined that in cultured T-cells from healthy volunteers ($n = 42$) the mean PI values of CD_4^+ and CD_8^+ T-cells were 3.6 ± 1.9 and 3.2 ± 1.8, respectively (unpublished). In this study, no significant effects of oral gemcitabine on T-cell PI were found. In Part A, for example, the mean PI of CD_4^+ cells altered from 3.4 ± 2.6 on day 1 (predose) to 3.0 ± 2.6 on day 14 and to 3.9 ± 3.5 on day 21 ($p = 0.714$) and the PI of CD_8^+ cells altered from 4.6 ± 3.7 on day 1 to 3.3 ± 2.9 on day 14 and to 3.7 ± 2.5 on day 21 ($p = 0.482$).

Table 3A. Pharmacokinetic parameters of dFdC and dFdU in plasma and dFdCTP and dFdUTP in PBMCs after once-daily dosing of oral gemcitabine (Part A). Data are presented as median and range.

Variable					
Dose-levels (mg)	1	2	4	6	8
Day 1					
N of evaluable patients	3	3	6	3	3
dFdC					
C_{max} (ng/mL)	1.1	0.6 (0.5-0.7)	1.6 (0.7-7.7)	0.8 0.6-1.1)	2.3 0.6-3.5
dFdU					
C_{max} (ng/mL)	13 (13-15)	27 (25-31)	60 (46-90)	88 (53-113)	127 (111-137)
AUC_{0-24} (h*ng/mL)	277 (76-320)	471 (379-487)	1139 (957-1609)	1709 (1146-2022)	2379 (2338-2889)
dFdCTP					
C_{max} (ng/mg protein)	0.41 (0.33-0.48)	0.9 (0.6-1.3)	1.3 (0.3-4.1)	1.7 (0.5-2.0)	3.3 (1.4-4.8)
AUC_{0-24} (h*ng/mg protein)	5.0 (1.3-8.7)	4.3 (2.9-5.7)	19 (0.2-45)	26 (0.2-28)	36 (19-63)
dFdUTP					
C_{max} (ng/mg protein)	0.9 (0.7-1.0	0.7 (0.4-0.9)	2.1 (1.2-33)	5.9 (1.5-7.4)	4.6 (4.1-6.2)
AUC_{0-24} (h*ng/mg protein)	13 (8.0-18	4.7 (4.4-4.9)	38 (16-178)	97 (27-131)	64 (42-88)
Day 14					
N of evaluable patients	2	3	5	3	2
dFdC					
C_{max} (ng/mL)	n.a.	n.a.	1.7 (0.7-7.2)	1.4	4.4 (2.7-6.2)
dFdU					
C_{max} (ng/mL)	78 (57-99)	107 (40-121)	325 (246-374)	368 (320-499)	631 (620-645)
AUC_{0-24} (h*ng/mL)	1695 (1216-2173)	2147 (653-2353)	7002 (5055-7480)	8473 (6971-11538)	13747 (13119-14375)
$t_{1/2}$ (h)	106 (81-130)	46 (16-157)	89 (58-146)	209 (58-249)	101 (86-115)
dFdCTP					
C_{max} (ng/mg protein)	0.7 (0.5-0.9	1.1 (0.9-1.1)	2.7 (0.9-9.9)	3.1 (1.5-4.7)	4.1 (3.2-5.0)
AUC_{0-24} (h*ng/mg protein)	2.2 (1.7-2.7)	6.8 (0.6-15)	29 (13-87)	28 (22-33)	40 (31-49)
dFdUTP					
C_{max} (ng/mg protein)	1.3 (1.1-1.5	3.3 (2.2-4.4)	9.0 (5.0-18)	13 (6-13)	28 (17-39)
AUC_{0-24} (h*ng/mg protein)	23 (20-25	55 (40-71)	143 (107-281)	129 (101-228)	467 (240-694)

n.a., not available; individual values are given if n < 3.

Table 3B. Pharmacokinetic parameters of dFdC and dFdU in plasma and dFdCTP and dFdUTP in PBMCs after every-other-day dosing of oral gemcitabine (Part B). Data are presented as median and range.

Variable				
Dose-levels (mg)	8	12	16	20
Day 1				
N of evaluable patients	3	3	3	3
dFdC				
C_{max} (ng/mL)	1.6	3.5	2.7	6.8
	(0.7-2.5)	(2.0-6.7)	(1.8-6.6)	(2.6-12)
dFdU				
C_{max} (ng/mL)	150	221	373	333
	(117-155)	(151-301)	(311-532)	(286-469)
AUC_{0-24} (h*ng/L)	2582	3736	7833	6207
	(2280-3292)	(2991-6472)	(6804-7896)	(5167-6797)
dFdCTP				
C_{max} (ng/mg protein)	2.2	6.5	2.6	4.3
	(1.4-2.5)	(1.3-8.2)	(1.9-5.8)	(1.1-4.7)
AUC_{0-24} (h*ng/mg protein)	24	69	14	15
	(7.0-40)	(23-87)	(12-68)	(4.3-72)
dFdUTP				
C_{max} (ng/mg protein)	3.0	4.0	7.7	n.a.
	(2.4-3.8)	(2.5-5.0)	(4.3-11)	
AUC_{0-24} (h*ng/mg protein)	47	38	76	n.a.
	(41-69)	(28-47)	(48-151)	
Day 21				
N of evaluable patients	3	3	3	3
dFdC				
C_{max} (ng/mL)	6.3	2.2	1.7	2.3
	(1.9-6.3)	(2.1-5.8)	(0.6-4.1)	(1.6-6.2)
dFdU				
C_{max} (ng/mL)	365	746	974	825
	(303-445)	(488-908)	(757-1078)	(791-1134)
AUC_{0-24} (h*ng/mL)	14125	24823	33235	32552
	(11245-16432)	(17496-29066)	(24471-36547)	(21435-39674)
$t_{1/2}$ (h)	84	80	48	49
	(79-103)	(76-104)	(34-59)	(39-79)
dFdCTP				
C_{max} (ng/mg protein)	1.7	4.7	3.4	1.4
	(1.5-2.9)	(1.6-9.5)	(2.9-3.8)	(1.2-4.5)
AUC_{0-24} (h*ng/mg protein)	26	72	20	18
	(6.7-62)	(26-130)	(13-32)	(7.5-29)
dFdUTP				
C_{max} (ng/mg protein)	5.2	11	14	n.a.
	(4.8-8.7)	(6.2-15)		
AUC_{0-24} (h*ng/mg protein)	151	211	248	n.a.
	(97-438)	(112-310)		

n.a., not available; individual values are given if n < 3.

Discussion

In this clinical phase I study we administered gemcitabine orally to patients with advanced solid tumors for the first time.

Overall, low dose oral gemcitabine was well tolerated. The study was discontinued, mainly because of the unfavourable PK of dFdC after oral gemcitabine. More precisely, QD administration for 14 days of oral gemcitabine at a dose of 8 mg (corresponding to a 225-fold lower dose compared to i.v. gemcitabine 1000 mg/m^2), resulted in the following mean systemic exposures: dFdC C_{max} of 4.4 ng/mL (about 5700-fold lower compared to i.v. gemcitabine), dFdU AUC_{0-24} of 13.8 x 10^3 h*ng/mL (about 25-fold lower compared to i.v. gemcitabine), and dFdCTP AUC_{0-24} of 40 h*ng/mg protein or 13.5 h*pmol/10^6 PBMCs (about 100 to 200-fold lower compared to i.v. gemcitabine). Following single i.v. gemcitabine, dFdCTP AUC_{0-24} values of approximately 1400 h*pmol/10^6 PBMCs (30) (31) (32) and a cumulative dFdCTP AUC over 3 weeks of 9700 h*pmol/10^6 PBMCs have been reported (11). These data illustrate the significant difference in PK of gemcitabine following oral and i.v. administration.

The main pattern of toxicity observed in this study is GI toxicity, whereas hardly any hematological toxicity was observed, probably consistent with the low systemic exposure to dFdC. The incidence of GI related toxicity was similar between Part A (QD) and Part B (QOD) although the severity seemed to be less in Part B compared to Part A (grade 2/3 toxicity was observed in 52% of the patients with GI toxicity in Part A and in 30% of the patients with GI toxicity in Part B). In the single patient at the 8 mg dose-level in Part A with lethal liver- and kidney toxicity, exposure levels to dFdC, dFdU and dFdCTP were comparable with those of other patients, however, levels of dFdUTP in this patient were high, with an AUC of 694 h*pmol/mg protein on day 14, compared to the other patients, in which AUC levels ranged from 20 to 270 h*pmol/mg protein after multiple daily dosing.

The study was terminated before the MTD was achieved because of the unfavourable pharmacokinetic profile of oral gemcitabine (low exposure to dFdC and dFdCTP and long $t_{1/2}$ of dFdU) and the lethal liver toxicity observed in one patient. We hypothesised that there was a relationship between the PK findings and

toxicity of oral gemcitabine. Therefore, we carried out preclinical studies to investigate cytotoxicity, uptake, metabolism, and biodistribution of dFdC, dFdU, and phosphorylated metabolites. In brief, in HepG2 cells, the IC_{50} values of dFdC and dFdU were about 1 nM (~0.3 ng/mL) and 2.5 µM (~660 ng/mL) (33), respectively, after 14 days drug exposure, comparable to the concentrations found in patients in this study. Furthermore, we discovered that both deamination of dFdCMP to dFdUMP by deoxycytidylate deaminase as well as phosphorylation of dFdU results in the formation of dFdUTP, which was incorporated into DNA and RNA (34). The long $t_{1/2}$ of dFdU and its accumulation in patients after continuous oral administration of gemcitabine might result in pharmacologically relevant concentrations for prolonged periods of time, and dFdU might contribute to the activity/toxicity of gemcitabine (e.g. by incorporation of dFdUTP into nucleic acids). Of note, accumulation of ara-UTP in leukemic blasts has been reported after treatment with cytarabine (ara-C) 0.5 g/m^2/h administered as 2- or 4-hour infusion (35).

The best response was SD in 7 patients with a median duration of 3 cycles in 6 out of 7 patients. Remarkably, the patient with advanced LMS had SD during 39 cycles of therapy after low dose oral gemcitabine. Second-line treatment with single agent i.v. gemcitabine was shown to be active in patients with LMS (36, 37).

In conclusion, this is the first study that tested oral administration of gemcitabine in patients. It demonstrates that the systemic exposure to dFdC was low due to extensive first-pass metabolism to dFdU, which must be overcome in order to successfully deliver gemcitabine orally. We discovered for the first time the formation of dFdUTP in PBMCs of patients. Recently, different approaches have been attempted to decrease deamination of dFdC to dFdU, such as coupling a long chain fatty acid or an isoprenoid chain of squalene to the terminal amino group of dFdC (38) (39), thereby protecting it from deamination by CDA. Whether these strategies might ultimately lead to higher intracellular concentrations of dFdC and its active phosphorylated metabolites, possibly leading to an increased cytotoxicity, has to be further elucidated.

Acknowledgements

We thank Annemarie Nol for her logistic assistance, Enaksha Wickremsinhe, Irina Kapsh, Vanaja Raguvaran, Ernest Wong, and Henrianna Pang for their work on the analysis of the dFdC and dFdU samples and Philip Marder, Lisa Green, and Joanne Hom for their work on the T-cell proliferation assay.

References

1 Hertel LW, Boder GB, Kroin JS, et al. Evaluation of the antitumor activity of gemcitabine (2',2'-difluoro-2'-deoxycytidine). Cancer Res 1990;50:4417-22.

2 Noble S, Goa KL. Gemcitabine. A review of its pharmacology and clinical potential in non-small cell lung cancer and pancreatic cancer. Drugs 1997;54:447-72.

3 Mackey JR, Yao SY, Smith KM, et al. Gemcitabine transport in xenopus oocytes expressing recombinant plasma membrane mammalian nucleoside transporters. J Natl Cancer Inst 1999;91:1876-81.

4 Heinemann V, Hertel LW, Grindey GB, Plunkett W. Comparison of the cellular pharmacokinetics and toxicity of 2',2'-difluorodeoxycytidine and 1-beta-D-arabinofuranosylcytosine. Cancer Res 1988;48:4024-31.

5 Huang P, Chubb S, Hertel LW, Grindey GB, Plunkett W. Action of 2',2'-difluorodeoxycytidine on DNA synthesis. Cancer Res 1991;51:6110-7.

6 Heinemann V, Xu YZ, Chubb S, et al. Cellular elimination of 2',2'-difluorodeoxycytidine 5'-triphosphate: a mechanism of self-potentiation. Cancer Res 1992;52:533-9.

7 Grunewald R, Kantarjian H, Du M, Faucher K, Tarassoff P, Plunkett W. Gemcitabine in leukemia: a phase I clinical, plasma, and cellular pharmacology study. J Clin Oncol 1992;10:406-13.

8 Heinemann V, Xu YZ, Chubb S, et al. Inhibition of ribonucleotide reduction in CCRF-CEM cells by 2',2'-difluorodeoxycytidine. Mol Pharmacol 1990;38:567-72.

9 Plunkett W, Huang P, Xu YZ, Heinemann V, Grunewald R, Gandhi V. Gemcitabine: metabolism, mechanisms of action, and self-potentiation. Semin Oncol 1995;22:3-10.

10 Camiener GW, Smith CG. Studies of the enzymatic deamination of cytosine arabinoside. I. Enzyme distribution and species specificity. Biochem Pharmacol 1965;14:1405-16.

11 Zhang L, Sinha V, Forgue ST, et al. Model-based drug development: the road to quantitative pharmacology. J Pharmacokinet Pharmacodyn 2006;33:369-93.

12 Braakhuis BJ, Visser GW, Stringer I, Peters GJ. In vitro antiproliferative and metabolic activity of eight novel 5-fluorinated uracil nucleosides. Eur J Cancer 1991;27:250-3.

13 Abbruzzese JL, Grunewald R, Weeks EA, et al. A phase I clinical, plasma, and cellular pharmacology study of gemcitabine. J Clin Oncol 1991;9:491-8.

14 Tempero M, Plunkett W, Ruiz van Haperen VW, et al. Randomized phase II comparison of dose-intense gemcitabine: thirty-minute infusion and fixed dose rate infusion in patients with pancreatic adenocarcinoma. J Clin Oncol 2003;21:3402-8.

15 Kroep JR, Giaccone G, Voorn DA, et al. Gemcitabine and paclitaxel: pharmacokinetic and pharmacodynamic interactions in patients with non-small-cell lung cancer. J Clin Oncol 1999;17:2190-7.

16 Patel SR, Gandhi V, Jenkins J, et al. Phase II clinical investigation of gemcitabine in advanced soft tissue sarcomas and window evaluation of dose rate on gemcitabine triphosphate accumulation. J Clin Oncol 2001;19:3483-9.

17 Buesa JM, Losa R, Fernandez A, et al. Phase I clinical trial of fixed-dose rate infusional gemcitabine and dacarbazine in the treatment of advanced soft tissue sarcoma, with assessment of gemcitabine triphosphate accumulation. Cancer 2004;101:2261-9.

18 Ruiz van Haperen VW, Veerman G, Vermorken JB, Pinedo HM, Peters GJ. Regulation of phosphorylation of deoxycytidine and 2',2'-difluorodeoxycytidine (gemcitabine); effects of cytidine 5'-triphosphate and uridine 5'-triphosphate in relation to chemosensitivity for 2',2'-difluorodeoxycytidine. Biochem Pharmacol 1996;51:911-8.

19 Verschuur AC, Van Gennip AH, Leen R, Van Kuilenburg AB. Increased cytotoxicity of 2',2'-difluoro-2'-deoxycytidine in human leukemic cell-lines after a preincubation with cyclopentenyl cytosine. Nucleosides Nucleotides Nucleic Acids 2004;23:1517-21.

20 Ruiz van Haperen VW, Veerman G, Boven E, Noordhuis P, Vermorken JB, Peters GJ. Schedule dependence of sensitivity to 2',2'-difluorodeoxycytidine (Gemcitabine) in relation to accumulation and retention of its triphosphate in solid tumour cell lines and solid tumours. Biochem Pharmacol 1994;48:1327-39.

21 Alvino E, Fuggetta MP, Tricarico M, Bonmassar E. 2'-2'-difluorodeoxycytidine: in vitro effects on cell-mediated immune response. Anticancer Res 1998;18:3597-3602.

22 Margreiter R, Fischer M, Roberts K, et al. Gemcitabine--a novel immunosuppressive agent--prevents rejection in a rat cardiac transplantation model. Transplantation 1999;68:1051-3.

23 Horton ND, Young JK, Perkins EJ, Truex LL. Toxicity of single-dose oral gemcitabine in mice. Amer Assoc Cancer Res 2004;45:486 (abstract 2115).

24 DeGeorge JJ, Ahn CH, Andrews PA, et al. Regulatory considerations for preclinical development of anticancer drugs. Cancer Chemother Pharmacol 1998;41:173-85.

25 Therasse P, Arbuck SG, Eisenhauer EA, et al. New guidelines to evaluate the response to treatment in solid tumors. European Organization for Research and Treatment of Cancer, National Cancer Institute of the United States, National Cancer Institute of Canada. J Natl Cancer Inst 2000;92:205-16.

26 Veltkamp SA, Hillebrand MJ, Rosing H, et al. Quantitative analysis of gemcitabine triphosphate in human peripheral blood mononuclear cells using weak anion-exchange liquid chromatography coupled with tandem mass spectrometry. J Mass Spectrom 2006;41:1633-42.

27 Beal SL, Sheiner LB. NONMEM User's Guide, University of California, San Fransisco, 1998.

28 U.S. Food and Drug Administration - Center for Drug Evaluation and Research: Oncology Tools Product Label Details for Prescribing gemcitabine 1998;
http://www.accessdata.fda.gov/scripts/cder/onctools/prescribe.cfm?GN=gemcitabine.

29 Gilbert JA, Salavaggione OE, Ji Y, et al. Gemcitabine pharmacogenomics: cytidine deaminase and deoxycytidylate deaminase gene resequencing and functional genomics. Clin Cancer Res 2006;12:1794-1803.

30 Rademaker-Lakhai JM, Crul M, Pluim D, et al. Phase I clinical and pharmacologic study of a 2-weekly administration of cisplatin and gemcitabine in patients with advanced non-small cell lung cancer. Anticancer Drugs 2005;16:1029-36.

31 Van Moorsel CJ, Kroep JR, Pinedo HM, et al. Pharmacokinetic schedule finding study of the combination of gemcitabine and cisplatin in patients with solid tumors. Ann Oncol 1999;10:441-8.

32 Kuenen BC, Rosen L, Smit EF, et al. Dose-finding and pharmacokinetic study of cisplatin, gemcitabine, and SU5416 in patients with solid tumors. J Clin Oncol 2002;20:1657-67.

33 Veltkamp SA, Ong FHG, Bolijn MJ, Garcia-Ribas I, Beijnen JH, Schellens JHM. In vitro toxicity of gemcitabine and its metabolite 2',2'-difluorodeoxyuridine in human cancer cells (abstract). Naunyn Schmiedeberg's Archives of Pharmacology 2007;375:145.

34 Veltkamp SA, van Eijndhoven MAJ, Pluim D, et al. Gemcitabine metabolite, 2',2'-difluorodeoxyuridine (dFdU), can be phosphorylated and incorporated into nucleic acids (abstract). Proc Amer Assoc Cancer Res 2007;48:366.

35 Gandhi V, Xu YZ, Estey E. Accumulation of arabinosyluracil 5'-triphosphate during arabinosylcytosine therapy in circulating blasts of patients with acute myelogenous leukemia. Clin Cancer Res 1998;4:1719-26.

36 Look KY, Sandler A, Blessing JA, Lucci JA 3rd, Rose PG. Phase II trial of gemcitabine as second-line chemotherapy of uterine leiomyosarcoma: a Gynecologic Oncology Group (GOG) Study. Gynecol Oncol 2004;92:644-7.

37 Silvestris N, Piscitelli D, Crucitta E, Fiore M, De Lena M, Lorusso V. Unusual response to second-line single-agent gemcitabine in locally advanced primary leiomyosarcoma of the lung: a case report. J Chemother 2003;15:507-9.

38 Castelli F, Sarpietro MG, Ceruti M, Rocco F, Cattel L. Characterization of lipophilic gemcitabine prodrug-liposomal membrane interaction by differential scanning calorimetry. Mol Pharm 2006;3:737-44.

39 Couvreur P, Stella B, Reddy LH, et al. Squalenoyl nanomedicines as potential therapeutics. Nano Lett 2006;6:2544-8.

Chapter 3.4

Quantitative analysis of gemcitabine triphosphate in human peripheral blood mononuclear cells using weak anion exchange liquid chromatography coupled with tandem mass spectrometry

Journal of Mass Spectrometry 2006;41:1633-1642

Stephan A. Veltkamp
Michel J.X. Hillebrand
Hilde Rosing
Robert S. Jansen
Enaksha R. Wickremsinhe
Everett J. Perkins
Jan H.M. Schellens
Jos H. Beijnen

Abstract

Gemcitabine triphosphate (dFdCTP) is a highly active metabolite of gemcitabine. It is formed intracellularly via the phosphorylation of gemcitabine by deoxycytidine kinase. The monitoring of dFdCTP in human peripheral blood mononuclear cells (PBMCs), in addition to plasma concentrations of gemcitabine and its metabolite 2',2'-difluorodeoxyuridine, is considered very useful in determining pharmacokinetic - pharmacodynamic relationships.

We describe a novel sensitive assay for the quantification of dFdCTP in human PBMCs. The method is based on weak anion-exchange liquid chromatography and detection with tandem mass spectrometry (LC-MS/MS). The assay has been validated from 1 ng/mL (lower limit of quantification, LLOQ) to 25 ng/mL (upper limit of quantification, ULOQ) using 180 μL aliquots of peripheral blood mononuclear cell (PBMC) extracts containing approximately 0.648 mg protein or 3.8 x 10^6 lysed PBMCs. The LLOQ is equivalent to 94 fmol/10^6 cells (1 ng/mL = 0.18 ng/180 μL or 0.18 ng/0.648 mg protein = 0.047 ng/10^6 cells or 94 fmol/10^6 cells). This highly sensitive assay is capable of quantifying about 200-fold lower concentrations of dFdCTP in human PBMCs than currently available methods.

Introduction

Gemcitabine (2',2'-difluorodeoxycytidine) belongs to the pyrimidine antimetabolites. It is registered for the treatment of a number of solid tumor types including pancreatic, non-small cell lung (NSCL), ovary, bladder, and breast cancer. Gemcitabine is a prodrug that is intracellularly phosphorylated to gemcitabine monophosphate (2´,2´-difluorodeoxycytidine monophosphate, dFdCMP) by deoxycytidine kinase (dCK) and subsequently to gemcitabine diphosphate (2´,2´-difluorodeoxycytidine diphosphate, dFdCDP) and gemcitabine triphosphate (2´,2´-difluorodeoxycytidine 5´-triphosphate, dFdCTP; Figure 1), a highly active metabolite of gemcitabine (1).

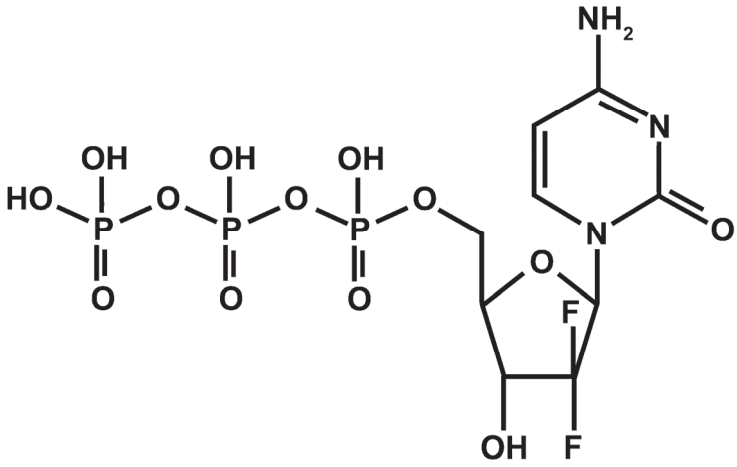

Figure 1. Structure of gemcitabine triphosphate (dFdCTP).

Gemcitabine is also converted to its inactive metabolite 2'2'-difluorodeoxyuridine (dFdU) by cytidine deaminase (CDA). The postulated mechanism of action of gemcitabine is incorporation as dFdCTP into DNA, causing inhibition of DNA synthesis and cell death (2). It has been shown *in vitro* that the intracellular dFdCTP levels and the extent of its incorporation into DNA increase in with gemcitabine in a concentration-dependent manner (2). Furthermore, pre-clinical models have demonstrated a good correlation between intracellular dFdCTP accumulation and cytotoxic activity of gemcitabine (3, 4). Therefore, dFdCTP can be considered the pharmacologically most important metabolite of gemcitabine. Studies have also shown the presence of dFdCTP in peripheral blood mononuclear

cells (PBMCs) during clinical trials (5). Consequently, clinical studies have often monitored dFdCTP levels in PBMCs in addition to the parent drug in plasma for the purpose of investigating the pharmacokinetic and pharmacodynamic relationships (6, 7, 8).

Rose and Brockman described an ion-exchange high performance liquid chromatography (HPLC) method with ultraviolet (UV) detection for the intracellular determination of 9-β-D-arabinofuranosyladenine 5'-triphosphate, a triphosphate metabolite of the nucleoside drug 9-β-D-arabinofuranosyladenine in mouse leukemia cells (9). This method was later adapted and used by others in preclinical and clinical studies with gemcitabine (5, 6, 10-18). Sparidans and co-workers described a method using ion-exchange liquid chromatography (IX-LC) with UV detection for the determination of dFdCTP in PBMCs (19). The lower limit of quantification (LLOQ) of dFdCTP of that assay was 0.4 μM (201 ng/mL, 10 ng/10^6 cells, 20 pmol/10^6 cells). A liquid chromatographic–tandem mass spectrometric (LC-MS/MS) method for the direct quantification of dFdCTP and other nucleoside triphosphates is desirable because of its potential to provide high specificity, sensitivity and simplicity. As nucleoside triphosphates are very hydrophilic compounds and have a strong ionic nature, ion-exchange liquid chromatography (IX-LC) is a useful technique for the separation of these compounds (20). Alternatively, ion-pairing liquid chromatography (IP-LC) has been demonstrated to have adequate chromatographic capacity and reasonable suitability for MS detection of intracellular nucleotides (21-23). However, IP-LC requires high concentration of ion-interaction reagents in the mobile phase that suppresses MS response. The use of weak anion exchange liquid chromatography-tandem mass spectrometry (WAX-LC-MS/MS) has been reported for the quantification of the triphosphate metabolite of D/D4FC, an investigational HIV nucleoside reverse transcriptase inhibitor (24). Our goal was to develop and validate an WAX-LC-MS/MS assay for the quantification of dFdCTP in human PBMCs with an improved sensitivity compared to the method of Sparidans and co-workers (19), to support a clinical trial with gemcitabine in patients receiving the drug at low dose levels.

Experimental

Materials

Gemcitabine triphosphate (dFdCTP), gemcitabine diphosphate (dFdCDP), and gemcitabine monophosphate (dFdCMP) were obtained from Eli Lilly and Company (Greenfield, USA). $^{13}C_9$,$^{15}N_3$-cytidine triphosphate (CTP, internal standard (IS); Figure 2) was obtained from Buchem BV, Apeldoorn, The Netherlands. Methanol (Supra-Gradient grade) was purchased from Biosolve Ltd (Amsterdam, The Netherlands). Ammonia (NH_3) 25%, acetic acid (CH_3COOH) 100%, ammonium acetate (NH_4Ac), acetonitrile (ACN), and perchloric acid ($HClO_4$) (70% (w/w)) (all analytical grade) were purchased from Merck (Darmstadt, Germany). Phosphate Buffered Saline (PBS) was purchased from Sigma Aldrich (Zwijndrecht, The Netherlands). Distilled water (B. Braun Medical, Emmenbrücke, Switzerland) was used throughout the analysis. Blank human buffy coat of leukocytes was purchased from Sanquin Bloodbank (Amsterdam, The Netherlands).

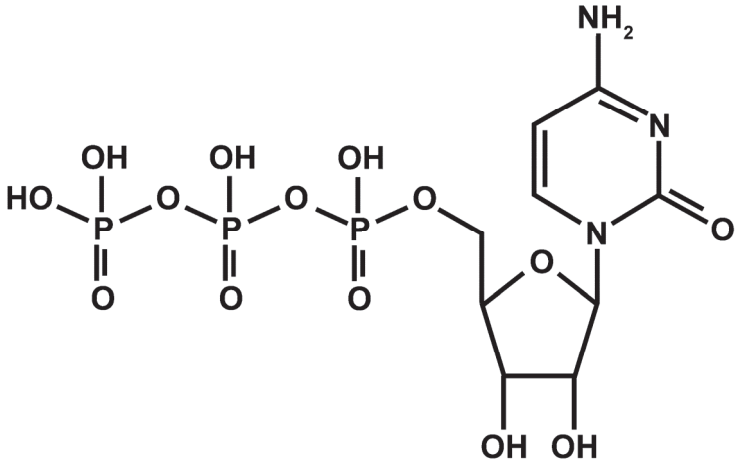

Figure 2. Structure of $^{13}C_9$,$^{15}N_3$-cytidine triphosphate, used as internal standard.

Instrumentation

Chromatographic separations were carried out using an Agilent 1100 series liquid chromatograph system (Agilent technologies, Palo Alto, CA, USA) consisting of a binary pump, an autosampler, a mobile phase degasser, and a column oven. A

Biobasic AX 5 µm, 50 x 2.1 mm column (Thermo Electron Corporation, Murrieta, CA, USA) was used with a step gradient mobile phase consisting of a mixture of 10 mM NH_4Ac in ACN/H_2O (30:70 v/v) pH 6.0 (A) and 1 mM NH_4Ac in ACN/H_2O (30:70 v/v) pH 10.5 (B) (see Table 1).

Table 1. HPLC conditions.

Time (min)	0.00	0.51	1.76	6.6	9.5	10
B%	10	50	100	10	10	10
Flow (ml/min)	0.25	0.25	0.25	0.50	0.25	0.25

The eluent pH was increased and the NH_4Ac concentration was decreased in mobile phase B relative to mobile phase A to obtain a good separation of the three phosphates (dFdCMP, dFdCDP, and dFdCTP). The autosampler temperature was maintained at approximately 4 °C. An injection volume of 25 µl was used and the total run time was 10 minutes. The liquid chromatography (LC) eluate was led directly to the API3000 triple quadrupole mass spectrometer using a turbo ionspray interface (Sciex, Thornhill, Ontario, Canada). A switching valve was used to direct the flow to waste during the first 4 minutes and after 8 minutes. The quadrupoles were operated with unit resolution in the negative ion mode. Nebuliser gas setting was set at 10, while the curtain gas and collision gas (both N_2) were operated at 8 and 9, respectively. Turbo gas flow was 7000 mL/min. The ionspray voltage was kept at -4.5 kV, with a source temperature of 500 °C. The following mass-to-charge (*m/z*) transitions were monitored: *m/z* from 502 to 159 for dFdCTP, *m/z* from 422 to 159 for dFdCDP, *m/z* from 342 to 231 for dFdCMP and *m/z* from 494 to 159 for $^{13}C_9$,$^{15}N_3$-CTP. A dwell time of 250 ms was used for dFdCTP and 50 ms for the other compounds. Data analysis was carried out using Analyst software version 1.2 (MDS Sciex, Toronto, Ontario, Canada).

Preparation of stock and working solutions

Two stock solutions of dFdCTP were prepared in water at a concentration of 1 mg/mL using separate weighings. These solutions were further diluted with water to obtain working solutions. One set of the working solutions was used to prepare

calibration standards while the other was used to prepare the validation samples. $^{13}C_9$,$^{15}N_3$-CTP internal standard stock solution was prepared in water at a concentration of 1 mg/mL and was subsequently diluted with water to a final concentration of 75 ng/mL (working solution). All solutions were stored at -70 °C.

Preparation of calibration standards, validation- and stability samples

Seven calibration standards were prepared ranging from 1 to 25 ng/mL by spiking 180 µL lysates of PBMCs in PBS/$HClO_4$ 1:1 v/v with 9 µL of working solution. Validation samples were prepared similar to the calibration standards at concentrations of 1, 10, and 25 ng/mL. Six replicates of each validation sample were analyzed in 3 analytical runs. Stability samples were prepared at concentrations of 3 and 20 ng/mL for freeze/thaw stability and short and long term stability. Stability sample aliquots of 189 µL were transferred to 1.5 mL polypropylene tubes (Eppendorf Merck) and stored at -70 °C.

Procedure to obtain PBMCs and determination of protein content and cell number

Human buffycoat of leukocytes (approximately 50 mL) were freshly derived out of whole blood (500 mL) of four individual blood donors obtained from Sanquin Bloodbank (Amsterdam, The Netherlands). The buffycoat was further handled according to the procedure described below for the patients. Whole blood samples (15 mL) were collected from patients in heparinized tubes and centrifuged at 4 °C for 5 min at 1500 *g*. The buffy coat of PBMCs at the erythrocyte-plasma interface was collected and transferred to a 15 mL polypropylene tube (Falcon®, Becton Dickinson, NJ, USA) and resuspended in 6 mL PBS. The suspension was carefully layered over 3 mL Ficoll-Paque Plus density gradient (Amersham, Biosciences, Sweden) in a 15 mL polypropylene tube and centrifuged at 4 °C for 20 min at 550 *g* (without brake). This resulted in 3 layers and the upper interface, containing the PBMCs, was transferred to a 50 mL tube (Falcon®, Becton Dickinson, NJ, USA) and washed with 35 mL cold PBS (4°C). Finally, after centrifugation for 5 min at 4 °C at 1500 *g*, the supernatant was removed and the cell pellet was resuspended in 100 µL cold PBS (4 °C). A volume of 10 µL of the cell suspension of PBMCs was removed for the analysis of protein concentrations using the Bio-Rad Protein Assay

(25). A volume of 100 µL of the remaining cell suspension was added to 100 µL 0.8 M $HClO_4$ and the cup was vortex mixed and centrifuged for 3 min at 1500 *g*. The addition of $HClO_4$ resulted in protein precipitation and inactivation and the acid soluble dFdCTP was extracted from the PBMC matrix (18, 19). A volume of 180 µL of the supernatant was transferred to a 1.5 mL polypropylene cup and immediately stored at -70 °C until analysis. The amount of protein was determined for all suspensions of PBMCs (including all individual patient samples) and used for the calculation of dFdCTP concentration in ng/mg protein. For practical purposes, we used the amount of protein instead of cell number to correct for differences in amount of isolated PBMCs between samples, because the samples could be stored for longer periods of time before analysis of protein concentrations, while determination of cell number requires immediate analysis. Furthermore, samples could be analyzed in one batch and if necessary re-analyzed quite easily. Moreover, normalization to cell number can have the disadvantage that the volume of PBMCs may influence the quantification of intracellular drug concentrations. This was shown by Arner and colleagues, who found that phosphorylation of 2-chlorodeoxyadenosine in PBMCs of patients was significantly different between patients with B-cell lymphocytic leukemia and hairy cell lymphoma after normalization to mg of protein, while this was not observed after normalization to cell number (26). They concluded that this was due to differences in cell volume of PBMCs between the two patient groups, and therefore intracellular drug concentrations in PBMCs might not perfectly reflect the exact intracellular drug amount if concentrations are normalized to cell number. Moreover, the quantification of intracellular drugs is often expressed per mg of protein in preclinical *in vitro* and *in vivo* studies when intracellular drug concentrations are determined in cells, organs or tumour tissue. Therefore, it also sounds reasonable to normalize intracellular drug concentrations in PBMCs to protein amount. In addition, we did assess the correlation between cellular protein content and cell number (see results). Therefore, cell number can always be easily calculated from the protein concentration. Furthermore, within PBMC samples of one specific healthy donor, the variability in protein amount was compared to the variability in cell number.

The cell suspension obtained from the blood donor was diluted to obtain an equal amount of mean protein as was determined for 18 patients. These aliquots were

then used for the validation experiments. Total cell concentration was determined for the cell suspension of PBMCs obtained from the blood donor and for the 100 µL cell suspensions of PBMCs in PBS obtained at 30 different samples from 5 individual patients, using a Casy 1 cell counter (Schärfe System GmbH, Reutlingen, Germany).

Sample processing

The frozen PBMC lysates in PBS/$HClO_4$ 1:1 v/v (180 µL) were placed on an ice-water bath to thaw. Calibration standards were prepared by adding 9 µL of working solution (concentrations of dFdCTP ranging from 20 to 500 ng/mL) to yield calibration standards in the range from 1 to 25 ng/mL. Validation samples were prepared by adding 9 µL of working solution containing 20, 200 and 500 ng/mL dFdCTP to obtain target concentrations of 1, 10 and 25 ng/mL. Clinical samples were prepared by adding 9 µL of water. Then, 50 µL of 1 M NH_4Ac was added to all samples, vortex mixed for 10 s, following addition of 20 µL of 10% ammonia and samples were again vortex mixed for 10 s. A volume of 10 µL of internal standard working solution (75 ng/mL) was added to all samples except for the double blank to which 10 µL of water was added. Finally, the samples were transferred to a glass autosampler vial with insert and 25 µl was injected onto the analytical column.

Validation procedures

To demonstrate that the method is reliable and reproducible for the intended use, the following parameters were assessed: linearity, accuracy and precision, carry-over, specificity and selectivity, stability, and matrix effect and recovery under various conditions. The validation was based on the Guidance for Industry on Bioanalytical Method Validation (27), however, some recommendations were adjusted or modified due to the complexity of analysing small molecules (nucleotides) in PBMCs. Based on the outcomes of pre-validation run, the pre-determined acceptance criteria were clearly established in a validation plan, prior to the initiation of the validation study. Procedures and applied criteria are discussed below.

Linearity

Seven non-zero calibration standards (1.0, 2.5, 5.0, 10, 15, 20, 25 ng/mL) were freshly prepared in control blank PBMCs in PBS/$HClO_4$ 1:1 v/v before each run and analyzed in duplicate in three separate analytical runs. Calibration curves were calculated by least-squares linear regression using a weighing factor of $1/x^2$. Linearity is evaluated by means of back-calculated concentrations of the calibration standards: these values should be within 20 % of the actual concentration. No more than 25% of the calibration standards may be rejected from the calibration curve.

Accuracy and precision

Accuracy and precision determination was conducted by analyzing six replicates each of validation samples in acidified PBMCs along with a front calibration curve performed over three analytical runs. The intra-assay accuracy was determined as the percent difference between the mean concentration per analytical run and the nominal concentration. The inter-assay accuracy was determined as the percent difference between the mean concentration after three analytical runs and the nominal concentration. The coefficient of variation (C.V.) was used to report the intra- and inter-assay precision. The accuracies and precisions should be within ± 20%. Clinical PBMC samples were diluted in control human acidified PBMCs and re-assayed when dFdCTP concentrations were above the upper limit of quantification (25 ng/mL)

Carry-over

Carry-over was evaluated in duplicate in three analytical runs by injecting two matrix blanks immediately following the ULOQ sample(s). Carry-over is acceptable as long as the mean carry-over in the first blank is less than or equal to 30% of the peak area of the LLOQ and is less than or equal to 20% in the second blank.

Specificity and selectivity

Four individual batches of control human acidified PBMC blank samples (without IS) were analyzed to evaluate specificity and selectivity. The objective was to determine whether any endogenous compounds interfere at the mass transitions chosen for dFdCTP and the internal standard. Interference can occur when co-

eluting endogenous compounds produce ions at the same *m/z* values that are used to monitor the analyte and internal standard. The peak areas of interference peaks co-eluting with the analyte should not exceed 20% of the analyte peak area at the LLOQ or 5 % of the internal standard area. The selectivity of the LC system was evaluated by the analyses of a system suitability sample prior to the start of each analytical run. The system suitability sample contained dFdCMP and dFdCDP in addition to dFdCTP in order to establish good separation of the three phosphates.

Stability

The stability of dFdCTP was evaluated in the stock solutions after 24 h at ambient temperatures and after 5.3 months of storage at -70 °C. The stability of the internal standard working solution was evaluated after 24 h at ambient temperatures and after 7.3 months of storage at -70°C. The analytes are considered stable at the respective concentrations when 95-105 % of the initial concentration is found. Matrix stability of dFdCTP was evaluated in acidified PBMCs at 3 and 20 ng/mL and analyzed in triplicate. The evaluation included 2 cycles of freeze/thaw stability (frozen at -70 °C and thawed at room temperature) compared with freshly prepared validation samples. We determined 2 instead of 3 cycles of freeze/thaw stability since the total sample of 180 µL was used for the quantification. If clinical samples were diluted in blank PBMCs, a sample volume remains for one re-assay. Short term matrix stability was evaluated for 2 hours at ambient temperatures and long-term matrix stability was conducted following storage at -70 °C for 6 months. The analyte was considered stable in the biological matrix or extracts thereof when 80-120% of the initial concentration was found. During the validation, the reinjection reproducibility was assessed to determine if an analytical run may be reanalyzed in the case of instrument failure. A validation sample set was reinjected and analyzed at least 24 h after the first injection at 4 °C. Accuracies should be within ± 20% of the actual values and the precisions should not exceed ± 20%. Also, final extract stability was studied at 4 °C for 4 weeks.

Matrix effect and recovery

The matrix effect is relevant in LC-MS/MS as co-eluting, mainly endogenous compounds can interfere during the ionization process. This could lead to a

decrease of the MS signal with increasing amounts of biological sample. In addition, recovery is important, because loss of the analyte might occur during cell lysis and centrifugation. The matrix effect was determined as a function of the amount of protein in PBMCs obtained after isolation from a leukocyte buffycoat from an individual donor as described above. Samples containing protein concentrations from 0 to 20 ng/mL were spiked with 3, 10, and 20 ng/mL of dFdCTP. Samples were spiked before lysis (90 µL of cell suspension with 10 µL dFdCTP working solution following mixing with 100 µL $HClO_4$ and addition of 9 µL of H_2O to 180 µL of supernatant) and after lysis (addition of 10 µL H_2O to 90 µL of cell suspension and mixing with 100 µL $HClO_4$ following addition of 9 µL of dFdCTP working solution to 180 µL of supernatant). The dFdCTP signals were compared between the samples before and after lysis for each protein concentration.

Application of the dFdCTP assay

To test the applicability of the method we measured dFdCTP concentrations in PBMCs obtained from patients who received a 300 mg/m^2 dose of i.v. gemcitabine. Blood samples were collected at the following time points: before start of infusion, at time of end of infusion, and 1 h, 2 h, 8 h, and 24 h after end of infusion. PBMCs were isolated after centrifugation as described previously in the article. Finally, 180 µl of PBMC suspension in PBS/0.8 M $HClO_4$ (1:1 v/v) was stored at -70 °C until analysis.

Results and discussion

Mass spectrometry

Figure 3 shows an MS/MS spectrum of dFdCTP following the fragmentation of the deprotonated molecular ion ($[M-H]^-$). The most abundant fragment ion can be observed at *m/z* 159 corresponding to the diphosphate fragment ion. The fragment at *m/z* 422 corresponds to dFdCDP, which is formed after cleavage of the terminal phosphate group from the parent molecular ion. The transition from 502 to 159 was used for multiple reaction monitoring (MRM). The proposed fragmentation pattern of dFdCTP is depicted in Figure 4.

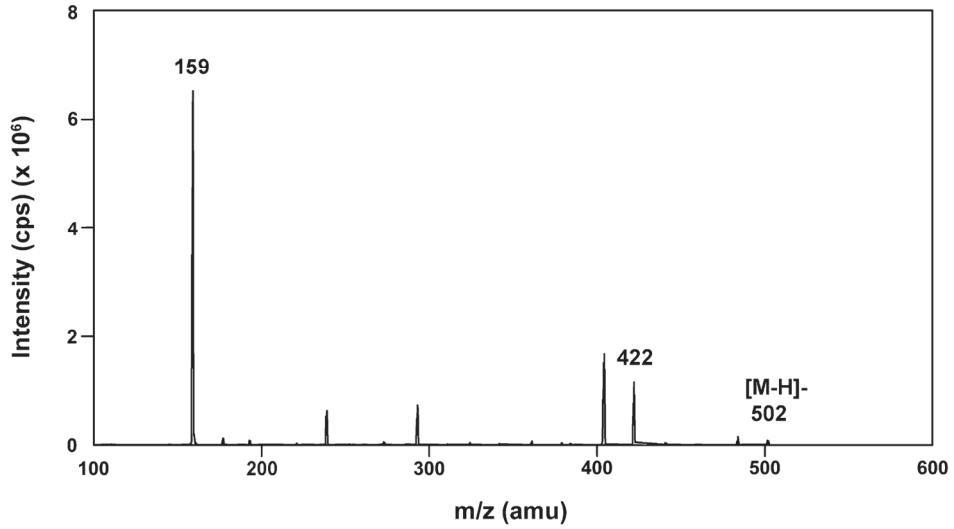

Figure 3. Product ion MS/MS spectrum of dFdCTP from the deprotonated molecular ion at *m/z* 502.

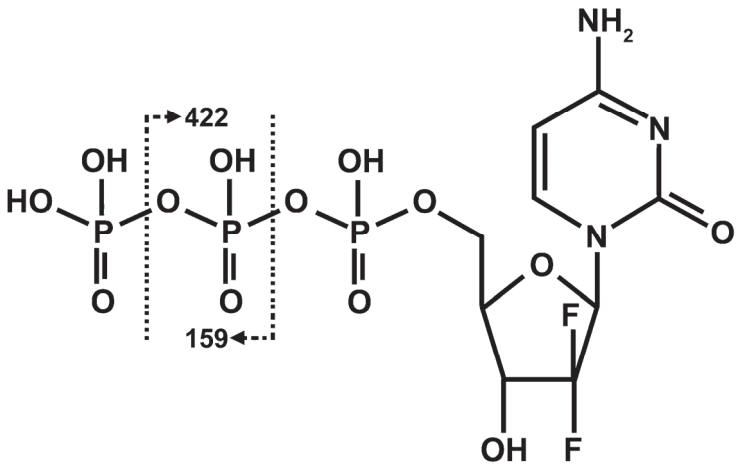

Figure 4. Proposed fragmentation scheme for dFdCTP.

Figure 5 shows an MS/MS spectrum of the internal standard following the fragmentation of the deprotonated molecular ion ($[M-H]^-$). The transition from 494 to 159 was used for MRM. IX-LC often requires the use of high salt concentrations in the mobile phase, with the disadvantage of causing ion-suppression and

deposition of non-volatile salts (24). We chose a mobile phase containing NH_4Ac in ACN/H_2O (30:70 v/v), which is compatible with MS detection. The lower concentration of NH_4Ac of 1 mM in mobile phase B reduced possible ion-suppression and was performed to get a good separation of the three gemcitabine phosphates (dFdCMP, dFdCDP, and dFdCTP) (24).

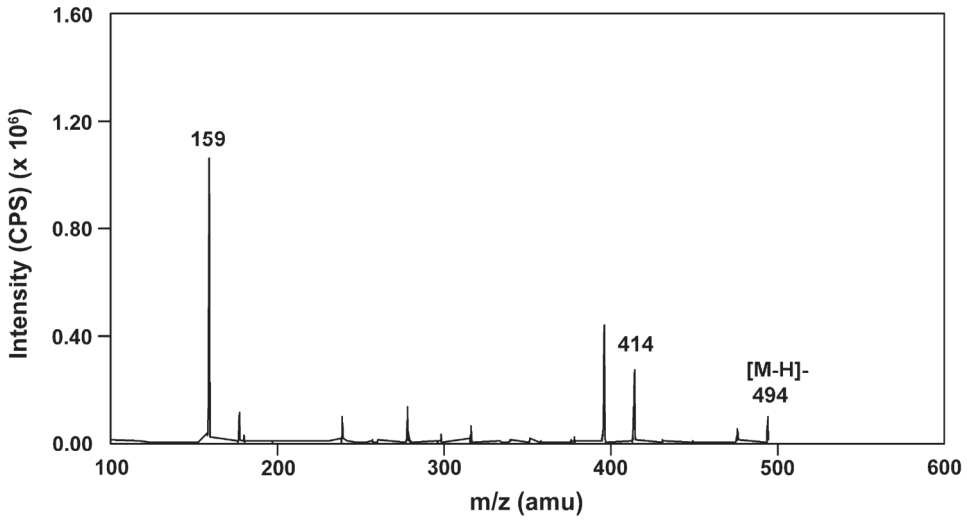

Figure 5. Product ion MS/MS spectrum of the internal standard CTP from the deprotonated molecular ion at *m/z* 494.

Chromatography

Representative chromatograms of a LLOQ calibration sample and a zero blank (blank + IS) are shown in Figure 6. An endogenous substance elutes around 6 min. The peak is well separated from dFdCTP, which has a retention time of 6.6 min, and did not interfere with the quantification of dFdCTP.

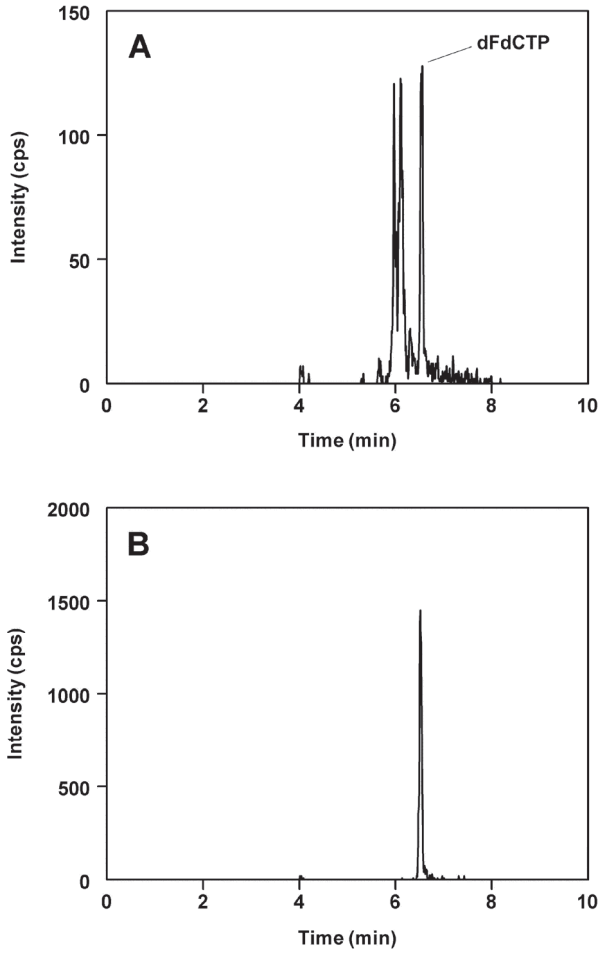

Figure 6. Representative chromatograms of (A) a dFdCTP calibration sample at the LLOQ (1 ng/mL) (retention time = 6.6 min) (*m/z* transition from 502 to 159) and (B) IS at 4.5 ng/mL (retention time = 6.6 min) (*m/z* transition from 494 to 159) in human acidified PBMCs.

Figure 7 demonstrates that dFdCTP, dFdCDP, and dFdCMP are well separated, using the WAX-LC method with the gradient of pH from pH 6 to 10.5 together with a decreasing NH_4Ac concentration in mobile phase B relative to that in mobile phase A as described by others (24).

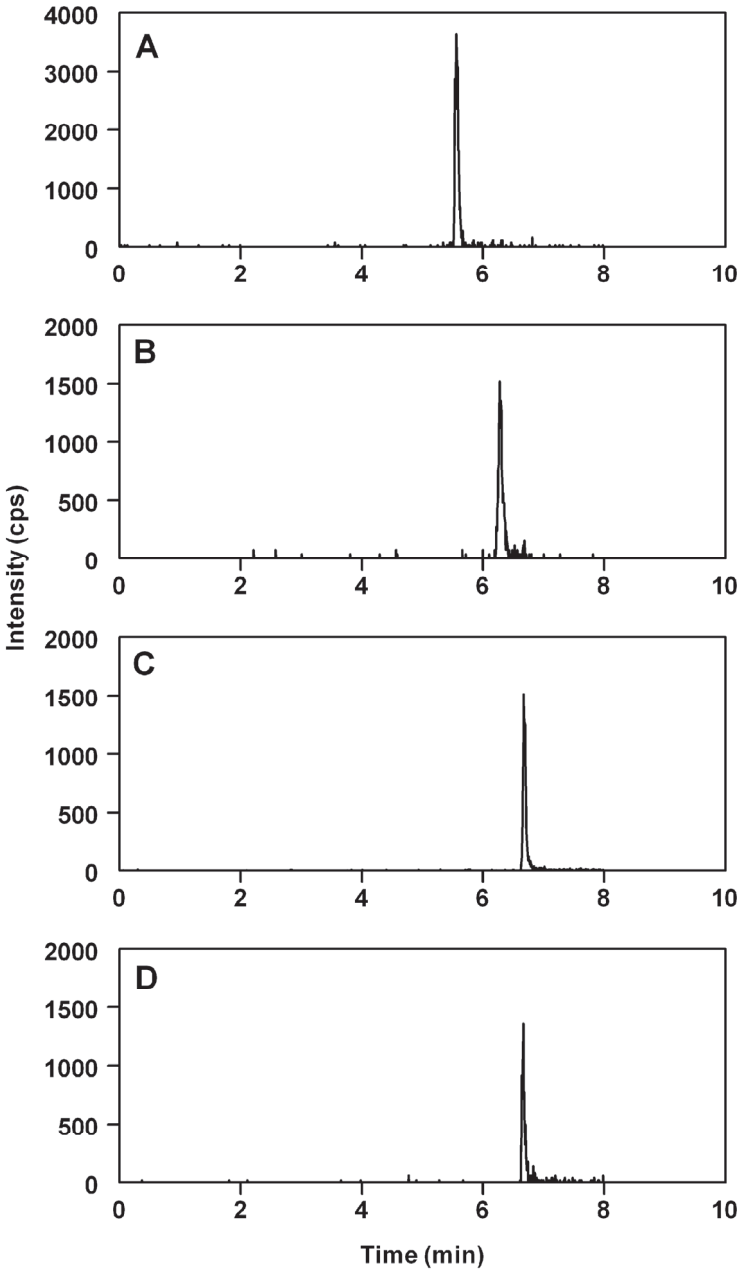

Figure 7. Representative chromatograms of a system suitability test for (A) dFdCMP (retention time = 5.6 min) (*m/z* transition from 342 to 231), (B) dFdCDP (retention time = 6.3 min) (*m/z* transition from 422 to 159), (C) dFdCTP (retention time = 6.6 min) (*m/z* transition from 502 to 159), and (D) IS (retention time = 6.6 min) (*m/z* transition from 494 to 159).

Procedure to obtain PBMCs and determination of protein content and cell number

The mean protein and cell concentration in the patient samples of 100 µL PBMCs in PBS was 7.205 mg/mL (C.V. = 64%) and 42 x 10^6 cells/mL (C.V. = 86%), respectively. Thus, after 1:1 dilution with 0.8 M $HClO_4$ the PBMC cell suspension contained 3.603 mg/mL proteins and 21 x 10^6 cells/mL. Therefore, the final 180 µL PBMC extract samples used for analysis contained approximately 0.648 mg protein or 3.8 x 10^6 lysed PBMCs. The control PBMCs used for the validation experiments obtained from freshly derived PBMC suspensions from healthy human volunteers were diluted with PBS to approximate a final protein concentration of 7.205 mg/mL which upon 1:1 dilution with $HClO_4$ yielded total protein concentrations and cell counts similar to the lysed PBMC patient samples. Within samples of one specific healthy donor, the variability in protein amount (C.V. = 2.4%) was comparable with the variability in cell number (C.V. = 2.5%).

Validation procedures

Linearity

The best fit for the calibration curves was obtained by using a weighting factor of the reciprocal of the squared concentration (Figure 8). The correlation coefficients were 0.991 or better. The calibration standards were back-calculated from the responses. The deviations of the nominal concentrations were between -4.67 and 4.07% for all concentrations of dFdCTP. The C.V. values ranged from 4.27 to 10.9% (data not shown).

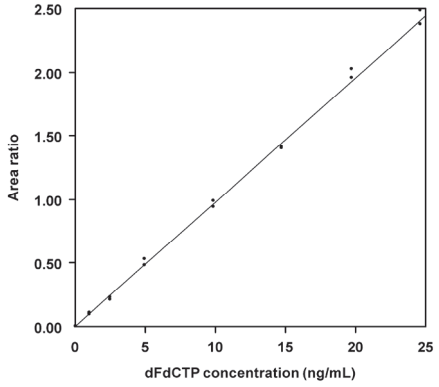

Figure 8. Representative calibration curve for dFdCTP in acidified PBMCs.

Accuracy and Precision

Intra- and inter-assay performance data for dFdCTP are summarized in Table 2. The intra-assay accuracy ranged from -5.08 % to 7.63%, while the inter-assay accuracy ranged from –3.82 % to 2.84 %. The mean intra-assay precision did not exceed 9.71% and the inter-assay precision did not exceed 8.58% for all tested concentrations. Both accuracy and precisions where within ± 20% over the validated assay range of 1 to 25 ng/mL.

Table 2. Assay performance data for dFdCTP in human acidified PBMCs.

Run	Nominal concentration (ng/mL)	Mean calculated concentration (ng/mL)	Accuracy (% deviation)	Precision (% CV)	Number of replicates
1	0.983	1.06	7.63*	8.03#	6
2	0.983	0.993	0.983*	9.20#	6
3	0.983	0.982	-0.102*	7.85#	6
Average	0.983	1.01	2.84**	8.58^	18
1	9.83	9.55	-2.87*	2.89#	6
2	9.83	9.72	-1.17*	5.74#	6
3	9.83	10.9	1.90*	7.99#	6
Average	9.83	9.76	-0.712**	5.99^	18
1	24.6	23.4	-5.08*	8.97#	6
2	24.6	24.3	-1.29*	3.95#	6
3	24.6	23.4	-5.08*	9.71#	6
Average	24.6	23.7	-3.82**	7.36^	18

* Intra-assay accuracy (%); # Intra-assay precision (%); ** Inter-assay accuracy (%); ^ Inter-assay precision (%).

Carry-over

The mean carry-over in the first blank was 19.6% and in the second blank 13.6% of the dFdCTP peak area in the LLOQ sample, indicating acceptable carry-over. Because nucleoside triphosphates have the tendency to stick to stainless steel surfaces, PEEK tubing was used to directly connect the autosampler to the column. The relatively high percentage of dFdCTP in the second blank may be due to the tendency of nucleotides to adsorb on stainless steel surfaces. Therefore PEEK tubing was used in the flow path where possible, to minimize this effect.

Specificity and selectivity

Double blank and blank samples prepared from four individual batches of human acidified PBMCs did not show any peaks that co-eluated with dFdCTP with areas exceeding 20% of the LLOQ nor any peaks that co-eluted with the internal standard with areas that exceeded 5% of the internal standard. The relative interferences in the tested blanks were less than 8% for dFdCTP and none were observed for the internal standard. A system suitability test showed that dFdCMP, dFdCDP and dFdCTP were separated, demonstrating a good chromatographic system. We considered the capability of separating dFdCTP from dFdCDP and dFdCMP to be a minimum requirement for the chromatographic method, but this was not necessary for the quantitation of only dFdCTP because of the high selectivity of the MS/MS instrumentation. All four individual batches exhibited endogenous peaks as shown in Figure 6, which were well separated from dFdCTP and did not interfere with the quantification of dFdCTP. Although, gemcitabine was not combined with other nucleoside drugs in the treatment of cancer patients at our Institute, other nucleoside drugs could theoretically interfere with the assay when combined with gemcitabine. Therefore, we checked the specificity against the active phosphate metabolites of other nucleoside drugs, by comparing the mass of gemcitabine (average MW = 263.2) with other commonly used nucleoside analogues (and consequently the mass of dFdCTP (average MW = 503) with the triphosphate of these nucleoside analogues), which were: cladribine (285.7), fludarabine (285.2), cytarabine (243.2), thioguanosine (299.3), lamivudine (229.3), zidovudine (267.2), zalcitabine (211.2), stavudine (224.2), dideoxyadenosine (ddA) (235.2) (active nucleoside of didanosine (ddI)), carbovir (247.3) (active nucleoside of abacavir), acyclovir (225.2), emtricitabine (247.2), ganciclovir (255.2), penciclovir (253.3), and tenofovir diphosphate (446.0) (metabolite of tenofovir (PMPA). Based on this comparison no interferences were expected, guaranteeing sufficient specificity for the quantification of dFdCTP.

Stability

The results of the stability experiments for dFdCTP are summarized in Table 3. dFdCTP was stable in stock solution for 24 hours at ambient temperatures and after 5.3 months of storage at -70 °C. Furthermore, dFdCTP was stable in human

acidified PBMCs for 2 freeze/thaw cycles and is stable in human PBMCs for 2 hours at ambient temperatures and after storage for 6 months at -70°C. In addition, re-injection reproducibility was established for 24 hours enabling the reinjection of samples within 24 h when stored at 4 °C. Moreover, dFdCTP was found to be stable in the final PBMC extract for 4 weeks at 4 °C. The IS was stable in stock solution for 24 hours at ambient temperatures and after 7.3 months of storage at -70 °C.

Table 3. Stability data of dFdCTP and IS.

Matrix	Conditions	Initial Conc. (ng/mL)	Found Conc. (ng/mL)	Dev. (%)	C.V. (%)	Number of replicates
dFdCTP, water	Ambient, 24 h	1.00	0.986	-1.36	2.17	3
(stock solution)	-70 °C, 5.3 months	1.00	1.00	1.44	14.1	3
	2 freeze (-70 °C)/	2.65	2.64	-0.503	7.97	3
	thaw cycles	18.0	16.8	-6.85	13.2	3
dFdCTP, human acidified	Ambient, 2 h	2.65	2.79	5.28	17.7	3
PBMCs		18.0	17.3	-3.89	2.45	3
	-70 °C, 6 months	2.91	3.14	7.79	11.0	3
		19.4	19.8	1.89	4.30	3
	2-8 °C, 4 weeks	2.91	2.84	-2.29	17.9	3
dFdCTP,		19.4	21.4	10.5	15.9	3
final extract	Reinjection reproducibility,	0.983	1.05	7.04	8.55	6
	2-8 °C, 24 h	9.83	9.53	-3.02	7.31	6
		24.6	23.4	-4.74	5.64	6
IS, water	Ambient, 24 h	75.0	75.5	0.600	5.08	3
(working solution)	-70 °C, 7.3 months	75.0	75.3	0.464	1.74	3

Matrix effect and recovery

The matrix effect for dFdCTP at 10 ng/mL vs. the amount of protein is shown in Figure 9. The signal for dFdCTP decreases in samples containing 0 to 2 mg/mL of protein, after which it remains stable up to 20 mg/mL of protein. The same pattern is seen for the IS, and therefore the IS corrects very well for the influence of the matrix on the dFdCTP signal. The normalized dFdCTP/IS ratio remained within ± 20% in the range from 0 to 20 mg/mL of protein, which is acceptable for quantification. The protein concentration did not significantly affect the

quantification of dFdCTP at all tested levels. Our patient samples could be directly measured without requiring dilution, because protein concentrations were within the tested range. By comparing the area ratios of the samples spiked with 10 ng/mL of dFdCTP before and after lysis, the recovery was established at 94 ± 23%.

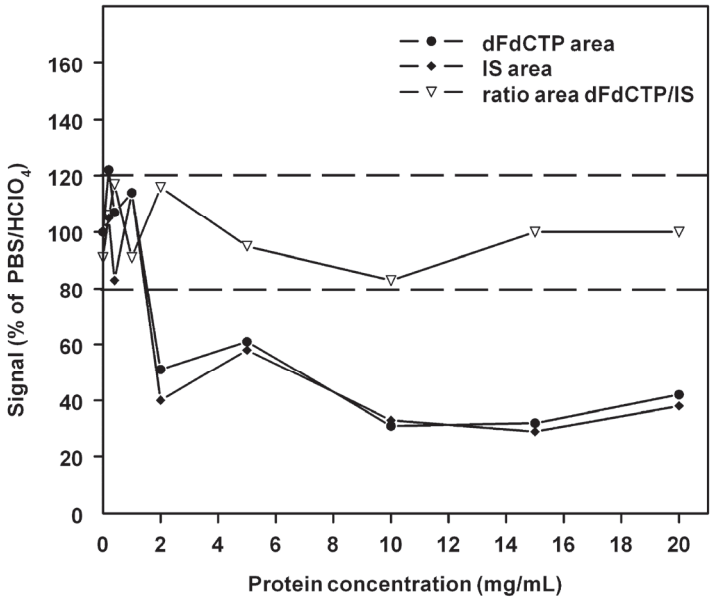

Figure 9. Matrix effect (signal as % of PBS/$HClO_4$ 1:1 v/v) of 10 ng/mL dFdCTP, IS and normalized dFdCTP/IS ratio with various amounts of PBMC protein.

Application of the dFdCTP assay

A chromatogram showing dFdCTP extracted from the PBMCs of a patient treated with gemcitabine is shown in Figure 10. Figure 11 shows a concentration *versus* time profile of dFdCTP in PBMCs of a patient receiving 300 mg/m^2 of i.v. gemcitabine demonstrating the applicability of this methodology for monitoring patient populations. For practical purposes, the dFdCTP concentrations are normalized to the protein content of the respective PBMC sample to account for differences in PBMC counts among individual patient samples. The sensitivity of this methodology is demonstrated by the fact that dFdCTP concentrations can be quantified at concentrations below 0.5 ng/mg protein.

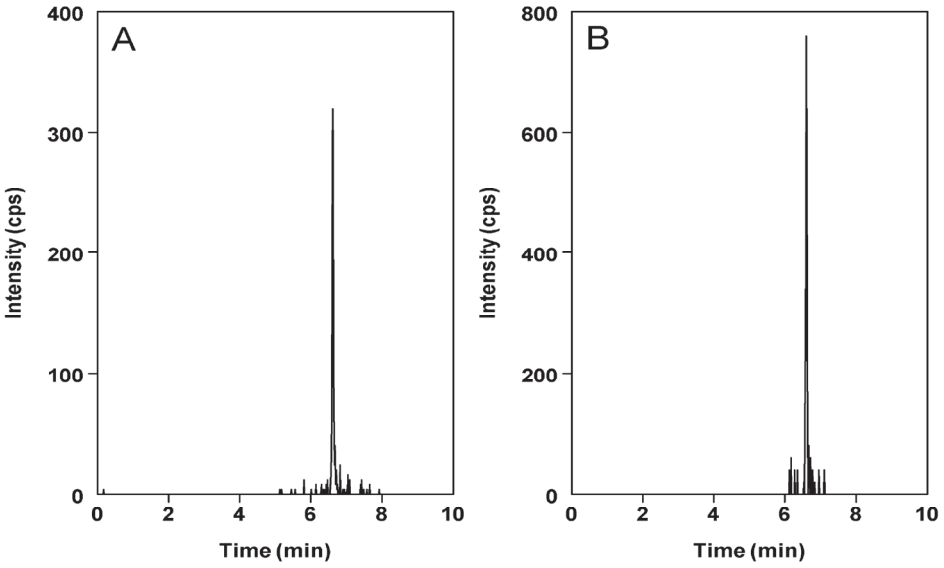

Figure 10. Representative chromatograms from a patient PBMC sample (A) dFdCTP 16.3 ng/mL (retention time = 6.6 min) (*m/z* transition from 502 to 159) and (B) IS (retention time = 6.6 min) (*m/z* transition from 494 to 159).

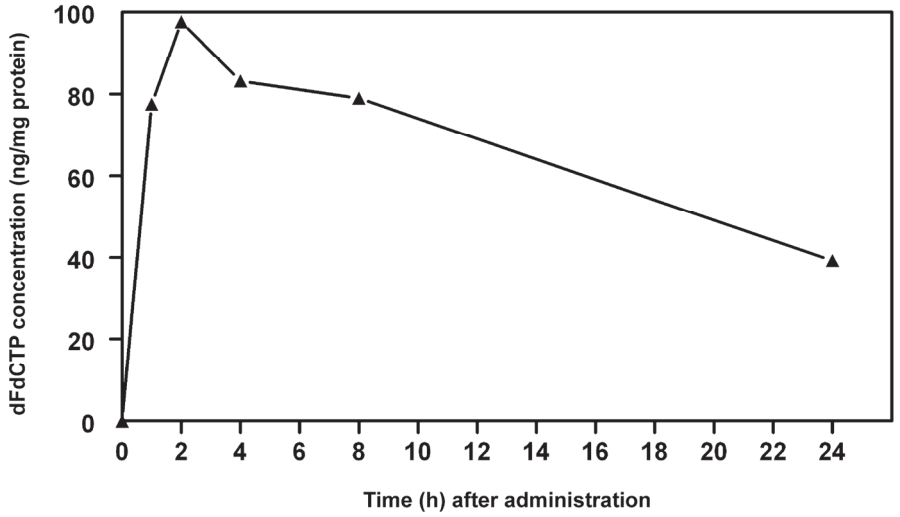

Figure 11. Profile of dFdCTP in PBMCs (expressed as ng/mg protein) versus time from an individual patient.

Conclusion

The method presented here is sensitive and specific in the quantification of dFdCTP in human PBMC's. The validated range for dFdCTP was from 1 to 25 ng/mL using 180 µL aliquots of human acidified extracts of PBMCs containing approximately 0.648 mg protein and 3.8 x 10^6 lysed PBMCs (1 ng/mL = 0.18 ng/180 µL or 0.18 ng/0.648 mg protein = 0.047 ng/10^6 cells or 94 fmol/10^6 cells). The methodology presented here was approximately 200 times more sensitive for the quantification of dFdCTP in human PBMCs compared to the methodology reported by Sparidans and co-workers (19) and is useful to quantify lower concentrations of dFdCTP in patient samples following the administration of lower doses of gemcitabine.

References

1. Plunkett W, Huang P, Gandhi V. Preclinical characteristics of gemcitabine. Anticancer Drugs 1995;6:7-13.

2. Huang P, Chubb S, Hertel LW, Grindey GB, Plunkett W. Action of 2',2'-difluorodeoxycytidine on DNA synthesis. Cancer Res 1991;51:6110-6117.

3. Ruiz van Haperen VW, Veerman G, Vermorken JB, Pinedo HM, Peters G. Regulation of phosphorylation of deoxycytidine and 2',2'-difluorodeoxycytidine (gemcitabine); effects of cytidine 5'-triphosphate and uridine 5'-triphosphate in relation to chemosensitivity for 2',2'-difluorodeoxycytidine. Biochem Pharmacol 1996;51:911-918.

4. Verschuur AC, Van Gennip AH, Leen R, Van Kuilenburg AB. Increased cytotoxicity of 2',2'-difluoro-2'-deoxycytidine in human leukemic cell-lines after a preincubation with cyclopentenyl cytosine. Nucleosides Nucleotides Nucleic Acids 2004;23:1517-1521.

5. Grunewald R, Abbruzzese JL, Tarassoff P, Plunkett W. Saturation of 2',2'-difluorodeoxycytidine 5'-triphosphate accumulation by mononuclear cells during a phase I trial of gemcitabine. Cancer Chemother Pharmacol 1991; 27:258-262.

6. Kroep JR, Giaccone G, Voorn DA, Smit EF, Beijnen JH, Rosing H, et al. Gemcitabine and paclitaxel: pharmacokinetic and pharmacodynamic interactions in patients with non-small-cell lung cancer. J Clin Oncol 1999; 17:2190-2197.

7. Patel SR, Gandhi V, Jenkins J, Papadopolous N, Burgess MA, Plager C, et al. Phase II clinical investigation of gemcitabine in advanced soft tissue sarcomas and window evaluation of dose rate on gemcitabine triphosphate accumulation. J Clin Oncol 2001;19:3483-3489.

8. Buesa JM, Losa R, Fernandez A, Sierra M, Esteban E, Diaz A, et al. Phase I clinical trial of fixed-dose rate infusional gemcitabine and dacarbazine in the treatment of advanced soft tissue sarcoma, with assessment of gemcitabine triphosphate accumulation. Cancer 2004;101:2261-2269.

9. Rose LM, Brockman RW. Analysis by high-pressure liquid chromatography of 9-beta-D-arabinofuranosyladenine 5'-triphosphate levels in murine leukemia cells. J Chromatogr 1977;133:335-343.

10. Abbruzzese JL, Grunewald R, Weeks EA, Gravel D, Adams T, Nowak B, et al. A phase I clinical, plasma, and cellular pharmacology study of gemcitabine. J Clin Oncol 1991;9:491-498.

11. Grunewald R, Kantarjian H, Du M, Faucher K, Tarassoff P, Plunkett W. Gemcitabine in leukemia: a phase I clinical, plasma, and cellular pharmacology study. J Clin Oncol 1992;10:406-413.

12. Heinemann V, Hertel LW, Grindey GB, Plunkett W. Comparison of the cellular pharmacokinetics and toxicity of 2',2'-difluorodeoxycytidine and 1-beta-D-arabinofuranosylcytosine. Cancer Res 1988;48:4024-4031.

13. Peters GJ, Laurensse E, Leyva A, Lankelma J, Pinedo HM. Sensitivity of human, murine, and rat cells to 5-fluorouracil and 5'-deoxy-5-fluorouridine in relation to drug-metabolizing enzymes. Cancer Res 1986;46:20-28.

14. Ruiz van Haperen VW, Veerman G, Boven E, Noordhuis P, Vermorken JB, Peters GJ. Schedule dependence of sensitivity to 2',2'-difluorodeoxycytidine (Gemcitabine) in relation to accumulation and retention of its triphosphate in solid tumour cell lines and solid tumours. Biochem Pharmacol 1994;48:1327-1339.

15. Bergman AM, Ruiz van Haperen VW, Veerman G, Kuiper CM, Peters GJ. Synergistic interaction between cisplatin and gemcitabine in vitro. Clin Cancer Res 1996;2:521-530.

16. Smitskamp-Wilms E, Pinedo HM, Veerman G, Ruiz van Haperen VW, Peters GJ. Postconfluent multilayered cell line cultures for selective screening of gemcitabine. Eur J Cancer 1998;34:921-926.

17. Van Moorsel CJ, Kroep JR, Pinedo HM, Veerman G, Voorn DA, Postmus PE, et al. Pharmacokinetic schedule finding study of the combination of gemcitabine and cisplatin in patients with solid tumors. Ann Oncol 1999;10:441-448.

18. Plunkett W, Chubb S, Alexander L, Montgomery JA. Comparison of the toxicity and metabolism of 9-beta-D-arabinofuranosyl-2-fluoroadenine and 9-beta-D-arabinofuranosyladenine in human lymphoblastoid cells. Cancer Res 1980;40:2349-2355.

19. Sparidans RW, Crul M, Schellens JHM, Beijnen JH. Isocratic ion-exchange chromatographic assay for the nucleotide gemcitabine triphosphate in human white blood cells. J Chromatogr B Analyt Technol Biomed Life Sci 2002;780:423-430.

20. Khym JX. An analytical system for rapid separation of tissue nucleotides at low pressures on conventional anion exchangers. Clin Chem 1975;21:1245-1252.

21. Claire RL, III. Positive ion electrospray ionization tandem mass spectrometry coupled to ion-pairing high-performance liquid chromatography with a phosphate buffer for the quantitative analysis of intracellular nucleotides. Rapid Commun Mass Spectrom 2000;14:1625-1634.

22. Pruvost A, Becher F, Bardouille P, Guerrero C, Creminon C, Delfraissy JF, et al. Direct determination of phosphorylated intracellular anabolites of stavudine (d4T) by liquid chromatography/tandem mass spectrometry. Rapid Commun Mass Spectrom 2001;15:1401-1408.

23. Fung EN, Cai Z, Burnette TC, Sinhababu AK. Simultaneous determination of Ziagen and its phosphorylated metabolites by ion-pairing high-performance liquid chromatography-tandem mass spectrometry. J Chromatogr B Biomed Sci Appl 2001;754:285-295.

24. Shi G, Wu JT, Li Y, Geleziunas R, Gallagher K, Emm T, et al. Novel direct detection method for quantitative determination of intracellular nucleoside triphosphates using weak anion exchange liquid chromatography/tandem mass spectrometry. Rapid Commun Mass Spectrom 2002;16:1092-1099.

25. Bradford MM. A rapid and sensitive method for the quantitation of microgram quantities of protein utilizing the principle of protein-dye binding. Anal Biochem 1976;72:248-254.

26. Arner ES, Spasokoukotskaja T, Juliusson G, Liliemark J, Eriksson S. Phosphorylation of 2-chlorodeoxyadenosine (CdA) in extracts of peripheral blood mononuclear cells of leukaemic patients. Br J Haematol 1994;87:715-718.

27. U.S. Department of Health and Human Services, Food and Drug Administration, Center for Drug Evaluation and Research, Center for Veterinary Medicine. World Wide Web. Guidance for Industry - Bioanalytical Method Validation, 2001. Available from URL: http://www.fda.gov/cder/guidance/4252fnl.htm.

Chapter 3.5

Severe pulmonary toxicity in patients with leiomyosarcoma after treatment with gemcitabine and docetaxel

Investigational New Drugs 2007;25:279-281

Stephan A. Veltkamp
Jetske M. Meerum Terwogt
Michel M. van den Heuvel
Hester H. van Boven
Jan H.M. Schellens
Sjoerd Rodenhuis

Introduction

Gemcitabine/docetaxel (G/D) combination therapy has shown favourable response rates in patients with leiomyosarcoma (LMS) (1-3). Although, G/D treatment is generally well tolerated, it can cause side effects, such as myelosuppression and fatigue. We describe two out of nine patients with advanced LMS, refractory to doxorubicin who developed acute pulmonary toxicity after treatment with 3-weekly gemcitabine 900 mg/m^2 as 90-min infusion on day 1 and 8 followed by docetaxel 100 mg/m^2 as 60-min infusion on day 8 and s.c. pegfilgrastim on day 9.

Case 1

A 67-year old woman presented with intra-abdominal metastasis from recurrent LMS of the ovary. G/D treatment was started. After the second cycle some lesions had regressed. After the fourth cycle she complained of fatigue and developed a dry cough. Chemotherapy was discontinued, however, she became progressively more dyspnoeic and hypoxic. She was afebrile and on ausculatation she had normal breathing sounds. Her haemoglobin level was 5.2 mmol/L and her leukocyte count was 24.5x10^9/L (91% neutrophils). Chest radiography clearly showed massive interstitial infiltrates (Figure 1). There was no prior history of cardiac or pulmonary illness. Antibiotic therapy was empirically started. All cultures were negative. Her respiratory status deteriorated and she was mechanically ventilated. Subsequently methylprednisolone (1 g daily for three days) was started. After an initial improvement, she developed pulmonary edema. Furosemide was supplied but her condition worsened and she died from respiratory failure. At autopsy, histologic findings confirmed acute lung injury consistent with the exudative and organising stage of diffuse alveolar damage (DAD) (Figure 2).

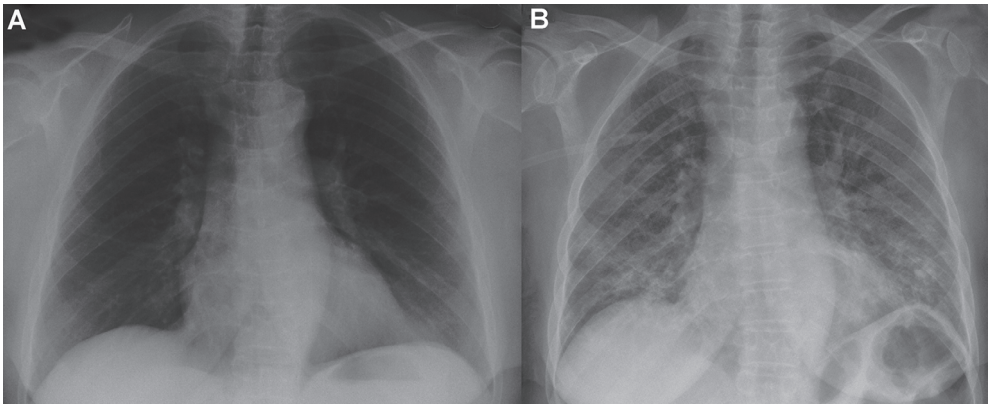

Figure 1. Case 1. Chest radiographs: Before treatment with G/D (A) and after the fourth cycle of G/D (B), showing diffuse interstitial infiltrates.

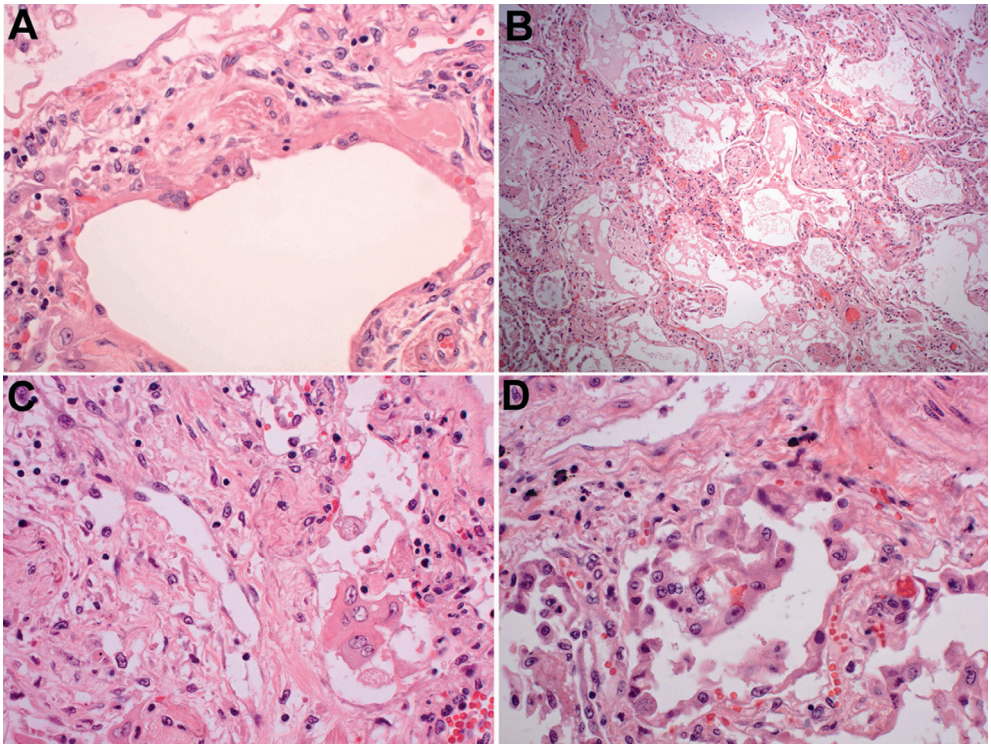

Figure 2. Case 1. Findings at autopsy: Severe acute lung injury manifested by diffuse alveolar damage. Exudative stage with edema and hyaline membrane lining edematous alveolar septa (A+B). Organizing stage with fibroblast proliferation in interstitium and focally in alveolar spaces, interstitial inflammation and alveolar lining cell hyperplasia (C+D).

Case 2

A 58-year old woman presented with LMS of the arm. After previous treatment with doxorubicin/ifosfamide, radiotherapy and resection of lung metastases, the disease metastasized to the left clavicle, thoracic wall, lung, liver and spleen. Radiotherapy at the left clavicle and G/D treatment were initiated. After two cycles, CT demonstrated a partial response. After the third cycle, she developed progressive complaints of dyspnea, edema, fever and peripheral neuropathic pain. Therefore, docetaxel was discontinued. A fourth cycle with gemcitabine monotherapy was given and CT confirmed the partial response. However, after ten cycles of gemcitabine monotherapy, she suffered from progressive dyspnea. Echocardiography, ECG, and bronchoalveolar lavage did not reveal the cause but a CT scan of the chest showed diffuse interstitial markings in the lung with ground-glass appearance (Figure 3). Gemcitabine was discontinued and furosemide 40 mg and prednisone 100 mg were started. She recovered and was discharged from the hospital. The patient is alive at the time of this writing.

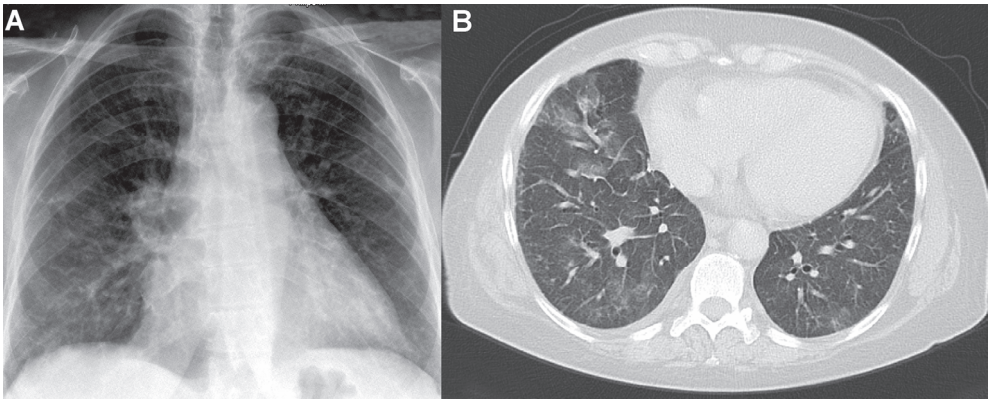

Figure 3. Case 2. Chest radiography (A) and CT scan (B) after three cycles of G/D followed by ten cycles of gemcitabine monotherapy, showing diffuse interstitial markings in both lungs with a ground-glass appearance.

Discussion

In our group of LMS patients treated with G/D, two patients developed severe lung injury. Our results show that G/D therapy has a serious risk of pulmonary toxicity in line with others (4-6). Possibly, gemcitabine-induced cytokine release can potentiate the lung toxicity of docetaxel, however, docetaxel might also augment gemcitabine-induced cytokine release. In addition, concurrent chest radiotherapy can increase the risk of pulmonary toxicity (5).

When patients develop pulmonary toxicity, G/D treatment should be discontinued and both diagnostic and therapeutic interventions (steroids, diuretics) should be installed promptly.

References

1. Hensley ML, Maki R, Venkatraman E, Geller G, Lovegren M, Aghajanian C, et al. Gemcitabine and docetaxel in patients with unresectable leiomyosarcoma: results of a phase II trial. J Clin Oncol 2002;20:2824-2831.

2. Leu KM, Ostruszka LJ, Shewach D, Zalupski M, Sondak V, Biermann JS, et al. Laboratory and clinical evidence of synergistic cytotoxicity of sequential treatment with gemcitabine followed by docetaxel in the treatment of sarcoma. J Clin Oncol 2004;22:1706-1712.

3. Bay JO, Ray-Coquard I, Fayette J, Leyvraz S, Cherix S, Piperno-Neumann S, et al. Docetaxel and gemcitabine combination in 133 advanced soft-tissue sarcomas: a retrospective analysis. Int J Cancer 2006;119:706-711.

4. Kouroussis C, Mavroudis D, Kakolyris S, Voloudaki A, Kalbakis K, Souglakos J, et al. High incidence of pulmonary toxicity of weekly docetaxel and gemcitabine in patients with non-small cell lung cancer: results of a dose-finding study. Lung Cancer 2004;44:363-368.

5. Belknap SM, Kuzel TM, Yarnold PR, Slimack N, Lyons EA, Raisch DW, et al. Clinical features and correlates of gemcitabine-associated lung injury: findings from the RADAR project. Cancer 2006;106:2051-2057.

6. Vasey PA, Atkinson R, Osborne R, Parkin D, Symonds R, Paul J, et al. SCOTROC 2A: carboplatin followed by docetaxel or docetaxel-gemcitabine as first-line chemotherapy for ovarian cancer. Br J Cancer 2006;94:62-68.

Chapter 4

New paclitaxel formulations for oral application in patients

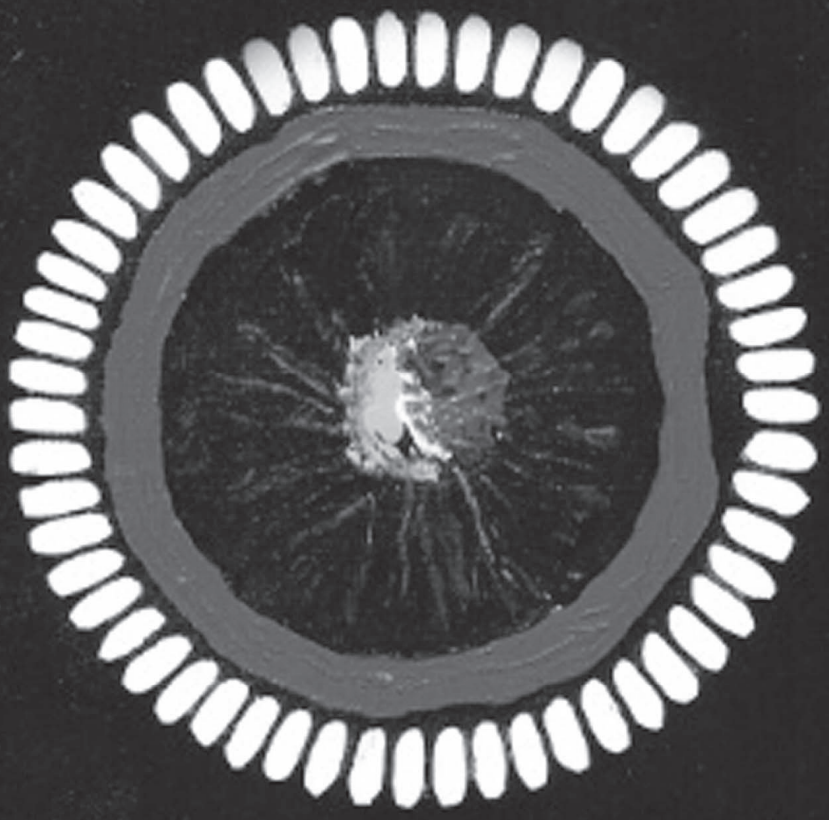

Chapter 4.1

A pharmacokinetic and safety study of a novel polymeric paclitaxel formulation for oral application

Cancer Chemotherapy and Pharmacology 2007;59:43-50

Stephan A. Veltkamp
Carolien Alderden-Los
Aruna Sharma
Hilde Rosing
Jos H. Beijnen
Jan H.M. Schellens

Abstract

To investigate the pharmacokinetics, safety, and tolerability of a new oral formulation of paclitaxel containing the polymer polyvinyl acetate phthalate in patients with advanced solid tumors.

A total of 6 patients received oral paclitaxel as single agent given as a single dose of 100 mg on day 1, oral paclitaxel 100 mg in combination with cyclosporin A (CsA) 10 mg/kg both given as a single dose on day 8, and i.v. paclitaxel (Taxol®) 100 mg as a 3-hour infusion on day 15.

The AUC (mean ± standard deviation) values of paclitaxel after oral administration without CsA and with CsA were 476 ± 254 ng/mL*h and 967 ± 779 ng/mL*h, respectively. T_{max} was 4.0 ± 0.9 hours after oral paclitaxel without CsA, and 6.0 ± 3.1 hours after oral paclitaxel with CsA. The mean AUC after oral administration as single agent was 13% of the AUC after i.v. administration of paclitaxel, and increased to 26% after co-administration with CsA. No hematological toxicities were observed, and only mild (CTC-grade 1 and 2) non-hematological toxicities occurred after oral intake of paclitaxel with or without CsA.

The AUC of the new polymeric paclitaxel formulation increased a factor 2 in combination with CsA, which confirms that CsA co-administration can also improve exposure to paclitaxel after oral administration of a polymeric formulation. Because of the delayed release of paclitaxel from this formulation, we hypothesize that a split-dose regimen of CsA where it is administered before and after paclitaxel administration will further increase the systemic exposure to paclitaxel up to therapeutic levels. The formulation was well tolerated at the dose of 100 mg without induction of severe toxicities.

Introduction

Paclitaxel is a potent anticancer agent and has antitumor activity against a variety of solid tumors, especially against lung, breast, ovarian, and head and neck tumors (4, 13). Paclitaxel is a taxane derivative that binds directly to tubulin, causing microtubular stabilisation that arrests cell division in the G_2 and M phase of the cell cycle. Currently, paclitaxel is only marketed as an intravenous (i.v.) formulation (Taxol®). Paclitaxel is poorly soluble in water, therefore, in the marketed i.v. formulation it is formulated in a 1:1 combination of the solubilising agent polyoxyethylated caster oil (Cremophor® EL (CrEL)) and dehydrated ethanol. CrEL has been reported to be responsible for severe hypersensitivity reactions (21) and the non-linear pharmacokinetic behaviour of i.v. administered paclitaxel (15, 19, 20).

Oral administration of paclitaxel is attractive, because it is more convenient for the patient than i.v. administration. Furthermore, oral paclitaxel administration may enable the development of treatment regimens resulting in plasma concentrations above a pharmacologically relevant level for more prolonged periods of time. Previous clinical studies using i.v. paclitaxel as 3-hour infusion have suggested that, the time above a paclitaxel concentration of 0.05 μM (43 ng/mL) or 0.1 μM (85 ng/mL) is positively related to the activity of the drug (2, 3). However, oral treatment with paclitaxel is severely hampered because of its low bioavailability, which is caused by several factors. Firstly, paclitaxel is a high affinity substrate for the efflux multidrug transporter P-glycoprotein (P-gp), which is highly expressed in the gastro-intestinal tract (14). Secondly, paclitaxel undergoes first-pass metabolism by the gut and liver cytochrome P450 (CYP) enzymes (CYP 2C8 and CYP 3A4).

Cyclosporin A (CsA) is a potent inhibitor of both P-gp and CYP3A4. Preclinical and clinical studies carried out at our institute revealed that co-administration of oral CsA, resulted in a significantly enhanced systemic exposure to oral paclitaxel (12, 18). As CsA is an inhibitor of P-gp and CYP3A4, both an increased absorption and reduced first pass effect may be responsible for the increased systemic exposure. We have shown previously that the effective dose of CsA resulting in a maximal P-gp inhibiting effect was reached at a dose of CsA of 10 mg/kg (7).

The i.v. paclitaxel formulation containing CrEL and ethanol was applied orally as a drinking solution diluted with water in previous studies (5, 6, 8, 10-12). CrEL affect paclitaxel pharmacokinetics by limiting the absorption of paclitaxel from the intestine after oral administration by entrapment of paclitaxel in micelles, thereby reducing the availability of paclitaxel for uptake (1, 9, 15, 16). Furthermore, the drinking solution has a disagreeable bitter taste. Although many attempts have been undertaken to improve systemic exposure of orally administered paclitaxel, a favourable oral formulation with paclitaxel has not been found yet. The paclitaxel formulation investigated in the current study is a capsule containing the polymer polyvinyl acetate phthalate, but no CrEL and ethanol, possibly leading to an improved systemic exposure and better tolerability.

The purpose of this study was to investigate the pharmacokinetics, safety, and tolerability of an innovative dosage form containing a modified formulation of paclitaxel for oral application in patients with advanced solid tumors. The paclitaxel formulation was administered as a single dose or co-administered with CsA to explore systemic exposure to paclitaxel as a basis for oral therapy in patients with solid tumors.

Patients and Methods

Patient Population

Patients with a histologic or cytologic proof of cancer, for whom no standard therapy of proven benefit existed, were eligible for the study. Previous radiotherapy or chemotherapy other than taxoid therapy was allowed as long as the last treatment was at least four weeks prior to study entry and any resulting toxicities were resolved. Patients had to have acceptable hematological parameters (absolute neutrophil count (ANC) $\geq$ 1.5 x 10^9/L, and platelets $\geq$ 100 x 10^9/L), hepatic function (serum bilirubin $\leq$ 25 µmol/L; transaminases $\leq$ 2 x UNL or $\leq$ 5 x UNL in case of liver metastasis) and renal function (serum creatinine $\leq$ 160 µmol/L or clearance $\geq$ 50 mL/min), and a World Health Organization (WHO) performance status $\leq$ 2. Patients were excluded if they suffered from uncontrolled infectious disease, neurologic disease, bowel obstruction or symptomatic brain metastasis. Further exclusion criteria were concomitant use of known P-gp inhibitors and chronic use of H2-receptor antagonists or proton pump inhibitors. The study

protocol was approved by the Medical Ethics Committee of the Institute, and all patients gave written informed consent.

Study design

Six patients were enrolled in the study and received paclitaxel as a single dose at three different occasions with 7 days between each treatment in the following sequence: 1) p.o. paclitaxel 100 mg, 2) p.o. paclitaxel 100 mg in combination with p.o. CsA 10 mg/kg 30 minutes before the intake of paclitaxel, and 3) i.v. paclitaxel (Taxol®) 100 mg.

Paclitaxel (Apotex Research Inc., Toronto, Ontario, Canada) was administered orally as 4 capsules of 25 mg paclitaxel in polyvinyl acetate phthalate each. Cyclosporin A (Neoral®, Novartis, Basel, Switzerland) was administered as capsules of 100 mg each. For patients who had difficulty swallowing the large CsA capsules, use of the drinking solution of CsA (Neoral® oral solution 100 mg/mL) was allowed in stead of the CsA capsules. Paclitaxel (Taxol® i.v. solution 6 mg/mL (Bristol-Myers Squibb)) was administered as a 3-hour infusion. The oral and i.v. dosages were administered early in the morning after a fasting period of at least 12 hours. The CsA capsules were ingested with 150 mL of tap water and the paclitaxel capsules were taken together with 150 mL of tap water and a cracker. Only 1.5 hours after the intake of paclitaxel were patients allowed to have a light breakfast. To prevent possible nausea, vomiting, and hypersensitivity reactions during both the treatment with oral paclitaxel and the combination of paclitaxel with CsA, patients were premedicated with oral granisetron (Kytril®) 1 mg 20 minutes before the intake of CsA, ranitidine (Zantac®) 50 mg p.o., and clemastine (Tavegil®) 1 mg p.o. 30 minutes before paclitaxel. To prevent hypersensitivity reactions, all i.v. occasions patients were premedicated with dexamethasone 20 mg orally 12 and 6 hours prior to, granisetron 1 mg orally 30 minutes prior to, i.v. ranitidine 50 mg, and i.v. clemastine 1 mg shortly prior to paclitaxel administration. If considered in their best interest, patients continued on a 3-weekly schedule of i.v. paclitaxel at a dose of 175 mg/m^2.

Sample collection and analysis

Blood samples for pharmacokinetic analysis of paclitaxel were collected via an indwelling catheter in 5 mL heparinized tubes for each treatment. Following oral

and i.v. administration samples were obtained pre-dosing, 45 minutes, and 1.5, 2, 3, 3.5, 4, 4.5, 5, 6, 8, 10, 12, and 24 hours after paclitaxel administration. Blood samples were centrifuged, and plasma was separated and immediately transferred into polypropylene tubes and stored at -20 °C until analysis. Paclitaxel concentrations in plasma were determined using a validated high performance liquid chromatographic - tandem mass spectrometric (HPLC-MS/MS) method (17).

Pharmacokinetic analysis

Pharmacokinetic parameters were determined by non-compartmental analysis, using Winnonlin™ (version 5.0, Pharsight Corporation, California, USA). The maximal paclitaxel concentration (C_{max}) and time to maximal concentration (T_{max}) were obtained directly from the experimental data. The terminal rate constant was determined by log-linear regression analysis of the terminal phase of the plasma concentration-time curve. The area under the plasma concentration time curve (AUC) was determined using the trapezoidal method up to the last measured concentration-time point and extrapolated to infinity ($AUC_{0-\infty}$) using the slope of the terminal rate of the logarithmic concentration versus time curve (λ_2). Furthermore, the terminal half-life ($t_{1/2}$) was calculated.

The apparent oral bioavailability (F) of paclitaxel was determined by the ratio of the $AUC_{0-\infty}$ after oral administration and $AUC_{0-\infty}$ after intravenous administration of paclitaxel.

Statistical analysis

The software package Statistical Product and Service Solutions (version 12.0.1 for Windows, SPSS Inc., Chicago, IL, USA) was used for statistical analysis. The a priori level of significance was $p = 0.05$. The paired t-test was applied on logarithmic-transformed values to make a comparison between the pharmacokinetic parameters of paclitaxel after the different study treatments.

Safety

Pretreatment evaluation included a complete medical history and thorough physical examination. Before each course, an interim history including concomitant medication taken, toxicities and performance status were registered and a physical examination was performed.

Non-hematological toxicities and hematology were checked prior to study entry (before the first treatment), 6 days after each oral treatment and two weeks after the i.v. treatment. The last assessment was done at the end of the study, which was two weeks after the i.v. treatment or after the patient's recovery from toxicities. To evaluate hepatic and renal function, the following parameters for blood chemistry were reported prior to study entry and at the end of study: alanine aminotransferase (ALT), aspartate aminotransferase (AST), gamma glutamyl transpherase (γ-GT), bilirubin, alkaline phosphatase (AP), albumin and serum creatinine. All toxicities observed were graded according to the National Cancer Institute Common Terminology Criteria for Adverse Events (NCI CTCAE) version 3.0, 2003 (http://ctep.cancer.gov/forms/CTCAEv3.pdf).

Results

Patient characteristics

In total six patients were enrolled in the study. Patient characteristics are outlined in Table 1.

Table 1. Patient characteristics.

Number of patients	6
Male/female	3/3
Median age (range)	50 (35 - 61)
Tumor type	
Gastric carcinoma	1
Bladder	1
Urothelial cell carcinoma	1
Small cell lung cancer (SCLC)	1
Oesophageal carcinoma	1
Carcinoma of unknown primary site	1

All patients had a performance status ≤ 2. All patients received paclitaxel orally as a single dose on day 1 (first treatment), paclitaxel orally as a single dose combined with oral CsA as a single dose on day 8 (second treatment), and i.v. paclitaxel as a 3-hour infusion on day 15 (third and last study treatment). If considered in their best interest, patients continued on a 3 weekly schedule of i.v. paclitaxel at a dose of 175 mg/m^2.

Drug administration

The first patient was administered both CsA as oral drinking solution 100 mg/mL and as capsules, because he experienced problems with swallowing. He received CsA 800 mg; 3 capsules of 100 mg each and 5 mL of oral solution 100 mg/mL. The second and third patient were given only the oral solution of CsA 100 mg/mL because they had swallowing problems; CsA 760 mg was administered to the second patient as 7,6 mL of the oral solution 100 mg/mL, and the third patient was administered CsA 540 mg as 5,4 mL of the oral solution 100 mg/mL. All other patients ingested the CsA capsules.

Pharmacokinetic and statistical analysis

Figure 1 depicts the plasma pharmacokinetic profiles (semi-logarithmic scale) of paclitaxel after treatment with p.o. paclitaxel as single agent, p.o. paclitaxel in combination with CsA, and i.v. administered paclitaxel (n = 6). A relatively large interpatient variability in paclitaxel plasma concentrations was observed after both oral and i.v. administration of paclitaxel.

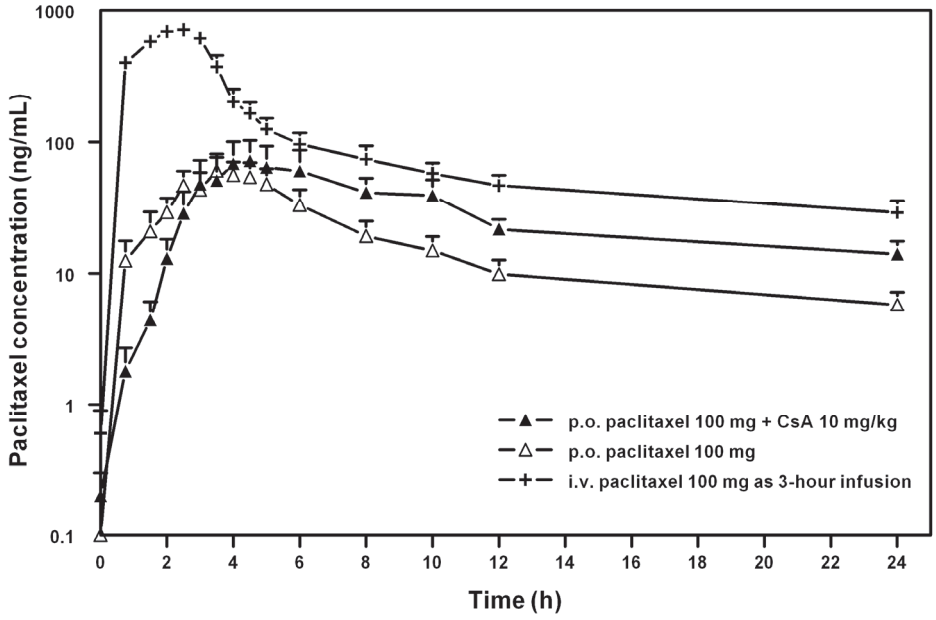

Figure 1. Plasma concentration versus time curves of p.o. paclitaxel 100 mg, p.o. paclitaxel 100 mg + CsA 10 mg/kg, and i.v. paclitaxel 100 mg as 3-hour infusion (n = 6). Data are represented as mean ± SEM on a semi-logarithmic scale.

Figure 2 shows the paclitaxel plasma concentration versus time curves (linear scale) after p.o. paclitaxel given as single agent and p.o. paclitaxel co-administered with CsA. Oral paclitaxel in combination with CsA resulted in a significant increase in systemic exposure to paclitaxel compared to administration of paclitaxel alone.

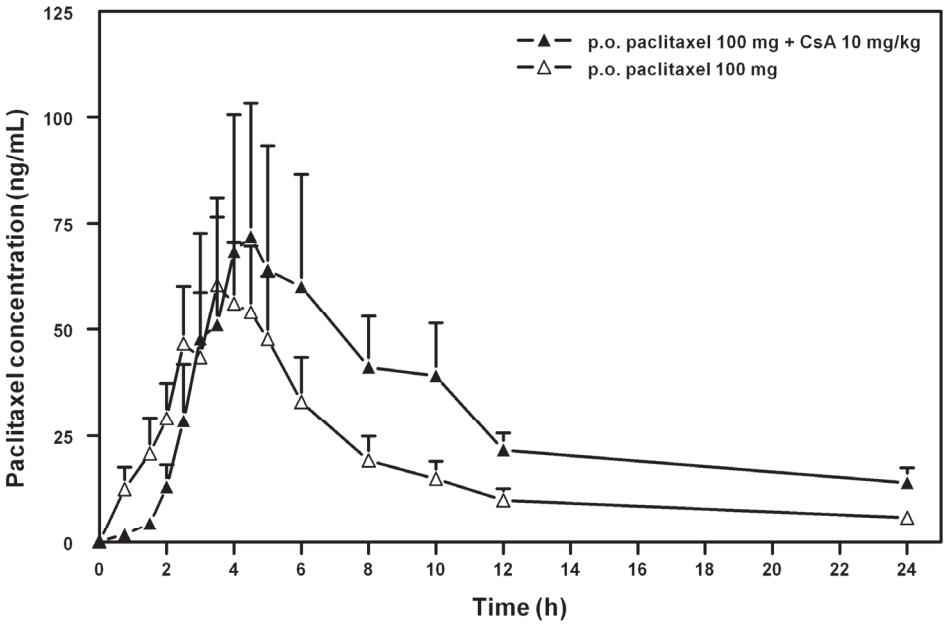

Figure 2. Plasma concentration versus time curves of p.o. paclitaxel 100 mg and p.o. paclitaxel 100 mg + CsA 10 mg/kg (n = 6). Data are represented as mean ± SEM on a linear scale.

Table 2 summarises the pharmacokinetic parameters (T_{max}, C_{max}, $AUC_{0-\infty}$, and $t_{1/2}$) of p.o. paclitaxel without CsA (treatment 1), p.o. paclitaxel + CsA (treatment 2), and i.v. administered paclitaxel (treatment 3). The $AUC_{0-\infty}$ (mean ± standard deviation, SD) of paclitaxel after treatment 2 was 967 ± 779 ng/mL*h, which was approximately 2-fold significantly higher ($p < 0.018$) than the mean $AUC_{0-\infty}$ of 476 ± 254 ng/mL*h of paclitaxel after treatment 1. No statistically significant differences were found for T_{max}, C_{max}, and $t_{1/2}$ between treatment 1 and 2. Paclitaxel $AUC_{0-\infty}$ and C_{max} after p.o. administration were substantially lower than after i.v. administration. The apparent bioavailability and percentage coefficient of variation

(%CV) of F for the new oral paclitaxel formulation was 13% (28%), and increased to 26% (54%) after co-administration with CsA. Plasma concentrations of paclitaxel above 0.05 μM and 0.1 μM were not reached in all patients. The mean duration of plasma levels above 0.05 μM was 3.0 ± 1.4 hours in a total of 5 patients after oral paclitaxel alone and 7.6 ± 8.4 hours in a total of 4 patients after oral paclitaxel with CsA (p = 0.314). In only 2 patients plasma concentrations above 0.1 μM were reached during 1.0 - 2.7 hours after oral paclitaxel alone and 1.6 - 10.4 hours after oral paclitaxel with CsA.

Table 2. Pharmacokinetic parameters of paclitaxel after p.o. paclitaxel (treatment 1), p.o. paclitaxel + CsA (treatment 2), and i.v. paclitaxel (treatment 3). Data are represented as mean (± SD).

Parameter	Treatment 1	Treatment 2	Treatment 3
n	6	6	6
T_{max} (h)	4.0 (0.9)	6.0 (3.1)	n.a.
C_{max} (ng/mL)	73 (35)	79 (72)	726 (230)
$AUC_{0-\infty}$ (ng/mL*h)	476 (254)	967 (779)	3761 (1626)
$t_{1/2}$ (h)	9.4 (3.0)	10 (3.1)	14.9 (5.5)
%CV of $AUC_{0-\infty}$	53	81	43
Apparent F (%)	13	26	
%CV of F	28	54	
T > 0.05 μM	3.0 (1.4) (n = 5)	7.6 (8.4) (n = 4)	15.2 (8.4) (n = 6)
T > 0.1 μM	1.0-2.7 (n = 2)	1.6-10.4 (n = 2)	6.4 (2.9) (n = 6)

n.a. = not applicable; %CV = % coefficient of variation.

Figure 3 depicts the $AUC_{0-\infty}$ of paclitaxel for each individual patient after treatment with p.o. paclitaxel as single agent and after p.o. paclitaxel in combination with CsA. In five of the six patients co-administration of p.o. paclitaxel with CsA resulted in an increase in $AUC_{0-\infty}$ compared to treatment with p.o. paclitaxel alone.

Safety evaluation

In none of the patients any grade 1-4 hematological toxicity (anemia, leukocytopenia, neutropenia, and thrombocytopenia) was observed 6 days after each oral treatment and two weeks after the first i.v. administration. Regarding blood chemistry, no clinically significant changes were observed at study end in any of the parameters (see Table 3).

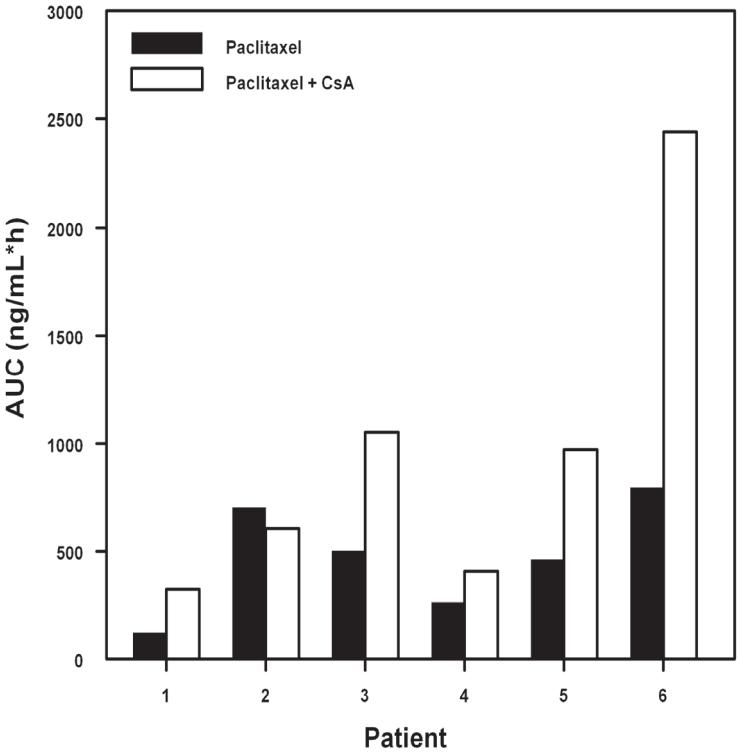

Figure 3. Individual $AUC_{0-\infty}$ values after treatment with paclitaxel alone and paclitaxel co-administered with CsA.

Table 3. Blood chemistry prior to study entry and at study end (n = 6).

Maximum severity NCI-CTC grade	CTC-Grade	Prior to study entry	Study end
Liver			
γ-GT	1	2	1
	2		1
	3	2	2
AP	1	3	4
	2	1	
	3		1

Table 4 summarises the non-hematological toxicities that were observed 6 days after p.o. paclitaxel (treatment 1), p.o. paclitaxel combined with CsA (treatment 2), and two weeks after i.v. paclitaxel (treatment 3). Non-hematological toxicities were mild (CTC-grade 1 and 2) for both oral treatments. The capsules were well tolerated by the premedicated patients, and nausea and vomiting were not reported

as drug-related adverse events, except for one patient who had nausea after treatment 2. Stomatitis was seen in one patient after all experimental treatments. Grade 2 fatigue was observed in two patients after oral treatment 2. In one patient constipation occurred after both oral treatments, as loss of appetite and grade 2 low back pain occurred after the second oral treatment. Only one patient developed fever, flushing, and sweating and grade 2 diarrhoea after the first oral treatment. Neuropathy was reported in one patient after the second oral treatment, and another patient had a tingling feeling of the tongue and sensitive corners of the mouth after all three experimental treatments.

Table 4. Non-hematological toxicity profile for all three study treatments (n = 6). Toxicities were possibly, probably, or definitely related to study medication. Duration of observation is from start of study until 2 weeks after the first i.v. infusion.

Maximum severity NCI-CTC grade	**CTC Grade ***	**p.o. treatment 1**	**p.o. treatment 2**	**i.v. treatment 3**	**Total**
Gastrointestinal disorders					
Stomatitis	1	1	1	1	3
Low back pain	1	-	-	-	-
	2	-	1	-	1
Constipation	1	1	1	-	2
Nausea	1	-	1	-	1
Diarrhea	1	-	-	-	-
	2	1	-	-	1
General disorders and administration site conditions					
Fatigue	1	-	-	1	1
	2	-	2	1	3
Fever	1	1	-	-	1
Sweating	1	1	-	-	1
Flushing	1	1	-	-	1
Central nervous system and other pain disorders					
Neuropathy	1	-	1	1	2
Tingling feeling in tongue	1	1	1	1	3
Sensitive corners of mouth	1	1	1	1	3
Metabolism and nutrition disorders					
Loss of appetite	1	-	1	-	1

* No grade 3-4 toxicities were observed.

Discussion

In this study we have shown that the apparent bioavailability of the new Cremophor-free formulation of paclitaxel containing the polymer polyvinyl acetate phthalate was 13% after oral administration at a dose of 100 mg in patients with advanced solid tumors. When the novel paclitaxel formulation was given orally in

combination with CsA 10 mg/kg, a P-gp and CYP3A4 inhibitor, an approximately two-fold increase in $AUC_{0-\infty}$ was achieved resulting in an apparent bioavailability of 26%. Previous studies showed that the orally applied i.v. Taxol® formulation containing CrEL and ethanol resulted in an $AUC_{0-\infty}$ of paclitaxel of 171 ng/mL*h and an apparent bioavailability of only 6% compared to i.v. Taxol® administration, but CsA co-administration resulted in an 8-fold increase of the $AUC_{0-\infty}$ to 1409 ng/mL*h and an apparent bioavailability of 47% (3, 12). Thus, oral administration of the new paclitaxel formulation without CsA resulted in a higher paclitaxel $AUC_{0-\infty}$ of 476 ng/mL*h than was obtained after the orally applied i.v. formulation. However, the 2-fold increase in $AUC_{0-\infty}$ of paclitaxel (from 476 to 967 ng/mL*h) after CsA co-administration in our current study was relatively low compared to the 8-fold increase that was observed with the orally applied i.v. formulation of Meerum Terwogt and co-workers (12).

The term bioavailability, however, should be interpreted with caution due to the non-linear pharmacokinetics of i.v. paclitaxel caused by the presence of CrEL (15, 19). Entrapment of paclitaxel in CrEL micelles in the central compartment causes a more than proportional increase in plasma paclitaxel concentrations with increasing doses. Studies in mice showed that these higher total drug levels in plasma did not result in higher drug levels in tissues (15). In previous studies it was shown that CrEL is not absorbed after oral administration. This pseudo-non-linearity of i.v. paclitaxel has two important implications for the pharmacology of oral paclitaxel. Firstly, the oral bioavailability of paclitaxel, calculated by comparing the AUC values after oral and i.v. administration, will be underestimated as the affinity of paclitaxel for the plasma compartment is increased after i.v. administration due to the presence of CrEL in the central circulation. Secondly, the pseudo-non-linearity of i.v. paclitaxel implies that after oral administration, when CrEL is not present, plasma levels of paclitaxel represent a higher fraction of free drug, which will result in enhancement of the availability of paclitaxel for the (tumor) tissues (19). Consequently, threshold values for the paclitaxel concentration established for i.v. paclitaxel (2, 3) can be different for oral administration of paclitaxel. Therefore, we did not use the duration of the paclitaxel plasma concentration above a certain level as a therapeutic endpoint. The pharmacokinetic parameters after i.v. paclitaxel 100 mg (treatment 3) were in line with previous observations (3, 11).

The new polymeric formulation of paclitaxel resulted in a higher T_{max} of 4.0 ± 0.9 hours after p.o. paclitaxel alone and 6.0 ± 3.1 hours after p.o. paclitaxel plus CsA compared to the orally applied i.v. formulation, which had a T_{max} of 2.4 ± 0.6 h and 2.4 ± 0.8 h without and with CsA, respectively (12).

It has been shown that in patients who were administered paclitaxel in combination with CsA maximum concentrations of CsA were reached at approximately 1.6-3.3 hours after intake (8). Since the T_{max} values of paclitaxel after oral administration of the new formulation were above 3 hours, we hypothesise that during the time period that paclitaxel was released from the formulation and taken up into the systemic circulation, already a large amount of the CsA had been absorbed and metabolised and relatively low concentrations of CsA were present at the site of uptake of paclitaxel. This may have caused less inhibition of P-gp in the gastro-intestinal tract leading to a less enhancing effect of CsA on paclitaxel uptake. Since we did not measure CsA concentrations, it remains, however, uncertain whether this was the case.

In summary, we demonstrated that the novel polymeric formulation of paclitaxel in polyvinyl acetate phthalate was well tolerated after oral administration at the given dose of 100 mg also when co-administered with CsA, without inducing severe toxicities. Regarding the almost uneventful oral administration of the 100 mg dose together with the relatively low $AUC_{0-\infty}$ after CsA co-administration, we suggest that new studies should be initiated with this new paclitaxel formulation to explore dose escalation and bi-daily administration in order to increase systemic exposure and to prolong exposure at therapeutic levels. Because of the delayed release profile of paclitaxel from this novel formulation, we hypothesize that a split-dose regimen in which CsA is both given before and after paclitaxel administration will further increase the systemic exposure of paclitaxel from this formulation.

References

1. Bardelmeijer HA, Ouwehand M, Malingré MM, Schellens JH, Beijnen JH, van Tellingen O. Entrapment by Cremophor EL decreases the absorption of paclitaxel from the gut. Cancer Chemother Pharmacol 2002;49:119-125.

2. Gianni L, Kearns CM, Giani A, Capri G, Vigano L, Lacatelli A, et al. Nonlinear pharmacokinetics and metabolism of paclitaxel and its pharmacokinetic / pharmacodynamic relationships in humans. J Clin Oncol 1995;13:180-190.

3. Huizing MT, Giaccone G, van Warmerdam LJ, Rosing H, Bakker PJ, Vermorken JB, et al. Pharmacokinetics of paclitaxel and carboplatin in a dose-escalating and dose-sequencing study in patients with non-small-cell lung cancer. The European Cancer Centre. J Clin Oncol 1997;15:317-329.

4. Huizing MT, Misser VH, Pieters RC, Bokkel Huinink WW, Veenhof CH, Vermorken JB, et al. Taxanes: a new class of antitumor agents. Cancer Invest 1995;13:381-404.

5. Malingré MM, Beijnen JH, Rosing H, Koopman FJ, Jewell RC, Paul EM, et al. Co-administration of GF120918 significantly increases the systemic exposure to oral paclitaxel in cancer patients. Br J Cancer 2001;84:42-47.

6. Malingré MM, Beijnen JH, Rosing H, Koopman FJ, van Tellingen O, Duchin K, et al. A phase I and pharmacokinetic study of bi-daily dosing of oral paclitaxel in combination with cyclosporin A. Cancer Chemother Pharmacol 2001;47:347-354.

7. Malingré MM, Beijnen JH, Rosing H, Koopman FJ, van Tellingen O, Duchin K, et al. The effect of different doses of cyclosporin A on the systemic exposure of orally administered paclitaxel. Anticancer Drugs 2001;12:351-358.

8. Malingré MM, Bokkel Huinink WW, Duchin K, Schellens JH, Beijnen JH. Pharmacokinetics of oral cyclosporin A when co-administered to enhance the oral absorption of paclitaxel. Anticancer Drugs 2001;12:591-593.

9. Malingré MM, Schellens JH, van Tellingen O, Ouwehand M, Bardelmeijer HA, Rosing H, et al. The co-solvent Cremophor EL limits absorption of orally administered paclitaxel in cancer patients. Br J Cancer 2001;85:1472-1477.

10. Malingré MM, Schellens JH, van Tellingen O, Rosing H, Koopman FJ, Duchin K, et al. Metabolism and excretion of paclitaxel after oral administration in combination with cyclosporin A and after i.v. administration. Anticancer Drugs 2000;11:813-820.

11. Malingré MM, Meerum Terwogt JM, Beijnen JH, Rosing H, Koopman FJ, van Tellingen O, et al. Phase I and pharmacokinetic study of oral paclitaxel. J Clin Oncol 2000;18:2468-2475.

12. Meerum Terwogt JM, Malingré MM, Beijnen JH, Bokkel Huinink WW, Rosing H, Koopman FJ, et al. Coadministration of oral cyclosporin A enables oral therapy with paclitaxel. Clin Cancer Res 1999;5:3379-3384.

13. Rowinsky EK, Donehower RC. Paclitaxel (taxol). N Engl J Med 1995;332:1004-1014.

14. Sparreboom A, van Asperen J, Mayer U, Schinkel AH, Smit JW, Meijer DK, et al. Limited oral bioavailability and active epithelial excretion of paclitaxel (Taxol) caused by P-glycoprotein in the intestine. Proc Natl Acad Sci USA 1997;94:2031-2035.

15. Sparreboom A, van Tellingen O, Nooijen WJ, Beijnen JH. Nonlinear pharmacokinetics of paclitaxel in mice results from the pharmaceutical vehicle Cremophor EL. Cancer Res 1996;56:2112-2115.

16. Sparreboom A, van Zuylen L, Brouwer E, Loos WJ, de Bruijn P, Gelderblom H, et al. Cremophor EL-mediated alteration of paclitaxel distribution in human blood: clinical pharmacokinetic implications. Cancer Res 1999;59:1454-1457.

17. Vainchtein LD, Thijssen B, Stokvis E, Rosing H, Schellens JH, Beijnen JH. A simple and sensitive assay for the quantitative analysis of paclitaxel and metabolites in human plasma using liquid chromatography/tandem mass spectrometry. Biomed Chromatogr 2005;20:139-148.

18. van Asperen J, van Tellingen O, van der Valk MA, Rozenhart M, Beijnen JH. Enhanced oral absorption and decreased elimination of paclitaxel in mice cotreated with cyclosporin A. Clin Cancer Res 1998;4:2293-2297.

19. van Tellingen O, Huizing MT, Panday VR, Schellens JH, Nooijen WJ, Beijnen JH. Cremophor EL causes (pseudo-) non-linear pharmacokinetics of paclitaxel in patients. Br J Cancer 1999;81:330-335.

20. van Zuylen L, Karlsson MO, Verweij J, Brouwer E, de Bruijn P, Nooter K, et al. Pharmacokinetic modeling of paclitaxel encapsulation in Cremophor EL micelles. Cancer Chemother Pharmacol 2001;47:309-318.

21. Webster LK, Linsenmeyer ME, Rischin D, Urch ME, Woodcock DM, Millward MJ. Plasma concentrations of polysorbate 80 measured in patients following administration of docetaxel or etoposide. Cancer Chemother Pharmacol 1997; 39:557-560.

Chapter 4.2

Novel paclitaxel formulations for oral application: a phase I pharmacokinetic study in patients with solid tumors

Cancer Chemotherapy and Pharmacology 2007;60:635-642

Stephan A. Veltkamp
Hilde Rosing
Alwin D.R. Huitema
Michael R. Fetell
Annemarie Nol
Jos H. Beijnen
Jan H.M. Schellens

Abstract

To explore the pharmacokinetics (PK) of paclitaxel and two major metabolites after three single oral administrations of a novel drinking solution and two capsule formulations in combination with cyclosporin A (CsA) in patients with advanced cancer. Moreover, the tolerability and safety of the formulations was studied. In addition, single nucleotide polymorphisms in the multidrug resistance (*MDR1*) gene were determined.

10 patients were enrolled and randomized to receive CsA 10 mg/kg followed by oral paclitaxel 180 mg given as (1) drinking solution (formulation 1), (2) capsule formulation 2B, and (3) capsule formulation 2C on day 1, 8, or 15.

The median C_{max} of paclitaxel was 0.42 (0.23-0.96), 0.48 (0.08-0.59), and 0.39 (0.11-1.03) µg/mL and the area under the plasma concentration-time curve (AUC) was 2.83 (1.69-5.12), 2.01 (1.57-3.04), and 2.67 (1.05-3.61) µg*h/mL following administration of formulation 1, 2B, and 2C, respectively. The novel formulations were tolerated after single oral dose without causing relevant gastrointestinal or hematological toxicity.

The PK and metabolism of paclitaxel were comparable between the oral formulations co-administered with CsA.

Introduction

Currently, paclitaxel is only marketed as an intravenous (i.v.) formulation. Paclitaxel is poorly soluble in most pharmaceutical solvents. Therefore, it is formulated in the marketed i.v. formulation in a 1:1 combination of the solubilising agent polyoxyethylated castor oil (Cremophor® EL (CrEL)) and dehydrated ethanol. CrEL has been reported to be responsible for severe hypersensitivity reactions (1) and the non-linear pharmacokinetic behaviour of i.v. administered paclitaxel (2-4).

Oral administration of paclitaxel is attractive because it may enable the development of treatment regimens resulting in plasma concentrations at a pharmacologically relevant level for more prolonged periods of time. Moreover, oral administration is more convenient for patients than i.v. administration. However, oral treatment with paclitaxel is severely hampered because of its low bioavailability (5), which is caused by two main reasons. Firstly, paclitaxel undergoes hepatic metabolism and biliary excretion. The formation of 6α-hydroxypaclitaxel is catalyzed by cytochrome P450 (CYP)2C8, while 3'p-hydroxypaclitaxel is formed via metabolism by CYP3A4, and both metabolites are further converted to 6α,3'p-dihydroxypaclitaxel (6). Secondly, paclitaxel is a high affinity substrate for the drug efflux transporter P-glycoprotein (P-gp), which is expressed in the biliary tract and intestine (7).

The search for agents that help to restore the drug sensitivity of multidrug resistant tumor cells has led to the identification and clinical testing of potent P-gp blockers, such as cyclosporin A (CsA) (8, 9). Previous studies carried out at our Institute revealed that co-administration of oral CsA resulted in a increased systemic exposure to oral paclitaxel (10). As CsA is an inhibitor of both P-gp and CYP3A4, both an increased absorption and a reduced first-pass effect may be responsible for the increased systemic exposure. In a previous study it was shown that 10 mg/kg CsA was sufficient for maximal enhancement of paclitaxel bioavailability (11).

P-gp is encoded by the multidrug resistance (*MDR1*) gene. Functional genetic single nucleotide polymorphisms (SNPs) of *MDR1* may be associated with variability of paclitaxel PK in patients (12). Hoffmeyer and co-workers described 15 SNPs in the human *MDR1* gene in a Caucasian population, including polymorphisms in C1236T in exon 12 and C3435T in exon 26 (13). They observed

that individuals with the homozygous TT genotype at position 3436 in exon 26 have significantly lower duodenal P-gp expression. This may influence the uptake of orally administered P-gp substrates. We determined genetic polymorphisms in exon 12, 21, and 26 of the *MDR1* gene.

In earlier studies the i.v. paclitaxel formulation containing CrEL and ethanol was ingested orally as a drink solution (8, 14-17). Although CrEL is not taken up from the gastrointestinal tract (18) it affects paclitaxel pharmacokinetics by limiting the absorption of paclitaxel from the intestine after oral administration. This is probably caused by entrapment of paclitaxel in micelles, thereby reducing the availability of paclitaxel for absorption (4, 19-22). Although, many attempts have been undertaken to improve systemic exposure of paclitaxel after oral administration, thus far a favourable oral formulation has not been found.

The novel oral formulations of paclitaxel used in the current study were a drinking solution (formulation 1) and two different liquid-filled capsules (formulations 2B and 2C). All three formulations consist of different pharmaceutical ingredients and do not contain CrEL (Table 1). Furthermore, the formulations contain a lower amount of ethanol compared to the orally administered i.v. paclitaxel formulations. The choice of the excipients used in the novel formulations was motivated by previous *in vivo* studies in rats in combination with CsA. In the three formulations, TPGS (D-alpha-tocopheryl polyethylene glycol 1000 succinate) has been selected for its ability to solubilise paclitaxel. TPGS is a derivative of vitamin E with amphiphilic properties and it is used as excipient in Agenerase® (amprenavir, GlaxoSmithKline, UK). TPGS has been shown to increase the bioavailability of poorly absorbed lipophilic drugs (23). The mechanism of action of TPGS can be explained, in part, by its solubilizing effect through improved micelle formation (24). Labrasol® (caprylocaproyl macrogol-8 glycerides), used in capsule formulation 2B, is a non-ionic amphiphilic excipient known as solubilizer and bioavailibilty enhancer for poorly soluble drugs. Labrasol® formulated in a liquid-filled capsule has been shown to increase the systemic exposure to UK 81252, an experimental drug with potential application as antihypertensive agent, after oral administration to dogs (25). It was suggested that this was partly caused by a permeability enhancing effect of Labrasol®. Labrafil® M 1944 CS (polyoxyethylated oleic glycerides), an excipient in capsule formulation 2C, is a biodegradable polyethylene glycol derivative used as co-surfactant in

pharmaceutical systems. It is used as a vehicle in Sandimmune® Oral Solution (cyclosporine, Novartis Pharma, Switzerland).
The main purpose of this study was to investigate the PK of paclitaxel and two major metabolites of the novel formulations of paclitaxel for oral application. In addition, tolerability and safety were studied.

Patients and Methods

Patient Population

Patients with a histological or cytological diagnosis of advanced non-hematological cancer for whom no curative therapy existed and for whom treatment with single agent paclitaxel was considered of potential benefit were eligible for the study. Patients had to have recovered from any toxicities of prior treatment. Previous chemotherapy was allowed as long as the last treatment had been at least four weeks prior to study entry and at least three weeks had elapsed since receiving any radiotherapy. Patients had to have acceptable hematological parameters (white blood cells (WBC) $\geq 3.0 \times 10^9$/L, absolute neutrophil count (ANC) $\geq 1.5 \times 10^9$/L, and platelets $\geq 100 \times 10^9$/L)), hepatic function (serum bilirubin ≤ 1.5 x upper limit of normal (ULN); AST and ALT ≤ 1.5 x ULN or ≤ 5 x ULN in case of liver metastases) and renal function (serum creatinine ≤ 2 ULN or creatinine clearance $\geq$ 40 mL/min as calculated by Cockcroft Gault formula), and a World Health Organization (WHO) Performance Status (PS) ≤ 2. Patients were excluded if they had experienced severe toxicities on prior taxane treatment, suffered from serious intercurrent illness or active infections, bowel obstruction or motility disorders that could have influenced the resorption of drugs, and heart disease. Further exclusion criteria were concomitant use of known P-gp and CYP 3A modulating compounds and chronic use of H2-receptor antagonists or proton pump inhibitors. Female patients were excluded when breast-feeding or pregnant (confirmed by a pregnancy test before study entry). The Medical Ethics Committee of the Institute approved the study protocol and all patients gave written informed consent.

Study design

Initially 9 patients were planned to enrol in the study and were randomly assigned to receive treatment with oral paclitaxel 180 mg as (1) drinking solution

(formulation 1) or (2) capsule formulation 2B or (3) capsule formulation 2C on day 1, 8, or 15 depending on the randomization. CsA was administered orally at a dose of 10 mg/kg 30 minutes prior to each oral administration of paclitaxel.

Drug composition and administration

The composition of the three oral formulations of paclitaxel (IVAX Research, Inc., Miami, Florida, USA) is depicted in Table 1.

Table 1. Composition of the oral formulations.

Formulation 1[a]	% (w/v)	Formulation 2B[b]	% (w/v)	Formulation 2C[c]	% (w/v)
Paclitaxel	1.2	Paclitaxel	7.5	Paclitaxel	7.5
TPGS[d]	40	TPGS[d]	46.8	TPGS[d]	46.8
Propylene glycol	40	Labrasol[e]	24.9	Labrafil M 1944 CS[f]	14.9
Vitamin E	0.5	Sorbitan monooleate	14.9	PEG 400	24.9
Ascorbyl palmitate	0.5	Ascorbyl palmitate	1.0	Ascorbyl palmitate	1.0
Anhydrous alcohol	17.8	Anhydrous alcohol	4.9	Anhydrous alcohol	4.9

[a]Formulation 1, oral drinking solution 15 mL; [b]Formulation 2B, liquid-filled capsule formulation 2B 0.6 mL; [c]Formulation 2C, liquid-filled capsule formulation 2C 0.6 mL; [d]TPGS, d alpha-tocopheryl polyethylene glycol 1000 succinate; [e]Labrasol®, caprylocaproyl macrogol-8 glycerides; [f]Labrafil® M 1944 CS, polyoxyethylated oleic glycerides.

Formulation 1, the drinking solution (180 mg paclitaxel in 15 mL), was administered orally to the patients within 2 hours after dilution with tap water to 100 mL. Capsule formulation 2B and capsule formulation 2C (containing 45 mg paclitaxel in 0.6 mL each) were ingested orally as 4 capsules per dose with 120 mL water. CsA was administered as capsules of 50 and 100 mg each (Galena, Opava, Czech Republic). No standard prophylactic anti-emetics were administered, but anti-emetics were allowed when the patient developed nausea and vomiting during previous treatment with paclitaxel or after prior treatment with one of the formulations in the current study. If necessary, patients were premedicated with oral granisetron (Kytril®) 1 mg approximately 1.5 - 2 hours before the intake of paclitaxel. All patients received a light breakfast (1 cracker) with each paclitaxel administration. Intake of a low-fat meal was allowed only 1 hour after the intake of oral paclitaxel. If considered in their best interest, patients continued on a 3-weekly schedule of i.v. paclitaxel administered at a dose of 175 mg/m^2 as 3-hour infusion.

Sample collection and analysis

Blood samples for pharmacokinetic analysis of paclitaxel, 6α-hydroxypaclitaxel, and 3'p-hydroxypaclitaxel were collected via an indwelling catheter in 5 mL heparinized tubes after all three p.o. administrations. Samples were obtained prior to administration, and 10, 15, 30 minutes, and 1, 2, 3, 5, 7, 10, and 24 hours after paclitaxel administration. Blood samples were centrifuged, and plasma was separated and immediately transferred into polypropylene tubes and stored at -20°C until analysis. Paclitaxel concentrations in plasma were determined using a validated HPLC tandem mass spectrometric (MS/MS) method (26).

For determination of the CsA concentration, blood samples were collected in 5 mL EDTA tubes 1 hour after paclitaxel administration (corresponding to 1.5 hours after CsA administration). These values were used as a surrogate for CsA exposure. Whole blood samples were stored at 4°C until analysis using a specific fluorescence polarization immunoassay (FPIA) (27). Three mL whole blood was collected from every patient in an EDTA tube before the start of the first course for determination of genetic polymorphisms of the *MDR1* gene.

Pharmacokinetics

The pharmacokinetic parameters of paclitaxel 6α-hydroxypaclitaxel, and 3'p-hydroxypaclitaxel were determined by non-compartmental analysis, using WinNonLin™ (version 5.0, Pharsight Corporation, Mountain View, CA, USA). The area under the plasma concentration time curve (AUC) was determined using the linear logarithmic trapezoidal method up to the last measured concentration-time point and extrapolated to infinity ($AUC_{0-\infty}$) using the slope of the terminal part of the logarithmic concentration versus time curve (λ_z). The maximal observed drug concentration (C_{max}) and time to maximal observed drug concentration (T_{max}) were obtained directly from the experimental data. Furthermore, the terminal half-life ($t_{1/2}$) was determined.

Statistics

An univariate General Linear Model (GLM) with treatment (formulation 1, 2B, and 2C) and day (1, 8, and 15) as fixed factors was applied to the logarithmic-transformed pharmacokinetic parameters of paclitaxel, to investigate the differences between the three study treatments using a LSD test. In addition, the

effect of the moment (day 1, 8, and 15) and order of treatment were investigated. The a priori level of significance was set at 0.05. The software package Statistical Product and Service Solutions (version 12.1.1 for Windows, SPSS Inc., Chicago, IL, USA) was used for statistical analysis.

Pharmacogenetics

Genetic polymorphisms in exon 12 (C1236T), exon 21 (G2677T), and exon 26 (C3435T) of the *MDR1* gene were determined. Genomic DNA was isolated according to the method by Boom et al (28). Genetic polymorphisms in *MDR1* were all analysed according to slightly modified methods previously described by Hoffmeyer et al (29) and Kim et al (30) DNA was amplified and sequences of the PCR products were analysed on an Applied Biosystems 3100-Avant DNA sequencer. For sequence alignment Seqscape v2.1 (Applied Biosystems, Foster City, CA, USA) was used and the polymorphisms were determined using Graphical Overview of Linkage Disequilibrium (GOLD) software v1.1.0.0.

Safety

All toxicities observed were graded according to the National Cancer Institute Common Terminology Criteria for Adverse Events (NCI CTCAE) version 3.0, 2003 (http://ctep.cancer.gov/forms/CTCAEv3.pdf).

Results

Patient characteristics

As one patient was not fully evaluable for pharmacokinetic analysis, one additional patient was included and in total 10 patients were entered into the study. Patient characteristics are specified in Table 2.

Drug administration and extent of exposure

All patients, except patient 4, received all three study treatments (Day 1, 8 and 15) at the single flat dose of 180 mg paclitaxel per formulation. The three formulations were administered in the following sequence: 1/2/3 to patients 3, 4, and 8, 2/3/1 to patients 2, 5, 9, and 10, and 3/1/2 to patients 1, 6, and 7. Patient 1 experienced vomiting within 15 and 30 minutes after administration of formulation 1 on day 8.

Table 2. Patient characteristics.

No. of patients	10
Male/Female	3/7
Median age, years (range)	58 (49-72)
Median PS (range)	1 (0-1)
Tumor type	
NSCL	3
Gastric	6
Bladder	1
Prior treatment	
Chemotherapy	10
Surgery	2
Radiotherapy	1

Therefore, administration of formulation 1 was repeated 7 days later with the use of pre-medication (dexamethasone 20 mg i.v. and granisetron 1 mg i.v. 30 min before CsA). Patient 4 also developed vomiting after administration of formulation 1 on day 1 and therefore administration of this formulation was repeated 7 days later. Regarding patient 4, pharmacokinetic sampling at 24 h after administration of formulation 2B could not be performed due to the poor clinical status of the patient. Patient 4 died due to progression of disease and was therefore not able to receive treatment with formulation 2C.

Pharmacokinetic and statistical analysis

Figure 1 depicts the plasma pharmacokinetic profiles of paclitaxel, 6α-hydroxypaclitaxel, and 3'p-hydroxypaclitaxel after treatment with formulation 1 (n = 10), formulation 2B (n = 9), and formulation 2C (n = 9). Interpatient variability in paclitaxel plasma concentrations was comparable between the formulations. Figure 2 presents the $AUC_{0-\infty}$ (μg*h/mL), C_{max} (μg/mL), and T_{max} (h) of paclitaxel after the three different oral formulations.

The plasma pharmacokinetic parameters (median and range) of paclitaxel after the three study treatments are given in Table 3. Mean $AUC_{0-\infty}$ and SD of paclitaxel was 2.89 ± 0.25 μg*h/mL (3.38 ± 0.29 μM*h), 2.10 ± 0.27 μg/mL (2.46 ± 0.32 μM*h) and 2.50 ± 0.27 μg/mL (2.93 ± 0.32 μM*h) after formulation 1, 2B, and 2C, respectively. $AUC_{0-\infty}$ of paclitaxel was not significantly different between formulation 1 and 2B (p = 0.10) and was also comparable for the other formulations.

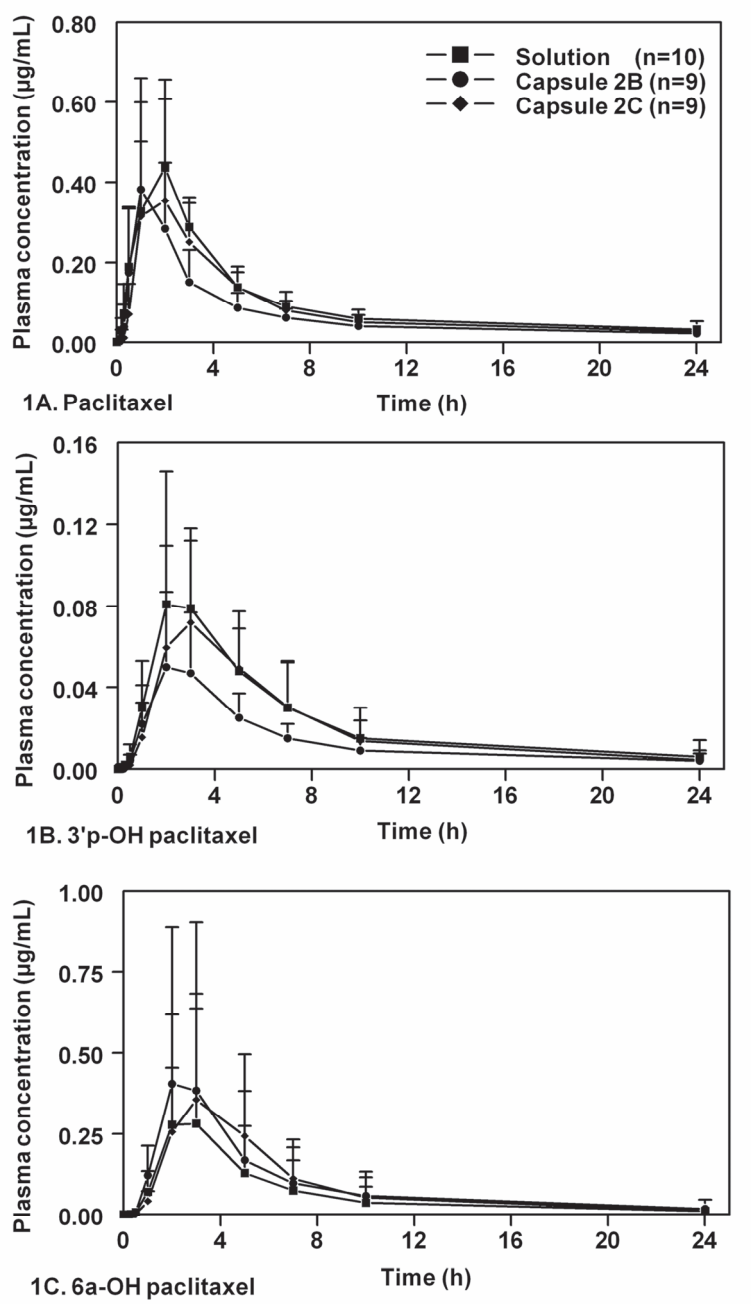

Figure 1. Paclitaxel plasma concentration versus time curves after p.o. paclitaxel 180 mg co-administered 30 minutes after p.o. CsA 10 mg/kg as formulation 1 (n = 10), formulation 2B (n = 9), and formulation 2C (n = 9). Data are represented as mean ± SD on a semi-logarithmic scale.

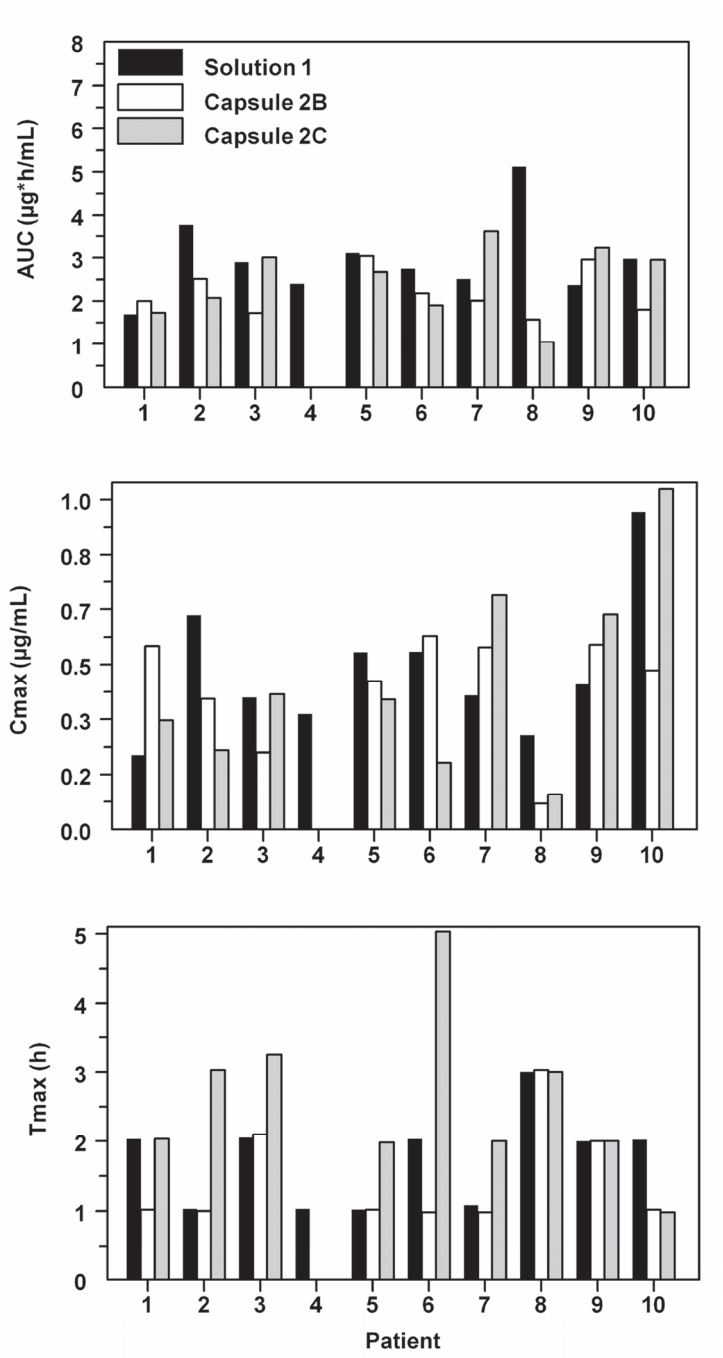

Figure 2. Individual $AUC_{0-\infty}$, C_{max}, and T_{max} values of paclitaxel after oral treatment with formulation 1 (n = 10), formulation 2B (n = 9), and formulation 2C (n = 9). All three paclitaxel formulations were administered 30-minutes after p.o. CsA 10 mg/kg.

In addition, mean C_{max} of paclitaxel was comparable between the three formulations and was 0.46 ± 0.06 μg/mL (0.54 ± 0.07 μM), 0.40 ± 0.07 μg/mL (0.47 ± 0.08 μM), and 0.42 ± 0.07 μg/mL (0.49 ± 0.08 μM) after formulation 1, 2B, and 2C, respectively. In addition T_{max} of paclitaxel after formulation 2B (1.6 ± 0.29 h) was substantially lower compared to formulation 2C (2.7 ± 0.3 h, p = 0.01). No significant effect of moment and order of treatment was found. The mean $AUC_{0-\infty}$ ratio of 6α-hydroxypaclitaxel/paclitaxel after formulation 1, 2B, and 2C was 0.61, 1.2, and 0.91, respectively, while the AUC ratio of 3'p-hydroxypaclitaxel/paclitaxel after these formulations was 0.23, 0.20, and 0.21, respectively. The median concentration of CsA at 1.5 h after administration was 1.08 (0.17-1.99) μg/mL, 1.82 (0.97-2.25) μg/mL, and 1.32 (0.47-2.54) μg/mL after co-administration with oral paclitaxel as formulation 1, formulation 2B, and formulation 2C, respectively. These results suggest that exposure to CsA was comparable between the different formulations.

Pharmacogenetics

Patient 2 and 5 had a homozygous T/T allele expressed in exon 26 and these patients also had homozygous SNPs in exon 12 and 21.A total of 8 patients (80%) had heterozygous C/T allele expression in exon 26.

Safety evaluation

Overall, the formulations were well tolerated. Few NCI CTCAE Grade 1-2 non-hematological toxicities were observed, consisting mainly of gastrointestinal disorders with the most common symptoms of nausea and vomiting; nausea was observed in 5 patients after both formulation 1 and formulation 2B, and occurred in 6 patients after formulation 2C. Vomiting was observed in 7 patients, 6 patients, and 5 patients after administration of formulation 1, 2B, and 2C, respectively. Five Grade 3 events were observed, consisting of nausea in patient 1 after formulation 1, and somnolence in patient 6 after all three administrations together with fatigue after formulation 2C. No life threatening adverse events (Grade 4) were reported in the study. Furthermore, no clinical relevant hematological toxicities occurred after the three treatments. In addition, no abnormal blood chemistry values were reported.

Table 3. Plasma pharmacokinetic parameters of paclitaxel, 6α-hydroxypaclitaxel, and 3'p-hydroxypaclitaxel after p.o. administration of paclitaxel 180 mg as formulation 1 (n = 10), formulation 2B (n = 9), and formulation 2C (n = 9). Data are presented as median (range).

Parameter	Formulation 1	Formulation 2B	Formulation 2C
Paclitaxel			
T_{max} (h)	2.0 (1.02-3.0)	1.0 (0.98-3.03)*	2.0 (0.98-5.03)
C_{max} (µg/mL)	0.42 (0.23-0.96)	0.48 (0.08-0.59)	0.39 (0.11-1.03)
$AUC_{0-\infty}$ (µg*h/mL)	2.83 (1.69-5.12)	2.01 (1.57-3.04)	2.67 (1.05-3.61)
%CV of $AUC_{0-\infty}$	32	24	34
$t_{1/2}$ (h)	8.9 (6.0-16)	10.6 (7.3-20)	9.7 (7.6-11)
6α-hydroxypaclitaxel			
T_{max} (h)	2.6 (2.0-6.9)	2.0 (2.0-5.02)	3.0 (2.0-5.03)
C_{max} (µg/mL)	0.20 (0.09-1.21)	0.24 (0.06-1.43)	0.43 (0.08-1.05)
$AUC_{0-\infty}$ (µg*h/mL)	1.16 (0.31-6.89)	1.03 (0.33-9.15)	1.51 (0.54-5.48)
%CV of $AUC_{0-\infty}$	117	118	90
$t_{1/2}$ (h)	5.2 (4.7-24)	5.6 (4.0-8.4)	5.0 (4.3-7.0)
3'p-hydroxypaclitaxel			
T_{max} (h)	3.0 (2.0-5.05)	2.0 (2.0-5.02)	3.1 (2.0-5.0)
C_{max} (µg/mL)	0.071 (0.046-0.25)	0.058 (0.015-0.13)	0.071 (0.021-0.18)
$AUC_{0-\infty}$ (µg*h/mL)	0.53 (0.18-1.66)	0.40 (0.19-1.16)	0.45 (0.25-1.17)
%CV of $AUC_{0-\infty}$	66	63	56
$t_{1/2}$ (h)	6.1 (4.5-14)	5.8 (4.3-24)	6.0 (4.9-7.5)

%CV = % coefficient of variation; * $p < 0.05$ in comparison with formulation 2C.

Discussion

We studied the PK of paclitaxel and two major metabolites of three novel formulations (one drinking solution and two capsules) for oral administration of paclitaxel 180 mg in combination with CsA 10 mg/kg. In addition, tolerability and safety were studied.

The release profile of paclitaxel from the formulations used in this study as well as the safety was previously tested in preclinical studies. It was observed from *in vitro* studies that propylene glycol solubilised the paclitaxel and Labrasol® and Labrafil® M 1944 CS helped to keep the paclitaxel in solution after dilution in simulated gastric fluid. Furthermore, *in vivo* studies in rats demonstrated that oral administration of formulation 2B and 2C resulted in a prolonged release profile of paclitaxel without causing an initially high C_{max} of paclitaxel (data on file). This was considered to be advantageous as this could result in plasma concentrations at a pharmacologically relevant level for prolonged periods of time.

In the present clinical study the systemic exposure of paclitaxel was comparable following oral administration of formulation 1, formulation 2B, and formulation 2C (all administered 30 minutes after CsA). Furthermore, the systemic exposure of paclitaxel after these oral formulations was comparable with recently tested novel oral paclitaxel formulations (31, 32) and with paclitaxel PK after i.v. administration of docosahexaenoic acid (DHA)-paclitaxel (33). The $AUC_{0-\infty}$ ratio of 6α-hydroxypaclitaxel/3'p-hydroxypaxlitaxel after formulation 1, 2B, and 2C was approximately 3, 6, and 4, respectively, which is comparable with previous findings (21). The differences in paclitaxel PK between the oral formulations were low. It would be interesting, however, to investigate capsule formulation 2C in future studies because of the generally better tolerability and safety profile of a capsule formulation above an oral drink solution (formulation 1), and because of the slightly higher AUC of paclitaxel compared to formulation 2B.

It is known that CrEL, which is present in the i.v. paclitaxel formulations, is responsible for the non-linear pharmacokinetics of i.v. paclitaxel (2, 4). This can be explained by entrapment of paclitaxel in micelles in the central compartment by CrEL, leading to a more than proportional increase in plasma paclitaxel concentrations with increasing doses. We previously described that CrEL could limit the absorption rate of paclitaxel due to encapsulation in CrEL micelles. As the concentration of CrEL in the gastro-intestinal tract decreases with time due to distribution, breakdown and elimination of CrEL, more unbound paclitaxel becomes available for absorption in the systemic circulation with time and consequently the absorption rate increases (34). The shorter T_{max} of formulation 2B could be caused by a more rapid dilution of micelles in the gastrointestinal tract

due to a higher contact surface area and/or lower critical micellar concentration of the excipients.

All 3 formulations have the advantage that they contain a substantially lower amount of ethanol compared to orally administered i.v. paclitaxel (Taxol®) at a similar paclitaxel dose of 180 mg; the amount of administered ethanol was approximately 2.7 g (formulation 1) and 0.1 g (for both formulation 2B and 2C), while this would be 11.9 g after the orally applied i.v. paclitaxel (Taxol®) formulation. Furthermore, C_{max} values of CsA were comparable to a previous study, which demonstrated that 10 mg/kg CsA is sufficient for maximal enhancement of paclitaxel bioavailability (11).

All three formulations were well tolerated and the main toxicities of the three different formulations were mild to moderate gastro-intestinal disorders (nausea and vomiting). However, the limited number of patients prohibited detailed safety analysis of the three study treatments. The fact that patients 2 and 5, having a homozygous T/T allele expressed in exon 26 and homozygous SNPs in exon 12 and 21, did not have different PK of paclitaxel compared to the other patients also supports the notion that CsA in the doses administered leads to maximal inhibition of PgP. However, to assess the influence of different SNPs in *MDR1* on the PK of paclitaxel, larger studies with paclitaxel administered as a single drug are warranted.

In summary, we demonstrated that three new paclitaxel formulations were well tolerated after oral administration at the given dose of 180 mg when co-administered with CsA, without induction of relevant gastrointestinal or hematological toxicity. The formulations demonstrated comparable PK of paclitaxel and metabolites. We suggest new studies especially with capsule formulation 2C to explore single daily administration of paclitaxel at higher dose levels and multiple daily dosing in order to increase the systemic exposure and to prolong exposure at therapeutic levels.

Acknowledgements

We thank Ms. Ciska Koopman and Ms. Carolien Alderden-Los for the assistance in paclitaxel and CsA analysis and Ms. Tessa Bosch and Ms. Valerie Doodeman for analysis of genetic polymorphisms.

References

1. Webster LK, Linsenmeyer ME, Rischin D, Urch ME, Woodcock DM, Millward MJ. Plasma concentrations of polysorbate 80 measured in patients following administration of docetaxel or etoposide. Cancer Chemother Pharmacol 1997;39:557-60.

2. van Tellingen O, Huizing MT, Panday VR, Schellens JHM, Nooijen WJ, Beijnen JH. Cremophor EL causes (pseudo-) non-linear pharmacokinetics of paclitaxel in patients. Br J Cancer 1999;81:330-5.

3. van Zuylen L, Karlsson MO, Verweij J, et al. Pharmacokinetic modeling of paclitaxel encapsulation in Cremophor EL micelles. Cancer Chemother Pharmacol 2001;47:309-18.

4. Sparreboom A, van Tellingen O, Nooijen WJ, Beijnen JH. Nonlinear pharmacokinetics of paclitaxel in mice results from the pharmaceutical vehicle Cremophor EL. Cancer Res 1996;56:2112-5.

5. Kruijtzer CM, Beijnen JH, Schellens JHM. Improvement of oral drug treatment by temporary inhibition of drug transporters and/or cytochrome P450 in the gastrointestinal tract and liver: an overview. Oncologist 2002;7:516-30.

6. Kivisto KT, Kroemer HK, Eichelbaum M. The role of human cytochrome P450 enzymes in the metabolism of anticancer agents: implications for drug interactions. Br J Clin Pharmacol 1995;40:523-30.

7. Sparreboom A, van Asperen J, Mayer U, et al. Limited oral bioavailability and active epithelial excretion of paclitaxel (Taxol) caused by P-glycoprotein in the intestine. Proc Natl Acad Sci USA 1997;94:2031-5.

8. Malingré MM, ten Bokkel Huinink WW, Duchin K, Schellens JHM, Beijnen JH. Pharmacokinetics of oral cyclosporin A when co-administered to enhance the oral absorption of paclitaxel. Anticancer Drugs 2001;12:591-3.

9. Britten CD, Baker SD, Denis LJ, et al. Oral paclitaxel and concurrent cyclosporin A: targeting clinically relevant systemic exposure to paclitaxel. Clin Cancer Res 2000;6:3459-68.

10. van Asperen J, van Tellingen O, van der Valk MA, Rozenhart M, Beijnen JH. Enhanced oral absorption and decreased elimination of paclitaxel in mice cotreated with cyclosporin A. Clin Cancer Res 1998;4:2293-7.

11. Malingré MM, Beijnen JH, Rosing H, et al. The effect of different doses of cyclosporin A on the systemic exposure of orally administered paclitaxel. Anticancer Drugs 2001;12:351-8.

12. Bosch TM, Meijerman I, Beijnen JH, Schellens JHM. Genetic polymorphisms of drug-metabolising enzymes and drug transporters in the chemotherapeutic treatment of cancer. Clin Pharmacokinet 2006;45:253-85.

13. Hoffmeyer S, Burk O, von RO, et al. Functional polymorphisms of the human multidrug-resistance gene: multiple sequence variations and correlation of one allele with P-glycoprotein expression and activity in vivo. Proc Natl Acad Sci U S A 2000;97:3473-8.

14. Malingré MM, Beijnen JH, Rosing H, et al. A phase I and pharmacokinetic study of bi-daily dosing of oral paclitaxel in combination with cyclosporin A. Cancer Chemother Pharmacol 2001;47:347-54.

15. Malingré MM, Meerum Terwogt JM, Beijnen JH, et al. Phase I and pharmacokinetic study of oral paclitaxel. J Clin Oncol 2000;18:2468-75.

16. Malingré MM, Schellens JHM, van Tellingen O, et al. Metabolism and excretion of paclitaxel after oral administration in combination with cyclosporin A and after i.v. administration. Anticancer Drugs 2000;11:813-20.

17. Meerum Terwogt JM, Malingré MM, Beijnen JH, et al. Coadministration of oral cyclosporin A enables oral therapy with paclitaxel. Clin Cancer Res 1999;5:3379-84.

18. Malingré MM, Beijnen JH, Schellens JHM. Oral delivery of taxanes. Invest New Drugs 2001;19:155-62.

19. Malingré MM, Schellens JHM, van Tellingen O, et al. The co-solvent Cremophor EL limits absorption of orally administered paclitaxel in cancer patients. Br J Cancer 2001;85:1472-7.

20. Bardelmeijer HA, Ouwehand M, Malingré MM, Schellens JHM, Beijnen JH, van Tellingen O. Entrapment by Cremophor EL decreases the absorption of paclitaxel from the gut. Cancer Chemother Pharmacol 2002;49:119-25.

21. Sparreboom A, van Zuylen L, Brouwer E, et al. Cremophor EL-mediated alteration of paclitaxel distribution in human blood: clinical pharmacokinetic implications. Cancer Res 1999;59:1454-7.

22. van Zuylen L, Verweij J, Sparreboom A. Role of formulation vehicles in taxane pharmacology. Invest New Drugs 2001;19:125-41.

23. Chang T, Benet LZ, Hebert MF. The effect of water-soluble vitamin E on cyclosporine pharmacokinetics in healthy volunteers. Clin Pharmacol Ther 1996;59:297-303.

24. Boudreaux JP, Hayes DH, Mizrahi S, Maggiore P, Blazek J, Dick D. Use of water-soluble liquid vitamin E to enhance cyclosporine absorption in children after liver transplant. Transplant Proc 1993;25:1875.

25. Chang RK, Shojaei AH. Effect of a lipoidic excipient on the absorption profile of compound UK 81252 in dogs after oral administration. J Pharm Pharm Sci 2004;7:8-12.

26. Vainchtein LD, Thijssen B, Stokvis E, Rosing H, Schellens JHM, Beijnen JH. A simple and sensitive assay for the quantitative analysis of paclitaxel and metabolites in human plasma using liquid chromatography/tandem mass spectrometry. Biomed Chromatogr 2006;20:139-48.

27. Malingré MM, Rosing H, Koopman FJ, Schellens JHM, Beijnen JH. Performance of the analytical assays of paclitaxel, docetaxel, and cyclosporin in a routine hospital laboratory setting. J Liq Chrom & Rel Technol 2001;24:2697-717.

28. Boom R, Sol CJ, Salimans MM, Jansen CL, Wertheim-van Dillen PM, van der Noordaa J. Rapid and simple method for purification of nucleic acids. J Clin Microbiol 1990;28:495-503.

29. Hoffmeyer S, Burk O, von RO, et al. Functional polymorphisms of the human multidrug-resistance gene: multiple sequence variations and correlation of one allele with P-glycoprotein expression and activity in vivo. Proc Natl Acad Sci USA 2000;97:3473-8.

30. Kim RB, Leake BF, Choo EF, et al. Identification of functionally variant MDR1 alleles among European Americans and African Americans. Clin Pharmacol Ther 2001;70:189-99.

31. Veltkamp SA, Thijssen B, Garrigue JS, et al. A novel self-microemulsifying formulation of paclitaxel for oral administration to patients with advanced cancer. Br J Cancer 2006;95:729-34.

32. Veltkamp SA, Alderden-Los C, Sharma A, Rosing H, Beijnen JH, Schellens JHM. A pharmacokinetic and safety study of a novel polymeric paclitaxel formulation for oral application. Cancer Chemother Pharmacol 2007;59:43-50.

33. Wolff AC, Donehower RC, Carducci MK, et al. Phase I study of docosahexaenoic acid-paclitaxel: a taxane-fatty acid conjugate with a unique pharmacology and toxicity profile. Clin Cancer Res 2003;9:3589-97.

34. de Jonge ME, Huitema AD, Schellens JH, Rodenhuis S, Beijnen JH. Population pharmacokinetics of orally administered paclitaxel formulated in Cremophor EL. Br J Clin Pharmacol 2005;59:325-34.

Chapter 4.3

A novel self-microemulsifying formulation of paclitaxel for oral administration to patients with advanced cancer

British Journal of Cancer 2006;95:729-734

Stephan A. Veltkamp
Bas Thijssen
Jean S. Garrigue
Gregory Lambert
Frédéric Lallemand
Florence Binlich
Alwin D.R. Huitema
Bastiaan Nuijen
Annemarie Nol
Jos H. Beijnen
Jan H.M. Schellens

Abstract

To explore the pharmacokinetics, safety and tolerability of paclitaxel after oral administration of SMEOF#3, a novel Self-Microemulsifying Oily Formulation, in combination with cyclosporin A (CsA) in patients with advanced cancer.

Seven patients were enrolled and randomly assigned to receive oral paclitaxel (SMEOF#3) 160mg + CsA 700mg on day 1, followed by oral paclitaxel (Taxol®) 160mg + CsA 700mg on day 8 (group I) or vice versa (group II). Patients received paclitaxel (Taxol®) 160mg as 3-hour infusion on day 15.

The median (range) area under the plasma concentration-time curve of paclitaxel was 2.06 (1.15-3.47) µg*h/mL and 1.97 (0.58-3.22) µg*h/mL after oral administration of SMEOF#3 and Taxol®, respectively and 4.69 (3.90-6.09) µg*h/mL after intravenous Taxol®. Oral SMEOF#3 resulted in a lower median T_{max} of 2.0 (0.5-2.0) h than orally applied Taxol® (T_{max} = 4.0 (0.8-6.1) h, p = 0.02). The median apparent bioavailability of paclitaxel was 40 (19-83) % and 55 (9-70)% for the oral SMEOF#3 and oral Taxol® formulation, respectively. Oral paclitaxel administered as SMEOF#3 or Taxol® was safe and well tolerated by the patients.

Interestingly, the SMEOF#3 formulation resulted in a significantly lower T_{max} than orally applied Taxol®, probably due to the excipients in the SMEOF#3 formulation resulting in a higher absorption rate of paclitaxel.

Introduction

Currently, paclitaxel is only marketed as an intravenous (i.v.) formulation. Paclitaxel is poorly soluble in most pharmaceutical solvents, therefore, in the marketed i.v. formulation it is formulated in a 1:1 combination of the solubilising agent polyoxyethylated caster oil (Cremophor® EL (CrEL)) and dehydrated ethanol.

CrEL has been reported to be responsible for severe hypersensitivity reactions (1) and the non-linear pharmacokinetic behaviour of i.v. administered paclitaxel (2-4). Oral administration of paclitaxel might be attractive because it is more convenient for patients than i.v. administration. Furthermore, oral paclitaxel administration may enable the development of treatment regimens resulting in plasma concentrations above a pharmacologically relevant level for more prolonged periods of time. However, oral treatment with paclitaxel is severely hampered because of its low bioavailability, which is caused by two main reasons. Firstly, paclitaxel is a high affinity substrate for the efflux multidrug transporter P-glycoprotein (P-gp), which is highly expressed in the gastrointestinal tract (5). Secondly, paclitaxel undergoes first-pass metabolism by the gut and liver cytochrome P450 (CYP) enzymes (CYP 2C8 and CYP 3A4).

Previous studies carried out at our Institute investigated the pharmacokinetics of the i.v. paclitaxel formulation after oral administration as a drinking solution diluted with water (6-13) and revealed that co-administration of oral CsA resulted in an increased systemic exposure to oral paclitaxel (13, 14). As CsA is an inhibitor of both P-gp and CYP3A4, both an increased absorption and a reduced first-pass effect may be responsible for the increased systemic exposure. We have shown previously that systemic exposure to paclitaxel did not increase with CsA doses higher than 10 mg/kg.

Although CrEL was reported to exhibit no oral absorption it affects paclitaxel pharmacokinetics by limiting the absorption of paclitaxel from the intestine after oral administration, probably by entrapment of paclitaxel in micelles, thereby reducing the availability of paclitaxel for uptake (2, 10, 15-17). Thus far, a favourable oral formulation with paclitaxel has not been found yet. SMEOF#3 is a novel oral Self-Microemulsifying Oily Formulation (SMEOF) of paclitaxel. The formulation consists of an isotropic mixture of oils and surfactants, which

solubilise paclitaxel and spontaneously forms a microemulsion upon contact with water.

Previous *in vivo* studies in *wild type* mice and *mdr1a/b (-/-)* knockout mice, which lack functional P-gp activity, showed that SMEOF#3 was a suitable delivery vehicle for oral administration of paclitaxel in combination with oral CsA (data on file). The choice of the excipients was motivated by a previous study exploring particle size, physical and chemical stability as well as cytotoxic activity *in vitro* of different formulations of paclitaxel (18). Furthermore, the physical stability of emulsions of different SMEOFs of paclitaxel was assessed after dilution in simulated gastric fluid (SGF). It was shown that after dilution of the i.v. paclitaxel (Taxol®) formulation in SGF, a major part of the micelles were destabilized and a massive precipitation immediately occurred (data on file). This phenomenon was thought to be due to diffusion of ethanol in the SGF after which the remaining CrEL could not maintain all paclitaxel in solution. SMEOF#3, however, showed a high stability for about 6 hours after dilution in SGF. In SMEOF#3, tyloxapol and TPGS (d-alpha-tocopheryl polyethylene glycol 1000 succinate) have been selected for their ability to solubilise paclitaxel. Tyloxapol is a non-ionic surfactant used in the product Exosurf® (GlaxoSmithKline, UK). Upon contact with water, tyloxapol was shown to form lyotropic liquid crystals, which are thought to contribute to the formation of microemulsions (19). Furthermore, it was shown that tyloxapol can be used as a co-solvent by increasing the solubility of paclitaxel in ethanol (18). TPGS is a derivative of vitamin E with amphiphillic properties and it is used as excipient in Agenerase® (amprenavir, GlaxoSmithKline, UK). TPGS has been shown to increase the bioavailability of poorly absorbed lipophilic drugs (20), probably by its solubilising effect through improved micelle formation (21). As compared to the commercial paclitaxel (Taxol®) formulation tested orally, the main advantages of SMEOF#3 are the absence of CrEL and the significantly lower ethanol/paclitaxel ratio, which allows the administered amount of ethanol to be reduced. The purpose of this study was to investigate the pharmacokinetics, safety and tolerability of this novel oral formulation of paclitaxel (SMEOF#3).

Patients and Methods

Patient Population

Patients with a histological or cytological diagnosis of advanced non-haematological cancer for whom no curative therapy existed and for whom treatment with single agent paclitaxel was considered of potential benefit were eligible for the study. Patients had to have recovered from any toxicities of prior treatment. Previous chemotherapy was allowed as long as the last treatment was at least four weeks prior to study entry and at least three weeks had elapsed since receiving radiotherapy. Patients had to have acceptable haematological parameters (white blood cells (WBC) $\geq$ 3.0 x 10^9/L, and platelets $\geq$ 100 x 10^9/L)), hepatic function (serum bilirubin $\leq$ 20 µmol/L; AST and ALT $\leq$ 1.5 x upper limit of normal (ULN) or $\leq$ 3 x ULN in case of liver metastases) and renal function (serum creatinine $\leq$ 160 µmol/L or creatinine clearance $\geq$ 50 mL/min as calculated by Cockcroft Gault formula), and a World Health Organization (WHO) performance status (PS) $\leq$ 2. Patients were excluded if they had experienced severe toxicities on prior taxane treatment, suffered from uncontrolled infectious disease, heart disease, bowel obstruction or motility disorders that could have influenced the resorption of drugs. Further exclusion criteria were concomitant use of known P-gp and CYP 3A modulating drugs and chronic use of H2-receptor antagonists or proton pump inhibitors. Female patients were excluded when breast-feeding or pregnant (confirmed by a pregnancy test before study entry). Patients had to be willing and able to follow the protocol requirements. The Medical Ethics Committee of the Institute approved the study protocol and all patients gave written informed consent.

Study design

Initially 6 patients were planned to enrol in the study and were randomly assigned to two groups of treatment. Group I received a combination of oral paclitaxel (SMEOF#3) 160 mg and CsA 700 mg on day 1, followed by oral paclitaxel (Taxol®) 160 mg in combination with CsA 700 mg on day 8, and Group II received oral paclitaxel (Taxol®) 160 mg in combination with CsA 700 mg on day 1, followed by oral paclitaxel (SMEOF#3) 160 mg and CsA 700 mg on day 8. CsA was administered orally at a fixed dose of 700 mg (approximately equivalent to 10

mg/kg CsA) 30 minutes prior to oral administration of paclitaxel. The patients in both groups received a single i.v. administration of paclitaxel (Taxol®) 160 mg as a three-hour infusion on day 15.

Drug composition and administration

The composition of SMEOF#3 (Novagali Pharma SA, Evry cedex, France) is presented in Table 1.

Table 1. Composition of SMEOF#3.

Component	Percentage % (w/v)	Function
Paclitaxel	1.6	Active substance
Vitamin E	5	Oil
TPGS*	30	Surfactant, co-solvent
Tyloxapol	30	Surfactant, co-solvent
Ethanol (anhydrous)	33.38	Solvent
Citric acid (anhydrous)	0.02	pH adjuster
Total	100	

*D alpha-tocopheryl polyethylene glycol 1000 succinate

SMEOF#3 (160 mg in 10 mL) was administered orally to the patients via a syringe within 30 minutes after 1:3 dilution with tap water to 40 mL resulting in a final paclitaxel concentration of 4 mg/mL. The commercially available i.v. paclitaxel (Taxol®) formulation (Bristol-Myers Squibb, Syracuse, NY, USA) containing paclitaxel 6 mg/mL, ethanol 396 mg/mL and CrEL 527 mg/mL was administered orally after dilution of 26.7 mL (160 mg) with water to 40 mL (4 mg/mL). The i.v. paclitaxel (Taxol®) formulation was administered intravenously at a fixed dose of 160 mg as 3-hour infusion to all patients on day 15. CsA was administered as 7 capsules of 100 mg each (Neoral®, Novartis, Basel, Switzerland). To prevent possible nausea and vomiting during both the treatment with oral SMEOF#3 and oral Taxol®, patients were premedicated with oral granisetron (Kytril®) 1 mg approximately 2 hours before the intake of paclitaxel. In addition, patients received a light standard breakfast (2 crackers and a cup of tea) at least two hours prior to each paclitaxel administration. Intake of food was not allowed until 2 hours following the intake of oral paclitaxel. Patients were pre-medicated with dexamethasone 20 mg p.o. 8-10 hours prior to, and ranitidine 50 mg i.v., clemastine 2 mg i.v. and dexamethasone 20 mg i.v., 30-60 minutes before i.v.

paclitaxel dosing, to prevent infusion-related hypersensitivity reactions. If considered in their best interest, patients continued on a 3-weekly schedule of i.v. paclitaxel at a dose of 175 mg/m^2.

Sample collection and analysis

Blood samples for pharmacokinetic analysis of paclitaxel were collected via an indwelling catheter in 5 mL heparinized tubes after both p.o. and i.v. administration. Following oral administration samples were obtained prior to administration, immediately after administration, and 15, 30, 45 min, and 1, 2, 4, 6, 8, 24, 48, and 72 hours after paclitaxel administration. Following i.v. administration samples were obtained prior to administration, 60, 120, and 165 min after start of infusion, at the end of infusion, and 15, 30, 45 min, and 1, 2, 4, 6, 8, 24, 48, and 72 hours after infusion. Blood samples were centrifuged, and plasma was separated and immediately transferred into polypropylene tubes and stored at -20°C until analysis. Paclitaxel concentrations in plasma were determined using a validated HPLC tandem mass spectrometric (MS/MS) method (22). For the pharmacokinetic analysis of CsA, blood samples were collected in 5 mL EDTA tubes at the same time points as for paclitaxel after the oral SMEOF#3 and oral Taxol® administrations. Whole blood samples were stored at 4°C until analysis using a specific fluorescence polarization immunoassay (FPIA) (23). Urine samples were collected prior to paclitaxel administration and at the intervals: 0-24, 24-48 and 48-72 hours after oral SMEOF#3 and oral Taxol® and after i.v. Taxol® administration. A volume of 19 mL of each urine sample was mixed with 1 mL of a mixture of 5 % Cremophor® EL (Sigma, Prague, Czech Republic) - ethanol (Merck, Darmstadt, Germany) 1:1 v/v to prevent paclitaxel precipitation. Subsequently, 5 mL was transferred into a 10 mL polypropylene tube and stored at -20°C until analysis. Paclitaxel concentrations in urine were determined using a validated high performance liquid chromatographic (HPLC) method with ultraviolet (UV) detection (24).

Pharmacokinetics

The pharmacokinetic parameters of paclitaxel and CsA were determined by non-compartmental analysis, using WinNonLin™ (version 5.0, Pharsight Corporation, Mountain View, CA, USA). The area under the plasma concentration time curve

(AUC) was determined using the linear logarithmic trapezoidal method up to the last measured concentration-time point and extrapolated to infinity ($AUC_{0-\infty}$) using the slope of the terminal part of the logarithmic concentration versus time curve (λ_z). Furthermore, the terminal half-life ($t_{1/2}$) was determined. The maximal observed drug concentration (C_{max}) and time to maximal observed drug concentration (T_{max}) were obtained directly from the experimental data. The apparent bioavailability (F) of paclitaxel was calculated by the ratio of the $AUC_{0-\infty}$ after oral administration and $AUC_{0-\infty}$ after intravenous administration of paclitaxel. Furthermore, the fraction of the paclitaxel dose that was excreted unchanged in urine was calculated.

Statistics

The software package Statistical Product and Service Solutions (version 12.1.1 for Windows, SPSS Inc., Chicago, IL, USA) was used for statistical analysis. The a priori level of significance was $p = 0.05$. The paired t-test was applied on logarithmic-transformed values to make a comparison between the pharmacokinetic parameters of paclitaxel after the different study treatments.

Safety

All toxicities observed were graded according to the National Cancer Institute Common Terminology Criteria for Adverse Events (NCI CTCAE) version 3.0, 2003 (http://ctep.cancer.gov/forms/CTCAEv3.pdf).

Results

Patient characteristics

As one patient was not fully evaluable for pharmacokinetic analysis, one additional patient was included and in total 7 patients were entered into the study. Patient characteristics are specified in Table 2. Patients 1, 4, 5 and 7 were assigned to Group 1 and patients 2, 3, and 6 were assigned to Group II. Four patients and three patients had a PS of 1 and 2, respectively. Age, height and weight appeared to be equally distributed over the two treatment groups.

Table 2. Patient characteristics.

No. of patients	7
Male/Female	5/2
Median age, years (range)	56 (29-63)
Median PS (range)	1 (1-2)
Tumor type	
NSCL	1
Stomach	1
Neuroendocrinal	1
Thyroid	1
Oesophagus Cardia	2
Parotid gland	1
Prior treatment	
Surgical therapy	5
Chemotherapy	7
Radiotherapy	4

Drug administration and extent of exposure

All patients received all three treatments (Day 1, 8 and 15) at the single flat dose of 160 mg per formulation. The i.v. administration of Taxol® during day 15 was temporarily interrupted in patient 1 due to infusion leakage. Patient 4, a 54 years old female, developed rash and dyspnoea 15 minutes following i.v. paclitaxel administration. The paclitaxel infusion was terminated and 2 mg clemastine i.v. was given, which resolved the hypersensitivity reaction. Therefore blood sampling for pharmacokinetics could not be performed and this patient was not fully eligible. Intravenous paclitaxel administration was restarted after one hour at a lower infusion rate, which did not cause any adverse reactions.

Pharmacokinetic and statistical analysis

Figure 1 depicts the plasma pharmacokinetic profiles of paclitaxel after treatment with p.o. paclitaxel (SMEOF#3), p.o. paclitaxel (Taxol®) (n = 7), and i.v. paclitaxel (Taxol®) 160 mg as 3-hour infusion (n = 6). Interpatient variability in paclitaxel plasma concentrations was comparable between p.o. SMEOF#3 and p.o. Taxol®, both co-administered with CsA, but was lower after i.v. administered Taxol®.

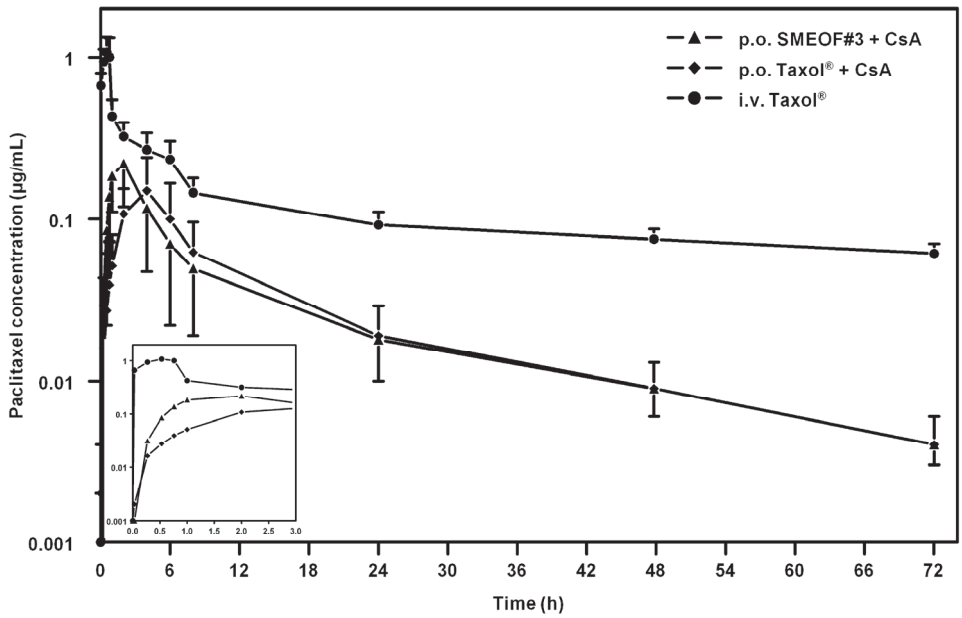

Figure 1. Paclitaxel plasma concentration versus time curves after p.o. SMEOF#3 160 mg + CsA 700 mg, p.o. Taxol® 160 mg + CsA 700 mg (n = 7), and i.v. Taxol® 160 mg as 3-hour infusion (n = 6). Data are represented as mean ± SD on a semi-logarithmic scale.

Figure 2 presents the $AUC_{0-\infty}$ (µg*h/mL), C_{max} (µg/mL), and T_{max} (h) of paclitaxel after p.o. SMEOF#3, p.o. Taxol® and after i.v. Taxol® given as 3 h infusion. T_{max} after oral SMEOF#3 was substantially lower compared to p.o. paclitaxel (Taxol®) ($p = 0.021$). The plasma pharmacokinetic parameters of paclitaxel after the three study treatments are depicted in Table 3. The median (range) $AUC_{0-\infty}$ of the SMEOF#3 formulation was 2.06 (1.15-3.47) µg*h/mL, which was not significantly higher than the $AUC_{0-\infty}$ of 1.97 (0.58-3.22) µg*h/mL after oral Taxol® ($p = 0.74$). The interpatient variability in $AUC_{0-\infty}$ was relatively high after both p.o. SMEOF#3 (%CV = 42) and p.o. Taxol® (%CV = 45). Furthermore, oral SMEOF#3 resulted in a not significantly higher median C_{max} of 0.21 (0.15-0.35) µg/mL compared to a C_{max} of 0.16 (0.10-0.29) µg/mL after oral Taxol® ($p = 0.15$). Remarkably, oral SMEOF#3 showed a significantly lower T_{max} of 2.0 (0.5-2.0) h than p.o. Taxol®, which had a T_{max} of 4.0 (0.8-6.1) h ($p = 0.021$). The median apparent bioavailability was 40% (19-83%) and 55% (9-70%) for the oral SMEOF#3 and oral Taxol® formulation, respectively. After both i.v. and oral administration

excretion of paclitaxel in the urine was low and more than 70% of the total urinary excretion occurred within 24 hours.

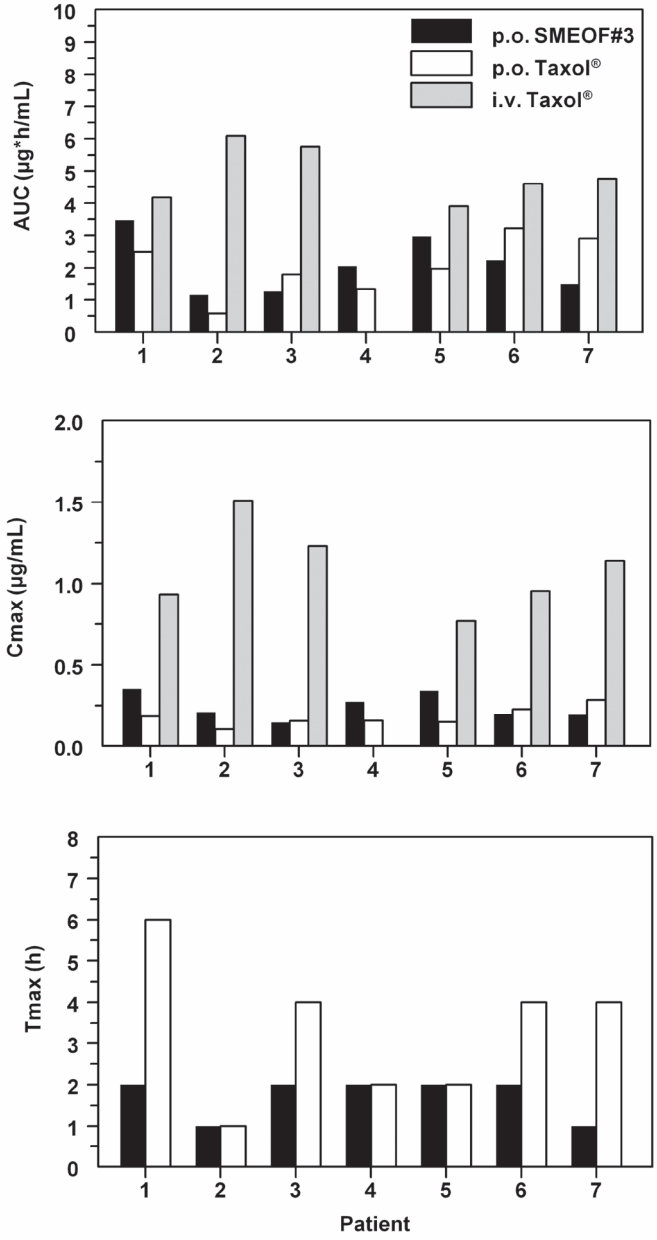

Figure 2. Individual $AUC_{0-\infty}$, C_{max}, and T_{max} values of paclitaxel after treatment with p.o. SMEOF#3 and p.o. Taxol® (n = 7), both co-administered with CsA, and after treatment with i.v. Taxol® (n = 6).

Table 3. Plasma pharmacokinetic parameters of paclitaxel after p.o. SMEOF#3 160 mg, p.o. Taxol® 160 mg (n = 7), and i.v. Taxol® 160 mg as 3-hour infusion (n = 6). Data are presented as median (range).

Parameter	SMEOF#3 p.o.	Taxol® p.o.	Taxol® i.v.
T_{max} (h)	2.0 (0.5-2.0)	4.0 (0.8-6.1)	n.a.
C_{max} (µg/mL)	0.21 (0.15-0.35)	0.16 (0.10-0.29)	1.05 (0.77-0.15)
$AUC_{0-\infty}$ (µg*h/mL)	2.06 (1.15-3.47)	1.97 (0.58-3.22)	4.69 (3.90-6.09)
%CV of AUC	42	45	18
$t_{1/2}$ (h)	23 (20-28)	22 (17-33)	23 (16-32)
F(%)	40 (19-83)	55 (9-70)	
%CV of F	59	48	
U_{excr} (% of dose)*	1.3 (0.5-2.1)	1.7 (0.6-3.6)	5.0 (3.4-8.3)

n.a. = not applicable; *U_{excr} = Urinary paclitaxel excretion; %CV = % coefficient of variation.

Figure 3 depicts the mean pharmacokinetic profiles of CsA after oral administration of CsA 700 mg in combination with p.o. SMEOF3# 160 mg and p.o. Taxol® 160 mg (n = 7).

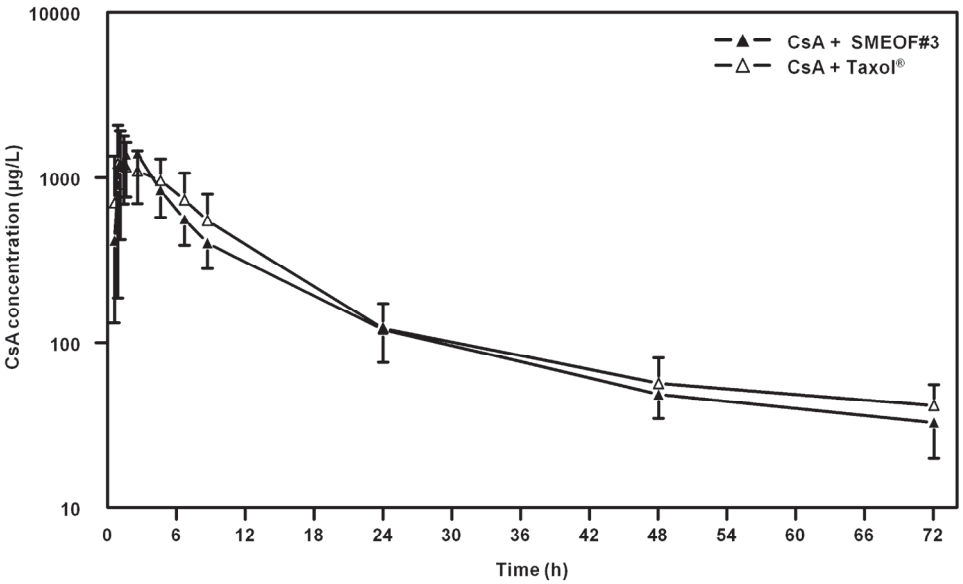

Figure 3. CsA blood concentration versus time curves after administration of CsA 700 mg in combination with oral SMEOF#3 and oral Taxol® (n = 7). Data are represented as mean ± SD on a semi-logarithmic scale.

The pharmacokinetic parameters of CsA of all three study treatments are summarized in Table 4. Figure 3 and Table 4 clearly show that CsA pharmacokinetics were not influenced by co-administration of either paclitaxel formulations.

Table 4. Plasma pharmacokinetic parameters of CsA after administration of CsA 700 mg in combination with p.o. SMEOF#3 160 mg and p.o. Taxol® 160 mg (n = 7). Data are presented as median (range).

Parameter	SMEOF#3	Taxol®
T_{max} (h)	2.6 (0.8-2.8)	1.5 (0.8-6.7)
C_{max} (µg/mL)	1.48 (0.86-2.89)	1.51 (0.80-2.71)
$AUC_{0-\infty}$ (µg*h/mL)	13.3 (10-23.8)	15.8 (8.95-25.1)
%CV of AUC	32	34
$t_{1/2}$ (h)	17 (12-28)	20 (8-34)

Safety evaluation

Non-haematological toxicities were CTCAE Grade 1-2, except for two Grade 3 events: one hypersensitivity reaction in patient 4 after i.v. paclitaxel administration, and muscular weakness in patient 1, that was considered to be probably related to SMEOF#3. No life threatening adverse events (Grade 4) and deaths (Grade 5) were reported in the study. Overall, the most frequently reported drug-related adverse events were gastrointestinal disorders with the most common symptoms of nausea occurring in 3 patients after oral administration of paclitaxel. Furthermore, abdominal pain, diarrhoea, and stomatitis were reported in 2 patients. No clinical relevant haematological toxicities occurred after the three treatments. Furthermore, no abnormal blood chemistry values were reported.

Discussion

In the present clinical study we tested the pharmacokinetics, safety and tolerability of SMEOF#3, a new micro-emulsifying formulation for oral administration of paclitaxel in combination with CsA. The apparent bioavailability of paclitaxel after oral administration of SMEOF#3 co-administered with CsA was estimated at 40% (19-83%) and was comparable to the apparent bioavailability of orally

administered Taxol®. These data were consistent with studies that showed that the apparent bioavailability of orally administered Taxol® in combination with CsA was approximately 47% (13, 25). The term bioavailability, however, should be interpreted with caution due to the non-linear pharmacokinetics of i.v. paclitaxel caused by the presence of CrEL (3). Entrapment of paclitaxel in CrEL micelles in the central compartment causes a more than proportional increase in plasma paclitaxel concentrations with increasing doses.

Studies in mice showed that these higher total drug levels in plasma did not result in higher drug levels in tissues (2). Previous studies showed that CrEL is not absorbed after oral administration. This pseudo-non-linearity of i.v. paclitaxel has two important implications for the pharmacology of oral paclitaxel. Firstly, the oral bioavailability of paclitaxel, calculated by comparing the AUC values after oral and i.v. administration, will be underestimated as the affinity of paclitaxel for the plasma compartment is increased after i.v. administration due to the presence of CrEL in the central circulation. Secondly, the pseudo-non-linearity of i.v. paclitaxel implies that after oral administration, when CrEL is not present, plasma levels of paclitaxel represent a higher fraction of free drug, which will result in enhancement of the availability of paclitaxel for the (tumor) tissues (3). Consequently, threshold values for the paclitaxel concentration established for i.v. paclitaxel (25, 26) can not be used for oral administration of paclitaxel. The pharmacokinetic parameters of CsA after co-administration with oral SMEOF#3 and orally administered Taxol® were comparable. Furthermore, pharmacokinetic parameters of CsA were in line with those obtained before (6, 12). It has been demonstrated that 10 mg/kg CsA was sufficient for maximal enhancement of paclitaxel bioavailability (6, 12). In combination, these facts suggest that a dose of 700 mg CsA as used in this study was sufficient.

Remarkably, the T_{max} of paclitaxel after oral administration of the SMEOF#3 formulation was lower compared to oral Taxol®. We previously described that CrEL limits the absorption rate of paclitaxel due to encapsulation in CrEL micelles. As the concentration of CrEL in the gastrointestinal tract decreases with time due to distribution, breakdown and elimination of CrEL, more unbound paclitaxel becomes available for absorption in the systemic circulation with time and consequently the absorption rate increases (27). The lower T_{max} after oral SMEOF#3 is probably due to the ability of the SMEOF#3 formulation to remain

stable in the gastrointestinal tract avoiding precipitation of paclitaxel leading to a major fraction of paclitaxel in solution, which is available for absorption. However, in the case of oral paclitaxel administered as Taxol®, a significant amount of paclitaxel probably precipitates due to quick diffusion and resorption of ethanol and the precipitated fraction of paclitaxel is slowly re-dissolved in the gastrointestinal fluids before being absorbed. Furthermore, a lower amount of ethanol was administered after SMEOF#3 160 mg compared to the orally applied i.v. paclitaxel (Taxol®) formulation 160 mg; the amount of administered ethanol was approximately 3.3 g and 10.6 g after SMEOF#3 and the orally applied i.v. paclitaxel (Taxol®) formulation, respectively. An extensive pharmacokinetic analysis demonstrated an increase in the systemic exposure to paclitaxel and a prolonged time of a paclitaxel concentration above a pharmacological relevant level with increasing doses of SMEOF#3 (data not shown).

In summary, we demonstrated that the novel SMEOF#3 formulation was well tolerated after oral administration at the given dose of 160 mg when co-administered with CsA, without induction of relevant gastrointestinal or haematological toxicity. Regarding the nearly uneventful oral administration of the 160 mg dose in combination with the relatively low $AUC_{0-\infty}$ after CsA co-administration, we suggest that new studies should be initiated with this novel SMEOF#3 formulation to explore single daily administration of paclitaxel at higher dose levels in order to increase systemic exposure and to prolong exposure at therapeutic levels.

Acknowledgements

We thank Ms. Ciska Koopman for her analytical support.

References

1. Webster LK, Linsenmeyer ME, Rischin D, Urch ME, Woodcock DM, Millward MJ. Plasma concentrations of polysorbate 80 measured in patients following administration of docetaxel or etoposide. Cancer Chemother Pharmacol 1997;39:557-60.

2. Sparreboom A, van Tellingen O, Nooijen WJ, Beijnen JH. Nonlinear pharmacokinetics of paclitaxel in mice results from the pharmaceutical vehicle Cremophor EL. Cancer Res 1996;56:2112-5.

3. van Tellingen O, Huizing MT, Panday VR, Schellens JHM, Nooijen WJ, Beijnen JH. Cremophor EL causes (pseudo-) non-linear pharmacokinetics of paclitaxel in patients. Br J Cancer 1999;81:330-5.

4. van Zuylen L, Karlsson MO, Verweij J, et al. Pharmacokinetic modeling of paclitaxel encapsulation in Cremophor EL micelles. Cancer Chemother Pharmacol 2001;47:309-18.

5. Sparreboom A, van Asperen J, Mayer U, et al. Limited oral bioavailability and active epithelial excretion of paclitaxel (Taxol) caused by P-glycoprotein in the intestine. Proc Natl Acad Sci USA 1997;94:2031-5.

6. Malingré MM, Beijnen JH, Rosing H, et al. A phase I and pharmacokinetic study of bi-daily dosing of oral paclitaxel in combination with cyclosporin A. Cancer Chemother Pharmacol 2001;47:347-54.

7. Malingré MM, Beijnen JH, Rosing H, et al. The effect of different doses of cyclosporin A on the systemic exposure of orally administered paclitaxel. Anticancer Drugs 2001;12:351-8.

8. Malingré MM, Beijnen JH, Schellens JHM. Oral delivery of taxanes. Invest New Drugs 2001;19:155-62.

9. Malingré MM, Meerum Terwogt JM, Beijnen JH, et al. Phase I and pharmacokinetic study of oral paclitaxel. J Clin Oncol 2000;18:2468-75.

10. Malingré MM, Schellens JH, van Tellingen O, et al. The co-solvent Cremophor EL limits absorption of orally administered paclitaxel in cancer patients. Br J Cancer 2001;85:1472-7.

11. Malingré MM, Schellens JHM, van Tellingen O, et al. Metabolism and excretion of paclitaxel after oral administration in combination with cyclosporin A and after i.v. administration. Anticancer Drugs 2000;11:813-20.

12. Malingré MM, ten Bokkel Huinink WW, Duchin K, Schellens JHM, Beijnen JH. Pharmacokinetics of oral cyclosporin A when co-administered to enhance the oral absorption of paclitaxel. Anticancer Drugs 2001;12:591-3.

13. Meerum Terwogt JM, Malingré MM, Beijnen JH, et al. Coadministration of oral cyclosporin A enables oral therapy with paclitaxel. Clin Cancer Res 1999;5:3379-84.

14. van Asperen J, van Tellingen O, van der Valk MA, Rozenhart M, Beijnen JH. Enhanced oral absorption and decreased elimination of paclitaxel in mice cotreated with cyclosporin A. Clin Cancer Res 1998;4:2293-7.

15. Bardelmeijer HA, Ouwehand M, Malingré MM, Schellens JHM, Beijnen JH, van Tellingen O. Entrapment by Cremophor EL decreases the absorption of paclitaxel from the gut. Cancer Chemother Pharmacol 2002;49:119-25.

16. Sparreboom A, van Zuylen L, Brouwer E, et al. Cremophor EL-mediated alteration of paclitaxel distribution in human blood: clinical pharmacokinetic implications. Cancer Res 1999;59:1454-7.

17. van Zuylen L, Verweij J, Sparreboom A. Role of formulation vehicles in taxane pharmacology. Invest New Drugs 2001;19:125-41.

18. Gursoy N, Garrigue JS, Razafindratsita A, Lambert G, Benita S. Excipient effects on in vitro cytotoxicity of a novel paclitaxel self-emulsifying drug delivery system. J Pharm Sci 2003;92:2411-8.

19. Gershanik T, Benita S. Self-dispersing lipid formulations for improving oral absorption of lipophilic drugs. Eur J Pharm Biopharm 2000;50:179-88.

20. Chang T, Benet LZ, Hebert MF. The effect of water-soluble vitamin E on cyclosporine pharmacokinetics in healthy volunteers. Clin Pharmacol Ther 1996;59:297-303.

21. Boudreaux JP, Hayes DH, Mizrahi S, Maggiore P, Blazek J, Dick D. Use of water-soluble liquid vitamin E to enhance cyclosporine absorption in children after liver transplant. Transplant Proc 1993;25:1875.

22. Vainchtein LD, Thijssen B, Stokvis E, Rosing H, Schellens JHM, Beijnen JH. A simple and sensitive assay for the quantitative analysis of paclitaxel and metabolites in human plasma using liquid chromatography/tandem mass spectrometry. Biomed Chromatogr 2006;20:139-48.

23. Malingré MM. Performance of the analytical assays of paclitaxel, docetaxel and cyclosporin in a routine hospital laboratory setting. J Liq Chrom & Rel Technol 2001;24:2697-717.

24. Huizing MT, Rosing H, Koopman F, Keung AC, Pinedo HM, Beijnen JH. High-performance liquid chromatographic procedures for the quantitative determination of paclitaxel (Taxol) in human urine. J Chromatogr B Biomed Appl 1995;664:373-82.

25. Huizing MT, Giaccone G, van Warmerdam LJ, et al. Pharmacokinetics of paclitaxel and carboplatin in a dose-escalating and dose-sequencing study in patients with non-small-cell lung cancer. The European Cancer Centre. J Clin Oncol 1997;15:317-29.

26. Gianni L, Kearns CM, Giani A, et al. Nonlinear pharmacokinetics and metabolism of paclitaxel and its pharmacokinetic/pharmacodynamic relationships in humans. J Clin Oncol 1995;13:180-90.

27. de Jonge ME, Huitema AD, Schellens JHM, Rodenhuis S, Beijnen JH. Population pharmacokinetics of orally administered paclitaxel formulated in Cremophor EL. Br J Clin Pharmacol 2005;59:325-34.

Chapter 4.4

A phase I safety and pharmacological study of a twice weekly dosing regimen of the oral taxane BMS-275183

Clinical Cancer Research 2007;13:3906-3912

Linda E. Bröker
Stephan A. Veltkamp
Elisabeth I. Heath
Bart C. Kuenen
Helen Gall
Ludovic Astier
Susan Parker
Louis Kayitalire
Patricia M. Lorusso
Jan H.M. Schellens
Giuseppe Giaccone

Abstract

BMS-275183, an orally administered C-4 methyl carbonate paclitaxel-analogue, showed promising activity in a phase I trial investigating a weekly treatment regimen, but was associated with a relatively high incidence of neuropathic side effects. The current dose escalation phase I trial was initiated to investigate whether twice weekly administration of BMS-275183 would improve its safety and tolerability. Additionally, the pharmacokinetics and possible antitumor activity were studied.

A cycle consisted of four weeks (i.e. 8 twice weekly oral doses). The starting dose was 60 mg/m^2 and the dose was increased by 20 mg/m^2 increments. Cohorts consisted of 3 patients and were expanded to at least 6 patients when toxicity was encountered. Plasma pharmacokinetics were performed on Day 1 and 15.

A total of 38 patients were enrolled. The maximum tolerated dose (MTD) was 100 mg/m^2 twice weekly. Seventeen patients were treated at the MTD; 3/17 patients experienced a dose limiting toxicity (DLT), consisting of a combination of neutropenia, neuropathy and diarrhea. BMS-275183 appeared to have a considerably lower incidence of neuropathic side effects compared to the weekly treatment regimen. Confirmed partial responses were observed in two patients with NSCLC, one patient with prostate cancer and one patient with melanoma. In addition, a long lasting PSA-response was observed in a prostate carcinoma patient with non-measurable disease.

BMS-275183 is preferably given in a twice weekly regimen and has considerable antitumor activity. A phase II trial in NSCLC using the twice weekly schedule has been initiated.

Introduction

BMS-275183 is an orally administered C-4 methyl carbonate analogue of paclitaxel containing additional modifications to the side chain (1). BMS-275183 has a higher oral bioavailability compared to paclitaxel. This is partially due to a lower affinity for the P-glycoprotein (P-gp) pump which is abundantly present in the intestinal brush border and limits the oral bioavailability of paclitaxel (1-3). The antitumor activity of BMS-2715183 was similar to intravenous (i.v.) paclitaxel in preclinical models (4). Paclitaxel is known to be a schedule-dependent drug that benefits from prolonged tumor exposure times (5). Therefore, oral administration may be preferable over i.v. administration, as it allows more prolonged or continued schedules. In addition, oral administration is often more convenient and is preferred by the majority of patients (6). BMS-275183 does not require the vehicle Cremophor EL®, which has been reported to be responsible for the hypersensitivity reactions and the non-linear pharmacokinetics of i.v. paclitaxel (7-9).

BMS-275183 has promising antitumor activity in patients. A recent phase I trial exploring once weekly dosing of BMS-275183 demonstrated a 24% response rate with a median duration of 8.7 months in a heavily pretreated group of patients with solid tumors. Most activity was observed in non-small cell lung cancer (NSCLC) and prostate carcinoma (10). Interestingly, the toxicity profile of oral BMS-275183 differs from that of i.v. paclitaxel. On a weekly treatment regimen, the main dose limiting toxicity (DLT) of BMS-275183 was peripheral neuropathy, whereas severe hematological side effects were infrequent (10). This is remarkable, because hematological toxicity and not neuropathy was dose limiting for both paclitaxel and docetaxel (11,12). For paclitaxel it is known that short infusion times (1-3 h) allow higher doses to be administered but neuropathy is a common side effect, whereas prolonged infusion times of 24 h or longer are associated with less neuropathy, but yield a higher incidence of myelosuppression (13). Mielke *et al.* demonstrated that patients with peripheral neuropathy had significantly higher overall systemic exposure to paclitaxel than those without development of peripheral neuropathy (14). As neutropenia was not an important DLT in the previous phase I study with once weekly dosing of BMS-275183 and systemic exposure to BMS-275183 proved to be predictive for toxicity (10), we

hypothesized that spreading the systemic exposure over a longer period of time would decrease the side effects of BMS-275183 and in particular neuropathy. We therefore amended the phase I trial in order to investigate a twice weekly administration of BMS-275183. The aims of the amended dose-escalating phase I trial were to investigate the safety, tolerability, pharmacokinetics (PK) and possible antitumor activity of BMS-275183 given in a twice weekly dosing regimen, and to define the recommended phase II dose.

Patients and Methods

Patients

Adult patients with histologically or cytologically confirmed diagnosis of a solid tumor not amenable to standard therapy were eligible for this study. They had to have an ECOG performance status (PS) of ≤ 2, a life expectancy of at least 3 months and adequate renal, liver and bone marrow function, defined as creatinine < 1.5 times upper limits of normal (ULN), bilirubin < 1.5 times ULN, alanine-aminotransferase < 2.5 times ULN, absolute neutrophil count (ANC) > 1.5 x 10^9/L and platelets > 100 x 10^9/L. An adequate method of birth control had to be used, and women of child-bearing potential had to have a negative serum or urine pregnancy test. At least 4 weeks had to have elapsed from prior anticancer treatment (including taxanes) and toxicities (except alopecia) had to be recovered to ≤ grade 1 (according to National Cancer Institute Common Toxicity Criteria version 2.0, NCI-CTCv2.0 (15)). Excluded were patients with a serious uncontrolled medical disease; active infection, significant pulmonary or cardiovascular disorder, QTc-interval > 450 msec, sensory or motor neuropathy ≥ grade 2, active brain metastasis, inability to swallow capsules, history of gastrointestinal disease, surgery or malabsorption that could impair the uptake of BMS-275183, concomitant use of known inducers or inhibitors of cytochrome P450 isoform CYP 3A4, and any psychiatric or other disorders such as dementia that would impair compliance. Concomitant radiotherapy or systemic anticancer therapy was not allowed. During the trial, the concomitant use of proton pump inhibitors (PPI) was added as an exclusion criterion, as an association between PPI-use and elevated exposure to BMS-275183 was found in ongoing clinical trials, suggesting a potential drug-drug interaction. The study was approved by the

medical ethics committees of the three participating institutes, and all patients gave written informed consent prior to study entry.

Study design

BMS-275183 (Bristol-Myers-Squibb, Princeton, NJ) was given orally on a continuous twice weekly schedule on an out-patient basis. One cycle consisted of four weeks of treatment, and the drug was given on days 1, 4, 8, 11, 15, 18, 22, and 25 of each 4-week treatment cycle. The starting dose was 60 mg/m^2, an estimation of a reasonably safe dose below the maximum tolerated dose (MTD) of 200 mg/m^2 identified with the weekly treatment regimen. Three patients were treated per cohort. Dose escalation took place according to predefined dose steps of 20 mg/m^2 (i.e. 80 mg/m^2, 100 mg/m^2 etc.), until a DLT was encountered. The cohort was then expanded to six patients, and dose escalation continued until a DLT was observed in two out of two to six patients. The MTD was defined as the highest dose at which no more than one out of six patients experienced a DLT. A minimum of 15 patients were to be treated at the MTD, to further establish the safety profile of a recommended phase II dose.

DLTs were predefined as any of the following drug-related side effects occurring during the first cycle: grade 4 neutropenia for ≥ 5 consecutive days, febrile neutropenia (fever ≥ 38.5°C), grade 4 thrombocytopenia or grade 3 with a bleeding episode requiring platelet transfusion, any grade ≥ 3 non-hematological toxicity, retreatment delay of more than one week due to drug-related toxicity, dose reduction or omission due to any drug-related toxicity before completion of the first cycle, QTc-interval > 500 msec and any clinically significant arrhythmia within 24 h following drug administration. Hypersensitivity reactions were not defined as DLTs. Dose reductions by one level were performed when a DLT or grade 2 neurotoxicity occurred.

Drug administration

BMS-275183 was provided in 5 and 25 mg capsules solubilized in PEG 400/PEG 1450 with Gelucire 44/14 as the excipient system at a loading of 4% w/w. The calculated dose was rounded to the nearest 5 mg. Patients ingested the capsules with 150 mL of water within 10 min. Patients were fasting for at least 8 h prior to drug administration and for 2 h post-dose. No prophylactic medication was

prescribed. Patients were planned to receive at least two cycles, unless toxicity or progressive disease required drug discontinuation.

Patient evaluation

Pretreatment evaluation included a complete history and physical examination, urinalysis including pregnancy test, a complete blood count, coagulation tests, serum chemistries, determination of serum tumor markers, tumor assessment, chest X-ray and ECG. Toxicity assessment and all blood tests except serum tumor markers, were repeated weekly. Physical examination was repeated before each cycle. Toxicities were graded according to NCI-CTCv2.0 (15). Patients were considered evaluable for toxicity if they received at least one dose of the study drug.

Because BMS-275183 moderately prolonged the action potential duration in isolated Purkinje fibers (unpublished data), ECG-monitoring was performed prior to drug administration and 2, 6 and 24 h after the first drug administration to assess potential prolongation of the QTc-interval (calculated using the Bazett's formula $QTc = QT/\sqrt{RR}$). If a QTc interval > 450 msec was observed, ECG monitoring was again performed after the second dose.

Objective response to therapy was assessed every other cycle according to World Health Organization criteria (16). To be evaluable for response patients had to complete at least two cycles, unless they had to prematurely discontinue treatment because of rapidly progressive disease.

Blood sampling and pharmacokinetic analysis

Pharmacokinetic monitoring was performed on Day 1 and 15 of the first cycle (after the first and fifth dose). Blood samples of 5 mL were collected via an indwelling catheter in potassium-EDTA vacutainers (Becton Dickinson, Franklin Lakes, NJ) up to 72 h after drug administration (time points 0, 0.5, 1, 1.5, 2, 3, 4, 5, 6, 8, 24 and 72 h). After collection, the tube was placed on ice and immediately centrifuged for 5 min at 2000 x *g* at 4 °C, and plasma was separated and stored at -80 °C until analysis. Plasma concentrations of BMS-275183 were determined by a validated liquid chromatography/mass spectrometry method, as described previously (10). PK profiles were evaluated by non-compartmental analysis using the software package Kinetica version 4.2 (InnaPhase Corporation, Philadelphia,

PA). The elimination half-life ($t_{½}$) was assessed from the elimination rate constant, estimated by linear regression of the terminal phase of the semi-logarithmic concentration versus time curve. The area under the plasma concentration versus time curve (AUC) was estimated by the trapezoidal method up to the last measured concentration-time point and extrapolated to infinity (AUC_{inf}). The maximal observed drug concentration (C_{max}) and the time to maximal observed drug concentration (T_{max}) were obtained directly from the experimental data.

Statistical analysis

Descriptive statistics were used for baseline characteristics, safety assessment and pharmacokinetic parameters (C_{max}, T_{max}, AUC_{inf}, $t_{½}$). The software package SAS® (version 8.2 for Unix) was used for statistical analysis. Analysis of variance (ANOVA) was used to estimate intra-subject variability in AUC_{inf}.

Results

Patients and treatment

Between January 2004 and December 2005, 38 patients were enrolled and treated in the trial at two participating centers in the Netherlands, and one center in the USA. Patient characteristics are summarized in Table 1. In summary, most patients were male (74%) with a median age of 61 years and 89% had an ECOG PS of 0-1. There were relatively large subgroups of patients with NSCLC (13 patients) and prostate carcinoma (6 patients).

The patients were treated at the following dose-levels: 60 mg/m^2 (n = 3), 80 mg/m^2 (n = 10), 100 mg/m^2 (n = 17), 120 mg/m^2 (n = 7). Inadvertently, one patient was treated for two doses with 140 mg/m^2. This patient experienced non-complicated grade 4 neutropenia 9 days after the first BMS-275183 administration (duration 3 days), and no further treatment was given. In addition, one patient receiving 80 mg/m^2 died a few days after his first dose due to disease-related complications, leaving 9 evaluable patients in this cohort. The median number of cycles administered was 2, with a range of 1-22 cycles.

Table 1. Patient characteristics.

Characteristic	No. (%)
Total no. of patients	38
Male	28 (74%)
Female	10 (26%)
Age (years)	
Median (range)	61 (40-73)
ECOG Performance status	
0	7 (18%)
1	27 (71%)
2	4 (11%)
Prior chemotherapy regimens	
0	2 (5%)
1	17 (45%)
2	13 (34%)
≥ 3	6 (16%)
Prior immunotherapy or hormonal therapy	13 (34%)
Prior radiotherapy	23 (61%)
Prior biological therapy	7 (18%)
Tumor type	
Non-small cell lung cancer	13 (34%)
Prostate carcinoma	6 (16%)
Melanoma	4 (10.5%)
Colorectal carcinoma	4 (10.5%)
Other	11 (29%)

Adverse events induced by BMS-275183

Table 2 summarizes the drug related adverse events. Clinically relevant toxicity was encountered from the 80 mg/m^2 dose-level. In the expanded cohort of six patients treated at this dose-level, one DLT consisting of grade 2 neuropathy was observed. In addition, one patient omitted a dose in the first cycle due to ongoing diarrhea which lasted only one day and never exceeded grade 2. After thorough discussion, this episode was considered too mild to qualify for a DLT, but for safety reasons, we further expanded this cohort to nine evaluable patients. In total, two DLTs were observed in nine evaluable patients treated at the 80 mg/m^2 dose-level, consisting of grade 3 fatigue and grade 2 neuropathy, respectively. Both events led to dose omission and reduction in the first cycle. Subsequently, we explored the 100 mg/m^2 dose-level. Although the first three patients tolerated this dose-level well, we decided to expand the cohort to six patients because one patient experienced a potentially drug-related grade 3 hematuria and increased urinary frequency during the first week of cycle 2. The first cycle in these additional three

patients was uneventful, and the next dose-level of 120 mg/m^2 was explored. This dose-level proved not to be feasible, as two DLTs were seen in 7 patients, consisting of dose omission and reduction in the first cycle due to grade 2 neuropathy and grade 2 gastrointestinal symptoms and grade 2 fatigue, respectively. In addition, one patient treated by mistake with 140 mg/m^2 developed grade 4 neutropenia after only 2 doses of BMS-275183.

We thus defined the MTD as 100 mg/m^2, and expanded this cohort to further assess this dose as the potentially recommended phase II dose. In total, 17 patients were treated at the dose of 100 mg/m^2. This dose-level was generally well tolerated, although three patients experienced severe but reversible toxicity during the first cycle, consisting of grade 3 neuropathy (n = 1), grade 4 neutropenia (n = 1), and grade 4 neutropenia combined with grade 3 diarrhea (n = 1). Other side effects were generally mild to moderate (Table 2). Gastrointestinal symptoms occurred in 28/38 of patients some time during their treatment with BMS-275183, but were usually mild to moderate and short lasting, and did not interfere with ingestion of the capsules. ECG-monitoring revealed a grade 1 prolongation of the QTc-interval in 1/38 patients, treated at 60 mg/m^2. This normalized on repeated ECGs and did not recur after the second dose, suggesting that BMS-275183 does not have clinically relevant effects on cardiac rhythm. Taken together, DLTs associated with twice weekly administration of BMS-275183 were neutropenia, neuropathy, fatigue and diarrhea. Other grade 3 and 4 toxicities were not dose limiting and consisted of increased urinary frequency and hematuria. The 100 mg/m^2 dose-level was identified as the recommended dose-level for future phase II trials.

Table 2. Adverse events caused by BMS-275183 (any cycle). Events considered possibly, probably or certainly related to BMS-275183 are presented. Several episodes in the same patient are counted as one adverse event and only the worst grade is mentioned (n = 38).

	Grades 1-2	Grade 3	Grade 4
Any adverse event	25	7	4
Hematologic			
Neutropenia	9		4
Anemia	2		
Thrombocytopenia	9		
Neurologic			
Sensory neuropathy	18	1	
Motor neuropathy	5	1	
Muskuloskeletal			
Myalgia	6		
Gastrointestinal			
Nausea	12		
Vomiting	10		
Diarrhea	16	4	
Mouth dryness	5		
Anorexia	9		
Taste disturbance	9		
Stomatitis/mucositis	3		
Abdominal cramping	2		
Flatulence	1		
Cardiovascular			
Prolonged QTc-interval	1		
Genitourinary tract			
Hematuria	1	1	
Increased urinary frequency	1	1	
Other			
Fatigue	14	4	
Alopecia	8		
Skin rash	3		
Epistaxis	11		
Nail changes	3		
Fever	2		
Flushing	2		
Dizziness	1		
Headache	1		
Pruritus	1		

Peripheral neuropathy

Overall, 47% (18/38) of patients developed a new or worsening neuropathy event in this trial. These patients belonged to the following dose cohorts: 1 in the 60 mg/m^2 cohort, 4 in the 80 mg/m^2 cohort, 7 in the 100 mg/m^2 cohort and 6 in the

120 mg/m^2 cohort. In most patients (11/18; 61%), the neuropathy was mild and did not exceed grade 1, whereas only 1/18 patients (5.6%) experienced severe grade 3 neuropathy (both sensory and motor). Nerve conduction studies were performed in this patient with severe neuropathy, and showed both sensory and motor axonal neuropathy.

Interestingly, neuropathy occurred less frequently in the twice weekly regimen than in the weekly schedule: overall incidence of 47% (18/38 patients) versus 65% (31/48 patients; (10)). Moreover, in only 7/18 (39%) of patients treated with the twice weekly schedule, the neuropathy exceeded grade 1, compared to 25/31 (81%) of patients treated with a weekly treatment regimen. In addition, the neuropathy induced by twice weekly administration of BMS-275183 developed more slowly than in the weekly treatment regimen. The median time to onset of any grade new or worsening neuropathy was 2.7 months (95% CI 1.4-∞ ; Figure 1) in patients treated with the twice weekly regimen, compared to 1.2 months (95% CI 0.3-10.8 months) in patients treated with weekly administration. In 17 out of 18 patients, the neuropathic symptoms recovered to baseline with a median time to resolution of 3.5 months (95% CI 2.9-5.3 months). This recovery was remarkably faster than observed in the weekly study protocol, in which the median time to resolution was 8.6 months (95% CI 5.8-17.5 months).

We studied whether prior treatment with neurotoxic chemotherapy was a risk factor for the development of peripheral neuropathy upon treatment with BMS-275183. From the 18 patients who developed peripheral neuropathy during this trial, 10 (56%) received prior treatment with at least one cytotoxic compound known to be associated with the development of peripheral neuropathy (defined as platinum compounds, taxanes, vinca alkaloids), and 8 (44%) patients were pretreated with a non-neurotoxic chemotherapeutic drug. In the group of 20 patients who did not experience any neurotoxic side effects from BMS-275183, 14 (74%) were pretreated with at least one neurotoxic drug, whereas 5 (26%) patients received prior treatment with a non-neurotoxic drug. One patient in the latter group did not receive any prior chemotherapeutic agents. Although the patient groups in this trial are small, these data suggest that prior treatment with neurotoxic agents does not predispose for the development of neuropathy upon treatment with BMS-275183, confirming our previous findings (10). It is, however, noteworthy that

patents with neuropathy greater than grade 1 resulting from prior therapies were excluded from participation in both trials, which may confound our results.

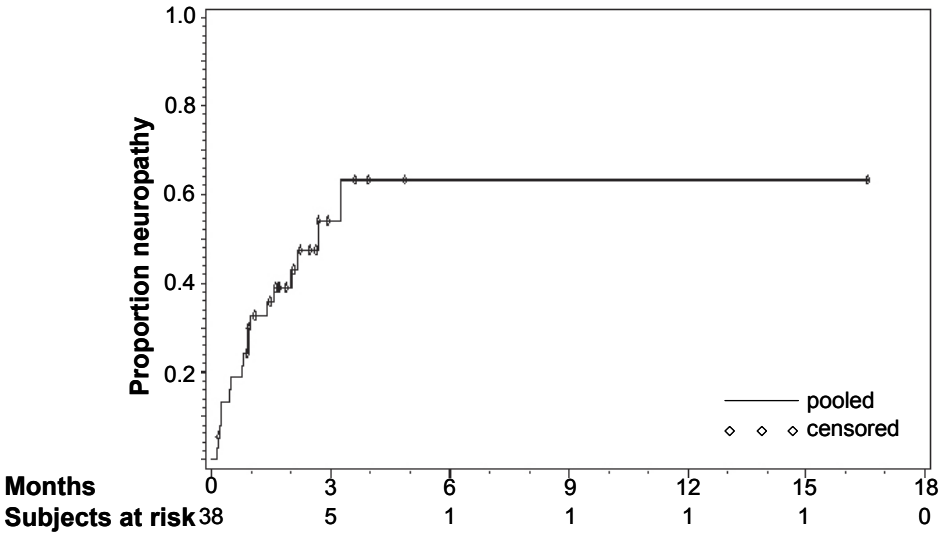

Figure 1. Time to onset of neuropathy (months). Analysis includes onset of any grade new or worsening sensory, motor or painful neuropathy in all patients treated with BMS-275183 (cohort pooled, n = 38). The curve estimates the time to onset if all patients would be treated until they develop neuropathy disregarding the other reasons for going off study. ♦: patients going off study without having developed neuropathy (censored data).

Pharmacokinetic analysis

Blood samples for PK analysis were available from 37 patients following the first dose Day 1), and from 32 patients following the fifth dose (Day 15). Figure 2 depicts the plasma PK profiles of BMS-275183 on Day 1 and Day 15 after twice weekly dosing of 60, 80, 100 and 120 mg/m^2 BMS-275183. Table 3 presents the PK parameters of BMS-275183 on Day 1 and 15. For all dose-levels (60 mg/m^2 - 120 mg/m^2) the compound was rapidly absorbed with a median T_{max} ranging from 0.5 to 1.0 h, suggesting that the rate of absorption was comparable among the four dose-levels. The mean $T_{½}$ over all dose-levels ranged from 25 - 35 h.

For increasing dose-levels of 60, 80, 100 and 120 mg/m^2, the median C_{max} and AUC_{inf} on Day 1 changed in the ratio of 1 : 0.75 : 0.78 : 0.67 and 1 : 1.03 : 0.93 : 1.16, respectively. As summarized in Table 3, the systemic exposure to BMS-275183 was comparable between Day 1 and 15 across the 4 dose-levels. The inter-

patient variability (%CV) of the AUC_{inf} in the patients treated at the recommended dose-level of 100 mg/m^2 was 94% on Day 1 (n = 17) and 93% on day 15 (n = 15). At other dose-levels, the inter-patient variability on Day 1 and 15 was lower compared to the 100 mg/m^2 dose cohort. One patient in the 100 mg/m^2 exhibited high exposure (AUC_{inf} = 7639 h*ng/mL, Day 1), which may have contributed to the higher interpatient variability in this dose cohort. This patient experienced a DLT after the second dose, consisting of grade 3 peripheral neuropathy. Provided that this outlier patient's data were excluded, the interpatient variability in AUC_{inf} for 100 mg/m^2 (Day 1) was 57%.

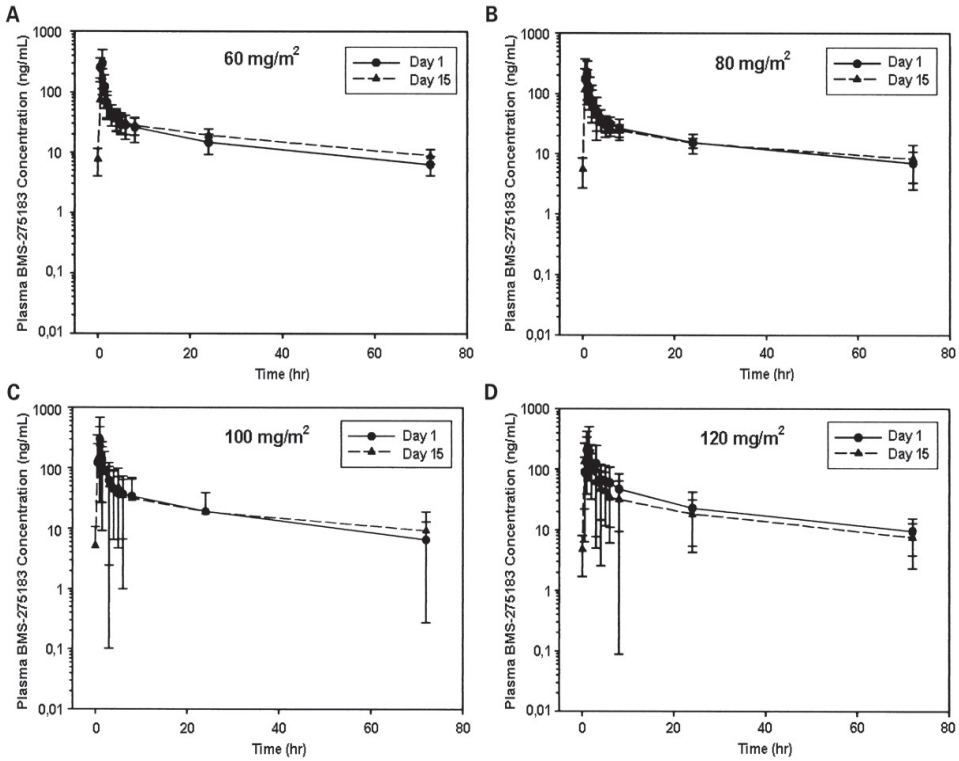

Figure 2. Plasma concentration versus time profiles of BMS-275183 on Day 1 and Day 15 following oral administration in a twice weekly regimen. **A.** 60 mg/m^2 (n = 3), **B.** 80 mg/m^2 (n = 10 for Day 1 and n = 8 for Day 15), **C.** 100 mg/m^2 (n = 17 for Day 1 and n = 15 for Day 15) and **D.** 120 mg/m^2 (n = 7 for Day 1 and n = 6 for Day 15). The lines represent the mean concentration and the error bars represent the standard deviation of the observed concentrations.

Table 3. Pharmacokinetic variables for BMS-275183.

	60 mg/m^2	80 mg/m^2	100 mg/m^2	120 mg/m^2
		Day 1		
No. of patients	3	10	17	7
C_{max} (ng/mL)†	299 (143-524)	223 (69-470)	233 (78-1700)	199 (80-429)
T_{max} (h) ‡	0.50 (0.5-1.0)	1.0 (0.5-2.0)	1.0 (0.5-3.0)	1.0 (1.0-3.0)
AUC_{inf}† (h*ng/mL)	1548 (954-2184)	1591 (1010-2649)	1437 (707-7640)	1803 (722-4541)
%CV of AUC_{inf}	38	37	94	68
$t_{½}$ (h)†	35 (30-35)	34 (24-52)	26 (19-76)	25 (21-29)
		Day 15		
No. of patients	3	8	15	6
C_{max} (ng/mL)†	196 (166-248)	202 (97-427)	265 (62-952)	200 (87-803)
T_{max} (h) ‡	1.0 (0.5-1.5)	1.0 (0.5-2.0)	1.0 (0.5-4.0)	1.0 (1.0-3.0)
AUC_{inf} † (h*ng/mL)	1887 (1381-2243)	1595 (965-3588)	1588 (708-8020)	1594 (813-4929)
%CV of AUC_{inf}	25	46	93	79
$t_{½}$ (h)†	41 (34-43)	37 (22-60)	30 (19-73)	35 (28-45)

*Geometric mean (range); **Median (range).

In general, patients in whom a DLT occurred, had a higher exposure to BMS-275183, (mean AUC_{inf} = 3731 h*ng/mL [n = 7]) than did patients who did not experience a DLT (mean AUC_{inf} = 1488 h*ng/mL [n = 30]). We could not identify a common denominator predicting drug exposure and development of side effects. In particular, patients with tumor involvement of the liver did not have lower drug clearance. Additionally, many potentially interacting concomitant medications were excluded by protocol. However, the use of PPIs was only excluded from July 2005, as at that time an association between PPI-use and elevated exposure to BMS-275183 was found in ongoing clinical trials, suggesting a potential drug-drug interaction (17). In this study, there were 11 patients using a PPI concomitantly with study medication. Of the 7 patients experiencing a DLT, 2 patients (29%) were concomitantly using a PPI. Of the 30 patients who did not experience a DLT, 9 (30%) were reported to use a PPI during their treatment with BMS-275183, suggesting that concomitant use of PPIs was not an important risk factor for developing severe toxicity in this trial.

Tumor response

We observed 4 confirmed partial responses in 30 evaluable patients with measurable disease. The tumor types of responding patients included: NSCLC (2 of

10 response evaluable patients), prostate carcinoma (1 of 3 response evaluable patients) and melanoma (1 of 3 response evaluable patients). In addition, a long lasting PSA-response (baseline PSA = 670 ng/mL, decreasing to 6.1 ng/mL with a response duration of 8 months) was seen in 1 patient with prostate carcinoma out of 4 patients with non-measurable disease. In total, 4 patients treated at 80, 100, 120 and 140 mg/m^2, went off study in the first cycle and were not evaluable for response. Computed tomography (CT) scans of a responding NSCLC patient as well as a responding prostate carcinoma patient are shown in Figure 3.

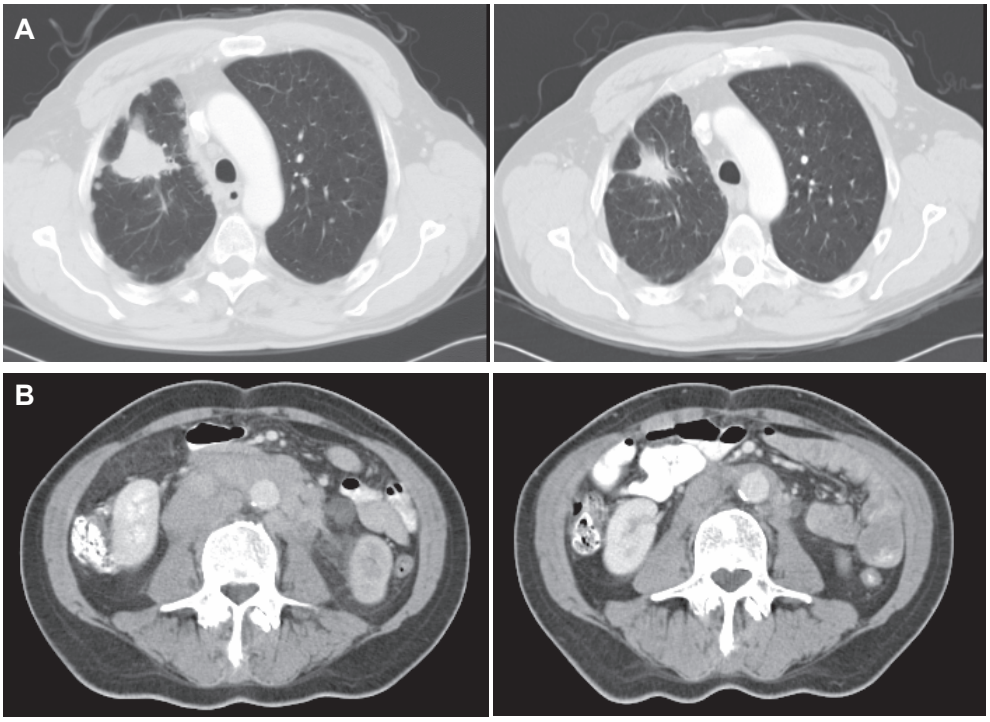

Figure 3. CT scans of two responding patients. **A.** CT scan of a 56-years-old male with NSCLC, previously treated with cisplatin/gemcitabine. Confirmed partial response (after 6 cycles) of the primary tumor and intrapulmonary metastases is presented. **B.** Abdominal CT scan of a chemotherapy-naïve 65-years-old male with prostate carcinoma. Confirmed partial response (after 3 cycles) of para-aortal lymph node metastases is presented.

Confirmed partial responses were observed after a mean of 2 cycles. The response duration was 6.5 and 15 months for the two NSCLC patients, 3.5 month for the prostate carcinoma patient and 1.75 month for the melanoma patient (mean

response duration of 6.7 months). Interestingly, one additional prostate carcinoma patient had a partial response (> 50% reduction of lymph node and pulmonary metastases) after only two doses of BMS-275183 (100 mg/m^2 dose-level), but the response was not confirmed, because he discontinued treatment due to development of grade 3 neurotoxicity. Upon recovery and progression, he was retreated at a lower dose-level of 60 mg/m^2, resulting in a minor response. All confirmed responses occurred in patients who were not previously treated with taxanes or other microtubule-interacting agents. Interestingly however, the one prostate carcinoma patient with an unconfirmed response after only two doses of BMS-275183 was resistant to docetaxel, as he had shown clear progressive disease after 3 courses of docetaxel.

Discussion

In the present clinical study, we have shown that BMS-275183 appears to be better tolerated in a twice weekly regimen than in a weekly schedule. In addition, we confirm that this drug has considerable antitumor activity. DLTs consisted of neutropenia, neuropathy and diarrhea, and other severe toxicities comprised fatigue and hematuria / increased urinary frequency and occurred only after prolonged treatment with BMS-275183. Remarkably, peripheral neuropathy occurred less frequently and was less severe than in our previous study with a weekly dosing schedule. This observation confirms our hypothesis that adapting the dosing regimen from once weekly to twice weekly dosing and thereby spreading the systemic exposure over a longer period of time would reduce the neurotoxic side effects of BMS-275183. Interestingly, we observed a similar incidence of myelosuppression after twice weekly administration of BMS-275183 compared to the weekly dosing regimen. Although we did not use prophylactic medication against anaphylaxis, we did not observe any hypersensitivity reactions, confirming the results of our previous trial with this compound (10).

In this study the systemic exposure to BMS-275183 on Day 15 was comparable to the exposure on Day 1 for all dose-levels, suggesting that twice weekly dosing does not result in accumulation of BMS-275183. No clinically relevant accumulation is expected based on the observed $t_{½}$ and the twice weekly dosing interval. The fact that no proportional increase in systemic exposure was seen in increasing dose-

levels, might be due to saturation of absorption of BMS-275183 after oral dosing. We identified 100 mg/m^2 twice weekly as the MTD. With this dose, we achieved a similar dose intensity as compared to the trial in which we studied weekly administration of BMS-275183 (MTD of 200 mg/m^2). The dose of 100 mg/m^2 given in a twice weekly regimen was generally well tolerated with 3/17 patients experiencing (reversible) grade 3 or 4 toxicity in the first cycle. Patients with a relatively high exposure to the drug were more prone to develop severe side effects. This relationship between drug exposure and adverse events is not unprecedented and has also been reported for other taxanes (18). Neither in our former study, nor in this trial could we identify a common denominator predicting drug exposure and development of side effects upon treatment with BMS-275183 (10). However, concomitant use of PPIs was not excluded from the start of the study, and a clinical study to explore the interaction between BMS-275183 and PPIs is ongoing.

In the 100 mg/m^2 dose cohort, one patient experienced a very high exposure (and a DLT), which may contribute to the high interpatient variability of 93% in this dose cohort. In our previous trial, we observed an interpatient variability of 53%, which is consistent with the average interpatient variability throughout all dose cohorts in this study. This variability is approximately two fold higher than for i.v. paclitaxel (historical data; (19)). Variations in absorption of the drug combined with individual differences in metabolism due to CYP3A4 polymorphism (20,21) may explain the observed high interpatient variability in systemic exposure to the drug. In the present study, concomitant use of CYP3A4 modifying drugs were prohibited and no violations of the protocol were made in this respect. However, no studies were undertaken to investigate the impact of CYP3A4 polymorphisms on the metabolism of BMS-275183, and future trials may elaborate on this important issue. The high interpatient variability may be of concern for the use of BMS-275183 in large scale phase II or III trials. Care should be taken to delay and reduce dosing upon the first signs of development of severe toxicity, in order to give the drug safely to those patients with an unexpected high exposure to the drug.

The response rate of 13% in the heavily pretreated patient group of this trial confirms our previous finding that BMS-275183 is a potent new taxane analogue. As expected, based on our previous trial and preclinical studies (1,4), most responses in this trial were observed in NSCLC and prostate carcinoma patients. In

preclinical studies, antitumor activity was observed in taxane resistant tumor models, including those harboring tubulin mutations or overexpressing P-gp (4). Our previous study indicated that BMS-275183 is active after prior taxane treatment, but no conclusion could be drawn on its activity in taxane-resistant tumors. In this study, all responses were in taxane-naïve patients, but interestingly, there were clear hints of activity in a taxane-resistant patient with prostate carcinoma.

In summary, BMS-275183 is a potent taxane analogue that is generally well tolerated at its MTD of 100 mg/m^2 in a twice weekly dosing schedule. A twice weekly regimen is preferred over a once weekly administration schedule, because of a considerably lower incidence of neuropathic side effects. BMS-275183 has antitumor activity in NSCLC and prostate carcinoma, and is currently being investigated in a phase II trial in NSCLC patients.

References

1. Mastalerz H, Cook D, Fairchild CR, et al. The discovery of BMS-275183: an orally efficacious novel taxane. Bioorg Med Chem 2003;11:4315-23.

2. Sparreboom A, van Asperen J, Mayer U, et al. Limited oral bioavailability and active epithelial excretion of paclitaxel (Taxol) caused by P-glycoprotein in the intestine. Proc Natl Acad Sci USA 1997;94:2031-5.

3. Trump DL, Egorin MJ, Ramesh R et al. A new oral taxane (BMS-275183): phase I trial with evaluation of pharmacokinetics, pharmacodynamics and bioavailability (abstract). Proc Am Soc Clin Oncol 2002;21:100a.

4. Rose WC, Long BH, Fairchild CR, Lee FY, Kadow JF. Preclinical pharmacology of BMS-275183, an orally active taxane. Clin Cancer Res 2001;7:2016-21.

5. Huizing MT, Giaccone G, van Warmerdam LJ, et al. Pharmacokinetics of paclitaxel and carboplatin in a dose-escalating and dose-sequencing study in patients with non-small-cell lung cancer. The European Cancer Centre. J Clin Oncol 1997;15:317-29.

6. Liu G, Franssen E, Fitch MI, Warner E. Patient preferences for oral versus intravenous palliative chemotherapy. J Clin Oncol 1997;15:110-5.

7. Sparreboom A, van Tellingen O, Nooijen WJ, Beijnen JH. Nonlinear pharmacokinetics of paclitaxel in mice results from the pharmaceutical vehicle Cremophor EL. Cancer Res 1996;56:2112-5.

8. Szebeni J, Muggia FM, Alving CR. Complement activation by Cremophor EL as a possible contributor to hypersensitivity to paclitaxel: an in vitro study. J Natl Cancer Inst 1998;90:300-6.

9. van Tellingen O, Huizing MT, Panday VR, Schellens JHM, Nooijen WJ, Beijnen JH. Cremophor EL causes (pseudo-) non-linear pharmacokinetics of paclitaxel in patients. Br J Cancer 1999;81:330-5.

10. Bröker LE, de Vos FY, van Groeningen CJ, et al. Phase I trial with BMS-275183, a novel oral taxane with promising antitumor activity. Clin Cancer Res 2006;12:1760-7.

11. Cortes JE, Pazdur R. Docetaxel. J Clin Oncol 1995;13:2643-55.

12. Rowinsky EK, Donehower RC. Paclitaxel (taxol). N Engl J Med 1995;332:1004-14.

13. Williams C, Collingwood M, Simera I, Grafton C. Short versus long duration infusions of paclitaxel for any adenocarcinoma. Cochrane Database Syst Rev 2003;CD003911.

14. Mielke S, Sparreboom A, Steinberg SM, et al. Association of Paclitaxel pharmacokinetics with the development of peripheral neuropathy in patients with advanced cancer. Clin Cancer Res 2005;11:4843-50.

15. Division of Cancer Treatment NCI. Guidelines for reporting of adverse drug reactions. Bethesda (MD): 1998.

16. World Health Organization Offset Publication No.48. WHO handbook for reporting results of cancer treatment. Geneva (Switzerland): 1979.

17. Marchetti S, Pluim D, Van Tellingen O et al. The novel orally available taxane derivative BMS-275183 is a substrate for P-glycoprotein (PgP, MDR1) and MRP2 and interacts with benzimidazole proton pump inhibitors (abstract). Proc Amer Assoc Cancer Res 2006;47:1272.

18. Huizing MT, Keung AC, Rosing H, et al. Pharmacokinetics of paclitaxel and metabolites in a randomized comparative study in platinum-pretreated ovarian cancer patients. J Clin Oncol 1993;11:2127-35.

19. Schiller JH, Storer B, Tutsch K, et al. Phase I trial of 3-hour infusion of paclitaxel with or without granulocyte colony-stimulating factor in patients with advanced cancer. J Clin Oncol 1994;12:241-8.

20. Goh BC, Lee SC, Wang LZ, et al. Explaining interindividual variability of docetaxel pharmacokinetics and pharmacodynamics in Asians through phenotyping and genotyping strategies. J Clin Oncol 2002;20:3683-90.

21. Henningsson A, Marsh S, Loos WJ, et al. Association of CYP2C8, CYP3A4, CYP3A5, and ABCB1 polymorphisms with the pharmacokinetics of paclitaxel. Clin Cancer Res 2005;11:8097-104.

Chapter 5

MEN 4901/T-0128: a new topoisomerase I inhibiter

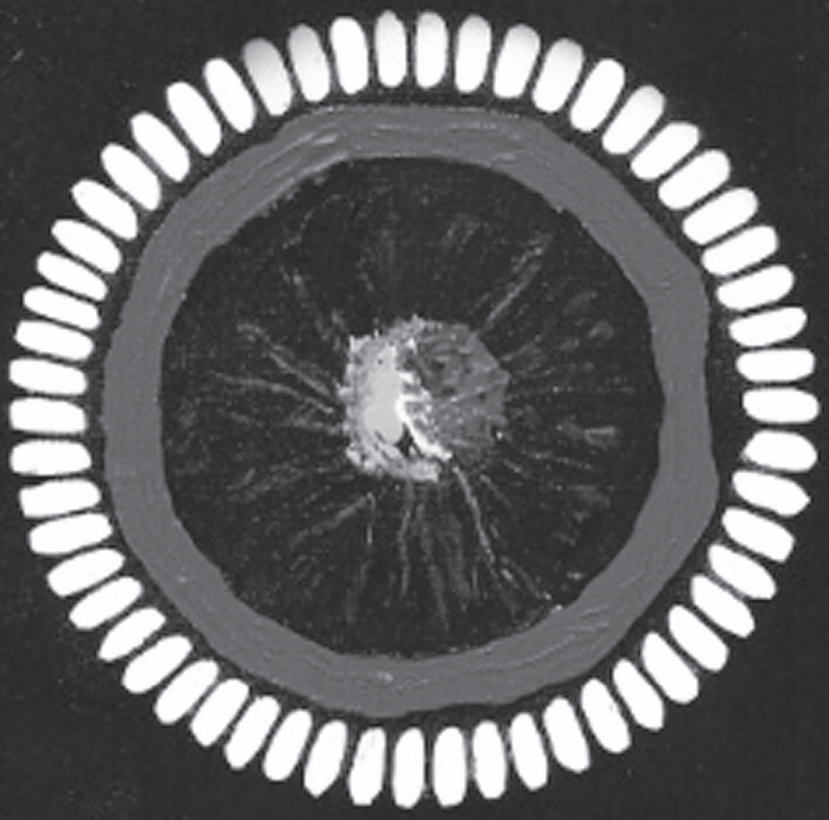

Chapter 5.1

Clinical and pharmacological study of the novel prodrug MEN 4901/T-0128 in patients with solid tumors

Submitted for publication

Stephan A. Veltkamp
Els O. Witteveen
Angela Capriati
Attillio Crea
Marja Voogel-Fuchs
Ingeborg J.G.M. van den Heuvel
Jos H. Beijnen
Emile E. Voest
Jan H.M. Schellens

Abstract

To evaluate the feasibility of intravenous (i.v.) administration of MEN 4901/T-0128, a carboxymethyldextran polymer prodrug of the active camptothecin derivative T-2513 and to assess the maximum tolerated dose (MTD), toxicity profile, clinical pharmacology, and antitumor activity of MEN 4901/T-0128 and metabolites.

Patients with solid tumors refractory to standard therapy received i.v. MEN 4901/T-0128 as a 3-hour infusion once every 6 weeks. The starting dose was 150 mg/m^2 following an accelerated dose escalation with at least 1 patient per dose-level. Pharmacokinetics (PK) of MEN 4901/T-0128, T-2513, and its metabolites SN-38, SN-38G, T-1335, T-0055, and T-3921 were assessed in plasma and urine and pharmacodynamics were determined by measuring the effect of the treatment on the decrease in white blood cells (WBC) and absolute neutrophil count (ANC).

Twenty-two patients received 35 courses. At a dose-level of 2400 mg/m^2, 2 out of 7 patients developed dose-limiting toxicities. One patient, receiving 5400 mg/m^2 MEN 4901/T-0128, experienced lethal multiorgan failure during the first cycle. At 1800 mg/m^2, only mild to moderate non-hematological toxicity occurred in 2 out of 7 patients and the mean AUC of SN-38 was 3261 h*nmol/mL. Overall, two partial responses were observed in patients with colorectal cancer (1800 mg/m^2) and head and neck cancer (2400 mg/m^2). MEN 4901/T-0128 had a long terminal half-life of 109 h, which resulted in a relatively high exposure to SN-38. The percentage decrease in WBC and ANC correlated significantly with the dose of MEN 4901/T-0128.

Based on the preliminary antitumor activity, the overall toxicity profile, and the PK, we recommend to evaluate MEN 4901/T-0128 administered as 3-hour infusion once every 6 weeks at a dose-level of 1800 mg/m^2 in a Phase II study.

Introduction

MEN 4901/T-0128 is a new polysaccharide prodrug comprising the active moiety 10-(3'-amino-propyloxy)-7-ethyl-(20S)-camptothecin (T-2513) bound to carboxymethyldextran (CM-dextran) via a triglycyl chain (Figure 1). This semi-synthetic prodrug with high solubility was designed to improve the pharmacological profile (higher efficacy/lower toxicity) in comparison to clinically available camptothecins (CPTs), such as irinotecan (CPT-11), which is currently used as first and second-line therapy in advanced colorectal cancer following 5-fluoruracil (5-FU) based therapy (1, 2).

T-2513 is a selective inhibitor of topoisomerase I, responsible for relaxation of torsionally strained supercoiled DNA (3-5). T-2513 binds covalently to and stabilizes the topoisomerase I-DNA complex, resulting into single strand DNA breaks, thereby inhibiting DNA replication and RNA synthesis, ultimately leading into cell death (5-7). The cytotoxic effects of T-2513 and metabolites are specific for the S-phase of the cell cycle (8), therefore prolonged exposure to MEN 4901/T-128 could increase antitumor activity as was shown previously for other topoisomerase I inhibitors (9, 10).

MEN 4901/T-0128 administered intravenously (i.v.) as a single dose and once-weekly for 4 weeks (q7dx4) demonstrated marked antitumor activity in human lung, oesophagal, gastric, colon and pancreatic tumor xenografts in nude mice (11, 12). A single i.v. administration of MEN-4901/T-0128 at a dose of 80 mg/kg (dose equivalent to T-2513) resulted in higher antitumor activity in human lung, colorectal, and oesophagal carcinomas in mice compared to i.v. CPT-11 given every fourth day for four times (q4dx4) at a total dose of 240 mg/kg (12). Reversible leukocytopenia and anemia, and decrease in body, thymus and testes weight, and lymphoid depletion were observed after single and repeated i.v. dosing of MEN 4901/T-0128. Dogs were more sensitive to toxicity than rodents. The dose of a single i.v. administration of MEN 4901/T-0128 severely toxic to 10% of the animals (STD_{10}) was 40 mg/kg (~ 800 mg/m^2) in dogs and 2000 mg/kg (~ 6200 mg/m^2) in mice following single i.v. administration (12). MEN 4901/T-0128 had a long terminal half-life ($t_{1/2}$) of 40-129 h. The AUC of T-2513 seemed to increase linearly with dose. Preclinical studies suggested that MEN-4901/T-0128 can permeate and accumulate in tumor tissue and is cleaved to T-2513 by cathepsin B,

which is overexpressed in tumors. These studies further showed that tumor-associated macrophages may play a key role in the uptake of MEN 4901/T-0128, and cleavage and local release of T-2513 (13, 14). T-2513 can be metabolized to the CPT analogues T-0055, T-1335, T-3921, and SN-38, which is glucuronidated to SN-38 glucuronide (SN-38G) (Figure 1).

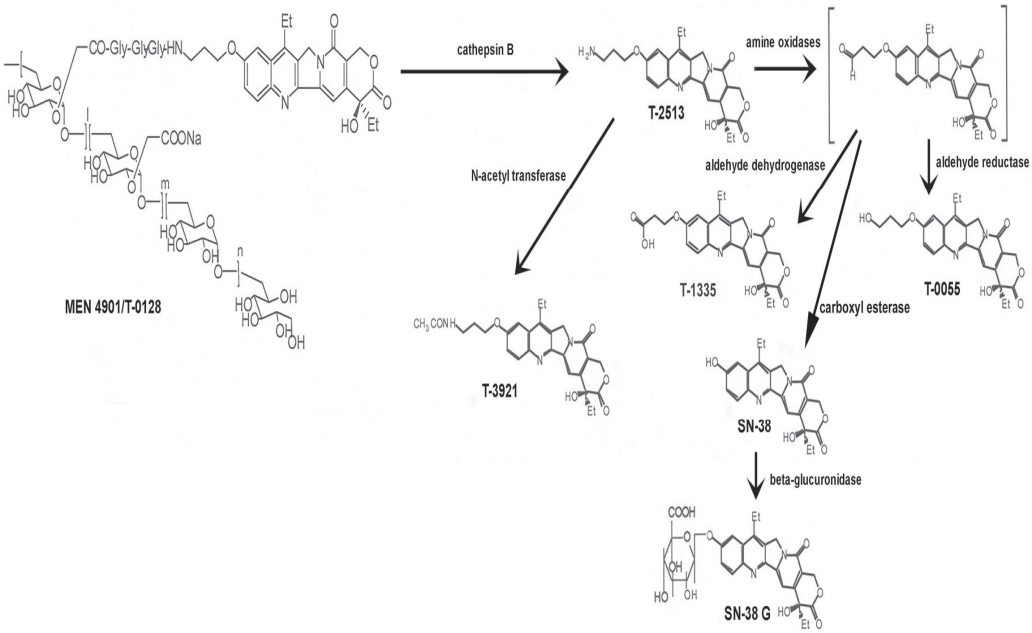

Figure 1. Proposed metabolic route and enzymatic activation of MEN 4901/T-0128

Based on the preclinical studies, which showed marked antitumor activity, moderate toxicity, and a long $t_{1/2}$ of MEN 4901/T0-128 following single i.v. dosing, a phase I study was initiated to investigate the feasibility of administering MEN 4901/T-0128 as 3-hour infusion once every 6 weeks in patients with solid tumors. A starting dose of 150 mg/m^2 MEN 4901/T-0128 was chosen based on the STD_{10} in dogs. The objectives of the study were to assess the maximum tolerated dose (MTD), to recommend a safe phase II dose, and to determine the dose-limiting toxicities (DLTs) of MEN 4901/T-0128 and its metabolites, pharmacodynamics (PD), and assessment of the antitumor activity of MEN 4901/T-0128.

Patients and methods

Patients

Patients with histologically or cytologically confirmed solid tumors refractory to standard therapy were eligible. Other criteria were: age ≥ 18 years, a World Health Organization (WHO) performance status (PS) ≤ 2 on the Eastern Cooperative Oncology Group (ECOG) scale, and an estimated life expectancy of ≥ 3 months. Previous chemotherapy and radiotherapy had to be discontinued for at least 4 weeks before study entry and 6 weeks in the case of mitomycin-C, nitrosourea, melphalan, and high dose carboplatin. Patients had to have adequate bone marrow function (white blood cells (WBC) ≥ 3.0 x 10^9/L, absolute neutrophil count (ANC) ≥ 1.5 x 10^9/L, and platelets ≥ 100 x10^9/L), kidney function (creatinine ≤ 1.5 the upper limit of normal (ULN)), and liver function (bilirubin < 1.5 mg/dL and/or alanine transaminase (ALT) and aspartate transaminase (AST) ≤ 1.5 times the ULN (or ≤ 2.5 times the ULN in the case of tumor involvement in the liver). The study protocol was approved by the Medical Ethics Committee of both participating hospitals and all patients signed informed consent.

Treatment plan, schedule of administration, and study design

The first patient was treated at a dose of 150 mg/m^2 MEN 4901/T-0128, which was administered as 3-hour infusion once every 6 weeks. Toxicities were graded according to the National Cancer Institute - Common Toxicity Criteria (NCI-CTC) version 3.0 (http://ctep.cancer.gov/forms/CTCAEv3.pdf). If none or minimal (≤ grade 1) toxicity was observed, dose escalation followed a modified Fibonacci scheme with 1 patient per dose-level and 100% dose increment. When ≥ grade 2 toxicity was observed, the dose was escalated by 67%, 50%, 40%, or 33% increments relative to the preceding dose-level, dependent on the toxicity profile, in a cohort of 3 patients per dose-level. If one patient experienced a DLT, the cohort was to be expanded to 6 patients. DLTs were defined as: grade 4 neutropenia lasting more than 5 days or complicated neutropenia (ANC < 0.5 x 10^9/L and T > 38.5 °C or clinical signs of infection), grade 4 thrombocytopenia and/or hemorrhagic complications or any bleeding episode requiring platelet transfusion, any ≥ grade 3 non-hematological toxicity (except nausea and vomiting

in case toxicity was grade 4 with maximum treatment), diarrhea ≥ grade 2 and lasting ≥ 3 days, and inability to receive the next cycle within two weeks after the scheduled date. The MTD was defined as one dose-level below the dose-level that induced DLTs in 2 out of 6 patients. Each patient had to be followed for at least six weeks before entering the next dose-level. Patients started a new cycle on day 43 in case of complete recovery from any toxicity of the previous cycle. In case of failure to recovery, treatment was to be delayed for a maximum of two weeks. Patients with a partial response (PR), complete response (CR), or stabilisation of disease (SD) who experienced any DLT were allowed to be retreated at a lower dose-level if this was in the best interest of the patient. In case there was no recovery after two weeks, the patient was taken off study.

Drug formulation

MEN 4901/T-0128 was supplied as a lyophilised powder in 24 mL glass vials by AG-Menarini Group (Galenic Department, Berlin-Chemie). Each vial contained 200 mg of active MEN 4901/T-0128 (comprising of 4.5-5.5% T-2513) and Na_2HPO_4 dihydrate and citric acid as inactive ingredients. Before use, it was constituted in 10 mL of 0.9% NaCl, and diluted with 0.9% NaCl to a final volume of at least 250 mL for infusion. The re-constituted solution was stable at room temperature for 6 h in glass or PVC bags.

Patient evaluation and follow-up

Pre-treatment evaluation was performed within 2 weeks before start of treatment and included a complete medical history and physical examination, vital signs, ECG, chest x-ray, tumor measurements, hematology (hemoglobin (Hb), WBC and differential count, platelets), serum chemistry (bilirubin, alkaline phosphatase (AP), AST, ALT, total protein, albumin, sodium, potassium, calcium, phosphate, y-glutamyltranspeptidase (y-GT), lactate dehydrogenase (LDH), glucose, creatinine, and β-human chorionic gonadotrophin (β-HCG) (in females with childbearing potential prior to the first dose and afterwards only on indication)), and urinalysis. Creatinine clearance had to be determined in case of creatinine > 1.5 x ULN. Before each cycle, the physical examination and vital signs were repeated, and hematology and serum chemistry were checked. During each cycle, hematology and serum chemistry were checked once weekly. Urinalysis was performed only

during the first week of each subsequent cycle or more often if clinically indicated. Patients were evaluated for efficacy after the 1st and 2nd cycle of therapy, and thereafter every two cycles. Tumor assessments were performed by palpable or visible examination at baseline and day 1 of every other cycle and were evaluated according to the RECIST criteria (15).

Pharmacokinetic studies

PK of MEN 4901/T-0128, T-2513 (total and free), SN-38, SN-38G, T-0055, T-3921, and T-1335 in plasma and urine were determined during the first cycle of therapy. Blood samples of approximately 3 mL of venous blood were drawn into sodium-heparinized tubes at the following prefixed time points: on day 1, prior to dosing, and at 0.5, and 1.5 h after start of infusion, at the end of infusion, and 4, 7, 8, 10, 24, 48, and 72 h after start of infusion, and on day 7, 10, 14, 21, 28, 35, and 42 after start of infusion. After collection of a blood sample, the tube was gently shaken, placed on ice, and immediately centrifuged at 1500 x *g* for 5 min at 4 °C. Then, plasma was transferred into a polypropylene tube and stored at -20 °C until analysis.

Urine was collected prior to start of infusion, and during 0-8 h, 8-24 h, and 24-48 h after start of infusion and was stored at 4 °C. For each collection interval the total volume of urine was determined and approximately 2 mL of each urine collection was transferred into a polypropylene tube and immediately stored at -20 °C until analysis. In addition, one urine sample was collected on day 4, 7, 10, 14, 21, 28, and 35 and handled as described above. Analysis of T-2513 and metabolites in plasma, urine, and tissue was performed using a sensitive validated high performance liquid chromatographic (HPLC) method with fluorescence detection. For analysis of total T-2513 in plasma and urine, 0.1 mL of sample was mixed with 0.2 mL of 6 M HCl and kept for 4 h at 100 °C to hydrolyse MEN 4901/T-0128. Then, 0.2 mL of 5.5 M NaOH was added, the mixture was vortexed, and 0.85 mL of formic ammonium buffer and 50 µL of internal standard (IS) (3 µg/mL) were added to 0.1 mL hydrolysate. After vortex mixing for 15 s, 0.1 mL of the content was taken and 0.3 mL formic ammonium buffer and 0.1 mL acetonitrile were added, vortex mixed for 10 s, the sample was centrifuged at 14,900 x *g* for 5 min at 4 °C and the supernatant was transferred into a sampler vial.

For analysis of free T-2513, T-1335, SN-38, SN-38G, T-3921, and T-0055 in plasma and urine, 50 µL of working solution (0.2 µg/mL) of the IS was added to 0.1 mL of sample. After gentle mixing, 0.3 mL acetonitril and 0.1 mL 0.1 M HCl were added. Each sample was vortex mixed for 10 s and centrifuged at 14,900 x *g* for 15 min at 4 °C. Then, 0.2 mL of the supernatant was transferred into a sampler vial containing 0.3 mL of 35 mM formic ammonium buffer pH 4.9.

For analysis of T-2513 and metabolites in tissues, each tissue was homogenized and an aliquot was extracted and analyzed following the plasma procedure applied as described above.

The injection volume was 50 µL. The HPLC system consisted of a model 125 solvent delivery pump (Beckman), automatic sample injector model 232 (Gilson), an Inertsil ODS-2 (5 µm) 250 x 4.6 mm column with a Lichrospher 100-RP-18 guard column (Ghrom), and a model RF-551 fluorescence detector (Shimadzu). The excitation and emission wavelength of the detector was 377 nm and 420 nm, respectively. Column temperature was kept at 40 °C, and the flow rate was 1 mL/min. The mobile phase consistent of gradient A (35 mM formic ammonium buffer pH 4.9) and gradient B (35 mM formic ammonium buffer pH 4.9/acetonitril (1:1, v/v) and the following gradient was used: t = 0-5 min: 70% A, t = 5-12 min: 70-40% A, 30-60% B, t = 15-22 min: 40% A, t = 22-29 min: 40-70% A, 60-30% B, and t = 29-33 min: 70% A. The injection volume and chromatographic conditions were the same as applied for analysis of total T-2513.

Pharmacokinetic analysis

The plasma pharmacokinetic parameters of MEN 4901/T-0128, T-2513, and metabolites were determined by non-compartmental analysis, using WinNonLin™ (version 5.0, Pharsight Corporation, Mountain View, CA, USA). The area under the plasma concentration time curve (AUC) was determined using the linear logarithmic trapezoidal method up to the last measured concentration-time point and extrapolated to infinity ($AUC_{0-\infty}$). Furthermore, terminal half-life ($t_{1/2}$), maximal drug concentration (C_{max}), time to maximum drug concentration (T_{max}), and apparent clearance (Cl) and volume of distribution (V_d) (for total T-2513 only) were generated from the data. The extent of metabolism of T-2513 to SN-38 was expressed by a metabolic ratio value, defined as the ratio of AUC of SN-38 + SN-38G over the AUC of total T-2513 (based on molar exposure values). The extent of

SN-38 glucuronidation was expressed by a glucuronidation ratio value, defined as the ratio of the AUC of SN-38G over the AUC of SN-38. The percentage of the administered dose of T-2513 recovered in the urine as unchanged drug (total and free T-2513), T-1335, SN-38, SN-38G, T-0055, and T-3921 during the first 48 h after start of infusion ($U_{excr,t=0-48h}$) was calculated as the amount excreted in the urine divided by the total administered dose times 100%. Data are reported as mean ± standard deviation (SD). Relationships between the dose of MEN 4901/T-0128 with the AUC of total T-2513, SN-38, and T-1335 were explored by scatter plots.

Pharmacokinetic-pharmacodynamic analysis

Relationships between the dose of MEN 4901/T-0128 and the AUC of T-2513, SN-38, and T-1335 with the percentage decrease in WBC count and ANC were explored with scatter plots. The percentage decrease in blood cells is defined as: [100 x (pre-treatment value - nadir)]/pre-treatment value. Furthermore, relationships between the AUC of T-2513, SN-38, and T-1335 with categorical toxicity data (intensity of diarrhea, nausea, vomiting, fatigue, and skin rash) were determined. Only data obtained in the first course were used.

Statistical analysis

Relationships between dose and AUC were assessed by Spearman correlation coefficients. Data on the relation between the dose of MEN 4901/T-0128 and percentage decrease in blood cells were fit to a sigmoidal maximum effect (E_{max}) model using WinNonLin™ according to the following formula: $E = E_{max} * [(DE)^{\gamma}/(DE_{50})^{\gamma}+(DE)^{\gamma}]$, where E represents the observed effect (i.e. % decrease), produced by drug exposure DE, E_{max} denotes the maximal elicitable effect, DE is a measure of drug exposure (i.e. the dose), DE_{50} represents the drug exposure associated with 50% of E_{max}, and γ is the Hill coefficient, which describes the sigmoidity of the curve.

Relationships between the AUCs and categorical toxicity data were explored by Spearman rank correlation tests. Statistical analysis was performed with the software package Statistical Product and Service Solutions (version 15.0 for Windows, SPSS Inc., Chicago, IL, USA). Differences were considered to be statistically significant at $p < 0.05$.

Results

Patient demographics

Twenty-two patients were enrolled onto the study and all patients were evaluable for toxicity. Patient characteristics are outlined in Table 1.

Table 1. Patient and disease characteristics.

Number of patients		22
Gender	Male	14
	Female	8
Age	Median	60
	Range	36-73
Race	Caucasian	22
Tumor types	Gall bladder	1
	Mesothelioma	3
	Colon	2
	Melanoma	1
	ACUP	2
	Colorectal	3
	Adenoid cystic carcinoma	1
	Cardia-oesophagal carcinoma	1
	Head & neck	2
	NSCLC	1
	Bronchial carcinoma	1
	Renal cell carcinoma	1
	Rectum	2
	Soft tissue sarcoma	1
Performance status	0	5
	1	11
	2	6
Number of cycles	Median	1
	Range	1-5
Prior therapy	Chemotherapy	21
	Surgery	19
	Radiotherapy	12
	Chemotherapy + radiotherapy	12
	Chemotherapy + radiotherapy + surgery	11
Number of involved organs	0	3
	1	3
	2	9
	≥3	7
Involved organs	Liver	10
	Lung	10
	Lymph nodes	11
	Other	16

Dose-levels and main drug related toxicities

At the lower dose-levels, patients tolerated therapy well and the dose was escalated by 100% with one patient per dose-level from 150 mg/m^2 to 1200 mg/m^2. The number of patients treated at each dose-level is depicted in Table 2. Overall, 35 cycles of therapy over seven dose-levels were administered. At the dose-level of 2400 mg/m^2, a male with an ACUP developed a grade 3 elevated AP on day 13 of the first cycle. No other drug-related toxicities were observed. The patient did not receive a second cycle and was taken off study because of progressive disease. The PK of T-2513 and metabolites was not aberrant from the expected pattern. A lower dose increment of 50% was applied resulting in a dose of 3600 mg/m^2 for the next cohort. A male patient with a colorectal carcinoma and lung and liver metastasis developed grade 3 pneumonitis and grade 4 dyspnea within 6 days after start of the first cycle, which was considered unrelated to the study drug, and which resolved within 10 days. Since no clinically relevant toxicity was seen at this dose-level, the dose was further escalated by 50% to 5400 mg/m^2. At this dose-level, a 47-year old female with a colon carcinoma and liver metastasis developed grade 3 skin rash on day 3 of the first cycle, followed by grade 3 fever, grade 3/4 hematological toxicity, grade 3 mucositis, and grade 4 oliguria, elevated AST/ALT, multiorgan failure and respiratory insufficiency (see DLTs and MTD). Plasmapheresis did not improve her clinical situation and she died 12 days after start of the treatment. Based on the severe toxicity and the PK data (see PK/PD of MEN 4901/T-0128, T-2513, and metabolites) in this patient, the dose was de-escalated to the previous level of 3600 mg/m^2 at which 2 more patients were treated. A female with colorectal carcinoma experienced a grade 3 rash on day 10 and stomatitis on day 22 (DLTs), and grade 4 neutropenia < 5 days on day 17. She developed PD after which she was taken off study. The other patient, a female with adenoid cystic carcinoma and lung metastasis, experienced grade 3 neutropenia and she was not given a second cycle, because of the toxicities observed in the other patients at this dose-level. Subsequently, the dose was de-escalated to 2400 mg/m^2. In total 7 patients were treated at this dose-level and DLTs (grade 3 skin rash and stomatitis) occurred in 2 patients. In two patients the second cycle was administered at a 25% reduced dose of 1800 mg/m^2. The dose was de-escalated to an intermediate dose-level of 1800 mg/m^2 at which in total 7 patients were treated.

Hematological and non-hematological toxicity

Hematological and non-hematological toxicities are outlined in Table 2. A total of 66 hematological drug related adverse events (AEs) were observed; 59% of these were ≤ grade 2, and 41% were grade 3/4. Leukocytopenia, neutropenia, thrombocytopenia, lymphocytopenia, and anemia contributed to 26%, 18%, 11%, 41%, and 4% of the grade 3/4 hematological AEs, respectively. In total 122 non-hematological AEs occurred, of which 82% were ≤ grade 2, and 18% were grade 3/4. The GI related toxicities (i.e. diarrhea, nausea, vomiting, anorexia, constipation, abdominal pain) contributed to 34%, 32%, and 14% of the grade 1, grade 2, and grade 3/4 non-hematological AEs, respectively. From the GI related toxicities (i.e. diarrhea, nausea, vomiting, anorexia, constipation, abdominal pain) 58.3% were grade 1, 33.3% were grade 2, and 8.3% were grade 3.

Table 2. Hematological and non-hematological toxicity per dose-level possibly, probably or definitively related to the study drug (as number of patients). Toxicities are presented as worst grade during all cycles.

Toxicity type	Dose (mg/m^2)	150	300	600	1200	1800	2400	3600	5400	Total
	No. of evaluable patients	1	1	1	1	7	7	3	1	22
Hematological	CTC grade									
Leukocytopenia	1	0	0	0	0	0	0	1	0	1
	2	0	0	0	0	1	1	1	0	3
	3	0	0	0	0	0	3	1	0	4
	4	0	0	0	0	0	1	1	1	3
Neutropenia	1	1	0	0	0	0	0	0	0	1
	2	0	0	0	0	0	2	0	1	3
	3	0	0	0	0	0	1	2	0	3
	4	0	0	0	0	0	1	1	0	2
Lymphocytopenia	1	1	1	0	0	1	0	0	0	3
	2	0	0	0	0	2	1	2	0	5
	3	0	0	1	0	3	5	1	0	10
	4	0	0	0	0	0	0	0	1	1
Anemia	1	1	1	1	1	3	1	1	0	9
	2	0	0	0	0	2	6	2	0	10
	3	0	0	0	0	0	0	0	1	1
	4	0	0	0	0	0	0	0	0	0
Thrombocytopenia	1	0	0	0	0	1	1	2	0	4
	2	0	0	0	0	0	0	0	0	0
	3	0	0	0	0	0	1	0	0	1
	4	0	0	0	0	0	1	0	1	2

Table 2. Continued.

Toxicity type	**Dose (mg/m^2)**	**150**	**300**	**600**	**1200**	**1800**	**2400**	**3600**	**5400**	**Total**
	No. of evaluable patients	1	1	1	1	7	7	3	1	22
Non-hematological	CTC grade									
Diarrhea	1	0	1	0	0	1	4	1	0	7
	2	0	0	0	0	1	1	1	0	3
	3	0	0	0	0	1*	0	0	0	1
Nausea	1	0	1	0	0	1	1	1	0	4
	2	0	0	0	0	2	0	1	0	3
	3	0	0	0	0	0	1	0	0	1
Vomiting	1	0	1	0	0	0	3	0	0	4
	2	0	0	0	0	1	0	1	0	2
	3	0	0	0	0	1	0	0	0	1
Anorexia	1	0	1	0	0	0	3	0	0	4
	2	0	0	0	0	1	1	0	0	1
Constipation	1	0	0	0	0	0	1	0	0	1
Abdominal pain	1	0	0	0	0	0	0	0	1	1
	2	0	0	0	0	0	2	0	0	2
Pyrosis	2	0	0	0	0	1	0	0	0	1
Muscle pain/cramp	1	0	1	0	1	0	1	0	0	3
Thorax pain	1	0	0	0	0	0	1	0	0	1
Peripheral neuropathy	1	0	0	0	0	0	1	0	0	1
Raynaud syndrome	1	0	0	1	0	0	0	0	0	1
Rash/skin reaction	1	0	0	0	0	2	2	0	0	4
	2	0	0	0	0	1	0	2	0	3
	3	0	0	0	0	0	1	1	1	3
Stomatitis	1	0	0	0	0	2	3	0	0	5
	3	0	0	0	0	0	0	1	0	1
Mucositis	1	0	0	0	0	0	0	1	0	1
	3	0	0	0	0	0	0	0	1	1
Fever	1	0	0	0	0	1	1	0	0	2
	2	0	0	0	0	1	0	1	0	2
	3	0	0	0	0	0	0	0	1	1
Infection	1	0	0	0	1	0	0	0	0	1
	2	0	0	0	0	0	0	1	0	1
	3	0	0	0	0	1	0	0	0	1
Malaise	2	0	0	0	0	0	1	0	0	1
Fatigue	1	0	0	1	1	1	0	0	0	3
	2	0	1	0	0	1	2	1	1	6
	3	0	0	0	0	3*	1	0	0	4
Alopecia	1	0	0	0	0	1	1	1	0	3
	2	0	0	0	0	1	0	2	0	3
Dyspnea	1	0	0	0	0	0	0	0	1	1
	2	0	0	0	0	0	1	0	0	1
Hypotension	3	0	0	0	0	0	0	0	1	1
Hypertension	1	0	0	0	0	0	1	0	0	1
	2	0	0	0	0	0	0	1	0	1
Tachycardia	1	0	0	0	0	0	1	0	1	2
Headache	1	0	1	0	0	0	0	1	1	3
Dizziness	2	0	0	0	0	0	2	0	0	2
Insomnia	1	0	0	0	0	1	0	0	0	1
Tremor	1	0	0	0	0	1	0	0	0	1
Flushing	1	0	0	0	0	0	1	1	0	2

Table 2. Continued.

Toxicity type	Dose (mg/m^2)	150	300	600	1200	1800	2400	3600	5400	Total
	No. of evaluable patients	1	1	1	1	7	7	3	1	22
Non-hematological	CTC grade									
Dehydration	1	0	0	0	0	0	1	0	0	1
	2	0	0	0	0	1	0	0	0	1
Oliguria	4	0	0	0	0	0	0	0	1	1
Proteinuria	1	0	0	0	1	0	1	0	0	2
AST/ALT rise	1	0	0	0	0	0	0	1	0	1
	2	0	0	0	0	1	0	0	0	1
	4	0	0	0	0	0	0	0	1	1
AP rise	3	0	0	0	0	0	2	0	0	2
γ-GT rise	3	0	0	0	0	0	1	0	0	1
Bilirubin rise	2	0	0	0	0	0	0	1	1	2
Creatinine rise	1	0	0	0	0	0	1	0	0	1
	2	0	0	0	0	0	0	0	1	1
Resp. insufficiency	4	0	0	0	0	0	0	0	1	1
Multiorgan failure	4	0	0	0	0	0	0	0	1	1

* These grade 3 toxicities were not significantly increased compared to their pre-treatment values and were therefore not considered DLTs.

Treatment related non-hematological and hematological toxicity of grade ≥ 3 occurred only at doses equal to or higher than 1800 mg/m^2. At this dose-level, the following grade 3 AEs were reported: diarrhea (n = 1), vomiting (n = 1), infection (n = 1), fatigue (n = 3), and lymphocytopenia (n = 3).

A total of 28 serious adverse events (SAEs) were experienced by 9 patients, of which 6 SAEs experienced by 4 patients were related to the study drug and included: grade 3 diarrhea (n = 1 at 1800 mg/m^2), grade 2 anorexia (n = 1 at 2400 mg/m^2), grade 3 stomatitis (n = 1 at 3600 mg/m^2), and grade 3 rash, grade 2 elevated serum creatinine, and grade 4 multiorgan failure (n = 1 at 5400 mg/m^2).

Eight patients received more than 1 cycle of therapy at the following dose-levels: 300 mg/m^2 (1 patient on 3 cycles), 600 mg/m^2 (1 patient on 3 cycles), 1800 mg/m^2 (1 patient on 5 cycles and 2 patients on 2 cycles each), 2400 mg/m^2 (2 patients on 2 cycles each), and 3600 mg/m^2 (1 patient on 2 cycles). Almost all hematological and non-hematological toxicities started during the first cycle and resolved or improved within 1-14 days. Toxicities did not significantly increase in number and/or severity after multiple cycles of therapy. Thus, no signs of cumulative toxicity were observed. These data should be interpreted with caution because of the low number of cycles that were administered and the low number of patients treated.

In total 13 DLTs were experienced by 4 patients: grade 4 thrombocytopenia (n = 1), grade 3 rash, grade 3 elevated γ-GT, and grade 3 elevated AP (n = 1) at 2400 mg/m^2; grade 3 rash and grade 3 stomatitis (n = 1) at 3600 mg/m^2; and grade 3 rash, grade 3 mucositis, grade 3 hypotension, grade 4 oliguria, grade 4 elevated AST/ALT, grade 4 multiorgan failure, and grade 4 respiratory insufficiency at 5400 mg/m^2 (n = 1). At a dose-level equal to or below 1800 mg/m^2, no DLTs were observed. Therefore, 1800 mg/m^2 resulted the MTD of MEN 4901/T-0128, worth to be further evaluated in a phase II study. This dose-level was evaluated in 7 patients. The safety assessment of the 1800 mg/m^2 dose-level was extended by two patients who initially received 2400 mg/m^2 at first cycle and after dose reduction 1800 mg/m^2.

Response

Two patients had a partial response: a patient with head and neck cancer treated at 2400 mg/m^2 and a patient with a colorectal carcinoma treated at 1800 mg/m^2. The duration of the partial response in the patient with head and neck cancer was 36 days. The patients had been heavily pretreated prior to inclusion in this study. Stable disease was observed in 9 patients with a median duration of 77 days (range: 34-202 days) at the following dose-levels: 300 mg/m^2 (n = 1), 600 mg/m^2 (n = 1), 1800 mg/m^2 (n = 3), 2400 mg/m^2 (n = 2), and 3600 mg/m^2 (n = 2). The patients with stable disease had the following tumor types: mesothelioma (n = 3), colorectal cancer (n = 2), adenoid cystic carcinoma (n = 1), bronchial carcinoma (n = 1), head and neck cancer (n = 1), and ACUP (n = 1). Eight patients had progressive disease and 3 patients were not evaluable for tumor response.

PK-PD of MEN 4901/T-0128, T-2513, and metabolites

Blood and urine sampling for pharmacokinetic analysis was performed in all patients. The plasma concentration versus time curves for total T-2513, free T-2513, SN-38, SN-38G, T-1335, T-3921, and T-0055 are depicted in Figure 2. The AUC values for total T-2513, SN-38, SN-38G and T-1335 are presented in Figure 3. The PK parameters in plasma and the urinary excretion values of all metabolites are presented in Table 3. MEN 4901/T-0128 (total T-2513) was slowly eliminated from plasma (Figure 2) with a median $t_{1/2}$ of 109 h (22 - 203 h).

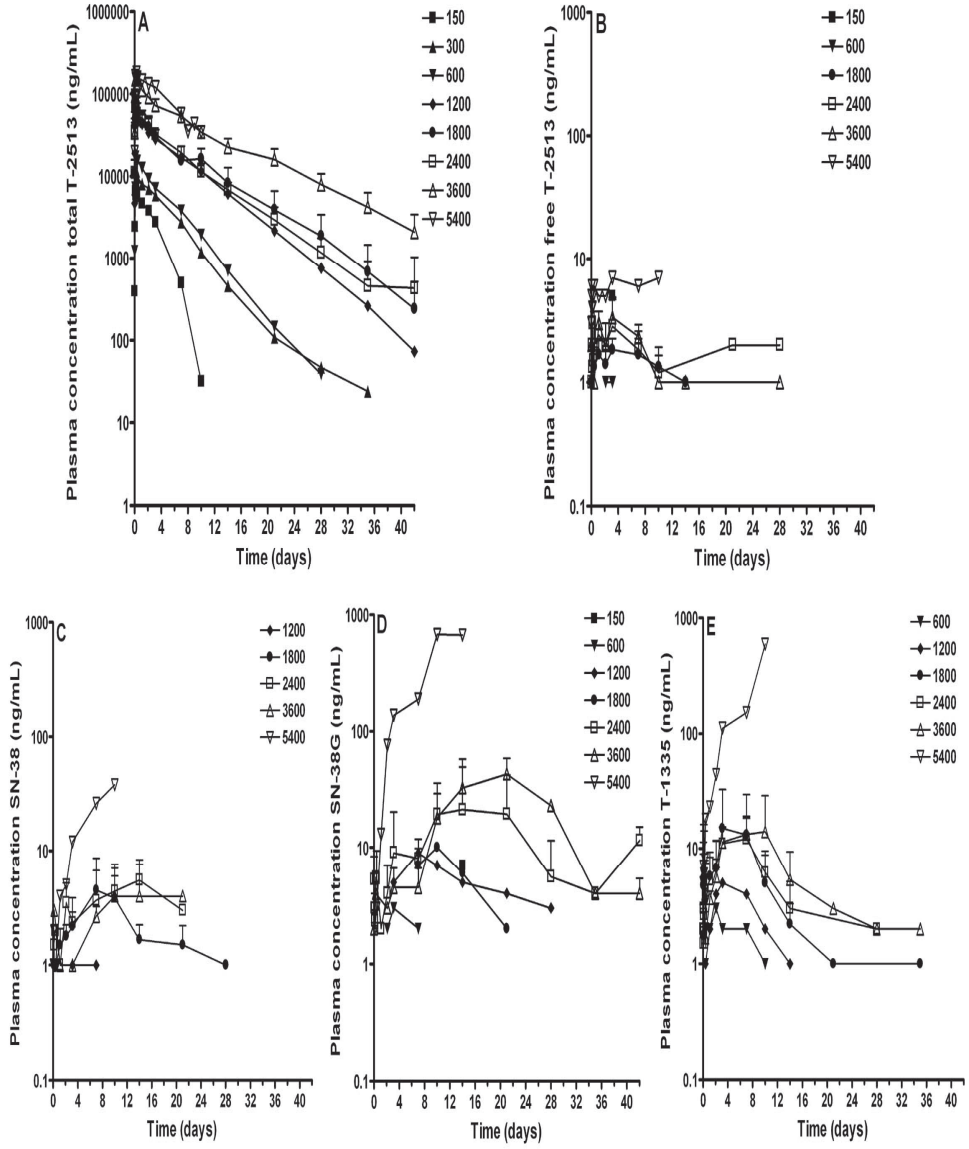

Figure 2. Plasma concentration versus time curves for total T-2513 (A), free T-2513 (B), SN-38 (C), SN-38G (D), and T-1335 (E).

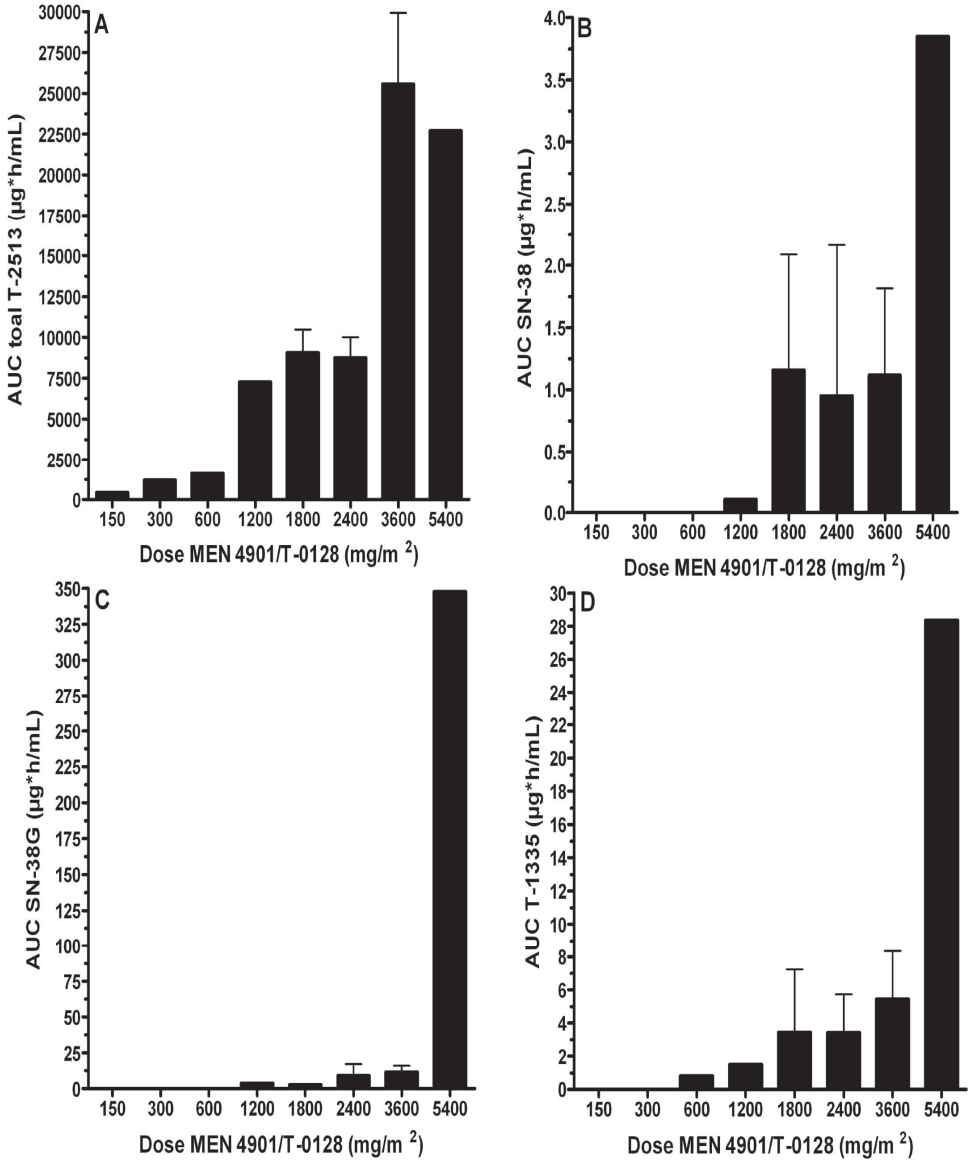

Figure 3. Area under the plasma concentration time curve (AUC) for total T-2513 (A), SN-38 (B), SN-38G (C), and T-1335 (D).

Table 3. Pharmacokinetic parameters of T-2513 (total and free) and metabolites at different dose-levels of i.v. MEN 4901/T-0128. Data are presented as mean ± SD (if n ≥ 3).

Dose-level (mg/m^2)	150	300	600	1200	1800	2400	3600	5400
Number of patients	1	1	1	1	7	7	3	1
Total T-2513								
C_{max} (µg/mL)	7	12	17	51	60 ± 13	82 ± 32	163 ± 31	183
AUC (h*µg/mL)	454	1188	1642	7283	9056 ± 1432	8754 ± 1255	25592 ± 4347	22673
$t_{1/2}$ (h)	22	154	75	109	119 ± 25	112 ± 31	165 ± 33	76
$U_{excr,\ t=0\text{-}48\ h}$ (%)	12	20	19	27	25 ± 5	25 ± 11	27 ± 5	52
Free T-2513								
C_{max} (µg/mL)	n.d.	n.d.	0.001	n.d.	0.002	0.004 ± 0.0002	0.003 ± 0.002	0.007
AUC (h*µg/mL)	n.d.	n.d.	0.11	n.d.	0.65 ± 0.44	1.7 ± 1.7	1.4 ± 0.6	1.3
$U_{excr,\ t=0\text{-}48\ h}$ (%)	0.07	0.12	0.08	0.11	0.14 ± 0.08	0.10 ± 0.02	0.09 ± 0.02	0.09
SN-38								
C_{max} (µg/mL)	n.d.	n.d.	0.001	n.d.	0.005 ± 0.004	0.005 ± 0.003	0.006 ± 0.003	0.04
AUC (h*µg/mL)	n.d.	n.d.	0.11	n.d.	1.2 ± 0.9	1.3 ± 1.3	1.3 ± 0.7	3.8
$U_{excr,\ t=0\text{-}48\ h}$ (%)	0.04	0.07	0.07	0.05	0.07 ± 0.06	0.07 ± 0.04	0.02 ± 0.006	0.08
SN-38G								
C_{max} (µg/mL)	n.d.	n.d.	0.003	0.009	0.01	0.03 ± 0.03	0.04 ± 0.02	0.78
AUC (h*µg/mL)	n.d.	n.d.	0.29	3.9	2.7	9.2 ± 8.0	11.7 ± 4.4	348
$U_{excr,\ t=0\text{-}48\ h}$ (%)	0.33	0.39	0.22	0.34	0.24 ± 0.17	0.51 ± 0.68	0.10 ± 0.05	0.53
T-1335								
C_{max} (µg/mL)	n.d.	n.d.	0.003	0.005	0.014 ± 0.016	0.015 ± 0.006	0.019 ± 0.01	0.6
AUC (h*µg/mL)	n.d.	n.d.	0.83	1.5	3.4 ± 3.8	4 ± 1.9	6.2 ± 3.1	28.3
$t_{1/2}$ (h)	n.d.	n.d.	162	139	143 ± 74	157 ± 90	236 ± 144	n.d.
$U_{excr,\ t=0\text{-}48\ h}$ (%)	0.76	0.49	0.49	0.49	0.49 ± 0.30	0.37 ± 0.28	0.19 ± 0.05	0.38
T-0055								
C_{max} (µg/mL)	n.d.	n.d.	n.d.	n.d.	n.d.	0.001	n.d.	0.006
AUC (h*µg/mL)	n.d.	n.d.	n.d.	n.d.	n.d.	0.05	n.d.	0.42
$U_{excr,\ t=0\text{-}48\ h}$ (%)	0.07	0.02	0.01	0.02	0.01 ± 0.01	0.09 ± 0.2	0.006 ± 0.001	0.007
T-3921								
C_{max} (µg/mL)	n.d.	n.d.	n.d.	n.d.	n.d.	0.003	0.002 ± 0.002	n.d.
AUC (h*µg/mL)	n.d.	n.d.	n.d.	n.d.	n.d.	1.5	15.8 ± 21.8	n.d.
$U_{excr,\ t=0\text{-}48\ h}$ (%)	n.d.	n.d.	n.d.	0.004	0.002 ± 0.003	0.009 ± 0.009	0.001	0.001
Metabolic ratio* (x 10^{-3})	n.d.	n.d.	n.d.	0.44	0.20 ± 0.22	1.1 ± 0.9	0.4 ± 0.20	12
Glucuronidation ratio**	n.d.	n.d.	n.d.	25	0.8	5.9 ± 4.2	6.9 ± 2.8	62

* The metabolic ratio is calculated by the ratio of SN-38 + SN-38G AUC over total T-2513 AUC; ** The glucuronidation ratio is calculated by the ratio of SN-38G AUC over SN-38 AUC; n.d.; not detectable.

The median apparent Cl and V_d were 21 (10 - 35) mL/h and 3.3 (0.8 - 5.8) L, respectively. The interpatient variability (coefficient of variation, %CV) of the AUC of total T-2513 was 16%, 14%, and 17% at the dose-levels of 1800, 2400, and 3600 mg/m^2, respectively. The plasma AUC of free T-2513 corresponds with 0.01% (0 - 0.05%) of the total amount of administered T-2513, indicating a very low exposure to free T-2513 in plasma. As depicted in Figure 2, the AUC of total

T-2513, SN-38, and T-1335 increased with the dose of MEN 4901/T-0128 ($r = 0.857$, $p<0.0001$ for T-2513; $r = 0.513$, $p = 0.018$ for SN-38; $r = 0.760$, $p<0.0001$ for T-1335). The AUC of SN-38 did not increase linearly with the AUC of MEN 4901/T-0128 ($r = 0.224$, $p = 0.389$).

MEN 4901/T-0128 was mainly excreted in the form of T-2513 conjugate in the urine (Table 3). In addition, free metabolites were present in urine with a peak concentration between 7 to 10 days. The ratio of the amount of free metabolite over the amount of administered T-2513 x 100% that was excreted in urine during the first 48 h after start of infusion for the main metabolites was 23% (12-52%) for total T-2513, 0.1% (0.03-0.3%) for free T-2513, 0.05% (0.02-0.2%) for SN-38, 0.21 (0.03-2.0%) for SN-38G, and 0.4% (0.1-1.1%) for T-1335.

The decrease in WBC and ANC significantly correlated with the dose (D) of MEN 4901/T-0128 and this relationship could best be fit to a sigmoidal E_{max} model (parameters: E_{max} = 100%; DE_{50} = 2525 mg/m^2; $\gamma = 1.8$ for WBC, and E_{max} = 100%; DE_{50} = 2129 mg/m^2; $\gamma = 2.0$ for ANC). No significant relationships were found between the AUC of parent drug and metabolites and the intensity of diarrhea, nausea, vomiting, fatigue and skin rash.

In the female patient treated at 5400 mg/m^2 who developed lethal hepatic and renal failure, the dose-corrected AUC of SN-38 + SN-38G, and of T-1335 were significantly (> 3 x standard deviation) higher than in the other patients (Figure 3). Urinary excretion of total T-2513 ($U_{excr,t=0-48h}$ = 52%) was two-fold higher compared to the other patients. Post mortem sampling revealed high levels of free T-2513, SN-38, and T-1335 in kidney (734, 942, and 3748 ng/g) and liver (583, 216, and 718 ng/g) compared to plasma (7, 38, and 595 ng/mL) (Figure 4B). The ratio of the AUC of free T-2513 over the AUC of total T-2513 times 100% was 2 to 15% in organs and 0.02% in plasma (Figure 4A), indicating predominantly cleavage of MEN 4901/T-0128 in tissues. The glucuronidation ratio (AUC SN-38G/AUC SN-38) was lower in liver (ratio = 0.3), kidney (ratio = 1.5) and intestine (ratio = 0.6) compared to plasma (ratio = 12).

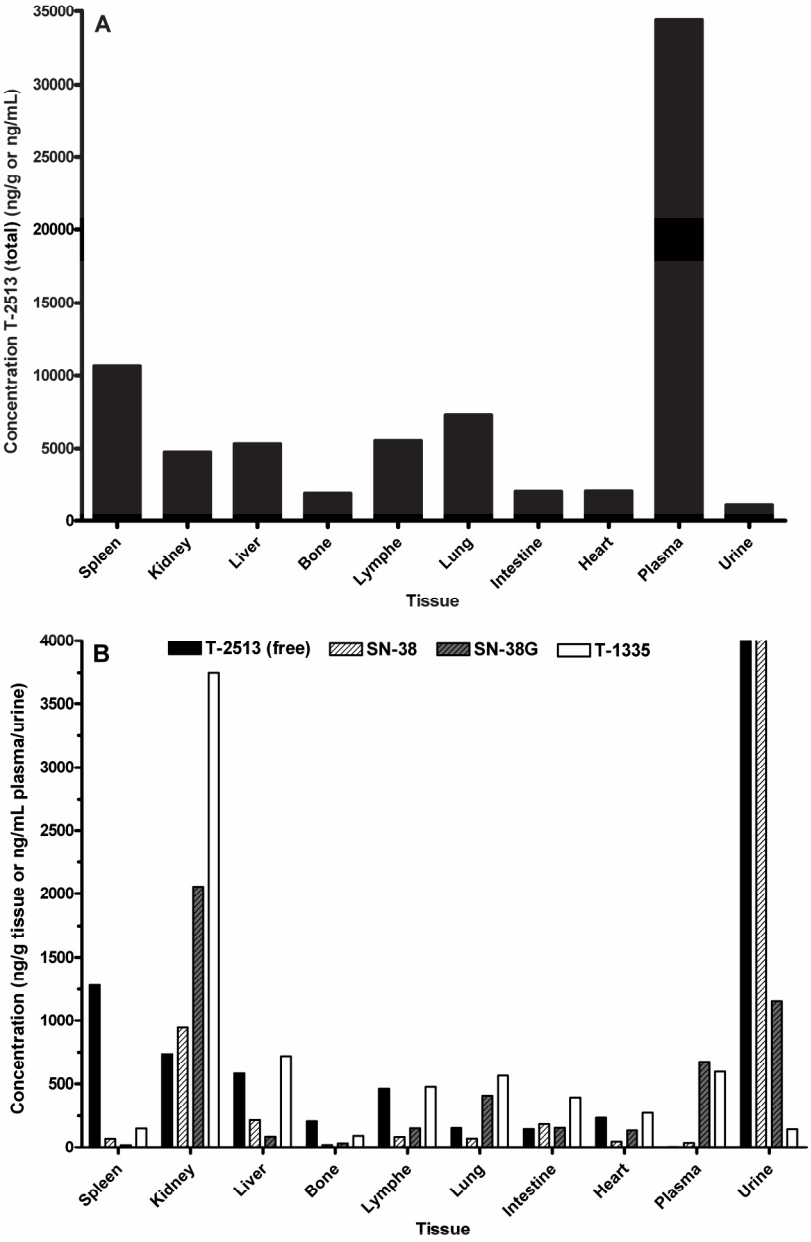

Figure 4. Concentrations of total T-2513 (A) and free T-2513, SN-38, SN-38G, and T-1335 (B) in organs, plasma, and urine collected from the single patient who developed multiorgan failure on day 10 after start of treatment with 5400 mg/m^2 MEN 4901/T-0128. Levels of free T-2513 and SN-38 in urine (B) were 10175 and 1154 ng/mL, respectively.

Discussion

This is the first study investigating the safety and pharmacology of the novel carboxymethyl-dextran conjugate prodrug MEN 4901/T-0128 as 3-hour infusion once every 6 weeks in patients with advanced solid tumors. During the past decades, synthetic drug-polymers have been developed to increase solubility and targeting of anticancer drugs (16, 17). Prodrugs of doxorubicin (PK-1), paclitaxel (PNU 166945), and camptothecin (MAG-camptothecin) have been used in the clinic (18-20). Furthermore, for S-phase cell cycle specific cytotoxic agents, prolonged low dose exposures have been suggested to be more effective than short lasting exposures at high concentrations (21). In addition, prolonged low dose infusion of CPT-11 demonstrated good tolerability, clinical activity, and resulted into enhanced conversion of CPT-11 to SN-38 (22, 23).

The toxicity of MEN 4901/T-0128 included hematological and non-hematological AEs, consisting mainly of grade 3/4 leukocytopenia, neutropenia, and lymphocytopenia, and grade 3 skin rash, fatigue, and diarrhea, nausea, and vomiting. Symptoms of the cholinergic syndrome (e.g. early onset diarrhea and flushing), which have been observed following CPT-11 therapy as a result of rapid reversible inhibition of acetylcholinesterase by CPT-11 (24), were not reported in this study, consistent with *in vitro* data demonstrating a 16-fold lower inhibitory activity of T-2513 than CPT-11 on acetylcholinesterase (12).

Clinical activity was observed in this group of heavily pre-treated patients. Two partial remissions were observed in a patient with colorectal cancer (1800 mg/m^2) and a patient with head and neck cancer (2400 mg/m^2).

The high plasma AUC of SN-38, SN-38G and T-1335 suggest relatively high metabolism of T-2513 in the single patient at the 5400 mg/m^2 dose-level compared to the other patients. The high exposure to SN-38 and T-1335 in liver and kidney compared to the other organs in this patient could be a result of high cleavage of MEN 4901/T-0128 to free T-2513 and high metabolic conversion to these metabolites. This might have contributed to the severe hepatic and renal toxicity in this single patient. Polymorphisms in uridine diphosphate glucuronosyltransferase 1A1 (UGT1A1) genes, encoding for proteins that are responsible for glucuronidation of SN-38 to SN-38G, have been associated with increased levels of SN-38 and conjugated bilirubin and with severe toxicity (neutropenia, diarrhea)

following CPT-11 treatment at high dose-levels and not at low dose-levels (25-27). However, the glucuronidation ratio was relatively high and only a moderate increase in unconjugated bilirubin was observed in this particular patient who experienced liver toxicity, suggesting no decrease in glucuronidation capacity. The observed rash in the patients was possibly related to SN-38 and/or T-1335, since MEN 4901/T-0128, T-2513, and CM-dextran did not cause allergic or immunogenic reactions in mice.

T-2513 had a low estimated clearance and volume of distribution of 21 mL/h and 3.3 L, respectively and a long $t_{1/2}$ of 109 h, suggesting that MEN 4901/T-0128 was present for prolonged periods of time mainly in the systemic circulation. This is consistent with the preclinical findings in mice (12). The PK in all patients showed a steep non-linear increase in the systemic exposure to total T-2513 with dose. Furthermore, SN-38, SN-38G, and T-1335 were the main metabolites formed. Preclinical studies determining the *in vitro* cytotoxicity (concentration inhibiting cell growth by 50% (GI_{50})) following 24 h drug incubation in a variety of human tumor cell lines, demonstrated that SN-38 had the highest cytotoxicity (GI_{50} ~ 1.5-15 ng/mL), followed by T-0055 (GI_{50} ~ 3.6-20 ng/mL), T-2513 (GI_{50} ~ 15-111 ng/mL), T-3921 (GI_{50} ~ 30-180 ng/mL) and T-1335 (GI_{50} ~ 73-1195 ng/mL) (28). SN-38 was detectable in plasma of patients who received doses of 1200 to 5400 mg/m^2 MEN 4901/T-0128. The mean AUC was 1331 h*µg/L corresponding to 3395 h*nmol/L, which was 2 to 7-fold higher than the values of 507-2080 h*nmol/L reported after CPT-11 7.5-40 mg/m^2/day (22, 29-31). This demonstrates efficient enzymatic conversion of T-2513 to SN-38. In this study only the total (lactone plus carboxylate) forms of T-2513, SN-38 were measured. Total drug concentrations correlated highly with lactone concentrations for CPT-11 and SN-38 in patients who received short drug infusions (32).

In conclusion, MEN 4901/T-0128 administered as 3-hour infusion at a dose of 1800 mg/m^2 is tolerated with only mild to moderate gastrointestinal toxicity and rash without relevant hematological toxicity. At this dose-level, clinical activity was observed. PK of MEN 4901/T-0128 demonstrated a long terminal half-life and a significant exposure to SN-38 at the 1800 mg/m^2 dose-level. Therefore, based on the safety profile, the preliminary antitumor activity, and the PK data, we recommend phase II testing of MEN 4901/T-0128 administered as 3-hour infusion once every 6 weeks at a dose-level of 1800 mg/m^2.

Acknowledgements

We thank Aurora Pacurar and Annelies Hiemstra for data management. We also thank the medical and nursing staff of the Netherlands Cancer Institute - Antoni van Leeuwenhoek Hospital and the University Medical Center Utrecht for the care and support of the patients in this study.

References

1 Douillard JY, Cunningham D, Roth AD, Navarro M, James RD, Karasek P, et al. Irinotecan combined with fluorouracil compared with fluorouracil alone as first-line treatment for metastatic colorectal cancer: a multicentre randomised trial. Lancet 2000;355:1041-1047.

2 Cunningham D, Pyrhonen S, James RD, Punt CJ, Hickish TF, Heikkila R, et al. Randomised trial of irinotecan plus supportive care versus supportive care alone after fluorouracil failure for patients with metastatic colorectal cancer. Lancet 1998;352:1413-1418.

3 Dallavalle S, Giannini G, Alloatti D, Casati A, Marastoni E, Musso L, et al. Synthesis and cytotoxic activity of polyamine analogues of camptothecin, J Med Chem 2006;49:5177-5186.

4 Pommier Y, Pourquier P, Fan Y, Strumberg D. Mechanism of action of eukaryotic DNA topoisomerase I and drugs targeted to the enzyme. Biochim Biophys Acta 1998;1400 :83-105.

5 Hsiang YH, Liu LF, Wall ME, Wani MC, Nicholas AW, Manikumar G, et al. DNA topoisomerase I-mediated DNA cleavage and cytotoxicity of camptothecin analogues. Cancer Res 1989;49:4385-4389.

6 Hsiang YH, Hertzberg R, Hecht S, Liu LF. Camptothecin induces protein-linked DNA breaks via mammalian DNA topoisomerase I. J Biol Chem 1985;260:14873-14878.

7 Hsiang YH, Lihou MG, Liu LF. Arrest of replication forks by drug-stabilized topoisomerase I-DNA cleavable complexes as a mechanism of cell killing by camptothecin. Cancer Res 1989;49:5077-5082.

8 Del Bino G, Lassota P, Darzynkiewicz Z. The S-phase cytotoxicity of camptothecin. Exp Cell Res 1991;193:27-35.

9 Houghton PJ, Cheshire PJ, Hallman JD, Lutz L, Friedman HS, Danks MK, et al. Efficacy of topoisomerase I inhibitors, topotecan and irinotecan, administered at low dose levels in protracted schedules to mice bearing xenografts of human tumors. Cancer Chemother Pharmacol 1995;36:393-403.

10 Furuta T, Yokokura T. [Effect of administration schedules on the antitumor activity of CPT-11, a camptothecin derivative]. Gan To Kagaku Ryoho 1990; 17:121-130.

11 Fujita F, Koike M, Fujita M, Sakamoto Y, Okuno S, Kawaguchi T, et al. MEN4901/T-0128, a new camptothecin derivative-carboxymethyldextran conjugate, has potent antitumor activities in a panel of human tumor xenografts in nude mice. Clin Cancer Res 2005;11:1650-1657.

12 Menarini Ricerche S.p.A. Investigator's Brochure MEN 4901/T-0128: Topoisomerase I inhibitor targeting solid tumors, 2003.

13 Harada M, Imai J, Okuno S, Suzuki T. Macrophage-mediated activation of camptothecin analogue T-2513-carboxymethyl dextran conjugate (T-0128): possible cellular mechanism for antitumor activity. J Control Release 2000;69:389-397.

14 Binaschi M, Parlani M, Bellarosa D, Bigioni M, Salvatore C, Palma C, et al. Human and murine macrophages mediate activation of MEN 4901/T-0128: a new promising camptothecin analogue-polysaccharide conjugate. Anticancer Drugs 2006;17:1119-1126.

15 Therasse P, Arbuck SG, Eisenhauer EA, Wanders J, Kaplan RS, Rubinstein L, et al. New guidelines to evaluate the response to treatment in solid tumors. European Organization for Research and Treatment of Cancer, National Cancer Institute of the United States, National Cancer Institute of Canada. J Natl Cancer Inst 2000;92:205-216.

16 Takakura Y, Hashida M. Macromolecular drug carrier systems in cancer chemotherapy: macromolecular prodrugs. Crit Rev Oncol Hematol 1995;18:207-231.

17 Onishi H, Machida Y. Macromolecular and nanotechnological modification of camptothecin and its analogs to improve the efficacy. Curr Drug Discov Technol 2005;2:169-183.

18 Vasey PA, Kaye SB, Morrison R, Twelves C, Wilson P, Duncan R, et al. Phase I clinical and pharmacokinetic study of PK1 [N-(2-hydroxypropyl)methacrylamide copolymer doxorubicin]: first member of a new class of chemotherapeutic agents-drug-polymer conjugates. Cancer Research Campaign Phase I/II Committee. Clin Cancer Res 1999;5:83-94.

19 Meerum Terwogt JM, ten Bokkel Huinink WW, Schellens JHM, Schot M, Mandjes IA, Zurlo MG, et al. Phase I clinical and pharmacokinetic study of PNU166945, a novel water-soluble polymer-conjugated prodrug of paclitaxel. Anticancer Drugs 2001;12:315-323.

20 Schoemaker NE, van Kesteren C, Rosing H, Jansen S, Swart M, Lieverst J, et al. A phase I and pharmacokinetic study of MAG-CPT, a water-soluble polymer conjugate of camptothecin. Br J Cancer 2002;87:608-614.

21 Gerrits CJ, de Jonge MJ, Schellens JHM, Stoter G, Verweij J. Topoisomerase I inhibitors: the relevance of prolonged exposure for present clinical development. Br J Cancer 1997;76:952-962.

22 Takimoto CH, Morrison G, Harold N, Quinn M, Monahan BP, Band RA, et al. Phase I and pharmacologic study of irinotecan administered as a 96-hour infusion weekly to adult cancer patients. J Clin Oncol 2000;18:659-667.

23 Herben VM, Schellens JHM, Swart M, Gruia G, Vernillet L, Beijnen JH, et al. Phase I and pharmacokinetic study of irinotecan administered as a low-dose, continuous intravenous infusion over 14 days in patients with malignant solid tumors. J Clin Oncol 1999;17:1897-1905.

24 Sheiner LB, Benet LZ. Premarketing observational studies of population pharmacokinetics of new drugs. Clin Pharmacol Ther 1985;38:481-487.

25 Hoskins JM, Goldberg RM, Qu P, Ibrahim JG, McLeod HL. UGT1A1*28 genotype and irinotecan-induced neutropenia: dose matters. J Natl Cancer Inst 2007;99:1290-1295.

26 Stewart CF, Panetta JC, O'Shaughnessy MA, Throm SL, Fraga CH, Owens T, et al. UGT1A1 promoter genotype correlates with SN-38 pharmacokinetics, but not severe toxicity in patients receiving low-dose irinotecan. J Clin Oncol 2007;25:2594-2600.

27 Ramchandani RP, Wang Y, Booth BP, Ibrahim A, Johnson JR, Rahman A, et al. The role of SN-38 exposure, UGT1A1*28 polymorphism, and baseline bilirubin level in predicting severe irinotecan toxicity. J Clin Pharmacol 2007;47:78-86.

28 Okuno S, Harada M, Yano T, Yano S, Kiuchi S, Tsuda N, et al. Complete regression of xenografted human carcinomas by camptothecin analogue-carboxymethyl dextran conjugate (T-0128). Cancer Res 2000;60:2988-2995.

29 Rothenberg ML, Kuhn JG, Burris HA, III, Nelson J, Eckardt JR, et al. Phase I and pharmacokinetic trial of weekly CPT-11. J Clin Oncol 1993;11:2194-2204.

30 Canal P, Gay C, Dezeuze A, Douillard JY, Bugat R, Brunet R, et al. Pharmacokinetics and pharmacodynamics of irinotecan during a phase II clinical trial in colorectal cancer. Pharmacology and Molecular Mechanisms Group of the European Organization for Research and Treatment of Cancer. J Clin Oncol 1996;14:2688-2695.

31 Schoemaker NE, Kuppens IE, Moiseyenko V, Glimelius B, Kjaer M, et al. A randomised phase II multicentre trial of irinotecan (CPT-11) using four different schedules in patients with metastatic colorectal cancer. Br J Cancer 2004;91:1434-1441.

32 Sasaki Y, Yoshida Y, Sudoh K, Hakusui H, Fujii H, Ohtsu T, et al. Pharmacological correlation between total drug concentration and lactones of CPT-11 and SN-38 in patients treated with CPT-11. Jpn J Cancer Res 1995;86:111-116.

Conclusions and Perspectives

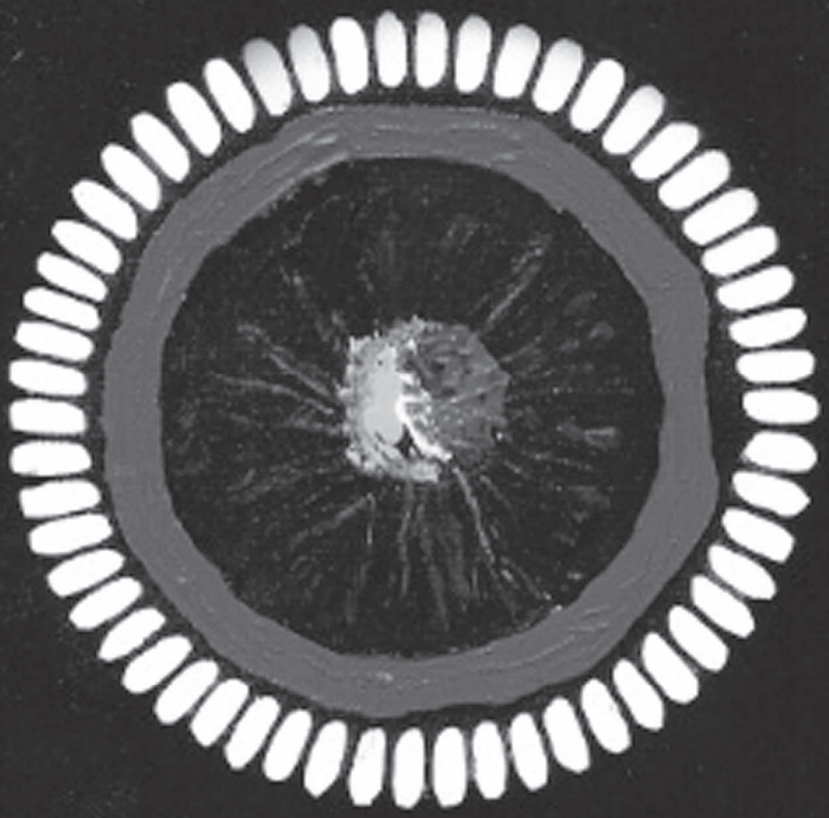

Conclusions and Perspectives

This thesis demonstrates the opportunities and main limitations of oral application of gemcitabine (2',2'-difluorodeoxycytidine, dFdC), new paclitaxel formulations and the i.v. administered novel polymer prodrug MEN 4901/T-0128 in patients with advanced solid tumors. By determining the pharmacokinetics (PK), pharmacodynamics (PD), toxicity profile, and preliminary antitumor activity it was investigated whether these drug formulations might be used to optimize therapy in patients with advanced cancer. Prolongation of the exposure time of a tumor to adequate concentrations of an anticancer drug may result in increased antitumor activity. This was investigated by continuous oral administration in the case of dFdC and BMS-275183 and by targeting the drug to the tumor site in the case of MEN 4901/T-0128.

Prolonged fixed dose rate (FDR) infusion of dFdC in patients was associated with an increased exposure to dFdCTP in leukemic cells and also in peripheral blood mononuclear cells (PBMCs). Future well designed randomized clinical studies in patients with various solid tumors should evaluate the potential benefits of FDR dosing compared to standard i.v. dosing of dFdC. The potential clinical activity and moderate toxicity of oral dFdC warrant further investigation of the concept of prolonged exposure to dFdC. The exposure to dFdC was low due to extensive deamination to dFdU, which had a long terminal half-life ($t_{1/2}$). We hypothesized that dFdU accumulated in the first-pass metabolizing organs, which was possibly associated with the hepatic toxicity observed in one patient. Our *in vitro* experiments revealed that dFdU was a good substrate for the concentrative nucleoside transporter type 1 (hCNT1), which is highly expressed in liver and kidney. This might contribute to (re)uptake of dFdU and to the long $t_{1/2}$ of dFdU. It was shown that dFdU is phosphorylated to its triphosphate metabolite (dFdUTP) and incorporated into DNA and RNA, which positively correlated with the cytotoxicity of dFdU. The compounds dFdUTP and dFdCTP showed comparable DNA incorporation in HepG2 cells at equitoxic concentrations of dFdC and dFdU, which suggests comparable intrinsic toxicity of these molecules. The novel developed sensitive LC-MS/MS method enabled us to quantify intracellular levels of dFdCTP in human PBMCs and revealed a relatively high exposure to dFdUTP

compared to dFdCTP in PBMCs of patients treated with low dose dFdC. The *in vivo* study in wild-type mice confirmed accumulation of dFdU and the phosphorylated metabolites dFdCTP and dFdUTP in liver and kidney following multiple dosing of dFdC. These phosphorylated metabolites were also found in plasma and urine, suggesting elimination of these toxic compounds from cells. The translational research on oral dFdC showed a higher extent of deamination and phosphorylation of dFdC in patients compared to mice. New metabolites of dFdC were discovered during this research; one of them, dFdUTP, likely contributes to the overall activity/toxicity of dFdC. The differences in PK of dFdC between tissues and between mice and humans could be explained by the extent of expression and localization of human equilibrative and concentrative nucleoside transporters and enzymes involved in dFdC metabolism. It is recommended to continue research on possible (bio)markers for antitumor activity of dFdC in patients. This could be performed by determination of 1) the exposure to dFdCTP in tumor tissue, 2) the incorporation of dFdCTP and dFdUTP into DNA, 3) the extent of inhibition of DNA synthesis, 4) the effects on intracellular natural (deoxy)nucleotide pools, and 5) the expression and single nucleotide polymorphisms of genes involved in dFdC activity. These studies should preferably be performed in solid tumors and PBMCs. The importance of dFdUTP relative to dFdCTP in the overall activity of dFdC as well as the main *in vivo* pathway(s) contributing to the synthesis of dFdUTP should be explored in more detail. A main topic for future investigation is the development of novel oral and i.v. formulations and derivatives of dFdC that protect the drug from extensive first-pass metabolism and that target the drug specifically to the tumor site.

Many attempts have been undertaken to administer paclitaxel orally to patients. However, so far no clinically applicable oral paclitaxel formulation has been discovered. Oral administration of paclitaxel is hampered by its low bioavailability, due to elimination by P-glycoprotein (P-gp) and hepatic metabolism by cytochrome P450 enzymes. In addition, it has been reported that cremophor® EL (CrEL), which is used as solubilizer for paclitaxel in the i.v. paclitaxel (Taxol®) formulation, limits absorption of paclitaxel from the intestinal lumen. This thesis described a number of clinical studies on novel oral formulations of paclitaxel without the cosolvent CrEL co-administered with

cyclosporin A (CsA). A capsule formulation containing the polymer polyvinyl acetate phthalate seemed to slowly release paclitaxel and its systemic exposure was slightly increased by CsA. Co-administration of CsA with oral paclitaxel formulated in a self-microemulsifying oily formulation (SMEOF) demonstrated systemic exposure to paclitaxel comparable to orally administered Taxol®.

We observed that BMS-275183, an orally administered C-4 methyl carbonate analogue of paclitaxel, resulted in considerable antitumor activity in patients with non-small cell lung cancer (NSCLC). These studies demonstrate the feasibility of oral delivery of paclitaxel in formulations without the cosolvent CrEL in combination with a P-gp inhibitor. Future studies should assess the PK, tolerability and safety of these paclitaxel formulations at higher doses or after bi-daily administration. Although a sceptic could define the development of these alternative formulations as old wine in a new bottle, slow progress has been made over the last years in the development of alternative paclitaxel formulations. It remains a challenge to successfully deliver paclitaxel orally and to increase the bioavailability of this drug. The paclitaxel analogue BMS-275183 showed a lower affinity for P-gp than paclitaxel and demonstrated clinical activity. An ongoing phase II study will address its antitumor activity in a selective population of patients with NSCLC.

The design of taxanes with low affinity for P-gp seems to be promising to improve oral bioavailability and penetration in (P-gp overexpressing) tumors. It is important that the antitumor activity of new taxanes is determined in preclinical models in multi-drug resistant solid tumors and in wild-type and P-gp knockout mice. Furthermore, sustained release formulations of paclitaxel may result in prolonged exposure to the drug. Besides a promising antitumor activity, new taxanes might cause less toxicity than the currently used taxane formulations.

The clinical study with the prodrug MEN 4901/T-0128, consisting of the new camptothecin analogue T-2513 bound to a carboxymethyldextran polymer, showed promising clinical activity. However, also significant hematological toxicity at high dose-levels was observed. PK analysis indicated a long circulation time of MEN 4901/T-0128 in the systemic circulation. The dose-level of 1800 mg/m^2 was tolerated and caused relatively high systemic exposure to SN-38. The safety and

antitumor activity of MEN 4901/T-0128 administered as 3-hour infusion once every 6 weeks should be further explored in a phase II study.

In summary, continuous exposure to novel oral and i.v. administered anticancer drugs is a promising strategy to improve the antitumor activity of these compounds. The low bioavailability of gemcitabine and paclitaxel are a major limitation for successful oral delivery of these drugs. Elucidation of the main pathways responsible for drug metabolism and the pharmacological actions of the metabolites are essential for optimal application of the drugs.

Summary
Samenvatting

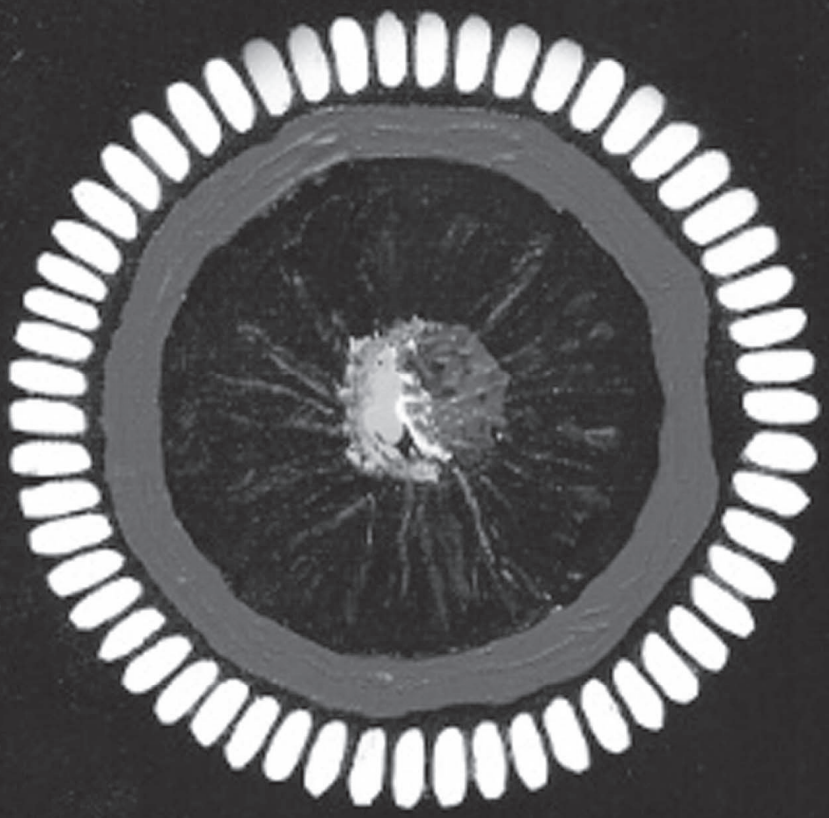

Summary

Chemotherapy is frequently used in the treatment of patients with advanced cancer. During the past years, significant progress has been made in cancer treatment and a range of new molecular targeted anticancer drugs have been developed. The intravenously (i.v.) administered conventional agents gemcitabine and paclitaxel are important in the treatment of patients with solid tumors, including non-small cell lung cancer (NSCLC) and ovarian cancer. However, there is a growing need for new treatment strategies to optimize the clinical use of these anticancer drugs.
One approach to increase antitumor activity is to prolong the exposure time of a tumor to sufficient concentrations of an anticancer drug. This strategy has been shown effective for the cell-cycle specific drugs gemcitabine, paclitaxel, and irinotecan. An increase in the exposure of the tumor to the drug can be achieved by continuous drug administration and by targeting the drug to the tumor site. Oral drug administration facilitates the use of continuous dosing regimens and is generally more convenient for patients than i.v. administration.
Novel preclinical discoveries are important for the development and application of new drugs and/or drug formulations in patients. Also, the clinical ("bed side") results often raise questions that are the basis for new preclinical ("bench side") research. This two-way traffic between preclinical and clinical research is called translational research.

In **Chapter 1**, a general introduction and description of the outline of this thesis is presented. In this thesis, the application of novel oral formulations of gemcitabine, paclitaxel, and an i.v. administered prodrug of a novel camptothecin analogue is investigated for the first time in patients with advanced cancer. More specifically, the aim of this thesis is to assess the pharmacokinetics (PK), pharmacodynamics (PD), toxicity profile, and preliminary antitumor activity of these novel formulations.

Gemcitabine (2',2'-difluorodeoxycytidine, dFdC) is used in the treatment of various solid tumors, including NSCLC, bladder, breast, pancreatic, and ovarian cancer. dFdC is currently marketed as i.v. formulation (Gemzar®) and usually administered as 30-min infusion at a dose of 1000-1250 mg/m^2 once weekly on day

1 and 8 of a 3-weekly cycle or on day 1, 8, and 15 of a 4-weekly cycle. dFdC is transported into the cell by human nucleoside transporters (hNTs). It is intracellularly phosphorylated by deoxycytidine kinase (dCK) to its monophosphate and subsequently to its active diphosphate and triphosphate metabolites. Gemcitabine triphosphate (dFdCTP) has been considered to be the main active metabolite that is incorporated into DNA and inhibits DNA synthesis. Furthermore, dFdC is highly deaminated by cytidine deaminase (CDA) to 2',2'-difluorodeoxyuridine (dFdU), which was considered an inactive metabolite.

Chapter 2 is a review of the literature about the use of prolonged fixed dose rate (FDR) infusion compared to standard 30-min infusion of dFdC. The rationale for FDR dosing is that it might increase the intracellular accumulation of dFdCTP leading to increased antitumor activity. The FDR dosing regimen has shown an increase in exposure to dFdCTP in leukemic cells and also in peripheral blood mononuclear cells (PBMCs), which are commonly used as a surrogate for tumor tissue. So far, only one clinical study demonstrated benefit of FDR dosing of dFdC in patients with pancreatic cancer. Future well designed randomized clinical trials in large patient populations and various tumor types should elucidate whether FDR administration is a better treatment option than standard i.v. dosing of dFdC.

Chapter 3 presents the preclinical and clinical studies on the cytotoxicity, metabolism, tissue distribution, and PK of oral and i.v. administered dFdC. The findings from a phase I (first in man) clinical study with oral dFdC were the basis for further *in vitro* and *in vivo* research in human cancer cell lines and mice. **Chapter 3.1** presents the results of an *in vitro* study, which demonstrates that the cytotoxicity of dFdU significantly increases with an increase in its exposure time. In human hepatocellular carcinoma HepG2 cells, the IC_{50} of dFdU is 2.5 μM following 14 days incubation, which is in the range of plasma concentrations in patients treated with oral dFdC. We show that dFdU is a good substrate for the human concentrative nucleoside transporter type 1 (hCNT1) that is highly expressed in liver and kidney. This might cause (re)uptake of dFdU and explain in part the long $t_{1/2}$ of dFdU. Furthermore, we demonstrate that dFdU is intracellularly phosphorylated to its triphosphate metabolite (dFdUTP) and incorporated into DNA and RNA, which obviously results in an increased cytotoxicity of dFdU. The

metabolites dFdUTP and dFdCTP have comparable DNA incorporation in HepG2 cells at equitoxic incubating concentrations of dFdC and dFdU, suggesting similar intrinsic toxicity of these molecules. **Chapter 3.2** presents the results of an *in vivo* study on oral and i.v. gemcitabine in wild-type mice. It is found that dFdU and the phosphorylated metabolites dFdCTP and dFdUTP accumulate in liver and kidney following multiple oral and i.v. administration of dFdC. Moreover, phosphorylated metabolites of dFdC and dFdU are also present in plasma and urine, suggesting elimination of these toxic compounds from cells. The extent of deamination and phosphorylation of dFdC seem to be significantly lower in mice than in patients, which shows important differences in PK of dFdC between mice and man. In **Chapter 3.3**, we describe the results of a clinical study with oral dFdC administered at low doses. The exposure to dFdC in plasma and to dFdCTP in PBMCs are low and do not significantly increase with dose. In addition, no significant effects of the treatment are observed on T-cell proliferation, which is used as a surrogate pharmacodynamic endpoint. dFdC is extensively deaminated to dFdU, which has a long terminal half-life ($t_{1/2}$ ~ 90 h) and is supposed to accumulate in the first-pass metabolizing organs. We assume that the lethal hepatic toxicity in one patient is associated with accumulation of the drug in the liver. Potential clinical activity and moderate toxicity of oral dFdC warrant further investigation of the concept of prolonged exposure to dFdC. In **Chapter 3.4**, the development and validation of a sensitive LC-MS/MS method for the quantification of dFdCTP in human PBMCs is presented. This assay is important to determine the intracellular levels of the active dFdCTP metabolite and was used to support the clinical study in patients treated with low doses of oral dFdC. **Chapter 3.5** describes two out of nine patients with leiomyosarcoma that develop severe pulmonary toxicity after treatment with gemcitabine and docetaxel. Based on these findings as well as the existing literature on lung toxicity due to gemcitabine and docetaxel, clinicians should take into account the risk of this combination.

Chapter 4 describes clinical research on novel oral paclitaxel formulations without cremophor® EL (CrEL) and the application of CsA to increase the systemic exposure to paclitaxel from these formulations. Paclitaxel is used for the treatment of a number of solid tumors, including NSCLC, ovarian cancer, and breast cancer. It is usually administered i.v. as 3-hour infusion at a dose of 175 mg/m^2 once every

3 weeks. In the i.v. paclitaxel (Taxol®) formulation, both CrEL and dehydrated ethanol are used to solubilise paclitaxel. CrEL has been reported to cause hypersensitivity reactions and non-linear PK of i.v. paclitaxel as a result of entrapment of paclitaxel in micelles in plasma. In addition, CrEL has been reported to limit absorption of paclitaxel from the intestinal lumen. These drawbacks have led to the development of alternative i.v. and oral formulations without CrEL. Oral paclitaxel administration is hampered because of its low bioavailability, due to elimination by P-glycoprotein (P-gp) and metabolism by cytochrome P450 (CYP450) enzymes. Combination of oral paclitaxel with cyclosporine A (CsA), which inhibits P-gp and CYP450 mediated elimination of paclitaxel, was shown to increase the systemic exposure to oral paclitaxel. **Chapter 4.1** describes the application of paclitaxel in a capsule formulation containing the polymer polyvinyl acetate phthalate. Paclitaxel seems to be released slowly from the formulation and its systemic exposure is slightly increased by CsA. In **Chapter 4.2**, it is found that co-administration of CsA with paclitaxel, formulated in an oral self-microemulsifying oily formulation (SMEOF), results in increased systemic exposure to paclitaxel. In **Chapter 4.3**, we demonstrate that a relatively high systemic exposure to paclitaxel could also be obtained by administration of the CrEL-free drinking solution and capsule formulations of paclitaxel after co-administration with CsA. In **Chapter 4.4**, we describe that BMS-275183, an orally administered C-4 methyl carbonate analogue of paclitaxel, results in antitumor activity in patients with NSCLC following twice weekly dosing.

Chapter 5 describes a clinical study with the topoisomerase I inhibiting prodrug MEN 4901/T-0128. This prodrug consists of the new camptothecin analogue T-2513 bound to a carboxymethyldextran polymer. Intravenous administration of MEN 4901/T-0128 as 3-hour infusion once every 6 weeks shows clinical activity in heavily pre-treated patients with solid tumors. Partial remissions are observed in patients with colorectal cancer (1800 mg/m^2) and head and neck cancer (2400 mg/m^2). At the dose-level of 1800 mg/m^2 only mild to moderate gastrointestinal toxicity and skin rash are observed without relevant hematological toxicity. MEN 4901/T-0128 has a long $t_{1/2}$ of 109 h and a significant exposure to SN-38 is obtained. It is recommended to further investigate the activity and safety of MEN

4901/T-0128 as 3-hour infusion once every 6 weeks at a dose-level of 1800 mg/m^2 in a phase II study.

Final remarks

In order to improve the treatment of patients with cancer, it is essential to continue research on the development of new (oral) drug formulations, dosing regimens, and tumor targeted formulations. Continuous exposure to novel anticancer drugs can result in clinical activity as is shown in this thesis for BMS-275183 and MEN 4901/T-0128. Extensive first-pass metabolism and elimination of gemcitabine and paclitaxel are important limitations for oral administration of these drugs. The studies described in this thesis emphasize the importance of elucidating the pharmacology of drugs, the pathways contributing to the metabolism of the drug, and the pharmacological action of the metabolites. Incorporation of pharmacodynamic markers in clinical studies to measure the effects of drugs may help to optimize the treatment in patients with cancer.

Samenvatting

Chemotherapie wordt regelmatig toegepast in de behandeling van patiënten met kanker. Gedurende de afgelopen jaren is er grote vooruitgang geboekt in de bestrijding van tumoren en een groot aantal nieuwe antitumor middelen zijn ontwikkeld. De toepassing van de intraveneus (i.v.) toegediende conventionele antikanker middelen gemcitabine en paclitaxel is effectief gebleken in de behandeling van patiënten met solide tumoren, waaronder niet-kleincellig longkanker en eierstokkanker. Desondanks is er een groeiende behoefte aan nieuwe behandelingsmethoden en alternatieve doseerschema's om de werking van de middelen verder te optimaliseren.

Eén benadering om de antitumor activiteit te verhogen is door de blootstellingstijd van de tumor aan adequate concentraties van het middel te verlengen. Deze aanpak is effectief gebleken voor chemotherapeutica die specifiek aangrijpen op de celcyclus waaronder gemcitabine, paclitaxel en irinotecan. De tijd dat een tumor wordt blootgesteld aan een antikanker middel kan worden verlengd door het middel continu toe te dienen en door er voor te zorgen dat het middel zo goed mogelijk het tumorgebied bereikt en zo min mogelijk het gezonde weefsel. Het continu toedienen van een middel kan worden gerealiseerd door het middel oraal (via de mond) toe te dienen wat tevens patiëntvriendelijker is dan i.v. (via de ader) toediening.

Nieuwe ontdekkingen in het laboratorium zijn belangrijk voor de ontwikkeling en toepassing van nieuwe antikanker middelen en/of nieuwe toedieningsvormen in patiënten. Echter, klinische resultaten in patiënten ('bedzijde') leiden vaak tot vraagstellingen die een basis vormen voor nieuw preklinisch ('labtafel') onderzoek. Dit tweerichtingsverkeer tussen preklinisch en klinisch onderzoek wordt ook wel translationeel onderzoek genoemd.

Hoofdstuk 1 is een algemene inleiding en beschrijft de opzet van dit proefschrift. In dit proefschrift wordt voor de eerste keer het onderzoek beschreven naar de toepassing van nieuwe orale formuleringen van gemcitabine, paclitaxel en een i.v. toegediend nieuwe camptothecine analoog in patiënten met een vergevorderd stadium van kanker. Het doel van dit onderzoek was het bepalen van de

farmacokinetiek, farmacodynamiek, het toxiciteitsprofiel en de antitumor activiteit van deze nieuwe formuleringen.

Gemcitabine (2',2'-difluorodeoxycytidine, dFdC) wordt toegepast bij de behandeling van verschillende soorten kanker waaronder niet-kleincellig longkanker, blaas, borst, pancreas en eierstokkanker. dFdC is op dit moment alleen geregistreerd als i.v. formulering (Gemzar®) en wordt over het algemeen toegediend als infuus met een inlooptijd van 30 minuten in een dosering van 1000-1250 mg/m^2 één keer per week op dag 1 en 8 van een 3-wekelijkse kuur of op dag 1, 8, en 15 van een 4-wekelijkse kuur. dFdC wordt opgenomen in de cel doormiddel van 'humane nucleoside transport eiwitten' (hNTs). Het wordt in de cel gefosforyleerd via een enzymatische reactie door het enzym deoxycytidine kinase (dCK) naar de monofosfaat vorm en vervolgens naar de actieve, difosfaat en trifosfaat metabolieten. Gemcitabine trifosfaat (dFdCTP), dat wordt beschouwd als de meest werkzame metaboliet, wordt in het DNA ingebouwd en remt de synthese van het DNA. Verder wordt dFdC in hoge mate gedeamineerd door cytidine deaminase (CDA) naar 2',2'-difluorodeoxyuridine (dFdU) dat tot op heden werd beschouwd als een niet relevante, onwerkzame metaboliet.

Hoofdstuk 2 is een overzichtsartikel van de literatuur omtrent het toedienen van dFdC als langzaam infuus met gefixeerde doseersnelheid (FDR) in vergelijking tot het gebruikelijke toedieningschema van dFdC waarbij het in 30 minuten als infuus wordt toegediend. De rationale voor het FDR doseerschema is dat dit tot een verhoging van de intracellulaire ophoping van dFdCTP kan leiden dat mogelijk resulteert in een sterker antitumor effect. Het FDR doseerschema heeft geleid tot een hogere blootstelling van leukemische cellen en witte bloedcellen (PBMCs) aan dFdCTP. Dit laatstgenoemde celtype wordt regelmatig gebruikt als vervangend patiëntmateriaal voor tumorweefsel. Tot dusver heeft slechts één klinische studie een voordeel aangetoond van het FDR doseerschema van dFdC in patiënten met pancreaskanker. Toekomstige klinische studies in grote patiëntenpopulaties en in patiënten met verschillende typen tumoren zullen moeten uitwijzen of FDR toediening een betere behandelingsoptie is dan de huidige standaardtoediening van dFdC.

In **hoofdstuk 3** worden preklinische en klinische studies beschreven naar de cytotoxiciteit, het metabolisme, de weefseldistributie en PK van oraal en i.v. toegediend dFdC. De gegevens van een fase 1 klinische studie met oraal toegediend dFdC vormden de basis voor verder *in vitro* en *in vivo* onderzoek in menselijke tumor cellijnen en muizen. **Hoodstuk 3.1** beschrijft de resultaten van het *in vitro* onderzoek, waaruit blijkt dat de cytotoxiciteit van dFdU significant toeneemt met de blootstellingstijd aan het middel. dFdU heeft een IC_{50} van 2.5 µM na een incubatieperiode met dFdC van 14 dagen in humane leverkanker (HepG2) cellen wat in dezelfde orde van grootte ligt als de dFdU plasma concentraties in patiënten die worden behandeld met oraal dFdC. Tevens is gevonden dat dFdU een goed substraat is voor de "human concentrative nucleoside transporter type 1" (hCNT1) die sterk tot expressie komt in de lever en de nieren. Dit kan (her)opname van dFdU veroorzaken en een verklaring zijn voor de lange halfwaardetijd van dFdU. Verder is aangetoond dat dFdU intracellulair wordt gefosforyleerd naar de trifosfaat vorm (dFdUTP) en wordt ingebouwd in het DNA en RNA wat correleert met de cytotoxiciteit van dFdU. De metabolieten dFdUTP en dFdCTP worden in gelijke mate ingebouwd in het DNA van HepG2 cellen na incubatie met vergelijkbare toxische concentraties van dFdC en dFdU. Dit suggereert dat deze moleculen een vergelijkbare intrinsieke toxiciteit hebben. In **hoofdstuk 3.2** worden de resultaten gepresenteerd van een *in vivo* studie in wildtype muizen. Er is aangetoond dat na herhaalde orale en i.v. toediening van dFdC zowel dFdU als de gefosforyleerde metabolieten dFdCTP en dFUTP ophopen in de lever en de nieren. De gefosforyleerde metabolieten werden ook gedetecteerd in plasma en urine wat er op wijst dat deze verbindingen kunnen worden geëlimineerd uit cellen. De mate van deaminering en fosforylering van dFdC blijkt in muizen significant lager te zijn dan in patiënten wat duidt op belangrijke verschillen in de farmacokinetiek van dFdC tussen muizen en mensen. In **hoofdstuk 3.3** beschrijven wij de resultaten van een klinische studie waarin dFdC in een lage dosering oraal is toegediend. De blootstelling aan dFdC in plasma en aan dFdCTP in PBMCs is laag en neemt niet significant toe bij hogere dosering. Daarnaast zijn geen significante effecten van de behandeling waargenomen op de delingscapaciteit van T-cellen. dFdC werd in hoge mate gedeamineerd naar dFdU welke een lange halfwaardetijd ($t_{1/2}$) had van circa 90 uur. Wij veronderstelden dat dFdU accumuleerde in de lever en dat dit een mogelijke verklaring zou kunnen zijn voor de ernstige levertoxiciteit die werd

waargenomen in één patiënt. Vanwege de potentiële klinische antitumor activiteit en de matige toxiciteit van oraal toegediend dFdC is het aanbevolen om onderzoek naar het concept van verlengde blootstelling aan dFdC te continueren. In **hoofdstuk 3.4** wordt de ontwikkeling en validatie van een gevoelige LC-MS/MS methode gepresenteerd. Deze methode is belangrijk voor het kwantificeren van dFdCTP in menselijke PBMCs en is gebruikt om de klinische studie te ondersteunen in patiënten die werden behandeld met een lage dosering van oraal toegediend dFdC. **Hoofdstuk 3.5** beschrijft twee patiënten met een leiomyosarcoom die na behandeling met gemcitabine en docetaxel ernstige longtoxiciteit ontwikkelen. Vanwege deze bevindingen alsmede de bestaande literatuur over longtoxiciteit als gevolg van gemcitabine en docetaxel is het aanbevolen dat artsen rekening houden met de risico's van deze combinatiebehandeling.

Hoofdstuk 4 beschrijft het onderzoek naar nieuwe oraal toegediende formuleringen van paclitaxel en een paclitaxel derivaat zonder cremophor® EL (CrEL) en de toepassing van CsA om de systemische blootstelling aan paclitaxel te verhogen. Paclitaxel wordt toegepast bij de behandeling van een aantal solide tumoren zoals niet-kleincellig longkanker, eierstok- en borstkanker. Over het algemeen word het i.v. toegediend als 3-uurs infuus in een dosering van 175 mg/m^2 éénmaal elke 3 weken. In de i.v. paclitaxel (Taxol®) formulering worden CrEL en ethanol gebruikt om paclitaxel in oplossing te houden. Van CrEL is beschreven dat het overgevoeligheidsreacties kan veroorzaken en ook niet-lineaire farmacokinetiek van i.v. toegediend paclitaxel kan veroorzaken als gevolg van het insluiten van paclitaxel in micellen in het plasma. Ook is van CrEL beschreven dat het de absorptie remt van paclitaxel vanuit de darm. Deze nadelen hebben geleid tot de ontwikkeling van alternatieve i.v. en orale formuleringen zonder CrEL. Orale toediening van paclitaxel wordt bemoeilijkt vanwege de lage biologische beschikbaarheid ten gevolge van eliminatie van paclitaxel door het P-glycoprotein (P-gp) eiwit en door metabolisering van het middel door cytochroom P450 (CYP450) enzymen. Het toedienen van oraal paclitaxel in combinatie met cyclosporine A (CsA), een remmer van P-gp en CYP3A4, leidde tot een toename in de systemische blootstelling aan paclitaxel. In **hoofdstuk 4.1** worden de resultaten gepresenteerd van onderzoek naar de toediening van paclitaxel in

capsules bestaande uit het polymeer polyvinyl acetaat ftalaat. Paclitaxel lijkt langzaam vrij te komen uit deze formulering en de systemische blootstelling werd verhoogd door CsA. In **hoofdstuk 4.2** is aangetoond dat oraal toegediend CsA in combinatie met oraal toegediend paclitaxel resulteert in een relatief hoge systemische blootstelling aan paclitaxel vanuit een "self micro-emulsifying oily formulation" (SMEOF). **Hoofdstuk 4.3** toont aan dat ook na het oraal toedienen van alternatieve CrEL vrije formuleringen (een drinkoplossing en twee type capsules) in combinatie met CsA een relatief hoge systemische blootstelling aan paclitaxel wordt verkregen. In **hoofdstuk 4.4** tonen we aan dat het middel BMS-275183, een oraal toegediend C-4 methyl carbonaat analoog van paclitaxel, in een tweewekelijks toedieningschema resulteert in antitumor activiteit in patiënten met niet-kleincellig longkanker.

In **hoofdstuk 5** beschrijven wij een klinische studie met de nieuwe topoisomerase-1 remmer MEN 4901/T-0128. Dit middel bestaat uit het nieuwe camptothecine analoog T-2513 die gebonden is aan een carboxymethyldextraan polymeer. Intraveneuze toediening van MEN4901/T-0128 als 3-uurs infuus éénmaal per 6 weken resulteerde in klinische activiteit in zwaar voorbehandelde patiënten met solide tumoren. In patiënten met colorectaal kanker (1800 mg/m^2) en hoofd en hals kanker (2400 mg/m^2) werd een partiële remissie waargenomen. De dosering van 1800 mg/m^2 leidde tot lichte maagdarm toxiciteit en huiduitslag zonder relevante hematologische toxiciteit. MEN 4901/T-0128 had een lange $t_{1/2}$ van 109 uur en een significante blootstelling aan SN-38 werd vastgesteld. Op basis van deze resultaten wordt aanbevolen om in een fase 2 studie de antitumor activiteit en veiligheid van MEN4901/T-0128 verder te onderzoeken middels toediening als 3-uurs infuus één maal per 6 weken in een dosering van 1800 mg/m^2.

Slot opmerkingen

Om de behandeling van patiënten met kanker verder te optimaliseren is het essentieel om het onderzoek naar de ontwikkeling van nieuwe (oraal toegediende) formuleringen, doseerschema's, en tumorgerichte antikanker middelen te continueren. Zoals in dit proefschrift is beschreven voor BMS-275183 en MEN4901/T-0128 kan continue blootstelling aan nieuwe antikanker middelen resulteren in klinische activiteit. De belangrijkste beperkingen van orale

toediening van gemcitabine en paclitaxel zijn de hoge mate van metabole afbraak en eliminatie van deze stoffen in de darm en lever.

Het onderzoek beschreven in dit proefschrift onderstreept het belang van het ophelderen van de farmacologie van antikanker middelen en van de routes die verantwoordelijk zijn voor het metabolisme van de stoffen en de farmacologische mechanismen van de metabolieten. Het toepassen van farmacodynamische "biomarkers" in klinische studies kan helpen om de effecten van antitumor middelen te meten en om de behandeling van patiënten met kanker te optimaliseren.

List of Abbreviations

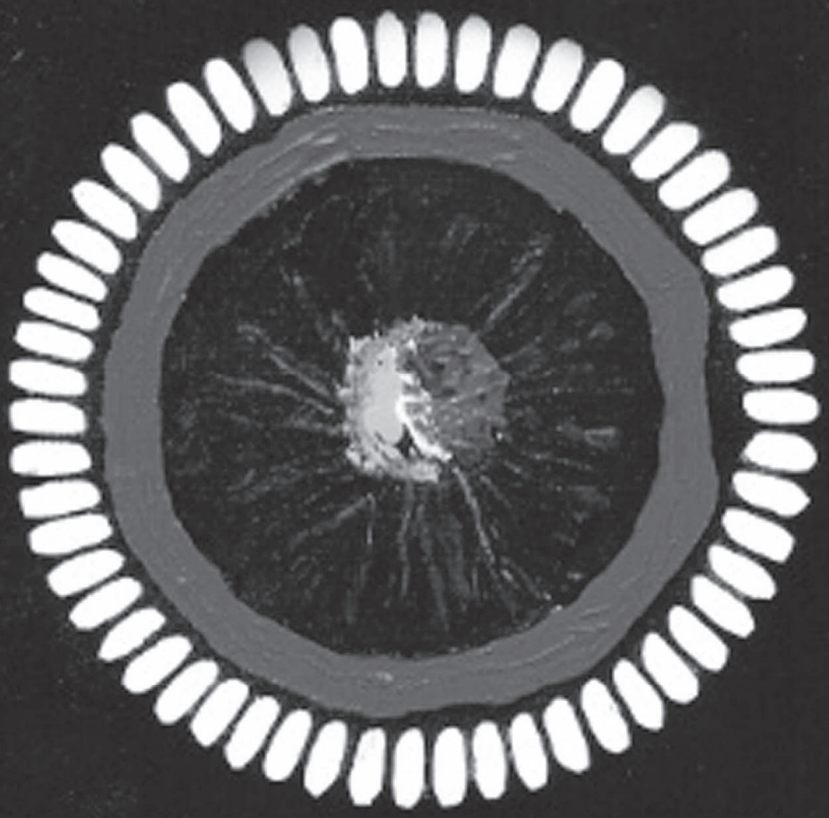

List of Abbreviations

AE	adverse event
AUC	area under the plasma concentration-time curve
CDA	cytidine deaminase
CDP	cytidine diphosphate
Cl	clearance
C_{max}	maximum drug concentration
CR	complete response
CrEL	cremophor EL
CTC	common toxicity criteria
CTP	cytidine triphosphate
CYP	cytochrome P450
dCMPD	deoxycytidine monophosphate deaminase
dFdC	2',2'-difluorodeoxycytidine (gemcitabine)
dFdCMP	gemcitabine monophosphate
dFdCDP	gemcitabine diphosphate
dFdCTP	gemcitabine triphosphate
dFdU	2',2'-difluorodeoxyuridine
dFdUMP	2',2'-difluorodeoxyuridine monophosphate
dFdUDP	2',2'-difluorodeoxyuridine diphosphate
dFdUTP	2',2'-difluorodeoxyuridine triphosphate
dATP	deoxyadenosine triphosphate
dCDP	deoxycytidine diphosphate
dCK	deoxycytidine kinase
dCTP	deoxycytidine triphosphate
DLT	dose limiting toxicity
DNA	desoxyribonucleic acid
hCNT	human concentrative nucleoside transporter
hENT	human equilibrative nucleoside transporter
HPLC	high performance liquid chromatography
IC_{50}	half-maximal inhibitory concentration
i.v.	intravenous
K_m	Michaelis-Menten constant

LC-MS/MS	liquid chromatography with tandem mass spectrometry detection
MDCK	Madin-Darby canine kidney cell line
MTD	maximum tolerated dose
NSCLC	non-small cell lung cancer
OS	overall survival
PD	pharmacodynamics / progressive disease
P-gp	P-glycoprotein
PK	pharmacokinetics
PR	partial response
PS	performance status
RNA	ribonucleic acid
RR	ribonucleotide reductase
SD	stable disease / standard deviation
SR	survival rate
THU	tetrahydrouridine
T_{max}	time to maximum drug concentration
TTP	time to progression
TTF	time to treatment failure
$t_{1/2}$	terminal half-life
V_d	volume of distribution
WHO	world health organization

Dankwoord / Acknowledgements

Curriculum Vitae

List of Publications

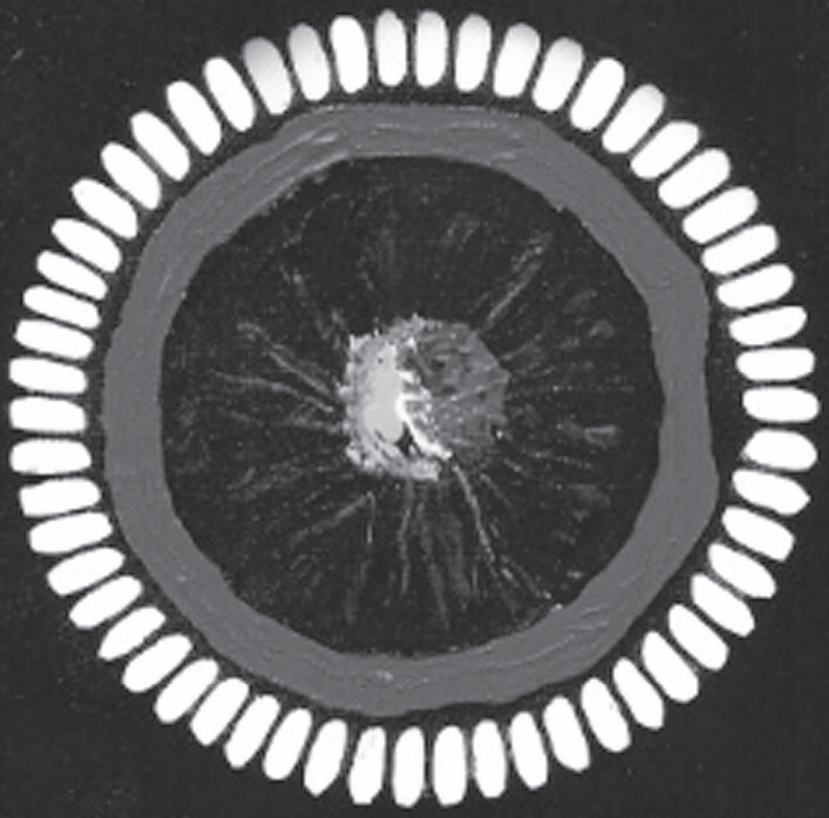

Dankwoord / Acknowledgements

De afgelopen jaren heb ik met veel plezier aan dit promotieonderzoek gewerkt. Er zijn heel wat mensen die hebben bijgedragen aan het tot stand komen van dit proefschrift. Een aantal personen wil ik in het bijzonder bedanken.

Allereerst wil ik de patiënten bedanken die hebben meegewerkt aan de klinische studies. Ik heb veel bewondering voor het optimisme, vertrouwen en de kracht waarmee zij in het leven staan en deelnemen aan het onderzoek. Het contact met de patiënten was plezierig en leerzaam in verschillende opzichten. Zo heb ik o.a. mijn repertoire aan recepten weten uit te breiden met Rendang.

Mijn promotoren, Jan Schellens en Jos Beijnen wil ik bedanken voor de begeleiding van mijn onderzoek. Beste Jan, heel erg bedankt voor de kans die je mij hebt gegeven om zowel klinisch als fundamenteel onderzoek te doen en de vrijheid die je mij gaf in het coördineren en uitvoeren van het onderzoek. Je was een stimulator en motivator. Je klinische blik en je snelle commentaar op mijn manuscripten en presentaties was leerzaam. Beste Jos, de gesprekken die we gehad hebben vond ik erg verhelderend. Je snelle reactie op de manuscripten en je suggesties voor verbeteringen waren zeer waardevol. Heel erg bedankt voor de analytische ondersteuning die je mogelijk maakte in de apotheek van het Slotervaart ziekenhuis.

Hilde, heel erg bedankt voor je suggesties voor de analyse van gemcitabine trifosfaat en super dat ik altijd kon langs komen voor overleg. Michel, Carolien, Bas, Joke, en anderen, bedankt voor jullie hulp bij de gemcitabine, paclitaxel en carboplatin metingen. Alwin, bedankt voor je krachtige en kinetische commentaar op de stukken en je inkortingscapaciteiten.

De verpleging van het AvL wil ik heel erg bedanken voor de hulp tijdens het “kinetieken”. Ans, het is fantastisch om te zien hoe vrolijk en enthousiast jij op 4C rond rent. Renske, Thea, Angela en alle anderen, bedankt voor jullie hulp. Alle nurse practitioners, bedankt voor jullie samenwerking.

Alle mensen van het trialbureau, het was fijn dat ik altijd terecht kon voor vragen over klinische studies. Ninja, bedankt voor het nakijken van mijn statistische analyses en je adviezen voor verbetering.

Tatiana, bedankt voor je hulp bij allerlei logistieke zaken voor de klinische studies. Het was leuk dat je daarnaast uitjes en barbecue avondjes organiseerde. Marja,

onze samenwerking tijdens de klinische studies heb ik heel prettig gevonden. Dilsha en Jolanda, bedankt voor jullie hulp bij allerlei administratieve zaken. Cécile, je inzet voor GCP is niet te evenaren.
Furthermore, I worked together with people from Eli Lilly on the gemcitabine studies. Sophie Callies, thanks for your patience and the answers to my questions regarding the pharmacokinetic model for oral gemcitabine. Furthermore, it was a good practice for me to improve my French-English language. Ignacio-Garcia Ribas, thanks for your interest and your suggestions in my preclinical research on gemcitabine. Thanks for the fruitful discussions. To be honest, I would have preferred that some of these conversations took place in the warmer atmosphere of Madrid.
Mijn zeer geslaagde tijd op het NKI kwam mede door mijn naaste collega's en kamergenoten. Dick, jouw hulp bij mijn promotie, met name het onderzoek naar gemcitabine, was van onschatbare waarde. Ik heb bewondering voor de manier waarop je een eenvoudige oplossing weet te bedenken om een experiment tot succes te brengen. Je hebt heel wat HPLC uurtjes op het radionucliden lab doorgebracht. Behalve dat de samenwerking erg vruchtbaar was, vond ik het ook leuk en leerzaam om met je gewerkt te hebben. Ik kon je droge humor zeer waarderen. Monique en Marije (M&M's), jullie gingen hand in hand ten strijde en zijn gelukkig niet gesmolten in onze hand(zame) besprekingen. Dankzij jullie kritische houding ten aanzien van de praktische haalbaarheid van de experimenten, hebben jullie mijn theoretische geneuzel tot effectieve proeven helpen transformeren.
Stefan (Mr. Figure), je behulpzaamheid heb ik zeer gewaardeerd. De dartavondjes in de LS kamer en de bierproeverijen in Bedier waren geslaagd. Roos, ik was blij toen ik hoorde dat je bij je afweging tussen verschillende werkplekken voor kamer 612 had gekozen. Ik zal de gezellige kletspraat en de koffiesessies 's morgens vroeg missen, alsmede de AACR scientific cocktail roof meeting. Maarten, bedankt voor je inbreng van de Senseo en de gezelligheid op de kamer. Houdt die kamer in balans met 3 vrouwen!
Marijn, bedankt voor de ritjes door Los Angeles en de gezelligheid tijdens de AACR. Wie weet beginnen we nog eens een bedrijfje. Jurjen, fantastisch hoe wij als duo opereerden op de OIO retreat op Texel. Gelukkig werden, na de voorbereidingen op de Cam, onze presentaties in Cambridge zeer goed ontvangen.

Sari, bedankt dat je mij wegwijs wilde maken in de wereld van het kloneren en het gebruik van siRNAs. De etentjes waren super en ik heb je vegetarische brouwsels langzaam weten te (vert)(waard)eren. Eitan, thanks for providing pSuper and your help with the transfections. Felix, bedankt dat je als student aan het *in vitro* gemcitabine onderzoek wilde meewerken.

Gerben, de tennispartijtjes waren gezellig. Hopelijk wordt je dit jaar wat sterker op gravel zodat we de symbolische Nadal - Haarhuis potjes kunnen omzetten in zenuwslopende Nadal - Federer partijen. Jimmy, bedankt voor je tennislesjes op de fameuze tennisclub Niet Winnen Toch Lol Donald Duck (NWTL-DD). Alle mensen van het NKI-AvL hockeyteam wil ik bedanken voor de gezellige hockeyavonden en toernooien. Hopelijk blijven jullie ondanks mijn afwezigheid opereren in de bovenste linie ;-).

Conchita, bedankt voor je ideeën voor mijn onderzoek. Het was voor mij bijzonder om iemand te ontmoeten die nog sneller praat dan ik. Adrian en Alfred, bedankt voor jullie suggesties en positieve commentaar. Adrian, in de toekomst laat ik je voor de verandering graag een keer rennen op de squash baan. Olaf, bedankt voor de prettige samenwerking en je uitleg ten aanzien van de muizen studies.

Frank en Anita, bedankt voor jullie ondersteuning bij de FACS en Lauran bedankt voor je hulp bij de microscopie. Henri en Theo, bedankt voor jullie bestellingen, ook al kwamen mijn aanvragen soms op ongebruikelijke uurtjes binnen.

De uitjes met de OIO's uit de Slotervaart bouwkeet waren geestverruimend! Der Markus, bedankt voor je hulp bij de platina metingen en de gezelligheid tijdens de borrels in Amsterdam.

Uiteraard kan ik niet iedereen uitgebreid bedanken. Buiten de directe collega's hebben veel vrienden gezorgd voor gezelligheid en ontspanning naast het harde werken aan mijn promotieonderzoek. Frans, Dimitri, Teun, Rogier, Wouter, Holger, de RB mannen, Sebastiaan, Frank, Theo-Hans, Tijmen en velen anderen dank ik voor de ontspannen avonden, sportieve activiteiten en luchtige gesprekken.

Beste paranimfen, ik ben blij dat jullie vandaag naast mij willen staan. Wouter, bedankt voor je rustige en intelligente kijk op de zaken. Het hardlopen, tennissen, en clubben gaan we zeker voortzetten. Robert, heel erg bedankt voor je waardevolle hulp bij de gemcitabine analyses en de nuttige discussies die we hadden ten aanzien van het gemcitabine onderzoek.

Lieve Pap en Mam, heel erg bedankt voor jullie steun en vertrouwen waardoor ik dit alles heb kunnen bereiken. Pap, ook heel veel dank voor je creatieve uitspatting op de omslag.

Allerliefste Annefloor, de slapsticks tijdens het salsa dansen waren perfect voor de ontspanning tijdens het onderzoek. Jammer dat ik een paar nachtjes met de NKI muisjes heb moeten doorbrengen in plaats van met jou en onze gezellige huismuisjes. Bedankt voor je begrip, liefde en je grote geduld met mijn enorme ongeduld.

Amsterdam, 2008

Curriculum Vitae

Sander Veltkamp was born on January 23, 1977 in Laren. In 1995, he received his VWO exam at the Rijks Scholengemeenschap (RSG) in Enkhuizen. In the same year, he started to study Pharmacy at Utrecht University. During his study he performed research at the Department of Dosage Form Development at Solvay Pharmaceuticals in Weesp. His main research project, entitled "Biodegradable implants as sustained drug delivery devices for CNS purposes" was performed at the Department of Novel Dosage Forms at Organon N.V. in Oss under supervision of Dr. Ir. M.A. Kruft, Prof. Dr. H. Vromans, and Prof. Dr. D.J.A. Crommelin. He conducted a literature study on neurophysiological functions of vasopressin and oxytocin and their role in the treatment of schizophrenia at the University Medical Center in Utrecht. As part of a student exchange program he temporarily worked at GlaxoSmithKline, San Jose, Costa Rica. He received his Master's degree in Pharmacy in April 2000 and started his specialisation to become Pharmacist. During this specialisation, he performed an internship at the Groote Schuur Hospital, Cape Town, South Africa. After receiving his Doctor of Pharmacy degree in May 2002, he started working as a pharmacist at the Hospital Pharmacy in The Hague where he performed research on the pharmacokinetics of gentamicin in preterm neonates. In December 2003, he started his PhD-project at the Division of Experimental Therapy and Department of Medical Oncology at the Netherlands Cancer Institute - Antoni van Leeuwenhoek Hospital in collaboration with the Department of Pharmacy & Pharmacology at the Slotervaart Hospital in Amsterdam. This project was supervised by Prof. Dr. J.H.M. Schellens and Prof. Dr. J.H. Beijnen. During his PhD-project he was trained in Clinical Pharmacology under auspicien of the Dutch Society of Clinical Pharmacology and Biopharmacy and received his Clinical Pharmacologist degree in September 2007.

List of Publications

Articles marked with an asterix (*) relate to the work described in this thesis.

1.* **Veltkamp SA**, Witteveen PO, Capriati A, Crea A, Voogel-Fuchs M, van den Heuvel IJGM, Beijnen JH, Voest EE, Schellens JHM. Clinical and pharmacological study of the novel prodrug MEN 4901/T-0128 in patients with solid tumors. *Submitted for publication*

2.* **Veltkamp SA,** Pluim D, van Tellingen O, Beijnen JH, Schellens JHM. Extensive metabolism and hepatic accumulation following multiple oral and i.v. dosing of gemcitabine in mice. *Submitted for publication*

3.* **Veltkamp SA,** Pluim D, van Eijndhoven MAJ, Bolijn MJ, Ong FHG, Govindarajan R, Unadkat J, Beijnen JH, Schellens JHM. New insights into the *in vitro* pharmacology and cytotoxicity of gemcitabine and its metabolite 2',2'-difluorodeoxyuridine. *Submitted for publication*

4.* **Veltkamp SA**, Beijnen JH, Schellens JHM. Prolonged versus standard gemcitabine infusion: translation of molecular pharmacology to new treatment strategy. *The Oncologist, accepted for publication*

5.* **Veltkamp SA**, Jansen RS, Callies S, Pluim D, Visseren-Grul CR, Rosing H, Beijnen JH, Slapak C, Schellens JHM. Oral administration of gemcitabine in patients with advanced solid tumors: a clinical and pharmacological study. *Clin Cancer Res, accepted for publication*

6. Sum BS, **Veltkamp SA**, Westerman EM, Sprij AJ, Touw DJ. An extended-interval gentamicin dosage regimen in newborns: a prospective study. *EJHP-S 2007;4:66-73*

7. **Veltkamp SA**, Westerman EM, Sprij AJ, Sum BS, Touw DJ. Gentamicin in preterm neonates: An extended interval dosing schedule. *EJHP-S 2007;4:59-64*

8.* Bröker LE, **Veltkamp SA**, Heath EI, Kuenen BC, Gall H, Astier L, Parker S, Kayitalire L, Lorusso PM, Schellens JHM, Giaccone G. A phase I safety and pharmacological study of a twice weekly dosing regimen of the oral taxane BMS-275183. *Clin Cancer Res 2007;13:3906-3912*

9.* **Veltkamp SA**, Meerum Terwogt JM, van den Heuvel MM, van Boven HH, Schellens JHM, Rodenhuis S. Severe pulmonary toxicity in patients with leiomyosarcoma after treatment with gemcitabine and docetaxel. *Invest New Drugs 2007;25:279-81*

10.* **Veltkamp SA**, Rosing H, Huitema ADR, Fetell MR, Nol A, Beijnen JH, Schellens JHM. Novel paclitaxel formulations for oral application: a phase I pharmacokinetic study in patients with solid tumors. *Cancer Chemother Pharmacol 2007;60:635-642*

11.* **Veltkamp SA**, Alderden-Los C, Sharma A, Rosing H, Beijnen JH, Schellens JHM. A pharmacokinetic and safety study of a novel polymeric paclitaxel formulation for oral application. *Cancer Chemother Pharmacol 2007;59:43-50*

12.* **Veltkamp SA**, Hillebrand MJ, Rosing H, Jansen RS, Wickremsinhe ER, Perkins EJ, Schellens JHM, Beijnen JH. Quantitative analysis of gemcitabine triphosphate in human peripheral blood mononuclear cells using weak anion-exchange liquid chromatography coupled with tandem mass spectrometry. *J Mass Spectrom 2006;41:1633-42*

13.* **Veltkamp SA**, Thijssen B, Garrigue JS, Lambert G, Lallemand F, Binlich F, Huitema AD, Nuijen B, Nol A, Beijnen JH, Schellens JHM. A novel self-microemulsifying formulation of paclitaxel for oral administration to patients with advanced cancer. *Br J Cancer 2006;18:729-34*

14. **Veltkamp SA**, Van Dongen A, Touw DJ, Bouvy PF, Teepe RGC. Kruisovergevoeligheid tussen SSRI's, mirtazapine en TCA's. *Pharm Weekbl 2003;46:1607*

Abstracts for oral and poster presentations

Veltkamp SA, Rosing H, Pluim D, Jansen RS, Callies S, Visseren-Grul CR, Slapak C, Beijnen JH, Schellens JHM. A clinical and pharmacological study of oral gemcitabine in patients with advanced solid tumors. *Basic & Clinical Pharmacology & Toxicology 2007;101:39.*

Veltkamp SA, Pluim D, Bolijn MJ, van Eijndhoven MAJ, Garcia-Ribas I, Wickremsinhe EM, Beijnen JH, Schellens JHM. Uptake, metabolism, and cytotoxicity of gemcitabine and its metabolite 2',2'-difluorodeoxyuridine in cell lines. *Basic & Clinical Pharmacology & Toxicology 2007;101:101*

Veltkamp SA, Huitema ADR, Rosing H, Nuijen B, Beijnen JH, Schellens JHM. Novel paclitaxel formulations for oral administration in patients with advanced solid tumors. *Basic & Clinical Pharmacology & Toxicology 2007;101:119*

Veltkamp SA, van Eijndhoven MAJ, Pluim D, Bolijn MJ, Jansen RS, Garcia-Ribas I, Wickremsinhe ER, Beijnen JH, Schellens JHM. Gemcitabine metabolite, 2',2'-difluorodeoxyuridine (dFdU), can be phosphorylated and incorporated into nucleic acids. *Proc Amer Assoc Cancer Res 2007;48:366*

Veltkamp SA, Ong FHG, Bolijn MJ, Garcia-Ribas I, Beijnen JH, Schellens JHM. In vitro toxicity of gemcitabine and its metabolite 2'2'-difluorodeoxyuridine in human cancer cells. *Naunyn Schmiedeberg's Archives of Pharmacology 2007;375:154*

Bröker LE, **Veltkamp SA**, Heath EI, Kuenen BC, Gall H, Astier L, Voi M, LoRusso PM, Schellens JHM, Giaccone G. The novel oral taxane BMS-275183 has a favorable activity and toxicity profile in a twice-weekly schedule; preliminary findings from an extended phase I trial. *Eur J Cancer, 2006;4:194*

Veltkamp SA, Callies S, Nol A, Visseren-Grul CM, Slapak C, Beijnen JH, Schellens JHM. Clinical pharmacology of oral gemcitabine in patients with advanced solid tumors. *Br J Clin Pharmacol 2006;62;6:735*